



**HAL**  
open science

# Finite element modeling of mechanical contact problems for industrial applications

Houssam Houssein

► **To cite this version:**

Houssam Houssein. Finite element modeling of mechanical contact problems for industrial applications. Solid mechanics [physics.class-ph]. Sorbonne Université, 2022. English. NNT: 2022SORUS011 . tel-03699706

**HAL Id: tel-03699706**

**<https://theses.hal.science/tel-03699706>**

Submitted on 20 Jun 2022

**HAL** is a multi-disciplinary open access archive for the deposit and dissemination of scientific research documents, whether they are published or not. The documents may come from teaching and research institutions in France or abroad, or from public or private research centers.

L'archive ouverte pluridisciplinaire **HAL**, est destinée au dépôt et à la diffusion de documents scientifiques de niveau recherche, publiés ou non, émanant des établissements d'enseignement et de recherche français ou étrangers, des laboratoires publics ou privés.

**SORBONNE UNIVERSITÉ**

**AIRTHIUM**

Doctoral School **École Doctorale Sciences Mathématiques de Paris Centre**

University Department **Laboratoire Jacques-Louis Lions**

Thesis defended by **Houssam HOUSSEIN**

Defended on **10<sup>th</sup> February, 2022**

In order to become Doctor from Sorbonne Université

Academic Field **Mathematics**

Speciality **Applied mathematics**

# Finite element modeling of mechanical contact problems for industrial applications

**Thesis supervised by** Frédéric HECHT    Supervisor  
Simon GARNOTEL    Co-Monitor

**Committee members**

<i>Referees</i>	Olivier PANTZ	Professor
	Rolf STENBERG	Professor
<i>Examiners</i>	Hervé LE DRET	Professor
	Christophe GEUZAINÉ	Professor
<i>Supervisor</i>	Frédéric HECHT	Professor at Sorbonne Université



**Keywords:** contact mechanics, signorini problem, friction, regularization , optimization, fixed point, penalization , interior point method, symmetric algorithm

**Mots clés :** mécanique des contacts, problème de signorini, frottement, régularisation, optimisation, point fixe, pénalisation, méthode des points intérieurs, algorithme symétrique



This thesis has been prepared at the following research units.

**Laboratoire Jacques-Louis Lions**

Sorbonne Université  
Campus Pierre et Marie Curie  
4 place Jussieu  
75005 Paris  
France

☎ +33 1 44 27 42 98  
Web Site <https://ljl1.math.upmc.fr/>



**Airthium**

Accelair - 1 chemin de la Porte des Loges  
78350 Les Loges-en-Josas  
France

Web Site <https://www.airthium.com>





*À mon père Ali et à ma mère Mona*

*À mon épouse Nada*

*À mon fils Dani*

*À mon frère Samer, ma famille et mes amis*



# Remerciements

Je tiens à remercier Airthium pour m'avoir offert la chance d'effectuer cette thèse chez eux, et je remercie le laboratoire LJLL (Laboratoire Jacques-Louis Lions) et tous ces membres pour m'avoir accueilli.

Je remercie Frédéric Hecht pour son soutien moral et technique, pour ses compétences scientifiques et pédagogiques, ainsi que pour ses qualités humaines et pour m'avoir suivi tout au long de ces trois dernières années.

Je remercie Simon Garnotel pour sa grande disponibilité, son soutien technique et aussi pour m'avoir suivi tout au long de ces trois dernières années, et sans oublier son humour. Je profite aussi pour remercier Pierre Jolivet pour son aide sur le sujet du parallélisme.

Je remercie Rolf Stenberg et Olivier Pantz pour avoir accepté de rapporter sur ma thèse, ainsi que les membres du jury Hervé Le Dret et Christophe Geuzaine.

Je remercie Andreï Klochko et Franck Lahaye pour leurs soutien moral, Franck Lahaye pour son soutien linguistique. Je n'oublie pas aussi les stagiaires qui ont fait leurs stage à Airthium, et aussi tous les doctorants du LJLL, sans citer les prénoms.

Je tiens à remercier également l'ANRT pour avoir financé partiellement cette thèse.



---

**FINITE ELEMENT MODELING OF MECHANICAL CONTACT PROBLEMS FOR INDUSTRIAL APPLICATIONS****Abstract**

The Airthium company uses FreeFEM software in order to study its energy storage system, and contact mechanics is a part of these studies. Therefore the principal aim of this thesis is to develop an algorithm, using FreeFEM and its tools, to solve mechanical contact problems between two bodies or more, for linear elastic or finite deformation problems.

The contact problem is considered as a minimization problem of an energy, where we can take advantage of several optimization techniques, in order to converge faster to the solution. For several reasons, the interior point method is the optimization method chosen to solve the generated minimization problems.

An algorithm is proposed in order to solve the frictionless contact between a hyperelastic body and a rigid foundation (obstacle). The non-penetration constraints between the body and the obstacle are described in a simple way, where there is no need to compute the normal vectors or the projection points on the obstacle, which simplifies the resolution of the contact problem.

The second aim of this thesis is to develop a symmetric algorithm where the user no longer needs to specify a slave body and a master one. Thus two algorithms were developed, one based on the penalty method, and the second one uses the interior point method. In the two cases a sequence of minimization problems with linear (or affine) constraints, using a fixed point algorithm, is employed in order to consider the non-penetration for finite deformation problems, where large deformations occur.

The friction is also taken into account, and the problem using Coulomb's criterion is written into a sequence of problems with Tresca's criterion, in order to obtain a sequence of minimization problems. A family of regularization for the Tresca's criterion are proposed, in order to obtain sufficiently smooth problems, which in some situations can have an experimental justifications.

**Keywords:** contact mechanics, signorini problem, friction, regularization , optimization, fixed point, penalization , interior point method, symmetric algorithm

---

### Résumé

La société Airthium utilise le logiciel FreeFEM afin d'étudier son système de stockage d'énergie, et la mécanique du contact fait partie de ces études. L'objectif principal de cette thèse est donc de développer un algorithme, utilisant FreeFEM et ses outils, pour résoudre des problèmes de contact mécanique entre deux corps ou plus, pour des problèmes d'élasticité linéaire ou de grandes déformations.

Le problème de contact est considéré comme un problème de minimisation d'une énergie, où nous pouvons tirer parti de plusieurs techniques d'optimisation, afin de converger plus rapidement vers la solution. Pour plusieurs raisons, la méthode de points intérieurs est la méthode d'optimisation choisie pour résoudre les problèmes de minimisation générés.

Un algorithme est proposé afin de résoudre le contact sans frottement entre un corps hyperélastique et une fondation rigide (obstacle). Les contraintes de non-pénétration entre le corps et l'obstacle sont décrites d'une manière simple, où il n'est pas nécessaire de calculer les vecteurs normaux ou les points de projection sur l'obstacle, ce qui simplifie la résolution du problème de contact.

Le second objectif de cette thèse est de développer un algorithme symétrique où l'utilisateur n'a plus besoin de spécifier un corps esclave et un corps maître. Ainsi deux algorithmes ont été développés, l'un basé sur la méthode de pénalisation, et le second utilise la méthode de points intérieurs. Dans les deux cas, une suite de problèmes de minimisation avec des contraintes linéaires (ou affines), utilisant un algorithme à point fixe, est employée afin de considérer la non-pénétration pour les problèmes où de grandes déformations se produisent.

Le frottement est également pris en compte, et le problème utilisant le critère de Coulomb est écrit en une séquence de problèmes avec le critère de Tresca, afin d'obtenir une séquence de problèmes de minimisation. Une famille de régularisation pour le critère de Tresca est proposée, afin d'obtenir des problèmes suffisamment lisses, qui dans certaines situations peuvent avoir une justification expérimentale.

**Mots clés :** mécanique des contacts, problème de signorini, frottement, régularisation, optimisation, point fixe, pénalisation, méthode des points intérieurs, algorithme symétrique

---

# Contents

<b>Remerciements</b>	<b>ix</b>
<b>Abstract</b>	<b>xi</b>
<b>Contents</b>	<b>xiii</b>
<b>Acronyms</b>	<b>1</b>
<b>Introduction (French version)</b>	<b>3</b>
<b>Introduction (english version)</b>	<b>5</b>
<b>1 State of the art</b>	<b>7</b>
1.1 Nonlinear mechanics . . . . .	8
1.1.1 kinematics . . . . .	8
1.1.2 Formulations and equations . . . . .	10
1.1.3 Hyperelastic materials . . . . .	11
1.2 Contact Theory . . . . .	15
1.2.1 Signorini’s contact problem . . . . .	15
1.2.2 Contact in finite deformation . . . . .	17
1.2.3 Contact between two elastic deformable bodies . . . . .	20

---

1.2.4	Friction in contact problems . . . . .	22
1.3	Contact numerical methods . . . . .	23
1.3.1	Inequality constrained problems . . . . .	26
1.4	Discretization methods . . . . .	28
1.4.1	Node-to-node . . . . .	28
1.4.2	Node-to-segment . . . . .	28
1.4.3	Quadrature-point-to-surface . . . . .	29
1.4.4	Mortar method . . . . .	29
1.4.5	Smoothing techniques . . . . .	30
1.4.6	Analytic contact detection . . . . .	31
1.5	Frictional contact algorithms . . . . .	31
1.6	Other contact methods . . . . .	34
1.6.1	Nitsche-based method . . . . .	34
1.6.2	Generalized Newton method . . . . .	34
1.6.3	Alternative discretization methods . . . . .	34
1.7	The need for a symmetric contact algorithm . . . . .	34
<b>2</b>	<b>Signorini's contact problem with Interior point optimizer</b>	<b>37</b>
2.1	Signorini's contact problem . . . . .	38
2.2	Minimization problem resolution . . . . .	40
2.2.1	Interior Point method . . . . .	40
2.2.2	Formulation of the problem . . . . .	43
2.2.3	Weak contact formulation . . . . .	45
2.3	Numerical validations . . . . .	46
2.3.1	Compression of a hyperelastic cube . . . . .	46

2.3.2 Hertz contact problem . . . . .	49
2.3.3 Press-fit problem . . . . .	51
2.3.4 Clamped body contact . . . . .	52
<b>3 Penalty method</b>	<b>55</b>
3.1 Signorini's problem for linear elasticity . . . . .	56
3.2 Finite deformations . . . . .	67
3.3 Contact between two bodies in linear elasticity . . . . .	69
3.4 Symmetric contact formulation . . . . .	70
3.5 Numerical integration . . . . .	71
3.6 Symmetric contact algorithm using penalty method . . . . .	75
3.7 Projection of the integration points . . . . .	76
3.8 Smoothing techniques . . . . .	79
3.8.1 Bézier curve . . . . .	79
3.9 Numerical validations . . . . .	80
3.9.1 Compression of two elastic blocks with imposed displacement . . . . .	80
3.9.2 Contact between two cylinders . . . . .	82
<b>4 Weak contact formulation and a simple symmetric algorithm</b>	<b>85</b>
4.1 Weak non-penetration condition for the contact . . . . .	86
4.1.1 Mesh discretization . . . . .	87
4.1.2 Non-penetration condition . . . . .	88
4.2 Numerical Integration . . . . .	89
4.2.1 Numerical integration of the weak constraints . . . . .	90
4.3 Contact problems with interior point method . . . . .	93
4.3.1 Symmetric formulation . . . . .	94

4.3.2	Numerical optimization by the interior point method . . . . .	94
4.3.3	Behavior of the barrier solutions . . . . .	98
4.3.4	Global convergence . . . . .	101
4.4	Alternative formulations . . . . .	103
4.4.1	First alternative formulation . . . . .	103
4.4.2	Mixed symmetric methods . . . . .	104
4.5	Symmetric contact algorithm . . . . .	104
4.6	Rigid body motions . . . . .	105
4.7	Numerical validations . . . . .	106
4.7.1	Compression of two elastic blocks with imposed displacement . . . . .	106
4.7.2	Hertz contact with two elastic bodies . . . . .	107
4.7.3	Contact between two cylinders . . . . .	109
4.7.4	Disc-in-disc . . . . .	110
4.7.5	Multi-body contact between three beams . . . . .	111
<b>5</b>	<b>The dynamic contact</b>	<b>113</b>
5.1	Formulation of the dynamic contact problem as a minimization one . . . . .	114
5.1.1	The minimization problem using Euler implicit scheme . . . . .	114
5.1.2	The problem using a special case of the Newmark scheme . . . . .	117
5.2	Numerical examples . . . . .	117
5.2.1	Impact between a ball and a block . . . . .	118
5.2.2	Impact between two balls and a foundation . . . . .	119
<b>6</b>	<b>Frictional contact problems with the interior point method</b>	<b>123</b>
6.1	Linear elasticity . . . . .	124
6.1.1	Tresca criterion . . . . .	125

6.1.2	Variational formulation for Tresca criterion . . . . .	125
6.1.3	Minimization formulation for the Tresca criterion . . . . .	126
6.1.4	Coulomb's criterion as a fixed point problem . . . . .	127
6.1.5	The quasi-static problem for Coulomb's criterion . . . . .	127
6.2	Regularization of the Tresca frictional problem . . . . .	128
6.2.1	Frictional criterion generated from the regularized problem . . . . .	130
6.2.2	Minimization formulation for the regularized problem . . . . .	134
6.2.3	Error between Tresca's solution and regularized Tresca's solution . . . . .	134
6.2.4	Coulomb's criterion as a fixed point problem for the regularized problem . . . . .	135
6.2.5	Quasi-static problem for the regularized one . . . . .	136
6.3	Finite deformation . . . . .	137
6.4	Fixed point algorithm convergence for the frictional regularized discretized problem . . . . .	143
6.4.1	Case of two bodies in contact . . . . .	149
6.4.2	Error between Tresca's discretized solution and regularized Tresca's discretized solution . . . . .	150
6.5	The Algorithm . . . . .	151
6.6	Numerical validations . . . . .	154
6.6.1	Validation of the regularized friction law . . . . .	154
6.6.2	Elastic bloc pressed against a rigid foundation . . . . .	155
6.6.3	Contact of a square plate against an obstacle . . . . .	157
6.6.4	Sliding on an inclined interface . . . . .	158
6.6.5	Frictional Hertz contact . . . . .	161
6.6.6	Shallow ironing . . . . .	164
<b>7</b>	<b>Conclusion and future works</b>	<b>167</b>

---

<b>A Contact method using indicator functions defined on triangles</b>	<b>169</b>
A.1 Indicator function of a triangle . . . . .	175
A.2 Non-penetration condition . . . . .	177
A.3 Contact problem formulation using indicator functions . . . . .	178
<b>Bibliography</b>	<b>179</b>

# Acronyms

- 2D Two-dimensional
- 3D Three-dimensional
- UL Length unit
- UF Force unit
- $P_1$  Piecewise linear continuous finite elements
- $P_2$  Piecewise quadratic continuous finite elements
- det Determinant operator
- Tr Matrix trace operator
- supp Support of a function
- meas Measure of a set
- *a.e* Almost everywhere



# Introduction (French version)

Les problèmes de contact mécanique et leurs simulations sont d'une grande importance dans l'industrie. Une des difficultés rencontrées dans ce type de problèmes est la non-linéarité résultant de la non-pénétration des corps en contact. Une autre non-linéarité peut provenir du matériau, en effet les matériaux élastiques linéaires ne sont pas utilisés en pratique pour modéliser les matériaux qui peuvent être soumis à de grandes déformations, au contraire les matériaux hyperélastiques sont considérés pour modéliser des matériaux comme le caoutchouc. La théorie sur les matériaux hyperélastiques est discutée dans [2, 17, 29, 83, 91]. Dans le cas du contact par frottement, une autre non-linéarité doit être prise en compte et rend le problème encore plus difficile.

Les solutions analytiques (le champ de déplacement ou la pression de contact) d'un problème de contact sont difficiles ou impossibles à trouver, cependant dans des cas particuliers comme le problème de Hertz, qui est le contact entre deux cylindres élastiques, une solution analytique peut être trouvée même si la friction est prise en compte [66].

Le problème de contact est en général transformé en une forme faible, l'existence et l'unicité de tels problèmes ne sont pas tout à fait faciles à prouver et dans certains cas impossibles, par exemple dans le cas des problèmes de contact sans frottement, l'existence et l'unicité du problème de contact de Signorini (contact avec une fondation rigide) pour les problèmes élastiques linéaires ont été prouvées dans [44], sinon dans le cas de grandes déformations et pour les matériaux hyperélastiques avec des propriétés spéciales, l'existence d'une solution peut être trouvée dans [29]. Cependant, dans le cas d'un problème de contact par friction utilisant le critère de Coulomb, la situation est plus compliquée, par exemple, seule l'existence d'une solution pour un petit coefficient de friction peut être trouvée dans [41]. Si la contrainte normale de contact est remplacée par une contrainte régularisée, l'existence d'une solution pour le problème de contact de Signorini avec frottement peut être prouvée [32] et il y a une unicité si le coefficient de friction est suffisamment petit.

Parmi les premiers articles sur la mécanique computationnelle des contacts, on peut citer : [24, 48, 65]. Différentes méthodes peuvent être utilisées pour résoudre un problème de contact, comme la méthode de pénalisation, la méthode des multiplicateurs de Lagrange et la méthode du Lagrangien augmenté. Pour plus de détails sur la mécanique du contact et les méthodes qui peuvent être utilisées pour résoudre ce type de problèmes, on peut se référer aux monographies [76, 69, 123] et aux références qui y figurent.

La méthode des contraintes actives est souvent utilisée en mécanique des contacts computa-

tionnelle afin de trouver la zone de contact. Par ailleurs la méthode de points intérieurs n'a pas été largement utilisée dans les problèmes de contact, on peut citer par exemple : [74, 112, 116].

La plupart des algorithmes de contact font intervenir le concept de maître/esclave, ce qui empêche la pénétration du corps esclave dans le corps maître, et entraîne donc la non-symétrie de l'algorithme. Autrement dit, les conditions de non-pénétration sont imposées au corps esclave, et lorsque la méthode des éléments finis est utilisée, des résultats différents peuvent être observés si le corps esclave devient le maître et le maître devient l'esclave. Par ailleurs, il existe des critères pour choisir un corps comme esclave mais dans certaines situations, il est très difficile de décider, d'où la nécessité d'un algorithme symétrique afin de résoudre ce problème.

L'objectif général de cette thèse, est de développer un algorithme simple utilisant FreeFEM [55] et ses outils afin de résoudre les problèmes de contact, avec ou sans frottement, pour les problèmes linéaires élastiques et pour les problèmes de grandes déformations, dans le but de simuler plusieurs phénomènes de contact dans notre système de stockage d'énergie. Le deuxième objectif de cette thèse est d'obtenir une formulation symétrique, afin de permettre à l'utilisateur de ne plus distinguer les corps esclaves et maîtres, ce qui est très utile pour les problèmes de contact multi-corps.

Enfin, ce manuscrit est organisé en plusieurs chapitres, dans le chapitre 1 nous présentons une introduction générale de la théorie des problèmes de contact, et les célèbres méthodes utilisées pour résoudre les problèmes de contact en plus de la nécessité d'un algorithme de contact symétrique.

Dans le chapitre 2, nous avons formulé le problème de contact de Signorini en un problème de minimisation sous contrainte. Les contraintes de non-pénétration sont formulées sous une forme simple qui rend la formulation du problème de contact bien adaptée à la méthode des points intérieurs. De plus, il n'est pas nécessaire de calculer les vecteurs normaux ou les points de projection sur l'obstacle pour décrire la non-pénétration, ce qui augmente la vitesse de résolution du problème de contact. Cette méthode permet de simuler le contact entre un joint en caoutchouc et une surface métallique.

Le chapitre 3 présente un algorithme pour résoudre les problèmes de contact mécanique entre deux corps ou plus, pour les problèmes d'élasticité linéaire et de grandes déformations. La méthode de pénalisation est utilisée afin de décrire les conditions de non-pénétration, cet algorithme est symétrique, et les points d'intégration de chaque zone de contact sont pénalisés pour pénétrer dans la zone de contact opposée.

Le chapitre 4 présente également un algorithme pour résoudre les problèmes de contact mécanique entre deux corps ou plus, pour les problèmes d'élasticité linéaire et de grandes déformations. Cependant, les conditions de non-pénétration sont écrites sous une forme faible, qui produit des solutions plus lisses. Cet algorithme est également symétrique et la méthode de points intérieurs a été utilisée pour résoudre le problème de minimisation contraint généralisé.

Dans le chapitre 5, le contact dynamique est considéré, et dans le chapitre 6, un algorithme pour résoudre les problèmes de contact avec frottement est présenté, où le problème est transformé en une séquence de problèmes de contact régularisés du critère de Tresca. En effet, le problème est transformé en une méthode de point fixe où un problème de minimisation est résolu à chaque itération.

# Introduction (english version)

Mechanical contact problems and their simulations are of great importance in the industry. One of the difficulties encountered in these kinds of problems is the non-linearity resulting from the non-penetration of the bodies in contact. Another non-linearity can come from the material, indeed linear elastic materials are not used in practice to model the materials which can be submitted to large deformations, instead hyperelastic materials are considered to model materials like rubber. The theory on the hyperelastic materials are discussed in [2, 17, 29, 83, 91]. In the case of frictional contact, another non-linearity must be considered and makes the problem even more difficult.

Analytical solutions (the displacement field or the contact pressure) of a contact problem are hard or impossible to find, however in special cases like the Hertz problem, which is the contact between two elastic cylinders, an analytical solutions can be found even if the friction is taken into account [66].

The contact problem is in general transformed into a weak form, the existence and the uniqueness of such problems are not quite easy to prove and in some cases impossible, for example in the case of frictionless contact problems (without friction), the existence and the uniqueness of Signorini's contact problem (contact with a rigid foundation) for linear elastic problems were proved in [44], otherwise in the case of large deformations and for hyperelastic materials with special properties, the existence of a solution can be found in [29]. However in the case of frictional contact problem using Coulomb's criterion the situation is more complicated, for example only the existence of a solution for a small coefficient of friction can be found in [41]. If the normal contact stress is replaced by a regularized one, the existence of a solution for Signorini's frictional contact problem can be found [32] and there is a uniqueness if the friction coefficient is small enough.

From the first papers in the computational contact mechanics we can cite [24, 48, 65]. Different methods can be used to solve a contact problem such as the penalty method, the Lagrangian multiplier method, and the augmented Lagrangian method. For more details about contact mechanics and methods that can be used for solving these type of problems, one can refer to the monographs [76, 69, 123] and the references therein.

Active-Set Strategy are often used in computational contact mechanics in order to find the contact zone. Otherwise the interior point method was not widely used in contact problems, we can cite for example [74, 112, 116].

Most of the contact algorithms involve the concept of master/slave, which prevents the penetration of the slave body into the master one, and therefore causes the non-symmetry of the algorithm. Otherwise speaking the non-penetration conditions are imposed on the slave body, and when the finite element method is used, a different results can be noticed if the slave body becomes the master and the master become the slave. Otherwise, there is some criterions to choose a body as slave but in some situations it's very hard to decide, hence the need for a symmetric algorithm in order to solve this issue.

The general aim of this thesis, is to develop a simple algorithm using FreeFEM [55] and its tools in order to solve contact problems, with or without friction, for linear elastic ones and for large deformations problems, for the purpose of simulating several contact phenomena in our energy storage system. The second goal of this thesis is to obtain a symmetric formulation, in order to allow the user to no longer distinguish between slave and master bodies, which is very useful for the self-contact and multi-body contact problems.

Finally, this manuscript is organized in several chapters, in the chapter 1 we present a general introduction of the contact problem theory, and the famous methods used to solve contact problems in addition to the need for a symmetric contact algorithm.

In chapter 2 we formulated the Signorini's contact problem into a constrained minimization one. The non-penetration constraints are formulated in a simple form which makes the contact problem formulation well fitted with the interior point method. In addition there is no need to compute the normal vectors or the projection points on the obstacle in order to describe the non-penetration, which increases the resolution speed of the contact problem. Such method can simulate the contact between a rubber gasket and a metallic surface.

The chapter 3 presents an algorithm to solve mechanical contact problems between two bodies or more, for linear elastic and finite deformation problems. Penalty method is used in order to describe the non-penetration conditions, this algorithm is symmetric, and the integration points of each contact area are penalized to penetrate the opposite contact area.

The chapter 4 also presents an algorithm to solve mechanical contact problems between two bodies or more, for linear elastic and finite deformation problems. However the non-penetration conditions are written into a weak form, which produce smoother solutions, this algorithm is also symmetric and the interior point method was used to solve the generated constrained minimization problem.

In chapter 5 the dynamic contact is considered, and in chapter 6 an algorithm to solve frictional contact problems is presented, where the problem is transformed into a sequence of regularized Tresca frictional contact problems. Indeed the problem is transformed into a fixed point method where a minimization problem is solved at each iteration.

# Chapter 1

## State of the art

### Outline of the current chapter

---

<b>1.1 Nonlinear mechanics</b>	<b>8</b>
1.1.1 kinematics . . . . .	8
1.1.2 Formulations and equations . . . . .	10
1.1.3 Hyperelastic materials . . . . .	11
<b>1.2 Contact Theory</b>	<b>15</b>
1.2.1 Signorini's contact problem . . . . .	15
1.2.2 Contact in finite deformation . . . . .	17
1.2.3 Contact between two elastic deformable bodies . . . . .	20
1.2.4 Friction in contact problems . . . . .	22
<b>1.3 Contact numerical methods</b>	<b>23</b>
1.3.1 Inequality constrained problems . . . . .	26
<b>1.4 Discretization methods</b>	<b>28</b>
1.4.1 Node-to-node . . . . .	28
1.4.2 Node-to-segment . . . . .	28
1.4.3 Quadrature-point-to-surface . . . . .	29
1.4.4 Mortar method . . . . .	29
1.4.5 Smoothing techniques . . . . .	30
1.4.6 Analytic contact detection . . . . .	31
<b>1.5 Frictional contact algorithms</b>	<b>31</b>
<b>1.6 Other contact methods</b>	<b>34</b>
1.6.1 Nitsche-based method . . . . .	34
1.6.2 Generalized Newton method . . . . .	34
1.6.3 Alternative discretization methods . . . . .	34
<b>1.7 The need for a symmetric contact algorithm</b>	<b>34</b>

---

The aim of this chapter is to present a general introduction of the finite deformation and contact problems theories, in addition to the famous methods used to solve contact problems. In the end we present why a symmetric contact algorithm is needed.

## 1.1 Nonlinear mechanics

In this part we will present some reminders on the large deformation mechanics or finite deformation [18, 102, 104, 126]. The bold type in the equations corresponds either to vectors or to matrices.

### 1.1.1 kinematics

In the following we will consider a deformable body which will undergo large deformations, we have to distinguish between two configurations, the reference configuration where this body is at its initial position and the actual configuration which corresponds to the deformed configuration of this body. The reference or the initial configuration is known in advance, on the other hand the current configuration which corresponds to the body deformed by the loads is to be determined.

Let  $\Omega \subset \mathbb{R}^3$  denotes this body (in its reference position) and  $\partial\Omega = \Gamma_0 \cup \Gamma_1$ , where  $\Gamma_0$  and  $\Gamma_1$  denote respectively the partition of the boundary ( $\Gamma_0 \cap \Gamma_1 = \emptyset$ ), where a displacement and a surface traction are applied. Assuming the static case, the application which describes the deformation of the body is denoted  $\phi$ . It maps the body from its initial configuration  $\Omega$  into its actual configuration  $\phi(\Omega)$ , see Figure 1.1.

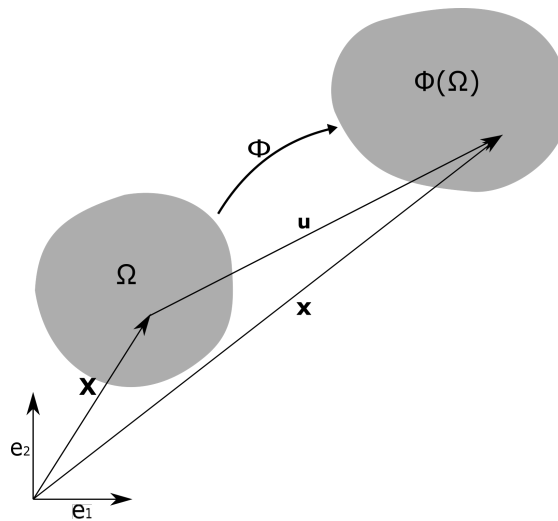


Figure 1.1 – Initial and actual configurations

In the following, the position vector of a particle in its initial and actual configurations are

respectively represented by  $\mathbf{X}$  and  $\mathbf{x} = \phi(\mathbf{X})$ . The displacement field vector is given by

$$\mathbf{u} = \mathbf{x} - \mathbf{X} = \phi(\mathbf{X}) - \mathbf{X} \quad (1.1)$$

In the Lagrangian description, all physical quantities are taken with respect to the reference configuration, in other words we follow in time the particles of the studied body along their trajectories, while in the Eulerian description the physical quantities are taken with respect to the current configuration. In solid mechanics the Lagrangian description is often used.

### The deformation gradient tensor

The deformation gradient tensor  $\mathbf{F}$  measures the deformation of the body  $\Omega$  and provides a relationship between a set of particles  $d\mathbf{X}$  in the reference configuration before deformation and the set  $d\mathbf{x}$  composed of the same particles in the current configuration after deformation. It is defined by

$$\mathbf{F} = \left( \frac{\partial \mathbf{x}}{\partial \mathbf{X}} \right)^T = \left( \frac{\partial \phi(\mathbf{X}, t)}{\partial \mathbf{X}} \right)^T$$

More precisely

$$\mathbf{F}_{ij} = \frac{\partial \phi_i}{\partial X_j}$$

In addition, we define

$$J = \det(\mathbf{F})$$

### Strain tensors

In order to measure and describe the deformations, we will present several strain tensors, like the right Cauchy-Green deformation tensor which is defined by

$$\mathbf{C} = \mathbf{F}^T \mathbf{F} \quad (1.2)$$

or the Green-Lagrange tensor defined by

$$\mathbf{E} = \frac{1}{2} (\mathbf{F}^T \mathbf{F} - \mathbf{I}) \quad (1.3)$$

where  $\mathbf{I}$  is the identity matrix. In the case of small deformations, the reference and actual configuration are no longer distinguished and the derivation with respect to  $\mathbf{X}$  or  $\mathbf{x}$  is the same, we define the strain tensor  $\epsilon$  as

$$\epsilon = \frac{1}{2} (\nabla_x \mathbf{u} + \nabla_x \mathbf{u}^T) \quad (1.4)$$

In other words

$$\epsilon_{ij} = \frac{1}{2} \left( \frac{\partial u_i}{\partial x_j} + \frac{\partial u_j}{\partial x_i} \right) \quad (1.5)$$

where  $\mathbf{x} = (x_1, x_2, x_3)$  and  $\mathbf{u} = (u_1, u_2, u_3)$ .

### Stress tensors

There are three different types of tensors describing the stress in a body, let's present these stress tensors.

- Let  $ds$  and  $\mathbf{n}$  denote respectively an infinitesimal surface in the body and the unitary normal vector at this surface (see Figure 1.2) in the actual configuration, thus the Cauchy stress tensor  $\boldsymbol{\sigma}$  provides the force  $d\mathbf{f}$  applied on  $ds$  by the following formula

$$d\mathbf{f} = (\boldsymbol{\sigma}\mathbf{n})ds \quad (1.6)$$

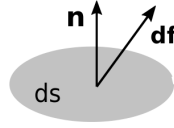


Figure 1.2 – Infinitesimal surface

- Let  $dS$  be the infinitesimal surface in the initial configuration, which corresponds to the surface  $ds$  in the actual configuration and let  $\mathbf{N}$  be the unitary normal vector at  $dS$ . Therefore, the force  $d\mathbf{f}$  in the actual configuration can also be given by

$$d\mathbf{f} = (\mathbf{P}\mathbf{N})dS \quad (1.7)$$

where  $\mathbf{P}$  denotes the first Piola-Kirchhoff stress tensor and can be obtained by the following

$$\mathbf{P} = J\boldsymbol{\sigma}\mathbf{F}^{-T} \quad (1.8)$$

and  $J = \det(\mathbf{F})$ .

- Finally, the force applied at  $dS$  in the initial configuration denoted by  $d\mathbf{F}$  can be provided by the following equation

$$d\mathbf{F} = (\mathbf{S}\mathbf{N})dS \quad (1.9)$$

where  $\mathbf{S} = \mathbf{F}^{-1}\mathbf{P}$  denotes the Second Piola-Kirchhoff stress tensor. For more details, refer to [102].

### 1.1.2 Formulations and equations

Let  $\rho$  be the actual density of the body and  $\mathbf{f}$  the body force per unit mass applied on the body (for example the gravity). Then the local balance of momentum in the actual configuration, where the Cauchy stress tensor is taken into account, is described by the following equation

$$\operatorname{div}_x \boldsymbol{\sigma} + \rho\mathbf{f} = 0 \quad (1.10)$$

or, by considering the components, it becomes

$$\sum_{j=1}^3 \frac{\partial \sigma_{ij}}{\partial x_j} + \rho f_i = 0 \quad i = 1, 2, 3 \quad (1.11)$$

The Cauchy stress tensor is symmetric ( $\boldsymbol{\sigma} = \boldsymbol{\sigma}^T$ ) by the local balance of angular momentum. Note that in the reference configuration the local balance of momentum for the body can also be described by

$$\operatorname{div} \mathbf{P} + \rho_0 \mathbf{f} = 0 \quad (1.12)$$

or, by considering the components, it becomes

$$\sum_{j=1}^3 \frac{\partial P_{ij}}{\partial X_j} + \rho_0 f_i = 0 \quad i = 1, 2, 3 \quad (1.13)$$

where  $\rho_0$  is the body density in the reference configuration. In addition, boundary conditions must be imposed on the body boundary, therefore if we suppose a null displacement on  $\Gamma_0$  and a surface traction  $\mathbf{t}$  applied on  $\Gamma_1$ , we will have the following conditions

$$\begin{cases} \mathbf{u} &= \mathbf{0} & \text{on } \Gamma_0 \\ \mathbf{PN} &= \mathbf{t} & \text{on } \Gamma_1 \end{cases} \quad (1.14)$$

In the following, the admissible displacements set is defined by

$$\mathcal{A} = \left\{ \mathbf{v} \in (H^1(\Omega))^3 ; \mathbf{v} = 0 \text{ on } \Gamma_0 \right\} \quad (1.15)$$

where  $H^1(\Omega)$  is the Sobolev space, such that if  $v_i \in H^1(\Omega)$  then  $v_i$  and its derivative are in  $L^2(\Omega)$  (square-integrable functions space). For more details on Sobolev spaces, refer to [6, 20].

The weak formulation in the initial configuration is the following

$$\int_{\Omega} \mathbf{P} : \operatorname{Grad} \mathbf{v} \, dV - \int_{\Omega} \rho_0 \mathbf{f} \cdot \mathbf{v} \, dV - \int_{\Gamma_1} \mathbf{t} \cdot \mathbf{v} \, dA = 0 \quad \forall \mathbf{v} \in \mathcal{A} \quad (1.16)$$

where  $(\operatorname{Grad} \mathbf{v})_{ij} = \frac{\partial v_i}{\partial X_j}$  and  $\mathbf{A} : \mathbf{B} = \operatorname{Tr}(\mathbf{A}^T \mathbf{B})$ .

### 1.1.3 Hyperelastic materials

Hyperelastic materials describe a group of materials that can be subject to large deformations, for example rubber material.

In order to describe the behavior of such materials, supposed to be isotropic, the strain energy function  $\hat{W}$ , a scalar function, can be used to show a relation between the stress tensors and the displacement field. Thus the second Piola-Kirchhoff stress tensor can be given by the following formula

$$\mathbf{S} = 2 \cdot \frac{\partial \hat{W}}{\partial \mathbf{C}} \quad (1.17)$$

or more explicitly by

$$\mathbf{S}_{ij} = 2 \cdot \frac{\partial \hat{W}}{\partial \mathbf{C}_{ij}} \quad (1.18)$$

where the tensor  $\mathbf{C}$  is presented by the equation (1.2) and the strain energy function  $\hat{W}$  depends on the invariants  $(I_1, I_2, I_3)$  of the tensor  $\mathbf{C}$ , which can be defined by

$$\begin{cases} I_1 = \text{Tr}(\mathbf{C}) \\ I_2 = \frac{1}{2}((\text{Tr}(\mathbf{C}))^2 - \text{Tr}(\mathbf{C}^2)) \\ I_3 = \det(\mathbf{C}) = J^2 \end{cases} \quad (1.19)$$

The theory on the Hyperelastic constitutive laws can be found in [2, 17, 29].

### Incompressible hyperelastic materials

In incompressible materials we have  $J = 1$  so the third invariant  $I_3 = 1$ . Several models to write the energy density function have been developed, we will present some interesting and well used models.

**Neo-Hookean model:** The Neo-Hookean model is the simplest model, indeed it depends only on one invariant  $I_1$ , it is a model based on physics. The energy density is expressed by

$$\hat{W}(I_1) = c_1(I_1 - 3)$$

where  $c_1$  is a constant that depends on the material.

For small deformations, less than 150%, the Neo-Hookean model is considered to be practical [83].

**Mooney model:** The energy density of a material for a Mooney model is written in the following form [83, 19, 2]

$$\hat{W}(I_1, I_2) = c_1(I_1 - 3) + c_2(I_2 - 3)$$

where  $c_1$  and  $c_2$  are two constants that depend on the material. For moderate deformations, less than 250%, this model can be used [83].

**Ogden model:** This model was proposed by Ogden [91], the energy density of this model depends on the principal stretches  $\lambda_1, \lambda_2, \lambda_3$ . The principal stretches are the eigenvalues square roots of the tensor  $\mathbf{C}$ . The energy density function is given by the following

$$\hat{W}(\lambda_1, \lambda_2, \lambda_3) = \sum_{i=1}^3 \frac{\mu_i}{\alpha_i} (\lambda_1^{\alpha_i} + \lambda_2^{\alpha_i} + \lambda_3^{\alpha_i} - 3)$$

where  $\{\alpha_i\}_{i=1,2,3}, \{\mu_i\}_{i=1,2,3}$  are 6 constants that depend on the material with  $\alpha_i \mu_i > 0 \forall i = 1, 2, 3$ . The difficulty of this model lies in the determination of these 6 material constants.

### Compressible hyperelastic materials

**Neo-Hookean model:** An example of an energy density function for this model is the following [29]

$$\hat{W}(I_1, I_2, I_3) = aI_1 + cJ^2 - d \ln(J)$$

where  $a, c, d > 0$  are constants.

**Mooney-Rivlin model:** An example of an energy density function for this model is the following [29]

$$\hat{W}(I_1, I_2, I_3) = aI_1 + bI_2 + cJ^2 - d \ln(J)$$

where  $a, b, c, d > 0$  are constants.

**Saint Venant-Kirchhoff model:** The Saint Venant-Kirchhoff model is also a simple model, however it must be used in the context of small deformations. Its energy density function depends directly on the Green-Lagrange tensor  $\mathbf{E}$  by the following formula [17, 29]

$$\hat{W}(\mathbf{E}) = \frac{\lambda}{2} (\text{Tr}(\mathbf{E}))^2 + \mu (\text{Tr}(\mathbf{E}^2))$$

where  $\lambda$  and  $\mu$  are the Lamé coefficients of the material.

### Nearly incompressible hyperelastic materials

The incompressible models like Mooney and Neo-Hookean can cause numerical problems, that is why the nearly incompressible models are introduced. These last models will be applicable for the incompressible materials and also can be valid for the compressible cases according to the bulk modulus  $\kappa$ . The energy density function is thus modified [2, 17, 19, 62] and it will be expressed in the following form

$$\hat{W} = \hat{W}_{inc}(\bar{I}_1, \bar{I}_2, \bar{I}_3) + \hat{W}_{VOL}$$

$\hat{W}_{inc}$  represents the energy density function of the incompressible model (Neo-Hookean or Mooney) with  $J = 1$ ,  $\hat{W}_{VOL}$  a volumetric function that depends on  $J$ . Otherwise  $\bar{I}_1, \bar{I}_2, \bar{I}_3$  are the invariants of the tensor  $\mathbf{C}' = J^{-\frac{2}{3}}\mathbf{C}$ , and are equal to

$$\begin{cases} \bar{I}_1 = J^{-\frac{2}{3}} I_1 \\ \bar{I}_2 = J^{-\frac{4}{3}} I_2 \\ \bar{I}_3 = 1 \end{cases} \quad (1.20)$$

Here are some formulas [19] for the volumetric function  $\hat{W}_{VOL}$

$$\hat{W}_{VOL}(J) = \begin{cases} \frac{\kappa}{2}(J-1)^2 \\ \frac{\kappa}{2}(\ln J)^2 \\ \kappa(J-1-\ln J) \end{cases} \quad (1.21)$$

When the bulk modulus  $\kappa$  has a high value, the nearly compressible model will represent the incompressible one. Indeed the bulk modulus can be seen as a penalty parameter, which penalizes the region where the incompressibility condition  $J = 1$  is not satisfied.

### Linear elastic materials

In the case of small deformations, the actual configuration is approximately equal to the initial configuration,  $\Omega \approx \phi(\Omega)$ . In this case the energy density function is equal to

$$\hat{W}(\boldsymbol{\epsilon}) = \frac{1}{2} \boldsymbol{\sigma} : \boldsymbol{\epsilon} = \frac{1}{2} \text{Tr}(\boldsymbol{\sigma}^T \boldsymbol{\epsilon}) \quad (1.22)$$

in addition to Hook's law

$$\boldsymbol{\sigma} = \lambda \text{Tr}(\boldsymbol{\epsilon}) \mathbf{I} + 2\mu \boldsymbol{\epsilon} \quad (1.23)$$

where  $\mathbf{I}$  is the identity matrix.

### Equivalence to a minimization problem

The displacement field  $\mathbf{u}$ , solution of the equation (1.16), minimizes the total potential energy  $\mathcal{E}$  over all of the admissible displacements. The total potential energy is defined by

$$\mathcal{E}(\mathbf{v}) = \int_{\Omega} \hat{W} dV - \int_{\Omega} \rho_0 \mathbf{f} \cdot \mathbf{v} dV - \int_{\Gamma_1} \mathbf{t} \cdot \mathbf{v} dA \quad (1.24)$$

Therefore

$$\mathbf{u} = \arg \min_{\mathbf{v} \in \mathcal{A}} (\mathcal{E}(\mathbf{v})) \quad (1.25)$$

where  $\mathcal{A}$  the admissible displacements set, defined by the equation (1.15). Note that the weak formulation (1.16) presented above can be obtained from the minimization problem (1.25), indeed it can be done by setting the Fréchet derivative of the energy  $\mathcal{E}$  to be equal to zero, and obtaining the Euler-Lagrange equation:

$$D\mathcal{E}(u)(v) = 0 \quad \forall v \in \mathcal{A} \quad (1.26)$$

## 1.2 Contact Theory

### 1.2.1 Signorini's contact problem

Signorini's contact problem is the contact between a deformable body and a rigid foundation (or obstacle) [106]. First of all, we suppose that we are in the case of small deformations, and we consider an elastic deformable body  $\Omega \subset \mathbb{R}^n$  with  $n = 2$  or  $n = 3$  with Lipschitz boundary, which will make contact with a rigid foundation  $S$ .

In the following  $\Gamma_1 \subset \partial\Omega$  represents the part where an external pressure  $\mathbf{t}_f$  is applied on the body  $\Omega$ ,  $\Gamma_0 \subset \partial\Omega$  represents the part where a null displacement is imposed on the body. Finally  $\Gamma_C \subset \partial\Omega$  is the potential contact area, otherwise speaking if  $\gamma_C = \phi(\Gamma_C)$  is  $\Gamma_C$  in the actual configuration, then the actual contact area is included in  $\gamma_C$ .

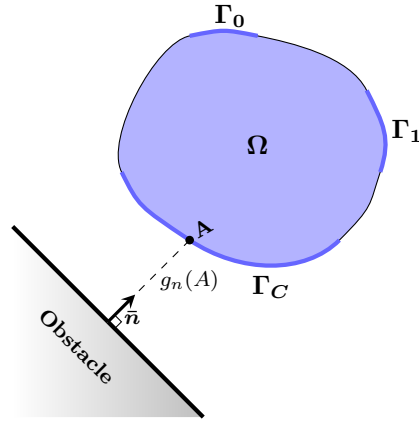


Figure 1.3 – The body, the obstacle and the normal gap at a point  $A \in \Gamma_C$

Under the assumption of small deformations, where there is no difference between the reference and the actual configuration, Signorini's problem is to find the displacement field  $\mathbf{u}$  such that the following equations and inequalities are valid.

$$\begin{cases} \nabla \cdot \boldsymbol{\sigma} + \mathbf{f} = 0 & \text{in } \Omega \\ \sigma_{ij}(\mathbf{x}) = E_{ijkl} \frac{\partial u_k}{\partial x_l} & \text{in } \Omega \quad (\text{Hook's law}) \\ \mathbf{u} = \mathbf{0} & \text{on } \Gamma_0 \\ \boldsymbol{\sigma} \mathbf{n} = \mathbf{t}_f & \text{on } \Gamma_1 \\ \boldsymbol{\sigma}_T = \mathbf{0} & \text{on } \Gamma_C \quad (\text{No friction}) \end{cases} \quad (1.27)$$

with the following contact conditions:

$$\begin{cases} (\mathbf{u} \cdot \bar{\mathbf{n}} + g_n) \sigma_n = 0 & \text{on } \Gamma_C \\ \mathbf{u} \cdot \bar{\mathbf{n}} + g_n \geq 0 & \text{on } \Gamma_C \\ \sigma_n \leq 0 & \text{on } \Gamma_C \end{cases} \quad (1.28)$$

where  $\mathbf{f}$  is a body force applied on the body. The second equation of (1.27) is another expression of the Hook's law where a summation on the 2 indexes  $k, l$  is considered and  $E_{ijkl} \in L^\infty(\Omega)$  are the components of the Hook tensor with the following symmetry conditions:  $E_{ijkl} = E_{jikl} = E_{klij}$  and  $\exists m > 0$   $E_{ijkl}\epsilon_{ij}\epsilon_{kl} \geq m\epsilon_{ij}\epsilon_{ij} \forall \epsilon \in \mathbb{R}^{n \times n}$  where  $\epsilon_{ij} = \epsilon_{ji}$ . In addition  $\boldsymbol{\sigma}_T$  represents the tangential component of the stress vector  $\boldsymbol{\sigma}\mathbf{n}$ , indeed  $\boldsymbol{\sigma}\mathbf{n} = \sigma_n\mathbf{n} + \boldsymbol{\sigma}_T$  where  $\mathbf{n}$  is the outward unit normal vector at the body  $\Omega$ . Finally  $g_n$  is the normal gap between the foundation  $S$  and the potential contact area  $\Gamma_C$ , see Figure 1.3, and  $\bar{\mathbf{n}}$  is the outward unit normal vector at the obstacle.

Note also that we can use  $-\mathbf{n}$  instead of  $\bar{\mathbf{n}}$  in the formulation (1.28). In addition at the real contact area we have  $\bar{\mathbf{n}} = -\mathbf{n}$ .

In order to reformulate the problem into a weak form and to prove the existence and the uniqueness for a solution of the Signorini's problem, some functional spaces must be defined.

By imposing a null displacement on  $\Gamma_0$ , the admissible set is defined as follows

$$\mathbf{V} = \{\mathbf{v} \in \mathbf{H}^1(\Omega) \mid \mathbf{v} = 0 \text{ a.e on } \Gamma_0\} \quad (1.29)$$

where  $\mathbf{H}^1(\Omega) = H^1(\Omega) \times H^1(\Omega)$ , endowed with the broken norm:

$$\|\mathbf{u}\|_1 = \|(u_1, u_2)\|_1 = (\|u_1\|_1^2 + \|u_2\|_1^2)^{\frac{1}{2}} \quad (1.30)$$

In addition,  $H^1(\Omega)$  denotes the Sobolev space endowed with its own norm  $\|\cdot\|_1$ , in other words if  $u \in H^1(\Omega)$  then

$$\|u\|_1 = \left( \int_{\Omega} u^2 dx + \int_{\Omega} \|\nabla u\|^2 dx \right)^{1/2} \quad (1.31)$$

More details about the functional spaces and the functional analysis can be found in [6, 20].

Let the symmetric continuous bilinear form  $a : \mathbf{V} \times \mathbf{V} \rightarrow \mathbb{R}$  and the continuous linear form  $f : \mathbf{V} \rightarrow \mathbb{R}$  be defined by

$$a(\mathbf{u}, \mathbf{v}) = \int_{\Omega} \boldsymbol{\sigma}(\mathbf{u}) : \boldsymbol{\epsilon}(\mathbf{v}) dx = \int_{\Omega} E_{ijkl} u_{k,l} v_{i,j} dx \quad \forall (\mathbf{u}, \mathbf{v}) \in \mathbf{V} \times \mathbf{V} \quad (1.32)$$

$$f(\mathbf{v}) = \int_{\Omega} \mathbf{f} \cdot \mathbf{v} dx + \int_{\Gamma_1} \mathbf{t}_f \cdot \mathbf{v} ds \quad \forall \mathbf{v} \in \mathbf{V} \quad (1.33)$$

In general the solution (the displacement field) of the contact problem involving a linear elastic body can be written as the following variational inequality.

Find  $\mathbf{u} \in \mathbf{K}$  such that:

$$a(\mathbf{u}, \mathbf{v} - \mathbf{u}) \geq f(\mathbf{v} - \mathbf{u}) \quad \forall \mathbf{v} \in \mathbf{K} \quad (1.34)$$

where  $\mathbf{K} = \{\mathbf{v} \in \mathbf{V} \mid \mathbf{v} \cdot \bar{\mathbf{n}} + g_n \geq 0 \text{ a.e on } \Gamma_C\}$ , the set where the displacement field satisfies the non-penetration condition for the Signorini's problem. The applications  $a(\cdot, \cdot)$  and  $f(\cdot)$  have the following properties.

$a(\cdot, \cdot) : \mathbf{V} \times \mathbf{V} \rightarrow \mathbb{R}$  is a continuous bilinear application, and it is elliptic.

$f(\cdot) : \mathbf{V} \rightarrow \mathbb{R}$  is a linear continuous application.  $f \in \mathbf{V}'$ , the dual of  $\mathbf{V}$ .

The subset  $\mathbf{K}$  is a nonempty closed convex subset of  $\mathbf{V}$ , therefore using Stampacchia's theorem, there exists a unique solution of the problem (1.34).

Otherwise, let the functional  $\mathcal{E} : \mathbf{V} \rightarrow \mathbb{R}$  denotes the potential energy of the problem and let it be defined by

$$\mathcal{E}(\mathbf{v}) = \frac{1}{2}a(\mathbf{v}, \mathbf{v}) - f(\mathbf{v}) \quad \forall \mathbf{v} \in \mathbf{V} \quad (1.35)$$

The problem (1.34) is equivalent to the following minimization problem.

Find  $\mathbf{u} \in \mathbf{K}$  such that:

$$\mathbf{u} = \arg \min_{\mathbf{v} \in \mathbf{K}} (\mathcal{E}(\mathbf{v})) \quad (1.36)$$

## 1.2.2 Contact in finite deformation

In this section we present several results about contact problems for hyperelastic materials, which can be found in [29]. Let  $\Omega$  be the body domain in  $\mathbb{R}^2$  or  $\mathbb{R}^3$  in its initial configuration. In addition, let the borders  $\Gamma_0, \Gamma_1, \Gamma_C$  be disjoint relatively to  $\partial\Omega$ , and  $\Gamma = \partial\Omega = \Gamma_0 \cup \Gamma_1 \cup \Gamma_C$ . The length of the border  $\Gamma_C$  is supposed to be strictly positive. Our unknown will be the actual position  $\phi$  instead of the displacement  $\mathbf{u}$ , which is not very different because  $\phi = \mathbf{X} + \mathbf{u}$ .  $\Gamma_0$  is the border where a displacement  $\phi_0$  is imposed,  $\Gamma_1$  is the border where a surface traction  $\mathbf{g}$  is applied, finally  $\Gamma_C$  is the potential contact area, otherwise speaking if  $\gamma_C = \phi(\Gamma_C)$  is  $\Gamma_C$  in the actual configuration, then the actual contact area is included in  $\gamma_C$ . In addition, a body force  $\mathbf{f}$  is applied over the body  $\Omega$ .

The obstacle or the rigid foundation is described by the open set  $\mathcal{C} \subset \mathbb{R}^2$  or  $\mathbb{R}^3$ , the strain energy function is denoted by  $\hat{W}$ , and the first Piola-Kirchhoff stress by  $\mathbf{P}$ . We have that  $\mathbf{P} = \frac{\partial \hat{W}}{\partial \mathbf{F}}$ , where  $\mathbf{F}$  is the deformation gradient tensor.

The admissible solutions set  $\Phi$  is defined by

$$\Phi = \{\psi : \bar{\Omega} \rightarrow \mathbb{R}^2; \det(\nabla\psi) > 0 \text{ in } \bar{\Omega}; \psi = \phi_0 \text{ on } \Gamma_0 \text{ with } \psi(\Gamma_C) \subseteq \mathcal{C}^c\} \quad (1.37)$$

where  $(\nabla\psi)_{ij} = (Grad\psi)_{ij} = \frac{\partial\psi_i}{\partial X_j}$ . The condition  $\psi(\Gamma_C) \subseteq \mathcal{C}^c$  (the complement of  $\mathcal{C}$ ) describes the non-penetration of the body into the obstacle. The actual position  $\phi = \mathbf{X} + \mathbf{u}$  satisfies the

following equations

$$\begin{cases} -\operatorname{div} \mathbf{P} = \mathbf{f} \text{ in } \Omega \\ \phi = \phi_0 \text{ on } \Gamma_0 \\ \mathbf{P}\mathbf{N} = \mathbf{g} \text{ on } \Gamma_1 \\ \phi(\Gamma_C) \subseteq \mathcal{C}^c \\ \mathbf{P}\mathbf{N} = \mathbf{0} \text{ if } \mathbf{X} \in \Gamma_C \text{ and } \phi(\mathbf{X}) \in \bar{\mathcal{C}}^c \quad (\notin \mathcal{C} \cup \partial\mathcal{C}) \\ (\mathbf{P}\mathbf{N}) \cdot \mathbf{n} = \lambda_n \text{ if } \mathbf{X} \in \Gamma_C \text{ and } \mathbf{x} = \phi(\mathbf{X}) \in \partial\mathcal{C} \text{ where } \lambda_n \leq 0 \\ \boldsymbol{\sigma}_T = 0 \text{ on } \phi(\Gamma_C) \cap \partial\mathcal{C} \end{cases} \quad (1.38)$$

where  $\boldsymbol{\sigma}_T$  is the tangential stress,  $\mathbf{N}$  and  $\mathbf{n}$  are respectively the unit outward normal vector on the initial and on the deformed surface of the body. Finally  $\boldsymbol{\sigma}$  is the Cauchy stress tensor and  $\boldsymbol{\sigma}\mathbf{n}$  has the same direction of  $\mathbf{P}\mathbf{N}$ .

Moreover, let the potential energy  $\mathcal{E}$  of the body  $\Omega$  be given by

$$\mathcal{E}(\psi) = \int_{\Omega} \hat{W}(\nabla\psi) dx - \int_{\Omega} \mathbf{f} \cdot \psi dx - \int_{\Gamma_1} \mathbf{g} \cdot \psi ds \quad (1.39)$$

and consider the following minimization problem

Find the displacement  $\phi \in \Phi$  such that:

$$\mathcal{E}(\phi) \leq \mathcal{E}(\psi) \quad \forall \psi \in \Phi \quad (1.40)$$

If the solution  $\phi$  of the minimization problem (1.40) is smooth enough, then it's a solution of the problem (1.38).

In the following  $\mathbb{M}^3$  is the set of all real square matrices of order 3,  $\mathbf{Cof} \mathbf{F}$  is the cofactor of the matrix  $\mathbf{F}$  and  $\mathbb{M}_+^3$  is the following set

$$\mathbb{M}_+^3 = \{\mathbf{F} \in \mathbb{M}^3 ; \det(\mathbf{F}) > 0\}$$

Let the matrix  $\mathbf{F}$  and the invariants  $I_1, I_2, I_3$  be defined as before, we have  $\mathbf{F} \in \mathbb{M}_+^3$  and the following equalities

$$\begin{cases} \|\mathbf{F}\|^2 = \operatorname{Tr}(\mathbf{F}^T \mathbf{F}) = I_1 \\ \|\mathbf{Cof} \mathbf{F}\|^2 = \operatorname{Tr}(\mathbf{Cof} \mathbf{F}^T \mathbf{F}) = I_2 \\ \det(\mathbf{F}) = I_3^{1/2} \end{cases} \quad (1.41)$$

where  $\|\cdot\|$  denotes the norm in  $\mathbb{M}^3$ .

The strain energy function  $\hat{W}$  of a given material can be written as a function of the variable  $\mathbf{F}$  as follows

$$\hat{W}(\mathbf{F}) = \mathbb{W}(\mathbf{F}, \mathbf{Cof} \mathbf{F}, \det(\mathbf{F})) \quad (1.42)$$

where  $\mathbb{W}$  is a function defined by

$$\mathbb{W} : \mathbb{M}^3 \times \mathbb{M}^3 \times ]0, +\infty[ \rightarrow \mathbb{R}$$

The existence of a solution in finite deformation for the frictionless contact problem is shown in [29, 69], and in [36] for two bodies in contact. Polyconvexity, coerciveness inequality and the behaviour properties of  $\hat{W}$  and the assumption  $\inf_{\psi \in \Phi} (\mathcal{E}(\psi)) < +\infty$  are considered for the proof of the solution existence. These properties are defined as follows

Polyconvexity: If there exist a convex function  $\mathbb{W}$  on  $\mathbb{M}^3 \times \mathbb{M}^3 \times ]0, +\infty[$  such that the equation (1.42) is valid, the strain energy function  $\hat{W}$  is said to be polyconvex.

In the next theorem we give an example of a polyconvex family of strain energy functions, which can be found in [29].

**Theorem 1.1.** *The strain energy function  $\hat{W} : \mathbb{M}_+^3 \rightarrow \mathbb{R}$  defined by*

$$\hat{W}(\mathbf{F}) = a\|\mathbf{F}\|^2 + b\|\mathbf{Cof}\mathbf{F}\|^2 + \Gamma(\det(\mathbf{F})) \quad (1.43)$$

*is polyconvex, where  $a > 0$ ,  $b > 0$  and finally  $\Gamma : ]0, +\infty[ \rightarrow \mathbb{R}$  is a convex function*

*Proof.* Indeed the function  $\hat{W}(\mathbf{F})$  can be written as

$$\hat{W}(\mathbf{F}) = \mathbb{W}(\mathbf{F}, \mathbf{Cof}\mathbf{F}, \det(\mathbf{F}))$$

where the function  $\mathbb{W} : \mathbb{M}^3 \times \mathbb{M}^3 \times ]0, +\infty[ \rightarrow \mathbb{R}$  is given by

$$\mathbb{W}(\mathbf{F}_1, \mathbf{F}_2, \gamma) = \mathbb{W}_1(\mathbf{F}_1) + \mathbb{W}_2(\mathbf{F}_2) + \mathbb{W}_3(\gamma)$$

The functions  $\mathbb{W}_1$ ,  $\mathbb{W}_2$  and  $\mathbb{W}_3$  are defined as follows

$$\begin{cases} \mathbb{W}_1(\mathbf{F}_1) = a\|\mathbf{F}_1\|^2 \\ \mathbb{W}_2(\mathbf{F}_2) = b\|\mathbf{F}_2\|^2 \\ \mathbb{W}_3(\gamma) = \Gamma(\gamma) \end{cases}$$

The functions  $\mathbb{W}_1$ ,  $\mathbb{W}_2$  and  $\mathbb{W}_3$  are convex, therefore we conclude that the function  $\mathbb{W}$  is convex and thus the strain energy function  $\hat{W}$  is polyconvex.  $\square$

Several strain energy functions can be found in [29]. The strain energy function of a Saint Venant-kirchhoff is not polyconvex, indeed it was proven in [99].

Coerciveness inequality: The strain energy function  $\hat{W}$  satisfies a coerciveness inequality if there exist constants  $\alpha, \beta, p, q, r$  such that:  $\alpha > 0$ ,  $p \geq 2$ ,  $q \geq \frac{p}{p-1}$ ,  $r > 1$  and

$$\hat{W}(\mathbf{F}) \geq \alpha(\|\mathbf{F}\|^p + \|\mathbf{Cof}\mathbf{F}\|^q + \det(\mathbf{F})^r) + \beta \quad \forall \mathbf{F} \in \mathbb{M}_+^3 \quad (1.44)$$

Behavior property: The strain energy function  $\hat{W}$  is supposed to have the following behavior

$$\lim_{\det(\mathbf{F}) \rightarrow 0^+} \hat{W}(\mathbf{F}) = +\infty \quad (1.45)$$

### 1.2.3 Contact between two elastic deformable bodies

In this section we briefly introduce the contact problem between two elastic bodies under the infinitesimal deformations assumption. As Signorini's problem, described above, the same approach can be used in order to prove the existence and the uniqueness for the displacement solution [16, 69]. Let these bodies be denoted by  $\Omega_1$  for the first and  $\Omega_2$  for the second. Like previously we will use the same notations, thus let  $\Omega = \Omega_1 \cup \Omega_2$ ,  $\partial\Omega = \partial\Omega_1 \cup \partial\Omega_2$ ,  $\Gamma_0 = \Gamma_0^1 \cup \Gamma_0^2 \subset \partial\Omega$  where a null displacement is imposed and  $\Gamma_1 = \Gamma_1^1 \cup \Gamma_1^2$  where a surface traction  $\mathbf{t} = (\mathbf{t}^1, \mathbf{t}^2)$  is imposed, the indexes 1 and 2 refer respectively for the body 1 and 2, in addition, a body force  $\mathbf{f} = (\mathbf{f}^1, \mathbf{f}^2)$  is applied over the body  $\Omega$ . Let  $\Gamma_{C1}$  and  $\Gamma_{C2}$  be respectively the potential contact surfaces of the first body  $\Gamma_{C1} \subset \partial\Omega_1$  and of the second body  $\Gamma_{C2} \subset \partial\Omega_2$ , see Figure 1.4, otherwise speaking if  $\phi = (\phi_1, \phi_2)$  denotes the transformation mapping which transforms the two bodies from their initial configurations to their actual ones, then the actual contact area is included in  $\phi_1(\Gamma_{C1}) \cap \phi_2(\Gamma_{C2})$ .

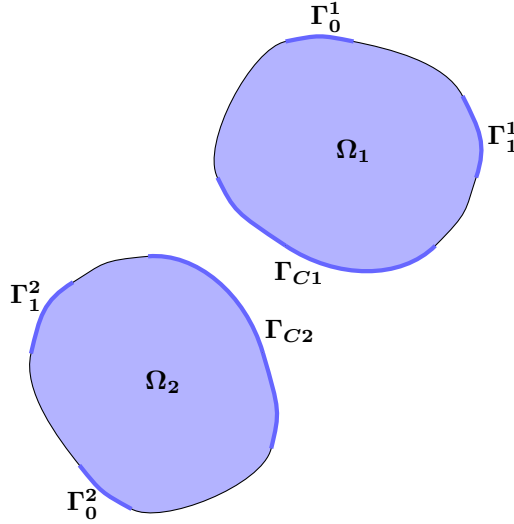


Figure 1.4 – The two bodies with the corresponding boundaries

We suppose that there exists a map  $\chi : \Gamma_{C1} \rightarrow \Gamma_{C2}$ , which maps any  $\mathbf{X}_1 \in \Gamma_{C1}$  to  $\chi(\mathbf{X}_1) \in \Gamma_{C2}$ , the closest point to  $\mathbf{X}_1$  on  $\Gamma_{C2}$ . We call  $g_n : \Gamma_{C1} \rightarrow \mathbb{R}$  the gap function which is equal to the distance between the two bodies in the normal direction at the initial configurations, otherwise speaking  $\forall \mathbf{X}_1 \in \Gamma_{C1}$  then  $g_n(\mathbf{X}_1) = (\mathbf{X}_1 - \chi(\mathbf{X}_1)) \cdot \bar{\mathbf{n}}$ , where  $\bar{\mathbf{n}}$  is the outward unit normal vector on  $\Gamma_{C2}$  at  $\chi(\mathbf{X}_1)$ .

The equations describing the contact between two deformable bodies are like the Signorini's problem equations, with a slightly difference in the contact conditions. The problem is described

as follows

$$\begin{cases} \nabla \cdot \boldsymbol{\sigma} + \mathbf{f} = 0 & \text{in } \Omega \\ \sigma_{ij}(\mathbf{x}) = E_{ijkl} \frac{\partial u_k}{\partial x_l} & \text{in } \Omega \quad (\text{Hook's law}) \\ \mathbf{u} = \mathbf{0} & \text{on } \Gamma_0 \\ \boldsymbol{\sigma} \mathbf{n} = \mathbf{t} & \text{on } \Gamma_1 \\ \boldsymbol{\sigma}_T = \mathbf{0} & \text{on } \Gamma_{C1} \cup \Gamma_{C2} \end{cases} \quad (1.46)$$

with the following contact conditions

$$\begin{cases} \sigma_n := (\boldsymbol{\sigma}_1 \mathbf{n}) \cdot \mathbf{n} = ((\boldsymbol{\sigma}_2 \circ \chi) \bar{\mathbf{n}}) \cdot \bar{\mathbf{n}} \leq 0 & \text{on } \Gamma_{C1} \\ ((\mathbf{u}_1 - \mathbf{u}_2 \circ \chi) \cdot \bar{\mathbf{n}} + g_n) \sigma_n = 0 & \text{on } \Gamma_{C1} \\ (\mathbf{u}_1 - \mathbf{u}_2 \circ \chi) \cdot \bar{\mathbf{n}} + g_n \geq 0 & \text{on } \Gamma_{C1} \end{cases} \quad (1.47)$$

where  $\mathbf{u}_1, \mathbf{u}_2$  denote respectively the displacement in the bodies  $\Omega_1$  and  $\Omega_2$ , indeed  $\mathbf{u} = (\mathbf{u}^1, \mathbf{u}^2)$  represents the displacement fields in the two bodies, the vector  $\mathbf{n}$  denotes the outward unit normal vector on  $\partial\Omega_1$  and  $\boldsymbol{\sigma}_1$  and  $\boldsymbol{\sigma}_2$  represent the Cauchy stress tensor in the first and the second body respectively.

We have selected the potential contact area  $\Gamma_{C1}$  of the first body in order to write the non-penetration conditions (equation (1.47)) with respect to it, by doing so, the first body is called the slave body and the second one is called the master one. If the finite element approach is used then the solution depends on the choice between the slave and the master bodies. One should note that there exist several approaches to describe the non-penetration conditions.

Otherwise, we define the admissible set  $\mathbf{V} = \mathbf{V}^1 \times \mathbf{V}^2$  where

$$\mathbf{V}^l = \{\mathbf{v} \in \mathbf{H}^1(\Omega_l) \mid \mathbf{v} = 0 \text{ a.e on } \Gamma_0^l\} \quad (1.48)$$

endowed with the broken norm

$$\|\mathbf{u}\|_1 = \|(\mathbf{u}_1, \mathbf{u}_2)\|_1 = (\|\mathbf{u}_1\|_1^2 + \|\mathbf{u}_2\|_1^2)^{\frac{1}{2}} \quad (1.49)$$

The contact problem in this case can be written as the following variational inequality

$$a(\mathbf{u}, \mathbf{v} - \mathbf{u}) \geq f(\mathbf{v} - \mathbf{u}) \quad \forall \mathbf{v} \in \mathbf{K} \quad (1.50)$$

where  $\mathbf{K} = \{\mathbf{v} \in \mathbf{V} \mid (\mathbf{u}_1 - \mathbf{u}_2 \circ \chi) \cdot \bar{\mathbf{n}} + g_n \geq 0 \text{ a.e on } \Gamma_{C1}\}$  the set of the admissible displacement fields, where the non-penetration condition is satisfied, in addition the applications  $a : \mathbf{V} \times \mathbf{V} \rightarrow \mathbb{R}$  and  $f : \mathbf{V} \rightarrow \mathbb{R}$  are defined as follows

$$\begin{cases} a(\mathbf{u}, \mathbf{v}) = a^1(\mathbf{u}, \mathbf{v}) + a^2(\mathbf{u}, \mathbf{v}) \\ f(\mathbf{v}) = f^1(\mathbf{v}) + f^2(\mathbf{v}) \end{cases} \quad (1.51)$$

where for  $l = 1, 2$

$$\begin{cases} a^l(\mathbf{u}, \mathbf{v}) = \int_{\Omega_l} \boldsymbol{\sigma}(\mathbf{u}^l) : \boldsymbol{\epsilon}(\mathbf{v}^l) dv \\ f^l(\mathbf{v}) = \int_{\Omega_l} \mathbf{f}^l \cdot \mathbf{v}^l dv + \int_{\Gamma_1^l} \mathbf{t}^l \cdot \mathbf{v}^l ds \end{cases} \quad (1.52)$$

Moreover, the contact problem can be written, equivalently, as the following minimization prob-

lem

$$\min_{\mathbf{v} \in \mathbf{K}} \frac{1}{2} a(\mathbf{v}, \mathbf{v}) - f(\mathbf{v}) \quad (1.53)$$

### 1.2.4 Friction in contact problems

The contact problems with friction were studied in many papers, for example in [41] the existence of solutions for elastic static contact problems with a small coefficient of friction was proved in the case of Coulomb's friction, where a penalty method was used. In the paper [32] existence of solutions for static Signorini's problem with Coulomb friction was proved where the normal component of the stress was replaced by a regularized one, in addition the uniqueness of the solution was proved for a small friction coefficient. In the chapter 3 of [40] several studies for elastic frictional problems were done in addition to the formulation into a variational inequality for the Signorini's problem with Coulomb's friction. In the case of small friction coefficient and of certain hypothesis on the tangential displacement, the uniqueness of the solution was proved in [103].

In the case of Signorini's problem, let  $\Gamma_C$  denotes the contact surface. The Coulomb's friction law is added to the problem described in the previous sections, indeed the tangential component of the stress  $\boldsymbol{\sigma}_T$  is no longer equal to zero, moreover there exists a relation between the tangential displacement  $\mathbf{u}_T$  and  $\boldsymbol{\sigma}_T$  on  $\Gamma_C$  as follows

$$\|\boldsymbol{\sigma}_T(\mathbf{u})\| \leq \mu(x) |\sigma_n(\mathbf{u})| \quad (1.54)$$

and

$$\begin{cases} \text{If } \|\boldsymbol{\sigma}_T(\mathbf{u})\| < \mu(x) |\sigma_n(\mathbf{u})| \Rightarrow \mathbf{u}_T = \mathbf{0} \text{ on } \Gamma_C \\ \text{If } \|\boldsymbol{\sigma}_T(\mathbf{u})\| = \mu(x) |\sigma_n(\mathbf{u})| \Rightarrow \exists \lambda \geq 0, \mathbf{u}_T = -\lambda \boldsymbol{\sigma}_T \text{ on } \Gamma_C \end{cases} \quad (1.55)$$

where  $\mu$  is the Coulomb's coefficient, hence a bounded and a measurable function defined on  $\Gamma_C$  where there exists  $\mu_0 > 0$  such that  $\mu \geq \mu_0$ .

In the dynamic case the Coulomb's friction law is the following (see also Figure 1.5)

$$\|\boldsymbol{\sigma}_T(\mathbf{u})\| \leq \mu(x) |\sigma_n(\mathbf{u})| \quad (1.56)$$

and

$$\begin{cases} \text{If } \|\boldsymbol{\sigma}_T(\mathbf{u})\| < \mu(x) |\sigma_n(\mathbf{u})| \Rightarrow \dot{\mathbf{u}}_T = \mathbf{0} \text{ on } \Gamma_C \\ \text{If } \|\boldsymbol{\sigma}_T(\mathbf{u})\| = \mu(x) |\sigma_n(\mathbf{u})| \Rightarrow \exists \lambda \geq 0, \dot{\mathbf{u}}_T = -\lambda \boldsymbol{\sigma}_T \text{ on } \Gamma_C \end{cases} \quad (1.57)$$

where the notations were taken as before.

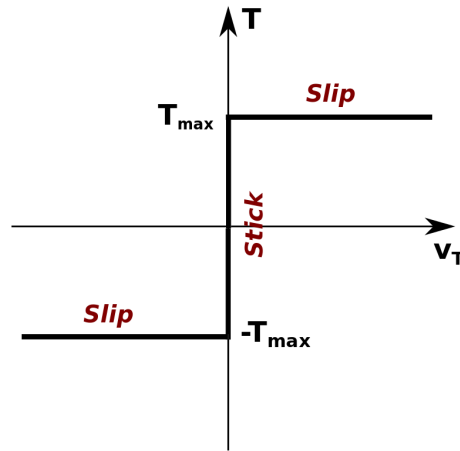


Figure 1.5 – Coulomb's friction law, where  $\mathbf{T} = \boldsymbol{\sigma}_T$ ,  $\mathbf{v}_T = -\dot{\mathbf{u}}_T$  and  $T_{max} = \mu|\sigma_n|$

The Coulomb's friction law says that on the contact area if the tangential stress norm  $\|\boldsymbol{\sigma}_T\|$  is equal to the normal stress norm multiplied by the Coulomb's coefficient  $\mu|\sigma_n|$ , then the body slips on its support, otherwise it sticks to its support.

Generally there is no uniqueness of the solution for a frictional contact problem, for example in [57] there is a simple example where it proposes 2 displacement fields in a triangular domain for a frictional Signorini's problem, the 2 displacement fields are solutions of the problem for a large friction coefficient.

We will talk more deeply about the friction problems in the chapter 6.

### 1.3 Contact numerical methods

As was stated before, different methods can be used to solve a contact problem such as the penalty method, the Lagrangian multiplier method, and the augmented Lagrangian method.

In [122], the penalty method was considered for a contact between a hyperelastic material and a rigid obstacle. The surface of the rigid obstacle was described by a  $C^2$  function that can be given analytically or by a cubic spline function. Mixed formulations are used for example in [56, 64], where the unknowns are the displacement field and the contact pressure, in [60] a stabilization method is used and the stabilization parameter is supposed to be small enough. A linear elasticity law is used to model the material and an Active-Set Strategy was used in [64] in order to find the contact zone. In [95], an algorithm for contact problems involving fluid-structure interactions is presented and uses the semi-smooth Newton method. Several methods can be found in [125] such as the Partial Dirichlet-Neumann method for the contact between a

body and a rigid foundation. Otherwise the interior point method or the barrier method were not widely used in contact problems, we can cite for example [71, 74, 88, 112, 116].

In Code\_Aster [3] Projected Conjugate Gradient method (see [113]) and the active-set method (see [39]) are used in the case of frictionless contact problems and the penalty method in the case of frictional contact problems. In [73] a Dirichlet-Neumann algorithm is presented to solve frictionless and frictional contact problems between two elastic bodies, using the mortar method for the contact discretization. The algorithm consists to solve and decompose in each iteration the two elastic bodies contact into a Neumann's problem and a Signorini's problem.

There exist many methods for the resolution of the contact problems, it can be found in the monographs [69, 123] or in [37]. In the following we will present some of these methods.

As we saw the contact problem is equivalent to a minimization problem in the case of frictionless contact, and can be equivalent to a sequence of a minimization problems in the case of frictional contact. Expressing the contact problem in a minimization form and solve it with optimization methods can be a robust way to solve it, indeed we can use several optimization techniques (for example line search method) in order to converge faster to the solution which is a minimum.

Inequality constraints occur in the contact problem, however in the following we will present some methods in order to solve minimization problems with equality constraints, indeed they can be useful to treat the minimization problem with inequality constraints as we will see in the section 1.3.1, especially when the active-set method is used.

Consider the following problem with equality constraints

$$\begin{cases} \min_{x \in \mathbb{R}^n} E(x) \text{ such that} \\ c_i(x) = 0 \quad \forall i = 1, \dots, m \end{cases} \quad (1.58)$$

where  $E$  is an energy and  $c_i$  are the constraints to satisfy. We have some famous methods to solve this problem, as follows

### Penalty method

The goal of the penalty method, is to transform the constrained optimization problem into an unconstrained one, by penalizing the domain where the constraints are not satisfied.

The problem (1.58) is transformed into the following unconstrained problem

$$\min_{x \in \mathbb{R}^n} E(x) + \mu \sum_{i=1}^m c_i^2(x) \quad (1.59)$$

where  $\mu > 0$  is called the penalty parameter. Let  $x_\mu$  be the solution of the previous problem (1.59) for the penalty parameter  $\mu$ , then when  $\mu \rightarrow \infty$ ,  $x_\mu$  converges to the solution of the problem (1.58).

The drawback of this method is the numerical ill-conditioning when taking large value for the parameter  $\mu$ , and the small violation of the constraints when the penalty parameter is not large enough.

### Lagrange multiplier method

The Lagrange multiplier method is used also for the constrained optimization problems, by introducing the Lagrangian function  $L$ , which is defined by

$$L(x, \lambda) = E(x) + \sum_{i=1}^m \lambda_i c_i(x) \quad (1.60)$$

where  $\lambda = (\lambda_1, \dots, \lambda_m)$  is the Lagrange multiplier vector to be determined. Therefore the problem (1.58) can be solved via the following saddle point problem

$$\nabla_{(x, \lambda)} L(x, \lambda) = 0 \quad (1.61)$$

or equivalently

$$\begin{cases} \nabla E(x) + \sum_{i=1}^m \lambda_i \nabla c_i(x) = 0 \\ c_i(x) = 0 \quad \forall i = 1, \dots, m \end{cases} \quad (1.62)$$

A Newton's method can be used to solve the problem (1.62).

### Augmented Lagrangian method

The augmented Lagrangian method is an another optimization method for constrained problems, it's a combination between the penalty and the Lagrange multiplier method. For more details one can refer to [82, 86, 123].

The augmented Lagrangian function  $L_A$  is defined by:

$$L_A(x, \lambda, \mu) = E(x) - \sum_{i=1}^m \lambda_i c_i(x) + \frac{\mu}{2} \sum_{i=1}^m c_i(x)^2 \quad (1.63)$$

where  $\lambda_i$  are the Lagrange multipliers and  $\mu$  is the penalty parameter.

The classical algorithm [86] to solve the minimizing problem with equality constraints is briefly presented in the following box.

- 1- Initialization: Choose a penalty parameter  $\mu_0$  and a starting Lagrange multiplier vector  $\lambda^0$
- 2- Loop on  $k = 0, 1, \dots$ 
  - 3- Compute a minimizer  $x^k$  of the augmented Lagrangian function  $L_A(x, \lambda^k, \mu_k)$
  - 4- Update the Lagrange multiplier:  $\lambda_i^{k+1} = \lambda_i^k - \mu_k c_i(x^k) \forall i = 1, \dots, m$
  - 5- Update the penalty factor such that:  $\mu_{k+1} \geq \mu_k$
- 6- Stop the loop when convergence

The augmented Lagrangian method does not require for the penalty factor to be very large, which avoids the ill-conditioning. There exist also methods like the perturbed Lagrange formulation which introduces a new Lagrangian depending on a parameter, where we obtain the Lagrange multiplier method if this parameter is very small.

### 1.3.1 Inequality constrained problems

As we saw, the contact problem can be in general written in the form of a minimization problem, with inequality constraints. After using the finite element method, the contact problem can be expressed as follows

$$\begin{cases} \min_{x \in \mathbb{R}^n} E(x) \text{ such that} \\ c_i(x) \geq 0 \quad \forall i = 1, \dots, m \end{cases} \quad (1.64)$$

where  $x \in \mathbb{R}^n$  denotes the degrees of freedom due to the finite element method,  $E$  denotes the total potential energy and  $c_i$  are the  $m$  constraints which describe the non-penetration condition.

In order to deal with the inequality constraints, we will present two famous methods: the active-set method and the interior point method.

#### Active-set method

The active-set method is an iterative method which briefly consists in activating some constraints  $\{c_i, i \in W_k\}$ , where  $W_k$  denotes the indices set of the active constraints at the iteration  $k$ , and solving at the iteration  $k$  an equality-constrained problem as follows

$$\begin{cases} \min_{x \in \mathbb{R}^n} E(x) \text{ such that} \\ c_i(x) = 0 \quad \forall i \in W_k \end{cases} \quad (1.65)$$

The working set  $W_{k+1}$  is updated at the iteration  $k+1$  if some constraints are violated, or the corresponding Lagrange multipliers are negative. The process is repeated until convergence. For more details about the active-set method, see [86].

### Interior-point method

The interior-point method is another method to solve inequality-constrained problems. We will briefly describe it, indeed it is presented in more details in the following chapters. First of all, by introducing slack variables  $s = (s_1, \dots, s_m) \in \mathbb{R}^m$ , the interior point method transforms the problem (1.64) into the following

$$\begin{cases} \min_{x \in \mathbb{R}^n} E(x) \text{ such that} \\ c_i(x) - s_i = 0 \quad \forall i = 1, \dots, m \\ s_i \geq 0 \quad \forall i = 1, \dots, m \end{cases} \quad (1.66)$$

where the inequality constraints are transformed into equality ones and they are all active. Then the problem (1.66) is transformed into a barrier one, as follows

$$\begin{cases} \min_{(x,s) \in \mathbb{R}^n \times \mathbb{R}^m} E(x) - \mu \sum_{i=1}^m \ln(s_i) \text{ such that} \\ c_i(x) - s_i = 0 \quad \forall i = 1, \dots, m \end{cases} \quad (1.67)$$

where  $\mu$  is the barrier parameter. The problem is solved for a sequence of barrier parameters  $\mu$ , converging to zero, which will make the solution of the problem (1.67) converges to the solution of the problem (1.64). For more details, one can refer to [47, 86].

### The selected method

The active-set method requires more iterations than the interior-point one, but at each iteration it's faster than the interior-point one, because all constraints are active in the latter. For large problems, generally the interior-point method is faster than the active-set method [53, 86]. In addition the active-set method may have a problem of cycling (the working set  $W_k$  may repeat itself after some iterations) [86].

Otherwise, in the two methods we have a sequence of linear systems to solve, the matrix structure or sparsity of the linear system remains the same for the interior-point method, however it changes for the active-set method, because the active constraints change at each iteration, therefore linear solvers can benefit from the fixed structure of the matrix in the interior-point method.

Finally, for the reasons we have selected the interior-point method as the method to solve our contact problem, furthermore as we want our contact problem to be symmetric (see section 1.7), which generates a linear dependent constraints, the interior-point method, as we will see in the chapter 4, is well fitted for this kind of issue.

## 1.4 Discretization methods

Discretization methods are a way to describe the non-penetration between two bodies, when a contact occurs and when the finite element method is used.

### 1.4.1 Node-to-node

Consider two bodies initially in contact at a common interface, we say that we have a conforming meshes (see Figure 1.6), if the nodes of each meshes of the first and the second body coincide at the interface. Let  $n_C$  be the number of the common nodes at the contact interface, the non-penetration conditions in this case are given as follows

$$(\mathbf{u}_i^1 - \mathbf{u}_i^2) \cdot \mathbf{n} \geq 0 \quad \forall i = 1, \dots, n_C \quad (1.68)$$

where  $\mathbf{u}_i^1$  and  $\mathbf{u}_i^2$  are respectively the displacement of the common node  $i$  at the interface of the first and of the second body, and  $\mathbf{n}$  the outward unit normal vector on the second body.

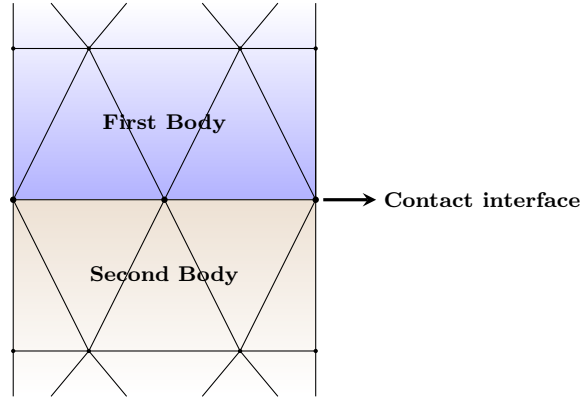


Figure 1.6 – Node to node discretization

This formulation is only efficient for small displacements and only for conforming meshes, which is not very practical in general. For this kind of formulation, one can cite [48].

### 1.4.2 Node-to-segment

In the case of non-conforming meshes, the node-to-segment discretization can be used [65]. The nodes of the slave body can not penetrate the segments of the master body. Let  $i$  be a node of the slave body, and  $s$  the closest segment of the master body to the node  $i$ , then the non-penetration conditions in this case can be given as follows

$$(\mathbf{x}_i - \bar{\mathbf{x}}_i) \cdot \mathbf{n} \geq 0 \quad \forall i = 1, \dots, n_C \quad (1.69)$$

where  $n_C$  is the number of slave nodes,  $\mathbf{x}_i$  the actual position of the node  $i$ ,  $\bar{\mathbf{x}}_i$  the projection of  $\mathbf{x}_i$  on the closest segment  $s$  (see Figure 1.7) and finally  $\mathbf{n}$  is the outward unit normal vector at  $\bar{\mathbf{x}}_i$ . Based on our experience, oscillations in the results can be observed.

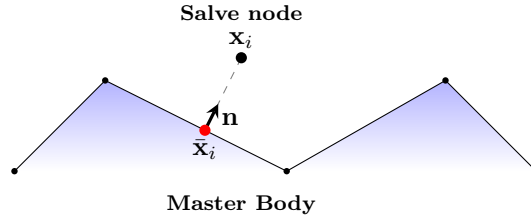


Figure 1.7 – Node to segment discretization

### 1.4.3 Quadrature-point-to-surface

In this discretization, the non-penetration conditions are done on the integration points, see [45, 46], otherwise speaking the integration points of each slave segment are forbidden to penetrate the master body.

### 1.4.4 Mortar method

In the case of a non matching meshes at the contact area between two bodies, the mortar method can be employed in order to define the contact conditions. The mortar method can be found in [15, 5, 59] in the case of the contact between two elastic bodies or in [96, 97, 118] for finite deformation.

Using the same notations as section 1.2.3 especially for the two applications  $a$  and  $f$ , in the case of linear elasticity, let  $[\mathbf{u} \cdot \mathbf{n}] = (\mathbf{u}_1 - \mathbf{u}_2) \cdot \mathbf{n}_1$  be the jump between the normal displacement of the two bodies at the contact area, where  $[\mathbf{u} \cdot \mathbf{n}] \leq 0$  describes the non-penetration between the two bodies with  $\mathbf{n}_1$  the outward unit normal vector at the contact area  $\Gamma_C$  of the first body. Therefore a saddle-point formulation (or a mixed formulation) can be used in order to describe the contact problem, as follows

Find  $\mathbf{u}_h \in \mathbf{V}_h$  and  $\lambda_h \in M_h$ , such that

$$\begin{cases} a(\mathbf{u}_h, \mathbf{v}_h) - \int_{\Gamma_C} \lambda_h [\mathbf{v}_h \cdot \mathbf{n}] ds = f(\mathbf{v}_h) & \forall \mathbf{v}_h \in \mathbf{V}_h \\ \int_{\Gamma_C} (\mu_h - \lambda_h) [\mathbf{v}_h \cdot \mathbf{n}] ds \geq 0 & \forall \mu_h \in M_h \end{cases} \quad (1.70)$$

where  $\mathbf{V}_h$  is the admissible displacement set, and  $M_h$  is the Lagrange multiplier space which can be generated from a nodal basis functions, or from a dual basis functions, see [121].

If  $(\mathbf{u}_h^*, \lambda_h^*)$  is a solution of the problem (1.70), then  $\mathbf{u}_h^*$  is the solution of the following varia-

tional inequality

Find  $\mathbf{u}_h \in \mathbf{V}_h$ , such that

$$a(\mathbf{u}_h, \mathbf{v}_h - \mathbf{u}_h) - f(\mathbf{v}_h - \mathbf{u}_h) \geq 0 \quad \forall \mathbf{v}_h \in \mathbf{K}_h \quad (1.71)$$

where  $\mathbf{K}_h = \left\{ \mathbf{v}_h \in \mathbf{V}_h \mid \int_{\Gamma_C} [\mathbf{v}_h \cdot \mathbf{n}] \phi \, ds \geq 0 \quad \forall \phi \in M_h \right\}$ .

In an equivalent manner,  $\mathbf{u}_h^*$  is a solution of the following minimization problem

Find  $\mathbf{u}_h \in \mathbf{V}_h$ , such that

$$\mathbf{u}_h = \arg \min_{\mathbf{v}_h \in \mathbf{K}_h} \left( E_h := \frac{1}{2} a(\mathbf{v}_h, \mathbf{v}_h) - f(\mathbf{v}_h) \right) \quad (1.72)$$

The constraints in this formulation are done in a weak sense, thus smoother results can be generated. In addition, when  $h \rightarrow 0$ , the Lagrange multiplier  $\lambda_h^*$  converges to the contact normal pressure  $\sigma_n$ .

Recently in [38] and in the case of contact between two elastic bodies, we can find the use of a local non-penetration condition, for example in the finite element method the set of the admissible displacement satisfying the non-penetration condition  $\mathbf{K}_h$  is given by

$$\mathbf{K}_h = \left\{ \mathbf{v}^h \in \mathbf{V}_h \text{ such that } \int_{I_m} [v_N^h] \, d\Gamma \leq 0 \quad \forall I_m \in I_M \right\} \quad (1.73)$$

where  $\mathbf{V}_h$  is the admissible displacement,  $[v_N^h] = v_{1N}^h + v_{2N}^h$  the jump between the normal displacement of the two bodies, where there is no initial gap.  $I_m, I_M$  are respectively the macro-segments and the macro-mesh, for more details see [38].

### 1.4.5 Smoothing techniques

Isogeometric analysis is a spatial discretization method which can be used to study computational contact mechanics, indeed this method uses splines functions such NURBS or B-splines as function basis, therefore it provides smoothness for the geometry and for the solution. See [117] for the application in contact mechanics.

Another smoothing method was used in [23], without going into details, for each slave node a smoothed contact surface is created using the weighted least-squares methods. In addition two adjustment techniques can be found in this paper, one for the penalty factor based on the gap and the other for the limitation of the status changes number of the contact nodes at each load step.

A famous patch test about sliding of two rectangular elastic bodies can be found in [115], it helps to give an indication about the robustness of the method used for the contact treatment between two bodies.

### 1.4.6 Analytic contact detection

We can see in the paper [61] different methods for contact detection between rigid bodies, the shapes of the bodies are supposed to be arbitrary in a way to corresponds to the granular material shapes, in addition the bodies can have a superquadratic shape. Indeed the superquadratic curves in 2D are defined by the following equation

$$F(x, y) = 0 \quad (1.74)$$

where the function  $F(x, y)$  is defined as follows

$$F(x, y) = \left| \frac{x}{a} \right|^{e_1} + \left| \frac{y}{b} \right|^{e_2} - 1 \quad (1.75)$$

The powers  $e_1$  and  $e_2$  belong to  $]0, +\infty[$ , moreover  $a$  and  $b$  correspond to the length of the principal axes. For example if  $e_1 = e_2 = 2$  we obtain an ellipse, and if  $e_1 = e_2 = 20$  we obtain a shape close to a rectangle.

Suppose that a body  $\Omega_1$  is described by a superquadratic curve  $F(x, y) = 0$ , and suppose that  $P = (X_2, Y_2)$  is a point belonging to the second body  $\Omega_2$ , then  $P$  penetrates the first body  $\Omega_1$  if  $F(X_2, Y_2) < 0$ , and is outside of it if  $F(X_2, Y_2) > 0$ . Finally if  $F(X_2, Y_2) = 0$  then the point  $P$  is on the boundary of  $\Omega_1$ .

## 1.5 Frictional contact algorithms

In [81] and in the case of linear elastic material, the Coulomb frictional contact problem is transformed into a sequence of Tresca frictional contact problems. Indeed the problem is transformed into a fixed point method where at each iteration a minimization problem over a convex set is solved.

The bi-potential method was used for frictional dynamic problem in [42, 43], indeed the contact forces are computed by a process of prediction and correction by a projection on the Coulomb cone. Then the contact forces are considered as an external loading. In these papers a first order time-stepping scheme was used for the dynamic problem.

A penalty formulation based on the integration points was considered in [46], to solve frictional contact problems. The numerical integration in [46] was done on the non-mortar segments (or the slave contact segments), with a fixed integration points on the non-mortar segment, and not on the overlapping regions between mortar and non-mortar areas, so the computational effort is reduced.

In [21, 90, 89] the elastic problems were considered, where a non-classical friction law was used in [90, 89], the idea was to fix the normal pressure at each iteration and update it for the next iteration.

Moreover we can cite another famous method to solve frictional contact problems, the return mapping method.

## Return mapping method

The returning mapping method is a method used for the frictional contact problems, this method was already been used in plasticity problems (see [34, 35]), where as the yield surface in plasticity problems, a surface which is dependent on the normal and on the tangential stress is created (see [52]).

Coulomb's friction law can be reformulated using the Kuhn-Tucker constraint conditions for friction as follows

$$\begin{cases} \zeta(\boldsymbol{\sigma}_T, \sigma_n) := \|\boldsymbol{\sigma}_T\| - \mu|\sigma_n| \leq 0 & (1.76) \\ \dot{\mathbf{u}}_T = -\xi \frac{\partial \zeta}{\partial \boldsymbol{\sigma}_T} & (1.77) \\ \xi \geq 0 & (1.78) \\ \xi \zeta = 0 & (1.79) \end{cases}$$

where  $\mu$  is the Coulomb friction coefficient. If at a point of the body  $\zeta = 0$  then this point slips, otherwise if  $\zeta < 0$  the point sticks, indeed from the equation (1.79) we have  $\xi = 0$  and from the equation (1.77) we obtain  $\dot{\mathbf{u}}_T = 0$ .

Always in the Coulomb friction case we have the following equation

$$\frac{\partial \zeta}{\partial \boldsymbol{\sigma}_T} = \frac{\boldsymbol{\sigma}_T}{\|\boldsymbol{\sigma}_T\|} \quad (1.80)$$

Note that from equations (1.77), (1.78) and (1.80) we can recover the equation (1.57).

Considering the dynamic case, the work of the contact forces at the time increment  $t + 1$  can be expressed as

$$W_c(\mathbf{u}_{t+1}, \mathbf{v}) = \int_{\gamma_C} \boldsymbol{\sigma}_{T_{t+1}} \cdot \mathbf{v} + \sigma_{n_{t+1}} \mathbf{n} \cdot \mathbf{v} \quad (1.81)$$

where  $\mathbf{u}_{t+1}$ ,  $\mathbf{v}$  denote respectively the displacement field at the increment  $t + 1$  and an admissible displacement, finally  $\gamma_C$  represent the current contact surface.

In [107] the penalty and the augmented Lagrangian methods were used. In the following we present the penalty method in addition to the return mapping method as it was shown in [107] (the sign change for the stresses in [107]). First for a penalty method the normal stress  $\sigma_n$  is replaced in the equation (1.81) by

$$\sigma_{n_{t+1}} = -\epsilon_n (-g(u_{t+1}))^+ \quad (1.82)$$

where  $g$  is the gap function,  $\epsilon_n$  the penalty factor and  $(\cdot)^+ = \max(\cdot, 0)$ . In order to calculate  $\boldsymbol{\sigma}_{T_{t+1}}$ , first a trial stick stress is defined as follows

$$\boldsymbol{\sigma}_{T_{t+1}}^{trial} = \boldsymbol{\sigma}_{T_t} - \epsilon_T (\mathbf{u}_{T_{t+1}} - \mathbf{u}_{T_t}) \quad (1.83)$$

where  $\epsilon_T$  is a penalty factor. Let  $\zeta_{t+1}^{trial} = \zeta(\boldsymbol{\sigma}_{T_{t+1}}^{trial}, \sigma_{n_{t+1}})$  then the tangential stress  $\boldsymbol{\sigma}_{T_{t+1}}$  at the

increment  $t + 1$  can be given by the return mapping as follows

$$\boldsymbol{\sigma}_{T_{t+1}} = \boldsymbol{\sigma}_{T_{t+1}}^{trial} - \epsilon_T \boldsymbol{\xi} \mathbf{s}_{t+1} \quad (1.84)$$

where  $\mathbf{s}_{t+1} = \frac{\boldsymbol{\sigma}_{T_{t+1}}^{trial}}{\|\boldsymbol{\sigma}_{T_{t+1}}^{trial}\|}$  and

$$\boldsymbol{\xi} = \begin{cases} 0 & \text{if } \zeta_{t+1}^{trial} \leq 0 \\ \frac{\zeta_{t+1}^{trial}}{\epsilon_T} & \text{if } \zeta_{t+1}^{trial} > 0 \end{cases} \quad (1.85)$$

The tangential stress  $\boldsymbol{\sigma}_{T_{t+1}}$  is replaced in the equation (1.81) which is used to compute the frictional contact problem using a Newton scheme.

The tangent matrix generated from the return mapping method is non-symmetric, thus an alternative algorithm (see [107]) was proposed.

The return mapping method and the penalty method were also presented in [124] for contact problems with large deformations. The finite element formulation for the dynamic contact problem leads to the following equation

$$G(U, t) = M\ddot{U} + F(U) + F_C - P = \mathbf{0} \quad \text{With } U \in \mathbb{R}^N \quad (1.86)$$

where  $U$  is the degree of freedom vector of the displacement field,  $\ddot{U}$  the second derivative with respect to time,  $F(U)$  the internal vector forces (for example in elasticity  $F(U) = KU$  where  $K$  is the stiffness matrix),  $M$  the mass matrix, finally  $F_C$  and  $P$  are the vector forces due to the contact and the external loads.

As the problem is dynamic, a Newton method is used at each time step. We present here in algorithm 1 a summary of the algorithm which can be found in [124].

---

**Algorithm 1** Summary of an algorithm for frictional contact problem

---

```

Initialization at time  $t = 0$  and setting the tolerance  $TOLER$ 
while  $t \leq T_{final}$  do
  while  $\|G\| > TOLER$  do
    for all elements in the body do
      for all slave nodes in the elements do
        Check for contact
        Compute the normal contact forces  $\sigma_n$ 
        Check for friction
        Return mapping for the friction
      end for
    end for
    Construct the vector  $G$  and the global tangent matrix  $K_T$ 
    Solve  $K_T \Delta U = -G$ 
     $U := U + \Delta U$ 
  end while
  Update the quantities for the time  $t + 1$ 
end while

```

---

The global tangent matrix  $K_T$  is built from the mass matrix, the tangent stiffness matrix of the body in addition to the contribution of the contact forces with friction. Note that the return mapping leads to a non-symmetric tangent matrices.

## 1.6 Other contact methods

### 1.6.1 Nitsche-based method

The unilateral contact for elastic bodies using Nitsche-based method was treated in [25, 27]. Indeed the method is based on the following contact condition which is equivalent to the Signorini's conditions.

$$\sigma_n(\mathbf{u}) = -\frac{1}{\gamma}(u_n - \gamma\sigma_n(\mathbf{u}))^+ \text{ on the contact area} \quad (1.87)$$

where  $\gamma > 0$  is a strictly positive value, and  $x^+ = \max(x, 0)$ .

### 1.6.2 Generalized Newton method

The generalized Newton method was used to solve contact problems in [7, 8]. Indeed a Newton algorithm is employed in order to solve a non-smooth non-linear equation.

### 1.6.3 Alternative discretization methods

The contact between two parameterized beams was treated in [84], where the interaction between the two beams is done at a point, and there is no distinction between slave and master body.

## 1.7 The need for a symmetric contact algorithm

In most contact algorithms the concept of slave and master body is used, indeed we impose contact conditions to forbid the penetration of the slave body into the master one, theoretically it does not impact the solution if we interchange the slave and the master body, but when we discretize and use the finite element method, a difference between the solutions appears when we swap the slave and the master body. In general the user must define at first the slave and the master in the contact algorithm.

There is different ways to help the user in defining the slave and the master body, for example a body can be chosen as slave if

- The body has the finest mesh
- The body is the least stiff
- The body has a curvature
- ...

As consequence we can see the difficulties to choose between the bodies, for example if the stiffest body has the finest mesh. In addition we can see the same problem in the case of self contact or in the case of a contact between more than two bodies. Hence the need for a symmetric algorithm where there is no difference between the slave and the master, or at least to reduce the difference between the results in the case of interchanging the roles of the bodies.

We can see some symmetric contact method for example in [12, 54, 92], or in [51, 72] where the symmetric contact method is based on the penalty method, and the Gauss points of the finite elements were used for the contact search instead of the nodes. In [108] a stabilized formulation was proposed in order to take the symmetry into account, indeed the difference between the two Lagrange multipliers of each contact area, was penalized.

In order to show the importance of the choice between the slave and the master in a non-symmetric algorithm and the advantage of a symmetric contact algorithm, we will consider a simple example of a contact between two elastic rectangular blocks. A first elastic rectangular block  $\Omega_1$  is set on a second one  $\Omega_2$  (see Figure 1.8). The two blocks have the same properties: a width  $L = 2UL$  ( $UL$ =length unit), a height  $H = 1UL$ , a Young's modulus  $E = 200 \frac{UF}{UL^2}$  ( $UF$ =force unit), a Poisson's ratio  $\nu = 0$ . The study is done under the plane strain hypothesis (2D). The frictionless case is always supposed, and a vertical displacement of  $U_0 = -0.1UL$  and a zero horizontal displacement are imposed on the upper face of the first block  $\Omega_1$ , the lower face of the second body  $\Omega_2$  is clamped.

Theoretically the value of the displacement field is equal to  $\mathbf{u}_{theo} = (0, 0.05y)$ , where the coordinate system is shown in the Figure 1.8.

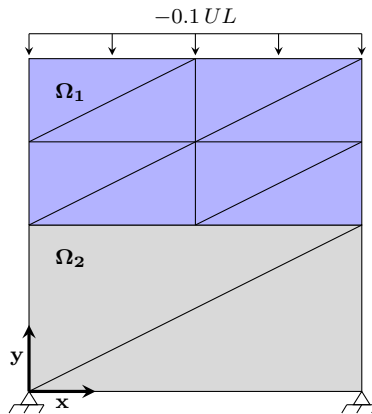


Figure 1.8 – The geometries and the meshes of the two rectangular bodies

We consider linear finite elements ( $P_1$ ) and the meshes shown in Figure 1.8. At the first stage, we consider the first body  $\Omega_1$  as slave and the second one  $\Omega_2$  as master, at the second stage, we consider the body  $\Omega_1$  as master and the second one  $\Omega_2$  as slave, and finally we consider the symmetric algorithm, where there is no difference between slave and master. For all of these three scenarios, the corresponding displacement field  $\mathbf{u}_h$  is computed using the contact algorithm developed in the chapter 4.

The relative error between the computed solution  $\mathbf{u}_h$  and the theoretical one is given by

$$error = \frac{\|\mathbf{u}_h - \mathbf{u}_{theo}\|_1}{\|\mathbf{u}_{theo}\|_1} \times 100 \quad (1.88)$$

where if  $\mathbf{u} = (\mathbf{u}_1, \mathbf{u}_2)$  is a displacement field of the body  $\Omega = \Omega_1 \cup \Omega_2$ , with  $\mathbf{u}_1, \mathbf{u}_2$  respectively the displacement fields of the bodies  $\Omega_1$  and  $\Omega_2$  then

$$\|\mathbf{u}\|_1 = (\|\mathbf{u}_1\|_1^2 + \|\mathbf{u}_2\|_1^2)^{1/2} \quad (1.89)$$

with

$$\begin{cases} \|\mathbf{u}_1\|_1 = \left( \int_{\Omega_1} \|\mathbf{u}_1\|^2 dv + \int_{\Omega_1} \|\nabla \mathbf{u}_1\|^2 dv \right)^{1/2} \\ \|\mathbf{u}_2\|_1 = \left( \int_{\Omega_2} \|\mathbf{u}_2\|^2 dv + \int_{\Omega_2} \|\nabla \mathbf{u}_2\|^2 dv \right)^{1/2} \end{cases} \quad (1.90)$$

where  $\|\cdot\|$  denotes the Euclidean norm.

The relative errors between the computed solutions  $\mathbf{u}_h$  and the theoretical one  $\mathbf{u}_{theo}$  are shown in the table (1.1).

Scenarios	Error (%)
$\Omega_1$ is the slave	$2 \times 10^{-5}$
$\Omega_2$ is the slave	0.38
Symmetric algorithm	$7 \times 10^{-6}$

Table 1.1 – The relative errors between the numerical solutions and the theoretical one

We note the advantage of the symmetric algorithm regarding the accuracy. Moreover, we noticed that the symmetric algorithm requires fewer iterations to converge.

# Signorini's contact problem with Interior point optimizer

## Outline of the current chapter

---

<b>2.1 Signorini's contact problem</b>	<b>38</b>
<b>2.2 Minimization problem resolution</b>	<b>40</b>
2.2.1 Interior Point method . . . . .	40
2.2.2 Formulation of the problem . . . . .	43
2.2.3 Weak contact formulation . . . . .	45
<b>2.3 Numerical validations</b>	<b>46</b>
2.3.1 Compression of a hyperelastic cube . . . . .	46
2.3.2 Hertz contact problem . . . . .	49
2.3.3 Press-fit problem . . . . .	51
2.3.4 Clamped body contact . . . . .	52

---

This chapter presents a method to solve the mechanical problems undergoing finite deformations and the contact problems without friction, between a hyperelastic body and an obstacle. In this chapter, we restrict ourselves to the contact between a hyperelastic body (where the linear elastic body is a particular case) and a rigid foundation (obstacle). The dynamical and frictional cases are not treated here. The goal of this chapter is to propose a simple method that uses the FreeFEM software [55] and its tools to solve a wide variety of contact problems.

The contact problem is formulated as a constrained minimization one, indeed the constraints which describe the non-penetration between the body and the obstacle are simple, and there is no need to compute the normal vectors or the projection points on the obstacle in order to describe the non-penetration, which increases the resolution speed of the contact problem, thus the contact formulation is well fitted with the interior point method. The IPOPT (interior

point optimizer) algorithm [120], which is already interfaced with FreeFEM, is used to solve the optimization problem and to reach the solution. The rigid foundation is supposed to be described by a  $C^2$  function, if this is not the case then the foundation can be approximated by a spline function which is also available in the FreeFEM language.

We also introduce two formulations of our contact problem, in the first one, the non-penetration between the body and the obstacle is done by forbidding the nodes of the body mesh to penetrate the obstacle, in the second one, the non-penetration is written in a weak form.

## 2.1 Signorini's contact problem

Signorini's contact problem [106] represents the contact between a deformable body and a fixed rigid foundation. An example is shown in Figure 2.1. Let  $\Omega \subset \mathbb{R}^3$  denote the body in its reference configuration,  $\Gamma_0$  which is a part of the boundary  $\partial\Omega$  where a null displacement is imposed,  $\Gamma_1 \subset \partial\Omega$  where a traction force  $\mathbf{t}$  is imposed, and  $\Gamma_C \subset \partial\Omega$  the potential contact part of the boundary  $\partial\Omega$ . We also suppose that  $\Gamma_0, \Gamma_1$  and  $\Gamma_C$  are disjoint and  $\partial\Omega = \Gamma_0 \cup \Gamma_1 \cup \Gamma_C$ , where  $\Gamma_C$  has a non null area.

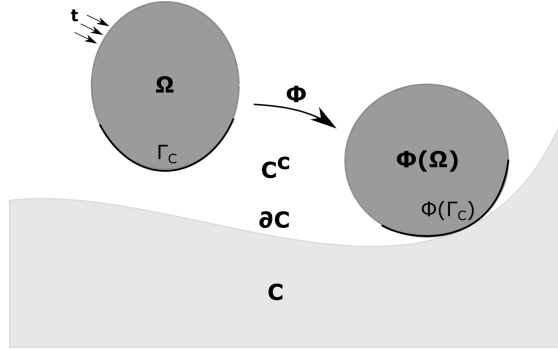


Figure 2.1 – Signorini's contact

Let  $\mathcal{C} \in \mathbb{R}^3$  be an open set in  $\mathbb{R}^3$  describing the rigid foundation or the obstacle where there is no penetration, and  $\mathcal{C}^c$  its complement. The Signorini's contact equations are the set of the local balance of the momentum equation, of the boundary conditions, and of the contact conditions. Giving a body force per unit volume  $\mathbf{f}$  applied on the body, and using the same notations as before, the equations in the reference configuration are

$$\begin{cases} \sum_{j=1}^3 \frac{\partial \mathbf{P}_{ij}}{\partial X_j} + f_i = 0 & \text{in } \Omega \quad (i = 1, 2, 3) \\ \mathbf{u} = \mathbf{0} & \text{on } \Gamma_0 \\ \mathbf{PN} = \mathbf{t} & \text{on } \Gamma_1 \end{cases} \quad (2.1)$$

with the following contact conditions

$$\begin{cases} \phi(\Gamma_C) \subseteq \mathcal{C}^c & \text{(Non-penetration in the foundation)} \\ \mathbf{PN} = 0 & \text{if } X \in \Gamma_C \text{ and } \mathbf{x} = \phi(\mathbf{X}) \in \bar{\mathcal{C}}^c \quad (\notin \mathcal{C} \cup \partial\mathcal{C}) \\ \mathbf{PN} = \lambda \mathbf{n} & \text{if } X \in \Gamma_C \text{ and } \mathbf{x} = \phi(\mathbf{X}) \in \partial\mathcal{C}, \text{ where } \lambda \leq 0 \end{cases} \quad (2.2)$$

For the hyperelastic materials, the first Piola-Kirchhoff stress tensor can be obtained by

$$\mathbf{P} = \frac{\partial \hat{W}}{\partial \mathbf{F}} \quad (2.3)$$

where  $\hat{W}$  is the strain energy function.

The contact formulation described in (2.1) and (2.2) can be formulated like in [29] as a constrained minimization problem, i.e if  $\mathbf{u}$  is the solution of Signorini's contact problem (2.1) and (2.2) then

$$\mathbf{u} = \arg \min_{\mathbf{v} \in \mathbf{K}} (\mathcal{E}(\mathbf{v})) \quad (2.4)$$

where  $\mathcal{E}$  is the total potential energy defined by

$$\mathcal{E}(\mathbf{v}) = \int_{\Omega} \hat{W} dV - \int_{\Omega} \mathbf{f} \cdot \mathbf{v} dV - \int_{\Gamma_1} \mathbf{t} \cdot \mathbf{v} dA \quad (2.5)$$

and  $\mathbf{K}$  is the set defined by

$$\mathbf{K} = \left\{ \mathbf{v} \in (H^1(\Omega))^3 ; \mathbf{v} = 0 \text{ on } \Gamma_0 ; \phi_{\mathbf{v}}(\Gamma_C) \subseteq \mathcal{C}^c \right\} \quad (2.6)$$

where  $\phi_{\mathbf{v}}(\mathbf{X}) = \mathbf{X} + \mathbf{v}$ . In most publications, the normal gap function  $g_n : \Gamma_C \rightarrow \mathbf{R}$  is used to describe the non-penetration condition:  $\phi(\Gamma_C) \subseteq \mathcal{C}^c$ . The normal gap function  $g_n$  is a signed distance function between the body  $\Omega$  and the foundation (see Figure 2.2). Let  $\mathbf{x} \in \phi(\Gamma_C)$  be a point of the deformed body  $\phi(\Omega)$ , then the normal gap function is defined as the following

$$g_n(\mathbf{x}) = (\mathbf{x} - \mathbf{y}) \cdot \mathbf{n}(\mathbf{y}) \quad (2.7)$$

where  $\mathbf{y}$  is the closest point of the rigid foundation to  $\mathbf{x}$  and  $\mathbf{n}(\mathbf{y})$  is the outward unit normal vector to the rigid foundation at  $\mathbf{y}$ . In this case, the non-penetration condition is given by

$$g_n(\mathbf{x}) \geq 0 \quad \forall \mathbf{x} \in \phi(\Gamma_C) \quad (2.8)$$

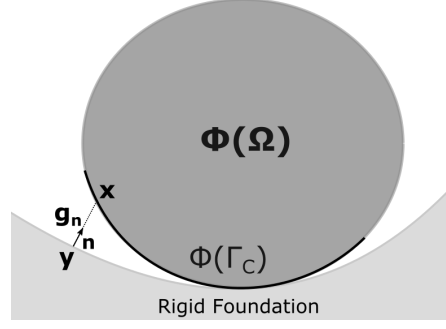


Figure 2.2 – Normal gap function

In other words, if  $g_n(\mathbf{x}) > 0$  there is no penetration between the point  $\mathbf{x}$  and the foundation, if  $g_n(\mathbf{x}) = 0$  the point  $\mathbf{x}$  and the foundation are in contact, and finally if  $g_n(\mathbf{x}) < 0$  the point  $\mathbf{x}$  penetrates the foundation.

The non-penetration condition used in this chapter, which is not based on the normal gap function, is mentioned in the section 2.2.2.

## 2.2 Minimization problem resolution

### 2.2.1 Interior Point method

One of the pieces of open source software for optimization is IPOPT. IPOPT uses the interior point method and can solve large scale constrained and unconstrained optimization problems, where the constraints can be nonlinear. In other words, it solves the following problem

$$\begin{cases} \arg \min_{u \in \mathbb{R}^n} f(u) & \text{such that} \\ g_{Lo} \leq g(u) \leq g_{Up} \\ u_{Lo} \leq u \leq u_{Up} \end{cases} \quad (2.9)$$

where  $f : \mathbb{R}^n \rightarrow \mathbb{R}$  is the function to minimize and  $g = (g^{(1)}, \dots, g^{(m)}) : \mathbb{R}^n \rightarrow \mathbb{R}^m$  the inequality constraints, the two symbols  $Lo$  and  $Up$  denote respectively the lower and upper bounds, and the inequality between vectors means the inequality between the components of the vectors. In addition, we suppose that  $g_{Lo}^{(i)}, u_{Lo}^{(j)} \in \mathbb{R} \cup \{-\infty\}$  and finally  $g_{Up}^{(i)}, u_{Up}^{(j)} \in \mathbb{R} \cup \{+\infty\}$  for all  $i = 1, \dots, m$  and  $j = 1, \dots, n$ . The functions  $f$  and  $g$  are supposed to be sufficiently smooth (for example  $C^2$ ).

By introducing the slack variables  $s = (s^{(1)}, \dots, s^{(m)}) \in \mathbb{R}^m$ , which convert the inequality constraints to equality constraints and bound constraints, the inequality constraint equations in

(2.9) can be expressed as

$$\begin{cases} g^{(i)}(u) - s^{(i)} = 0 \\ g_{Lo}^{(i)} \leq s^{(i)} \leq g_{Up}^{(i)} \quad \forall i = 1, \dots, m \end{cases} \quad (2.10)$$

Therefore the minimization problem (2.9) is simplified and can thus be reformulated as follows

$$\begin{cases} \arg \min_{(u,s) \in \mathbb{R}^n \times \mathbb{R}^m} f(u) \quad \text{such that} \\ g(u) - s = 0 \\ (u_{Lo}, g_{Lo}) \leq (u, s) \leq (u_{Up}, g_{Up}) \end{cases} \quad (2.11)$$

or in a simplified way and without loss of generality, the problem can be transformed as follows

$$\begin{cases} \arg \min_{u \in \mathbb{R}^n} f(u) \quad \text{such that} \\ g(u) = 0 \\ u \geq 0 \end{cases} \quad (2.12)$$

IPOPT solves the minimization problem in multiple steps, but we will only describe the principal ones. For more details see [119, 120]. The algorithm is briefly described in algorithm 2

---

#### Algorithm 2 IPOPT

---

Initial value for the barrier parameter  $\mu$ .

**while** No global convergence **do**

-The objective function  $f$  is transformed into a barrier function and the problem is reformulated as follows

$$\begin{cases} \arg \min_{u \in \mathbb{R}^n} f(u) - \mu \sum_{i=1}^n \ln(u^{(i)}) \quad \text{such that} \\ g(u) = 0 \end{cases}$$

**while** No convergence **do**

-First-order optimality condition for the barrier problem.

-Compute the descent directions  $(d_k^\mu, d_k^\lambda, d_k^z)$  at the iteration  $k$ .

-Line search by filter method.

**end while**

-Decrease the barrier parameter  $\mu$ .

**end while**

Return  $u \in \mathbb{R}^n$ .

---

The first-order optimality condition of the problem (2.12) is given by

$$\begin{cases} \nabla f(u) + \nabla g(u)\lambda - z = 0 \\ g(u) = 0 \\ UZe - \mu e = 0 \end{cases} \quad (2.13)$$

where  $\lambda \in \mathbb{R}^m$  and  $z \in \mathbb{R}^n$  correspond respectively to the constraints and bounds Lagrange multipliers,  $U = \text{diag}(u)$  (diagonal matrix with  $U_{ii} = u^{(i)}$ ),  $Z = \text{diag}(z)$  and finally  $e \in \mathbb{R}^n$  is the

vector  $e = (1, \dots, 1)^T$ .

A Newton method is applied to the system (2.13) in order to find the descent directions  $(d_k^u, d_k^\lambda, d_k^z)$  at each iteration  $k$ . If  $u_k, \lambda_k, z_k$  denote respectively the values of  $u, \lambda, z$  at the iteration  $k$ , then the following system is obtained

$$\begin{bmatrix} W_k & \nabla g(u_k) & -I \\ \nabla g(u_k)^T & 0 & 0 \\ Z_k & 0 & U_k \end{bmatrix} \begin{pmatrix} d_k^u \\ d_k^\lambda \\ d_k^z \end{pmatrix} = - \begin{pmatrix} \nabla f(u_k) + \nabla g(u_k)\lambda_k - z_k \\ g(u_k) \\ U_k Z_k e - \mu e \end{pmatrix} \quad (2.14)$$

where  $W_k = \nabla^2 \mathcal{L} = \nabla^2 f(u_k) + \sum_{j=1}^m \lambda_k^{(j)} \nabla^2 g^{(j)}(u_k)$ ,  $(j)$  denotes the components of a vector and  $\mathcal{L}$  is the Lagrangian function.

Otherwise, the linear system (2.14) can be reduced into the following

$$\begin{bmatrix} W_k + U_k^{-1} Z_k & \nabla g(u_k) \\ \nabla g(u_k)^T & 0 \end{bmatrix} \begin{pmatrix} d_k^u \\ d_k^\lambda \end{pmatrix} = - \begin{pmatrix} \nabla \phi_\mu(u_k) + \nabla g(u_k)\lambda_k \\ g(u_k) \end{pmatrix} \quad (2.15)$$

with the additional equation:

$$d_k^z = \mu U_k^{-1} e - z_k - U_k^{-1} Z_k d_k^u \quad (2.16)$$

where  $\phi_\mu = f(u) - \mu \sum_{i=1}^n \ln(u^{(i)})$  is the barrier function.

As the descent directions were computed, the quantities  $u_{k+1}, \lambda_{k+1}, z_{k+1}$  at the iteration  $k+1$  are given by

$$\begin{cases} u_{k+1} = u_k + \alpha_k d_k^u \\ \lambda_{k+1} = \lambda_k + \alpha_k d_k^\lambda \\ z_{k+1} = z_k + \alpha_k d_k^z \end{cases} \quad (2.17)$$

In order to improve the convergence of the algorithm, a line search method with a filter method is used to determine the parameters  $\alpha_k$ . Using the same notation as in [120], let  $\theta(u) = \|g(u)\|$  be the constraint violation. At first a parameter  $\alpha_k$  is proposed and a filter  $\mathcal{F}$  is a set of  $\mathbb{R}^2$ . It helps to determine if  $\alpha_k$  can be accepted as a step size and to avoid cycling between two successive iterations. Indeed when the optimization starts the filter is initialized as follows

$$\mathcal{F}_0 = \{(\theta, \phi) \in \mathbb{R}^2 \mid \theta \geq \theta^{max}\} \quad (2.18)$$

where  $\theta^{max}$  is a chosen value. After each iteration the filter is updated according to the situation, to:

$$\mathcal{F}_{k+1} = \mathcal{F}_k \cup \{(\theta, \phi) \in \mathbb{R}^2 \mid \theta \geq (1 - \gamma_\theta)\theta(u_k) \ \& \ \phi \geq \phi_\mu(u_k) - \gamma_\phi\theta(u_k)\} \quad (2.19)$$

or to:

$$\mathcal{F}_{k+1} = \mathcal{F}_k \quad (2.20)$$

where  $(\gamma_\theta, \gamma_\phi) \in ]0, 1[$  are two fixed values.

The step size  $\alpha_k$  can be accepted if  $(\theta(u_{k+1}(\alpha_k)), \phi_\mu(u_{k+1}(\alpha_k))) \notin \mathcal{F}_k$ . If this is not the case,

several actions may be possible [120].

Finally, the barrier parameter  $\mu$  is decreased and the iteration starts from the last converged solution. The solution of the above algorithm, which depends on the barrier parameter  $u(\mu)$ , converges to the solution of the original problem (2.9) as  $\mu \rightarrow 0$ .

### 2.2.2 Formulation of the problem

In this section and without loss of generality, we consider the two dimensional problem case. Using the same notations as section 2.1, let  $\mathbf{X}_r = (X, Y) \in \Gamma_C$  (the potential contact area of the body in the reference configuration),  $\mathbf{x} = (x, y) \in \gamma_C = \phi(\Gamma_C)$  in the actual configuration, and  $\mathbf{u} = \mathbf{x} - \mathbf{X}_r = (u_x, u_y)$  its corresponding displacement vector. The non-penetration condition in our analysis will be written in the form of  $F(\mathbf{u}) \geq 0$ , where  $F : \mathbb{R}^2 \rightarrow \mathbb{R}$  is a function of class  $C^2$ .

We suppose that the boundary of the foundation can be written in the form of a function  $\psi$  (see Figure 2.3) of class  $C^2$ , then the non-penetration condition is given by

$$y - \psi(x) \geq 0 \quad (2.21)$$

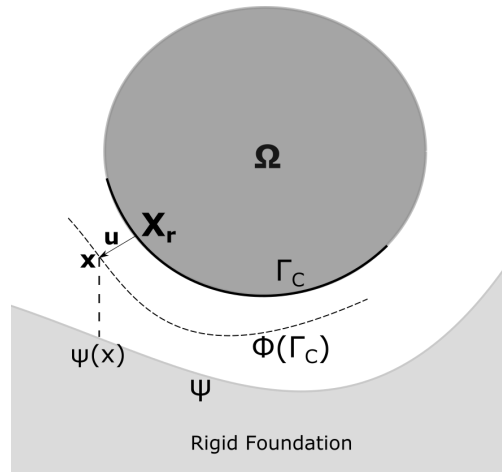


Figure 2.3 – The foundation function  $\psi$

This means that the body has to be always above the foundation in our case. By considering the reference configuration, this condition becomes

$$F(\mathbf{u}) = Y + u_y - \psi(X + u_x) \geq 0 \quad (2.22)$$

If the function  $\psi$  of the foundation is not subject to a large variations, then we can apply

Taylor's theorem to  $\psi(X_1 + u_1)$  and obtain a simpler non-penetration condition, as follows

$$F(\mathbf{u}) = Y - \psi(X) + u_y - \psi'(X).u_x \geq 0 \quad (2.23)$$

In the finite element method, the body domain  $\Omega$  can be approximated by a polygonal domain  $\Omega_h = \bigcup_{i=1}^{n_T} T_i$ , where  $T_i$  are the triangles which constitute  $\Omega_h$  and  $h$  is the mesh size. Let  $\mathcal{T}_h$  be the family of the triangles  $T_i$  and, without loss of generality, let  $V_h(P_1)$  be the linear finite element space defined on  $\Omega_h$  and given by

$$V_h(P_1, \mathcal{T}_h) = \left\{ v(x, y) = \sum_{k=1}^m v_k \Phi_k(x, y) \mid v_k \in \mathbb{R} \right\} \quad (2.24)$$

where  $m$  denotes the number of nodes (or vertex) in the mesh and  $\Phi_k$  is the shape function, which in our case is linear for each triangle and is equal to 1 at the node  $k$  and zero at the other nodes. The component  $v_k$  is called a degree of freedom of the function  $v$ . We can also note that the function  $v$  is a continuous piecewise function.

In our analysis, we are interested to find the displacement field  $\mathbf{u} = (u_x, u_y)$  for the Signorini's contact problem. First, we consider that  $u_x, u_y \in V_h$ , if  $\{U_{x,1} \dots U_{x,m}\}$  and  $\{U_{y,1} \dots U_{y,m}\}$  respectively denote the degrees of freedom of  $u_x$  and  $u_y$ , then the degrees of freedom of  $\mathbf{u}$  are given by

$$\mathbf{U} = \begin{pmatrix} U_0 \\ U_1 \\ \vdots \\ U_{2i} \\ U_{2i+1} \\ \vdots \\ U_{2(m-1)} \\ U_{2(m-1)+1} \end{pmatrix} = \begin{pmatrix} U_{x,1} \\ U_{y,1} \\ \vdots \\ U_{x,i} \\ U_{y,i} \\ \vdots \\ U_{x,m} \\ U_{y,m} \end{pmatrix} \quad (2.25)$$

The degrees of freedom vector  $\mathbf{U}$  of the displacement field describe the nodes displacement of the mesh. The coordinates vector  $\mathbf{X}$  of all mesh nodes in the reference configuration will be given by

$$\mathbf{X} = (X_0, X_1, \dots, X_{2(m-1)}, X_{2m-1})^T$$

Let  $n_C$  be the contact nodes number belonging to the contact boundary  $\Gamma_C$ , and suppose that the first  $2n_C$  components of the vector  $\mathbf{U}$  correspond to the degrees of freedom of the  $n_C$  contact nodes. Our contact problem can be formulated then as follows

$$\begin{cases} \arg \min_{\mathbf{U} \in \mathbb{R}^n} \mathcal{E}(\mathbf{U}) & \text{such that} \\ c_i(\mathbf{U}) := X_{2i+1} + U_{2i+1} - \psi(X_{2i} + U_{2i}) \geq 0 & \forall i = 0, \dots, n_C - 1 \end{cases} \quad (2.26)$$

where  $n = 2m$  and  $\mathcal{E}(\mathbf{U})$  the total potential energy of the body. More precisely the constraint  $c_i \geq 0$  represents the non-penetration condition with the rigid foundation or the obstacle, for the node  $i$  belonging to the boundary  $\Gamma_C$ .

Let the vector  $\mathbf{c}$  be defined by  $\mathbf{c} = (c_0, \dots, c_{n_C-1})^T$ . As the interior point method is used,

the Jacobian matrix of  $\mathbf{c}$  and the Hessian matrix of each  $c_i$  are needed (see equation (2.15)). The Jacobian matrix  $\text{Jac}(\mathbf{c})_{n_C \times n}$ , which is full row rank, can be given simply by

$$\text{Jac}(\mathbf{c}) = \begin{bmatrix} A_0 & \dots & 0 & 0 \\ \vdots & \ddots & \vdots & \vdots \\ 0 & \dots & A_{(n_C-1)} & 0 \end{bmatrix} \quad (2.27)$$

where only the matrices  $A_i$  are non zero, and  $A_i = \begin{bmatrix} -\psi'(X_{2i} + U_{2i}) & 1 \end{bmatrix} \quad \forall i = 0, \dots, n_C - 1$ ,  $\psi'$  denotes the derivative of  $\psi$ . The Hessian matrix of each  $c_i$ :  $\text{Hess}(c_i)_{n \times n}$  is equal to

$$\text{Hess}(c_i) = \begin{bmatrix} 0 & & & & & \\ & \ddots & & & & \\ & & h_{2i2i} & & & \\ & & & \ddots & & \\ & & & & 0 & \\ & & & & & 0 \end{bmatrix} \quad (2.28)$$

where only  $h_{2i2i}$  is not equal to zero, indeed  $h_{2i2i} = -\psi''(X_{2i} + U_{2i})$ , where  $\psi''$  is the second derivative of  $\psi$ .

Using the energy, its Jacobian matrix and its Hessian matrix, in addition to the constraints and the Jacobian and the Hessian of the constraints, the constrained minimization problem can be solved by the interior point method. In our case we used the IPOPT software.

In this formulation the non-penetration constraints are very simple and well fitted for the interior point method. In addition there is no need to compute the normal vectors and the projection points on the obstacle, which they depend on the solution of the problem, in order to define the non-penetration constraints. Therefore there is no need to use a fixed point algorithm or an active-set strategy.

Finally if the obstacle (rigid foundation) is defined by a mesh, then we can use for example a cubic spline in order to describe the potential contact area of the obstacle, if it can be described by a graph of a function, in other words to compute the function  $\psi$ .

### 2.2.3 Weak contact formulation

Instead of using the non-penetration condition for each node of the contact area  $\Gamma_C$  (problem 2.26), we can write the non-penetration conditions in a weak form and the constrained minimization problem becomes as follows

$$\begin{cases} \arg \min_{\mathbf{U} \in \mathbb{R}^n} \mathcal{E}(\mathbf{U}) & \text{such that} \\ \int_{\Gamma_C} F(\mathbf{u}) \Phi_i \geq 0 & \forall i = 0, \dots, n_C - 1 \end{cases} \quad (2.29)$$

where  $F(\mathbf{u})$  is given by the equation (2.22) and  $\Phi_i$  are the shape functions of the space  $V_h$  at the contact nodes of the contact surface  $\Gamma_C$ . We can see in this formulation that the non-penetration is done in an average sens, which makes the contact more softer, and gives smoother results.

However it's obvious that it takes more computational time due to the integrals calculation. Thus in the next section, we restrict our study with the first formulation. Note that the previous advantages remain for this formulation.

## 2.3 Numerical validations

In this section, we present several common numerical examples in order to validate our method. First, we will present two tests in 2D and 3D on the compression of a hyperelastic cube with two specific types of materials. In these tests, the contact is not taken into account, indeed the goal is to validate our algorithm in solving problems with a hyperelastic material behavior. Next, we present 3 contact tests, where one of them is Hertz contact problem with explicit analytic solution.

In FreeFEM, necessary quantities such as the energy and the constraints (Jacobian, Hessian) are computed. Then, IPOPT is used to solve our constrained minimization problem through the FreeFEM interface. To see how we can use IPOPT with FreeFEM, one can refer to [13, 55]. The advantage of this method is that only the contact problem needs to be formulated and then IPOPT will act like a black box to solve the optimization problem.

### 2.3.1 Compression of a hyperelastic cube

Here we handle the test presented in [4] using linear finite elements [93]. A unit cube of dimension equal to 1 *m* (meter) is considered (see Figure 2.4). The cube can move along the direction  $X_1$  and its two faces, which are perpendicular to the direction  $X_3$ , are fixed along this last direction. Finally, the lower face of this cube is fixed along the direction  $X_2$  (see Figure 2.4). A pressure of  $f = 0.876 Pa$  is applied to the upper face of the cube.

Two nearly incompressible hyperelastic material models [80] are considered for the cube: Neo-Hookean and Mooney. These models also describe the incompressibility of the two materials. The goal is to compute the displacement field (specifically the vertical displacement) and to compare it with the theoretical one. The strain energy functions of these two models are given as follows

$$\hat{W} = C_{10}(J^{-\frac{2}{3}}I_1 - 3) + C_{01}(J^{-\frac{4}{3}}I_2 - 3) + \frac{K}{2}(J - 1)^2 \quad (2.30)$$

where  $I_1, I_2, J$  the invariants defined in the equation (1.19),  $K = \frac{6(C_{01} + C_{10})}{3(1 - 2\nu)}$  [80] and  $\nu$  is the Poisson's ratio. The function  $\frac{K}{2}(J - 1)^2$  helps to satisfy the incompressibility constraint ( $J = 1$ ) by penalizing it. The coefficients  $C_{01}, C_{10}$ , and  $\nu$  are presented in the table 2.5

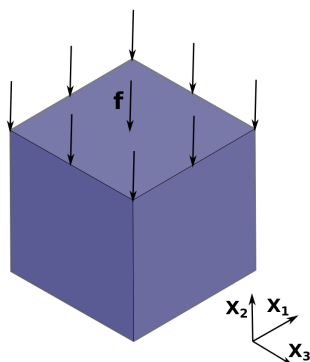


Figure 2.4 – The cube with the applied pressure

Figure 2.5 – Material coefficients

	Mooney	Neo-Hookean
$C_{10}$	0.709	1.2345
$C_{01}$	2.3456	0.
$\nu$	0.499	0.499

The linear finite elements  $P_1$  [55] were used for this study and the mesh contains 200 elements in the two dimensional case (plane strain situation because the cube is fixed along  $X_3$ ). In order to avoid the rigid movement of the structure and using the fact that the problem is symmetric, only half of the structure is modeled as can be seen in Figure 2.6 for the two dimensional case.

Using IPOPT in order to minimize the total potential energy of the cube and generate the displacement field, the maximum vertical displacement of the upper face is given in the table 2.1.

Table 2.1 – Vertical displacement  $w$  with FreeFEM in 2D

FreeFEM in 2D	Mooney	Neo-Hookean
$w$	0.034072	0.078331

The theoretical maximum vertical displacement of the upper face [4] is given in the table 2.2.

Table 2.2 – Theoretical vertical displacement  $w$

Theoretical	Mooney	Neo-Hookean
$w$	0.0340091	0.078180

The errors with respect to the theoretical values for our method and Code\_Aster [4] are presented in table 2.7, where similar results are seen.

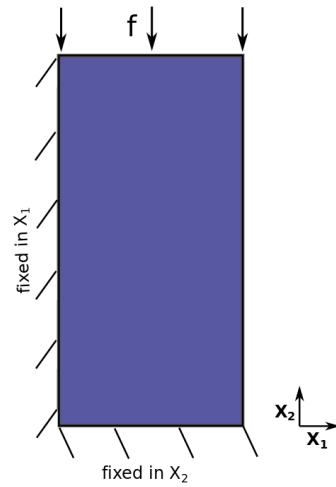


Figure 2.6 – The 2D symmetrical model of the cube

Figure 2.7 – Errors in 2D with respect to the theoretical values

	FreeFEM	Code_Aster
Mooney	0.19%	0.20%
Neo-Hookean	0.19%	0.20%

In Figure 2.8a, the deformed shape and the vertical displacement of the Neo-Hookean material case are shown. To see the FreeFEM script of the example presented above, please visit <https://modules.freefem.org/modules/nonlinear-elasticity/>.

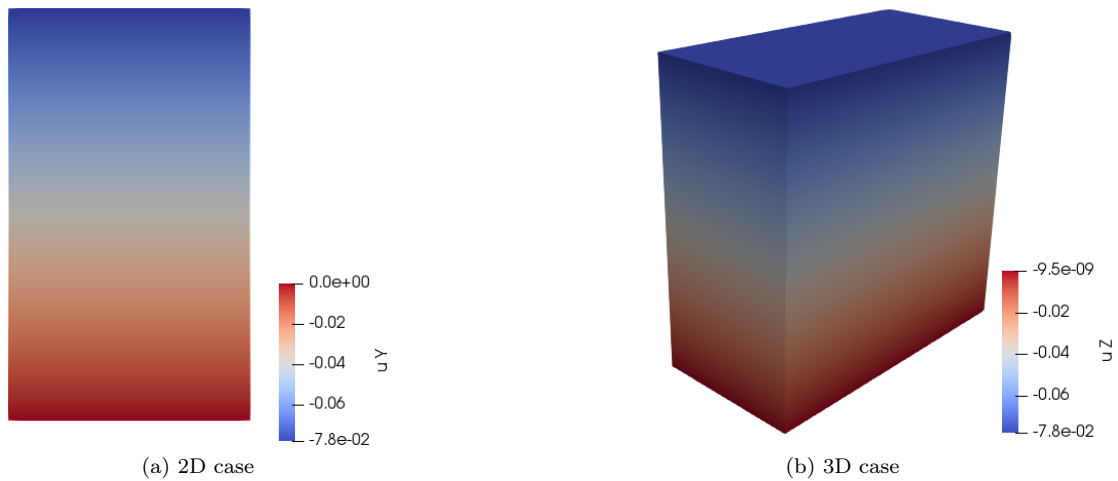


Figure 2.8 – Vertical displacement field (Neo-Hookean)

On the other hand, the exact same results were generated by considering the three dimensional case for the two types of materials. In addition, note that we obtained the same results for the displacement field by supposing that the cube is in contact on its lower face with a rigid

foundation, see Figure 2.8b for the three dimensional case.

### 2.3.2 Hertz contact problem

A classical contact problem is the contact between two deformable cylinders where their axis are parallel and a theoretical solution exists for this type of problem (see [66]). In the following, the plane strain situation is considered and it corresponds to the two dimensional case (2D). In other words, the height of the cylinders is large. Finally, the frictionless contact is assumed.

The zone of contact between the cylinders is a strip of width  $2a$ . The quantity of interest is the normal pressure at the contact zone. Let a force of magnitude  $P$  be applied on the first cylinder and let this force be normal to its axis in order to compress the two bodies and let them enter into contact. Therefore, by assuming the hypothesis of small deformations and linear elasticity, we can obtain analytically the half length of the contact zone  $a$  in addition to the profile of the normal pressure at the contact zone (see [66]).

Let  $R_1$  and  $R_2$  denote the radius of the cylinders,  $E_1$  and  $E_2$  the Young's modulus and  $\nu_1$  and  $\nu_2$  the Poisson's ratio of the first and second cylinder. Then, the half contact length  $a$  is given by

$$a = \sqrt{\frac{4PR}{\pi E^*}} \quad (2.31)$$

where  $R$  and  $E^*$  are computed as follows

$$\begin{cases} \frac{1}{R} = \frac{1}{R_1} + \frac{1}{R_2} \\ \frac{1}{E^*} = \frac{1-\nu_1^2}{E_1} + \frac{1-\nu_2^2}{E_2} \end{cases} \quad (2.32)$$

Let  $x$  denotes the abscissa along the contact zone, thus the normal pressure profile  $p$  is given as follows

$$p(x) = p_{max} \sqrt{1 - \frac{x^2}{a^2}} \quad (2.33)$$

where  $p_{max} = \frac{2P}{\pi a}$ , the maximum pressure, is located at the origin of the contact zone.

The second cylinder can be considered as a rigid foundation by taking a large value of its Young's modulus  $E_2 \rightarrow +\infty$ . Thus we obtain  $E^* \rightarrow \frac{E_1}{1-\nu_1^2}$  and the same equations presented above can be used.

In the same manner, the second cylinder can be replaced by a plane by taking  $R_2 \rightarrow +\infty$ , therefore  $R \rightarrow R_1$ .

Next, we present the numerical results of one contact example involving a deformable cylinder against a rigid foundation. The foundation is a plane for this example. Due to the two dimensional case and the symmetry of the problem, only a quarter of a disc, which represents

the cylinder, will be modeled. In this example,  $f$  denotes the pressure applied on the top face of the quarter disc.  $R_1$ ,  $E_1$  and  $\nu_1$  denote respectively the radius, Young's modulus, and the Poisson's ratio of the quarter disc. Note that the total force applied is equal to  $P = 2fR_1$ .

### Contact with a rigid plane foundation using the formulation (2.26)

The contact between the quarter disc and the rigid plane is shown below (Figure 2.9a). In order to compare our results to the theoretical ones, we suppose the following values: a radius  $R_1 = 1\text{ m}$ , a Young's modulus  $E_1 = 2.1 \times 10^9\text{ Pa}$ , a Poisson's ratio  $\nu_1 = 0.3$  and finally a top face pressure of  $f = 2.75 \times 10^6\text{ Pa}$ .

In this case, the half contact length  $a$  is equal to

$$a = \sqrt{\frac{8fR_1^2(1 - \nu_1^2)}{\pi E_1}} \quad (2.34)$$

The maximum pressure and the pressure profile at the contact zone are equal to

$$p_{max} = \frac{4fR_1}{\pi a} \quad (2.35) \quad p(x) = p_{max} \sqrt{1 - \frac{x^2}{a^2}} \quad (2.36)$$

The linear finite elements  $P_1$  were used for the simulation and the mesh was refined at the contact zone until satisfactory results are obtained. In Figure 2.9b, we can see the deformation of the quarter disc in addition to the distribution of the Von Mises stress and we also remark that the maximum Von Mises stress is not at the border where the contact occurs.

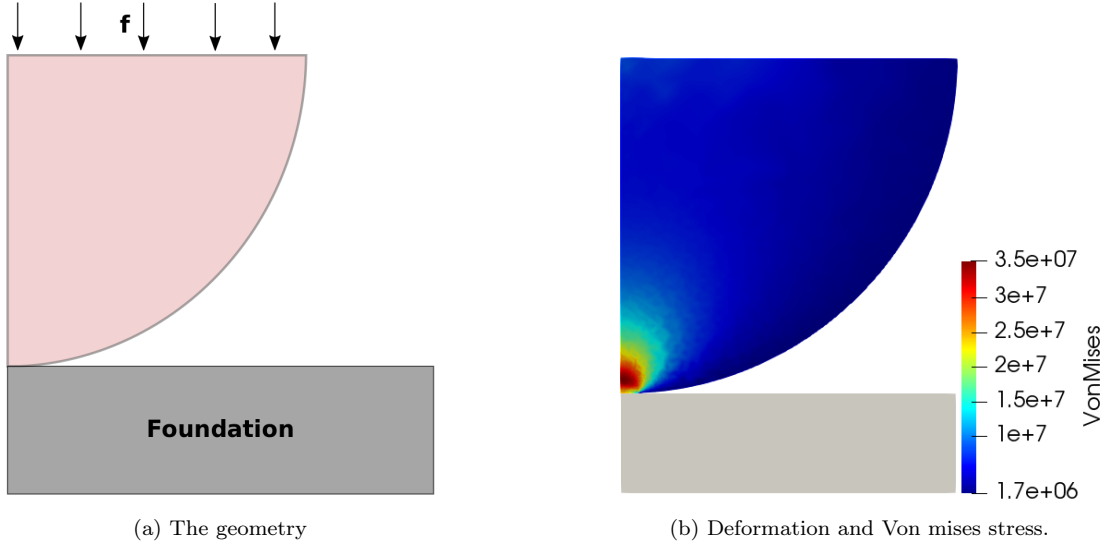


Figure 2.9 – Contact with a rigid plane foundation

The pressure at the contact zone  $p(x)$  computed with our algorithm is plotted with the theoretical one in the Figure 2.10.

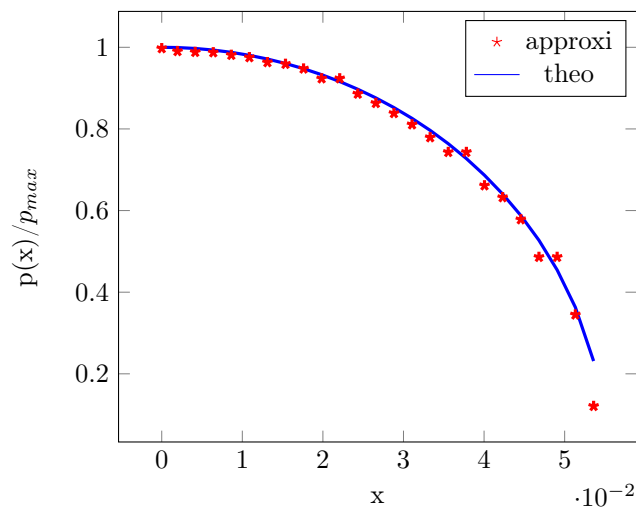


Figure 2.10 – Pressure at the contact zone

### 2.3.3 Press-fit problem

The following example, which can be found in [123], is considered in order to show that our algorithm can handle large deformations. A rectangular rubber material of length  $45\text{ cm}$  and width  $40\text{ cm}$  is pressed in a channel (see Figure 2.11), due to its high Young modulus with respect to the body, this channel is considered as an obstacle and is described by a cubic spline function, which interpolates the mesh nodes of the obstacle. The channel has a total length of  $190\text{ cm}$ , its first horizontal part has a length of  $80\text{ cm}$  and its second horizontal part has a length of  $90\text{ cm}$  with an opening of  $29.8\text{ cm}$ . In the first stage a vertical displacement of  $1\text{ mm}$  is imposed on the body in order to penetrate it in the channel, in the second stage a total horizontal displacement of  $130\text{ cm}$  is imposed on the left side of the body, this total displacement is done by 70 time steps. Neo-Hookean material is considered for the body, with the following properties  $E = 1000\text{ Mpa}$ ,  $\nu_h = 0.47$ . The deformation states of the rectangular body at the steps 0, 40, 70 are depicted in the following figures (Figure 2.11).

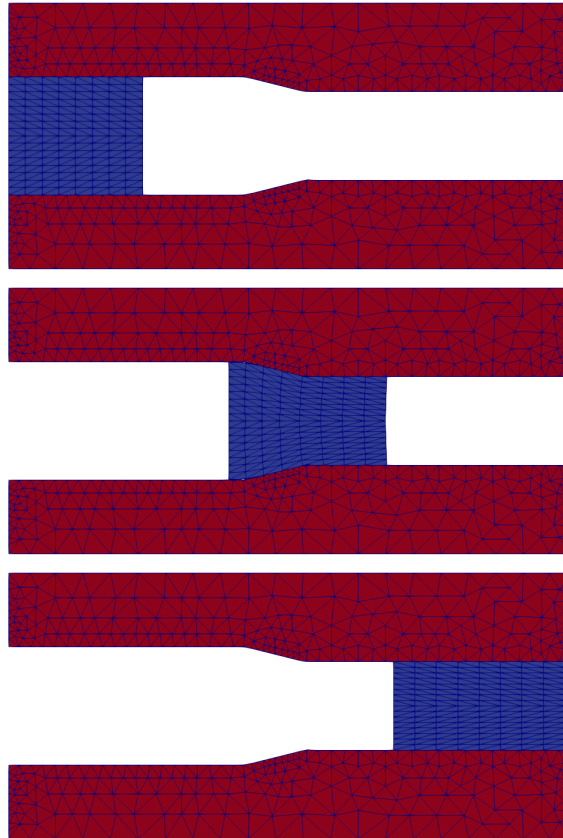


Figure 2.11 – The deformation states at the steps 0, 40, 70

### 2.3.4 Clamped body contact

In this test, an iron square  $\Omega$  of length equal to 1  $m$  is considered. The square is clamped on its side  $\Gamma_0$  and is initially in contact with a rigid plane on its side  $\Gamma_C$  (see Figure 2.12a). The body is subjected to its own weight, where  $\rho = 7800 \text{ kg.m}^{-3}$  and  $g = 9.81 \text{ m.s}^{-2}$ . The properties of the elastic body are the Young's modulus  $E = 2.1 \times 10^{11} \text{ Pa}$  and the Poisson's ration  $\nu = 0.3$ . This test was treated in [56]. A uniform mesh was taken with 51 nodes at each side and the finite element used is the  $P_2$  element.

The deformed configuration of the body is shown in the Figure 2.12b with an amplification factor.

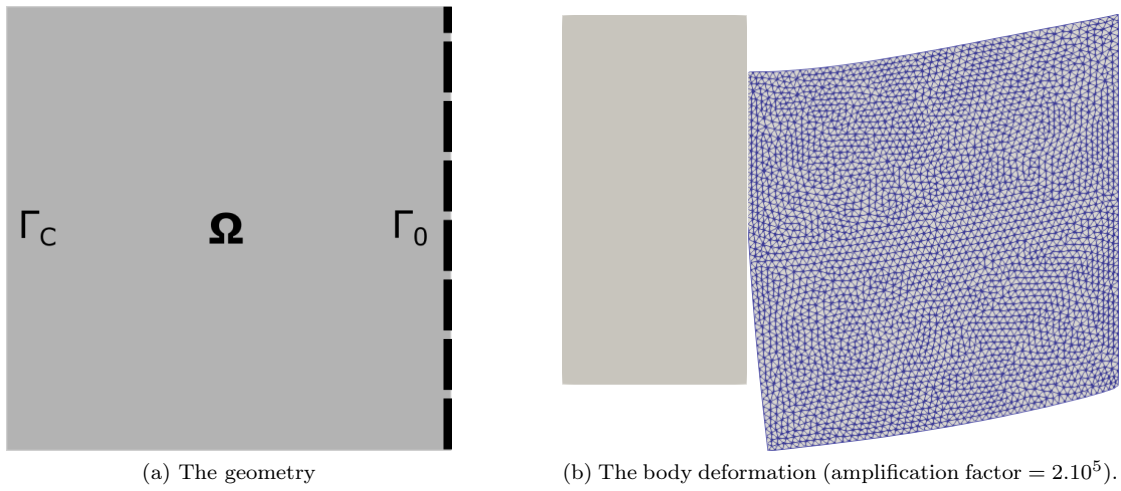
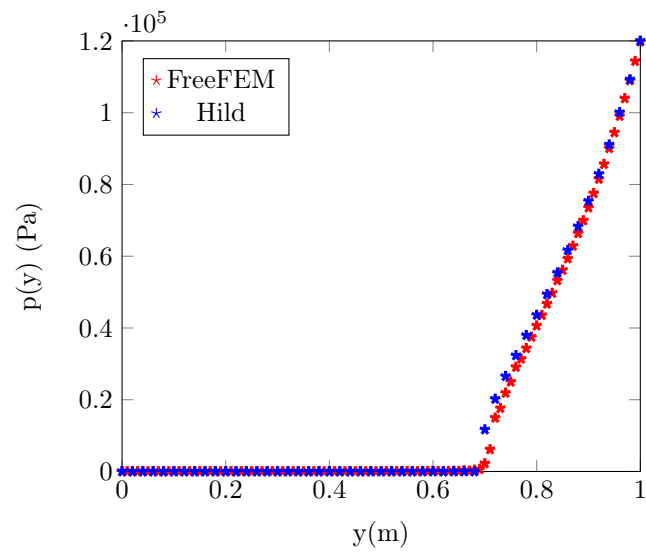


Figure 2.12 – The square iron problem

In Figure 2.13, the contact pressure on the left side  $\Gamma_C$  is plotted in comparison with the values found in [56].

Figure 2.13 – Contact pressure at the side  $\Gamma_C$  of the body



# Penalty method

## Outline of the current chapter

---

<b>3.1 Signorini's problem for linear elasticity</b>	<b>56</b>
<b>3.2 Finite deformations</b>	<b>67</b>
<b>3.3 Contact between two bodies in linear elasticity</b>	<b>69</b>
<b>3.4 Symmetric contact formulation</b>	<b>70</b>
<b>3.5 Numerical integration</b>	<b>71</b>
<b>3.6 Symmetric contact algorithm using penalty method</b>	<b>75</b>
<b>3.7 Projection of the integration points</b>	<b>76</b>
<b>3.8 Smoothing techniques</b>	<b>79</b>
3.8.1 Bézier curve . . . . .	79
<b>3.9 Numerical validations</b>	<b>80</b>
3.9.1 Compression of two elastic blocks with imposed displacement . . . . .	80
3.9.2 Contact between two cylinders . . . . .	82

---

In this chapter, an algorithm to solve frictionless contact problems is presented. A fixed point method is therefore used in order to transform the contact problem into a sequence of a minimization problems with linear (or affine) constraints especially in the case of large deformations. Two penalty functionals were employed to take care of the constraints, indeed each penalty functional penalizes the integration points to penetrate into the opposite body, which make the formulation and the algorithm symmetric. As the interior point is used to solve the minimization problem (we impose some bounds on the displacement field), the penalty functionals are chosen to be smooth enough. Some theoretical aspects are also addressed in this chapter.

### 3.1 Signorini's problem for linear elasticity

In order to simplify, we begin to consider Signorini's problem which is the contact between a body and a rigid foundation. In this section we treat only the linear elastic materials. Let  $\Omega$  denotes the body and  $\Gamma = \partial\Omega$  its boundary.  $\Gamma_0 \subset \Gamma$  denotes the boundary part where a displacement is imposed with  $meas(\Gamma_0) > 0$ ,  $\Gamma_1 \subset \Gamma$  is the boundary part where a traction vector is applied, finally  $\Gamma_C \subset \Gamma$  denotes the potential contact area. The boundary parts  $\Gamma_0, \Gamma_1, \Gamma_C$  form a partition of the body boundary  $\Gamma$ .

By imposing a null displacement on  $\Gamma_0$ , the admissible set is defined as follows

$$\mathbf{V} = \{\mathbf{v} \in \mathbf{H}^1(\Omega) \mid \mathbf{v} = 0 \text{ a.e on } \Gamma_0\} \quad (3.1)$$

where  $\mathbf{H}^1(\Omega) = H^1(\Omega) \times H^1(\Omega)$ , endowed with the broken norm:

$$\|\mathbf{u}\|_1 = \|(u_1, u_2)\|_1 = (\|u_1\|_1^2 + \|u_2\|_1^2)^{\frac{1}{2}} \quad (3.2)$$

The solution (the displacement field) of the contact problem involving a linear elastic body, can be written as the following minimization problem

$$\min_{\mathbf{v} \in \mathbf{K}} \frac{1}{2} a(\mathbf{v}, \mathbf{v}) - f(\mathbf{v}) \quad (3.3)$$

where  $\mathbf{K} = \{\mathbf{v} \in \mathbf{V} \mid \mathbf{v} \cdot \mathbf{n} + g_N \geq 0 \text{ a.e on } \Gamma_C\} = \{\mathbf{v} \in \mathbf{V} \mid \bar{g}_N - \mathbf{v} \cdot \mathbf{n} \leq 0 \text{ a.e on } \Gamma_C\}$ , the set where the displacement field satisfies the non-penetration condition for the Signorini's problem,  $g_N$  denotes the initial normal gap and  $\bar{g}_N = -g_N$ , finally  $\mathbf{n}$  is the normal vector at the foundation. The applications  $a(\cdot, \cdot)$  and  $f(\cdot)$  (see equations (1.32) and (1.33)) have the following properties.

$a(\cdot, \cdot) : \mathbf{V} \times \mathbf{V} \rightarrow \mathbb{R}$  is a continuous bilinear application, and it is elliptic.

$f(\cdot) : \mathbf{V} \rightarrow \mathbb{R}$  is a linear continuous application. Otherwise speaking  $f \in \mathbf{V}'$ , the dual of  $\mathbf{V}$ .

In order to present some theory results we need to recall the following definitions.

**Definition 3.1.** Let  $E$  be a Banach space, the functional  $F : E \rightarrow \mathbb{R}$  is said to be weakly sequentially lower semicontinuous in  $u \in E$ , if for each sequence  $u_n$  such that  $u_n$  converges weakly to  $u$  in  $E$ :  $u_n \rightharpoonup u$ , we have

$$F(u) \leq \liminf_{n \rightarrow +\infty} F(u_n) \quad (3.4)$$

**Definition 3.2.** The functional  $F : E \rightarrow \mathbb{R}$  is said to be coercive iff

$$\lim_{\|v\| \rightarrow +\infty} F(v) = +\infty \quad (3.5)$$

**Theorem 3.1.** The elastic energy  $E(\mathbf{v}) = \frac{1}{2} a(\mathbf{v}, \mathbf{v}) - f(\mathbf{v})$  is strictly convex.

*Proof.* Let  $\theta \in [0, 1]$  and  $\mathbf{u}, \mathbf{v} \in \mathbf{V}$ , after some calculations we obtain

$$E((1 - \theta)\mathbf{u} + \theta\mathbf{v}) - (1 - \theta)E(\mathbf{u}) - \theta E(\mathbf{v}) = -\frac{1}{2}\theta(1 - \theta)a(\mathbf{u} - \mathbf{v}, \mathbf{u} - \mathbf{v}) \quad (3.6)$$

$$\Rightarrow E((1 - \theta)\mathbf{u} + \theta\mathbf{v}) = (1 - \theta)E(\mathbf{u}) + \theta E(\mathbf{v}) - \frac{1}{2}\theta(1 - \theta)a(\mathbf{u} - \mathbf{v}, \mathbf{u} - \mathbf{v}) \quad (3.7)$$

Because the application  $a$  is elliptic then  $a(\mathbf{u} - \mathbf{v}, \mathbf{u} - \mathbf{v}) \geq M\|\mathbf{u} - \mathbf{v}\|^2$  with  $M > 0$ , therefore

$$E((1 - \theta)\mathbf{u} + \theta\mathbf{v}) \leq (1 - \theta)E(\mathbf{u}) + \theta E(\mathbf{v}) \quad (3.8)$$

If  $\mathbf{u} \neq \mathbf{v}$  and  $0 < \theta < 1$  then  $-\frac{1}{2}\theta(1 - \theta)a(\mathbf{u} - \mathbf{v}, \mathbf{u} - \mathbf{v}) < 0$ , thus

$$E((1 - \theta)\mathbf{u} + \theta\mathbf{v}) < (1 - \theta)E(\mathbf{u}) + \theta E(\mathbf{v}) \quad (3.9)$$

Hence the strict convexity.  $\square$

There exists a unique solution  $\mathbf{u}$  of the problem (3.3), indeed we can write the problem in the form of a variational inequality and use Stampacchia's theorem. Otherwise we can prove the existence and the uniqueness as follows: the set  $\mathbf{K}$  is closed and convex, the energy  $E$  is continuous and convex then  $E$  is weakly sequentially lower semicontinuous, as  $E$  is coercive then there exists a solution to the problem (3.3), this solution is unique because  $E$  is strictly convex.

## Boundary space

The open domain  $\Omega \subset \mathbb{R}^d$  is supposed to be a bounded set, with a Lipschitz-continuous (respectively  $C^1$ ) boundary  $\partial\Omega$ . Otherwise speaking and without going into details, there exist a finite number (let's say  $R$ ) of local coordinate systems  $(x'_1, \dots, x'_d)$ ,  $1 \leq r \leq R$  and  $R$  corresponding Lipschitz-continuous (respectively  $C^1$ ) functions  $\phi_r : \mathbb{R}^{d-1} \rightarrow \mathbb{R}$ , and two constants  $\alpha > 0$ ,  $\beta > 0$  such that (see also Figure 3.1).

$$\partial\Omega = \bigcup_{i=1}^R \{(x'_r, x'_d) \mid x'_d = \phi_r(x'_r); \|x'_r\| < \alpha\} \quad \text{where } x'_r = (x'_1, \dots, x'_{d-1}) \quad (3.10)$$

$$\{(x'_r, x'_d) \mid \phi_r(x'_r) < x'_d < \phi_r(x'_r) + \beta; \|x'_r\| \leq \alpha\} \subset \Omega \quad \forall 1 \leq r \leq R \quad (3.11)$$

$$\{(x'_r, x'_d) \mid \phi_r(x'_r) - \beta < x'_d < \phi_r(x'_r); \|x'_r\| \leq \alpha\} \subset (\bar{\Omega})^c \quad \forall 1 \leq r \leq R \quad (3.12)$$

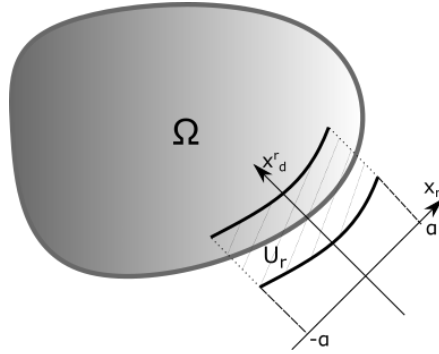


Figure 3.1 –  $\Omega$  and one of its local coordinate systems

where  $\|\cdot\|$  denotes the Euclidean norm in  $\mathbb{R}^{d-1}$ . For more details see for example (chapter 1 of [29]).

Each function  $\phi_r$  can define locally a surface measure, therefore to define the integral over  $\partial\Omega$ , a covering of the boundary is done with the sets

$$U_r = \{(x'_r, x'_d) \mid \phi_r(x'_r) - \beta < x'_d < \phi_r(x'_r) + \beta; \|x'_r\| < \alpha\} \quad (3.13)$$

and a partition of the unity of this covering is needed.

The partition of the unity of the covering  $\{U_r \mid 1 \leq r \leq R\}$  corresponds to the functions  $\theta_r : \mathbb{R}^d \rightarrow [0, 1]$  with  $1 \leq r \leq R$  such that

$$\begin{cases} \text{supp}(\theta_r) \subset U_r & \forall 1 \leq r \leq R \\ \sum_{i=1}^R \theta_r(x) = 1 & \forall x \in \partial\Omega \end{cases} \quad (3.14)$$

Finally the integral over  $\partial\Omega$  of a function  $v$  is defined as follows

$$\int_{\partial\Omega} v \, ds := \sum_{r=1}^R \int_{\|x'_r\| < \alpha} v(x'_r, \phi_r(x'_r)) \cdot \theta_r(x'_r, \phi_r(x'_r)) \cdot \sqrt{1 + \|\nabla\phi_r\|^2} \, dx'_r \quad (3.15)$$

The space  $L^p(\partial\Omega)$  is equipped with the norm

$$\|v\|_{L^p} = \left( \int_{\partial\Omega} |v|^p \, ds \right)^{\frac{1}{p}} \quad (3.16)$$

If  $\Gamma_C \subset \partial\Omega$  then

$$\int_{\Gamma_C} v \, ds = \int_{\partial\Omega} v \cdot \mathbf{1}_{\Gamma_C} \, ds \quad (3.17)$$

## Penalty method

Taking a penalty factor  $\mu > 0$ , we consider the following penalized problem

$$\min_{\mathbf{v} \in \mathbf{V}} \frac{1}{2} a(\mathbf{v}, \mathbf{v}) - f(\mathbf{v}) + \mu P(\mathbf{v}) \quad (3.18)$$

We note that it's an unconstrained minimization problem. The penalty functional  $P(\mathbf{v})$  is defined by

$$P(\mathbf{v}) = \int_{\Gamma_C} \eta(\bar{g}_N - \mathbf{v} \cdot \mathbf{n}) \, ds \quad (3.19)$$

In the following the function  $\eta(\cdot) \in \mathcal{P}$ , where  $\mathcal{P} = \{f \in C^2(\mathbb{R})\}$  is the set of functions  $f$  with the following properties

1.  $f \in C^2(\mathbb{R})$
2.  $f(x) = 0 \, \forall x \leq 0$  and  $f(x) > 0 \, \forall x > 0$

3.  $f$  is a convex function
4. There exist five constants  $C_1, C_2, C_3, C_4, C_5 \geq 0$  such that the function  $f$  and its derivative  $f'$  satisfy

$$\begin{cases} |f(x)| \leq C_1 x^2 + C_2 |x| + C_3 \\ |f'(x)| \leq C_4 |x| + C_5 \end{cases} \quad (3.20)$$

An example of functions that belong to the set  $\mathcal{P}$  is presented next.

### Example 3.1

1. Let the function  $f : \mathbb{R} \rightarrow \mathbb{R}$  be defined as follows

$$f(x) = \begin{cases} 0 & \text{if } x < 0 \\ x^3 & \text{if } 0 \leq x < 1 \\ 3x^2 - 3x + 1 & \text{if } 1 \leq x \end{cases} \quad (3.21)$$

The function  $f$  is  $C^2$ , convex because  $f'' \geq 0$ . Finally  $f(x) \leq 3x^2 + 3|x| + 1$  and  $f'(x) \leq 6|x| + 3$ , thus  $f \in \mathcal{P}$ .

2. Let  $0 < \nu < 1$ , the function  $f_\nu : \mathbb{R} \rightarrow \mathbb{R}$  is defined as follows

$$f_\nu(x) = \begin{cases} 0 & \text{if } x < 0 \\ \frac{1}{6\nu} x^3 & \text{if } 0 \leq x < \nu \\ \frac{1}{2} x^2 - \frac{\nu}{2} x + \frac{\nu^2}{6} & \text{if } \nu \leq x \end{cases} \quad (3.22)$$

The function  $f_\nu$  is  $C^2$ , convex because  $f_\nu'' \geq 0$ . Finally  $f_\nu(x) \leq \frac{1}{\nu} x^2 + \frac{\nu}{2} |x| + \frac{\nu^2}{6}$  and  $f_\nu'(x) \leq \frac{1}{\nu} |x| + \frac{\nu}{2}$ , thus  $f_\nu \in \mathcal{P}$ . We introduce this function in order to use it for the approximation of the function  $\max(0, x)^2$  (which is only  $C^1$ ), where theoretical results for the penalty formulation are available.

We suppose in the following that  $\bar{g}_N \in L^\infty(\Gamma_C)$ ,  $\mathbf{n} \in \mathbf{L}^\infty(\Gamma_C)$  and  $\eta \in \mathcal{P}$ . Thus by the fourth property of the set  $\mathcal{P}$  (Equation(3.20)), the functional  $P$  defined in (3.19) is well defined.

The functional  $P$  is convex, because the trace is linear and  $\eta$  is convex, indeed let  $\mathbf{u}, \mathbf{v} \in \mathbf{V}$  and  $\theta \in [0, 1]$  then

$$\begin{aligned} P(\theta \mathbf{u} + (1 - \theta) \mathbf{v}) &= \int_{\Gamma_C} \eta(\bar{g}_N - (\theta \mathbf{u} + (1 - \theta) \mathbf{v}) \cdot \mathbf{n}) \, ds \\ &= \int_{\Gamma_C} \eta(\theta(\bar{g}_N - \mathbf{u} \cdot \mathbf{n}) + (1 - \theta)(\bar{g}_N - \mathbf{v} \cdot \mathbf{n})) \, ds \\ &\leq \theta \int_{\Gamma_C} \eta(\bar{g}_N - \mathbf{u} \cdot \mathbf{n}) \, ds + (1 - \theta) \int_{\Gamma_C} \eta(\bar{g}_N - \mathbf{v} \cdot \mathbf{n}) \, ds \\ &= \theta P(\mathbf{u}) + (1 - \theta) P(\mathbf{v}) \end{aligned}$$

Let  $\mathcal{E}_\mu(\mathbf{v}) = \frac{1}{2}a(\mathbf{v}, \mathbf{v}) - f(\mathbf{v}) + \mu P(\mathbf{v})$ , then the functional  $\mathcal{E}_\mu$  is strictly convex, and as  $P \geq 0$  then  $\mathcal{E}_\mu$  is coercive. In order to prove the existence and uniqueness of the problem (3.18), it remains to prove that the functional  $\mathcal{E}_\mu$  is weakly sequentially lower semicontinuous.

**Theorem 3.2.** *Given  $\eta \in \mathcal{P}$ , then the functional  $P$  is continuous*

*Proof.* From the trace theorem we have

$$\|\mathbf{v}\|_{L^2(\Gamma)} \leq C\|\mathbf{v}\|_1 \quad (3.23)$$

Let  $\mathbf{u}_n$  be a sequence such that  $\mathbf{u}_n \xrightarrow{n \rightarrow +\infty} \mathbf{u}$  in  $\mathbf{V}$ , as

$$\|\mathbf{u}_n - \mathbf{u}\|_{L^2(\Gamma)} \leq C\|\mathbf{u}_n - \mathbf{u}\|_1 \quad (3.24)$$

Then  $\mathbf{u}_n \xrightarrow{n \rightarrow +\infty} \mathbf{u}$  in  $L^2(\Gamma)$ . We have

$$\int_{\Gamma} \|\mathbf{u}_n - \mathbf{u}\|^2 ds = \sum_{r=1}^R \int_{C_r} \|\mathbf{u}_n - \mathbf{u}\|^2 \cdot \theta_r \cdot J dx_r \quad (3.25)$$

The notations have been lightened by taking  $J = \sqrt{1 + \|\nabla \phi_r\|^2}$ ,  $C_r = \{\|x_r\| < \alpha\}$  and a convention:  $f(x_r) = f_r(x_r, \phi(x_r))$  for an arbitrary function  $f$ . As  $\mathbf{u}_n \xrightarrow{n \rightarrow +\infty} \mathbf{u}$  in  $L^2(\Gamma)$  then from the equation (3.25) we obtain that:

$$\sqrt{\theta_r} \mathbf{u}_n \rightarrow \sqrt{\theta_r} \mathbf{u} \text{ in } \mathbf{L}^2(C_r) \quad \forall 1 \leq r \leq R \quad (3.26)$$

Let  $w_n = \bar{g}_N - \mathbf{u}_n \cdot \mathbf{n}$  and  $w = \bar{g}_N - \mathbf{u} \cdot \mathbf{n}$  then

$$\sqrt{\theta_r} w_n \mathbf{1}_{\Gamma_C} \rightarrow \sqrt{\theta_r} w \mathbf{1}_{\Gamma_C} \text{ in } L^2(C_r) \quad \forall 1 \leq r \leq R \quad (3.27)$$

For any subsequence  $\sigma$ , and thanks to the reciprocal of the dominated convergence theorem, there exist a subsequence  $\sigma \circ \tau$  and  $g_r \in L^2(C_r)$  such that

$$\sqrt{\theta_r} w_{\sigma \circ \tau(n)} \mathbf{1}_{\Gamma_C} \rightarrow \sqrt{\theta_r} w \mathbf{1}_{\Gamma_C} \text{ a.e. } \quad \forall 1 \leq r \leq R \quad (3.28)$$

$$\sqrt{\theta_r} |w_{\sigma \circ \tau(n)}| \mathbf{1}_{\Gamma_C} \leq g_r \text{ a.e. } \quad \forall 1 \leq r \leq R \quad (3.29)$$

From equation (3.28) we have

$$\theta_r w_{\sigma \circ \tau(n)} \mathbf{1}_{\Gamma_C} \rightarrow \theta_r w \mathbf{1}_{\Gamma_C} \text{ a.e. } \quad \forall 1 \leq r \leq R \quad (3.30)$$

As  $\sum_{r=1}^R \theta_r = 1$  then

$$w_{\sigma \circ \tau(n)} \mathbf{1}_{\Gamma_C} \rightarrow w \mathbf{1}_{\Gamma_C} \text{ a.e. } \quad (3.31)$$

As  $\eta$  is continuous then

$$\eta(w_{\sigma \circ \tau(n)}) \mathbf{1}_{\Gamma_C} \rightarrow \eta(w) \mathbf{1}_{\Gamma_C} \text{ a.e. } \quad (3.32)$$

From equation (3.29):

$$\theta_r w_{\sigma \circ \tau(n)}^2 \mathbf{1}_{\Gamma_C} \leq g_r^2 \text{ a.e. } \quad \forall 1 \leq r \leq R \quad (3.33)$$

The function  $\eta \in \mathcal{P}$  (see equation (3.20)), thus from equation (3.33) and (3.29) we deduce that

$$\theta_r \eta(w_{\sigma \circ \tau(n)}) \mathbf{1}_{\Gamma_C} \leq \theta_r (C_1 w_{\sigma \circ \tau(n)}^2 + C_2 |w_{\sigma \circ \tau(n)}| + C_3) \mathbf{1}_{\Gamma_C} \quad (3.34)$$

$$\leq C_1 g_r^2 + C_2 g_r \sqrt{\theta_r} + C_3 \theta_r \quad (\in L^1(C_r)) \text{ a.e. } \forall 1 \leq r \leq R \quad (3.35)$$

Using the equations (3.32) and (3.35) and the dominated convergence theorem we obtain:

$$\int_{C_r} \eta(w_{\sigma \circ \tau(n)}) \cdot \theta_r \cdot \mathbf{1}_{\Gamma_C} \cdot J \, dx_r \longrightarrow \int_{C_r} \eta(w) \cdot \theta_r \cdot \mathbf{1}_{\Gamma_C} \cdot J \, dx_r \quad \forall 1 \leq r \leq R \quad (3.36)$$

By summing over  $r$  we obtain finally

$$P(\mathbf{u}_{\sigma \circ \tau(n)}) \longrightarrow P(\mathbf{u}) \quad (3.37)$$

Since it's true for any subsequence  $\sigma$ , therefore  $P$  is continuous.  $\square$

**Theorem 3.3.** *Given  $\eta \in \mathcal{P}$ , then the functional  $P$  is Gâteaux differentiable, and it's Gâteaux derivative is equal to*

$$DP(\mathbf{u}) \cdot \mathbf{v} = - \int_{\Gamma_C} \eta'(\bar{g}_N - u_N) \cdot v_N \, ds \quad (3.38)$$

where  $u_N = \mathbf{u} \cdot \mathbf{n}$  and  $v_N = \mathbf{v} \cdot \mathbf{n}$ .

*Proof.* First we have to prove that for a fixed  $\mathbf{u}$

$$\frac{P(\mathbf{u} + t\mathbf{v}) - P(\mathbf{u})}{t} \xrightarrow[t \rightarrow 0]{} - \int_{\Gamma_C} \eta'(\bar{g}_N - u_N) \cdot v_N \, ds \quad (3.39)$$

Let  $\zeta(\mathbf{v}) = \eta(\bar{g}_N - \mathbf{v} \cdot \mathbf{n})$ , then

$$\zeta(\mathbf{u} + t\mathbf{v}) - \zeta(\mathbf{u}) = \eta(\bar{g}_N - u_N - tv_N) - \eta(\bar{g}_N - u_N) \quad (3.40)$$

$$= \int_0^1 \eta'(\bar{g}_N - u_N - ltv_N) (-tv_N) \, dl \quad (3.41)$$

Thus for  $t \neq 0$

$$\frac{\zeta(\mathbf{u} + t\mathbf{v}) - \zeta(\mathbf{u})}{t} = \int_0^1 \eta'(\bar{g}_N - u_N - ltv_N) (-v_N) \, dl \quad (3.42)$$

We shall use the same abbreviated notations of the theorem 3.2 proof.

$$\begin{aligned} & \int_{C_r} \left| \frac{\zeta(\mathbf{u} + t\mathbf{v}) - \zeta(\mathbf{u})}{t} + \eta'(\bar{g}_N - u_N) \cdot v_N \right| \cdot \theta_r \cdot \mathbf{1}_{\Gamma_C} \cdot J \, dx_r \leq \\ & \int_{C_r} \int_0^1 | -\eta'(\bar{g}_N - u_N - ltv_N) + \eta'(\bar{g}_N - u_N) | |v_N| \cdot \theta_r \cdot \mathbf{1}_{\Gamma_C} \cdot J \, dl \, dx_r \end{aligned} \quad (3.43)$$

Otherwise  $\eta'$  is continuous then

$$| -\eta'(\bar{g}_N - u_N - ltv_N) + \eta'(\bar{g}_N - u_N) | |v_N| \cdot \theta_r \cdot \mathbf{1}_{\Gamma_C} \cdot J \xrightarrow[t \rightarrow 0]{} 0 \quad (3.44)$$

We suppose that  $|t| \leq 1$ . We have  $l \leq 1$  and  $\eta'(x) \leq C_4|x| + C_5$  because  $\eta \in \mathcal{P}$  (see equation

(3.20)), thus

$$| -\eta'(\bar{g}_N - u_N - tv_N) + \eta'(\bar{g}_N - u_N) | |v_N|. \theta_r. \mathbf{1}_{\Gamma_C}. J \leq f \quad (\text{a function } \in L^1(C_r)) \quad (3.45)$$

Therefore using Fubini's theorem and the dominated convergence theorem for the Fubini's measure, we obtain  $\forall 1 \leq r \leq R$

$$\int_{C_r} \frac{\zeta(\mathbf{u} + t\mathbf{v}) - \zeta(\mathbf{u})}{t} \cdot \theta_r. \mathbf{1}_{\Gamma_C}. J \, dx_r \xrightarrow{t \rightarrow 0} - \int_{C_r} \eta'(\bar{g}_N - u_N). v_N. \theta_r. \mathbf{1}_{\Gamma_C}. J \, dx_r \quad (3.46)$$

Therefore by summing over  $r$

$$\frac{P(\mathbf{u} + t\mathbf{v}) - P(\mathbf{u})}{t} \xrightarrow{t \rightarrow 0} - \int_{\Gamma_C} \eta'(\bar{g}_N - u_N). v_N \, ds \quad (3.47)$$

In addition

$$\begin{aligned} \left| \int_{\Gamma_C} \eta'(\bar{g}_N - u_N). v_N \, ds \right| &= \left| \int_{\Gamma} \eta'(\bar{g}_N - u_N). v_N. \mathbf{1}_{\Gamma_C} \, ds \right| \\ &\leq \int_{\Gamma} |\eta'(\bar{g}_N - u_N)| \cdot |v_N|. \mathbf{1}_{\Gamma_C} \, ds \\ &\leq \|\eta'(\bar{g}_N - u_N). \mathbf{1}_{\Gamma_C}\|_{L^2(\Gamma)} \|v_N. \mathbf{1}_{\Gamma_C}\|_{L^2(\Gamma)} \quad (\text{Cauchy-Schwarz}) \\ &\leq C \|\eta'(\bar{g}_N - u_N). \mathbf{1}_{\Gamma_C}\|_{L^2(\Gamma)} \|\mathbf{v}\|_{\mathbf{L}^2(\Gamma)} \\ &\leq C \|\eta'(\bar{g}_N - u_N). \mathbf{1}_{\Gamma_C}\|_{L^2(\Gamma)} \|\mathbf{v}\|_1 \quad (\text{Trace theorem}) \end{aligned}$$

Therefore the functional  $\int_{\Gamma_C} \eta'(\bar{g}_N - u_N). v_N \, ds$  is continuous, and it's already linear.  $\square$

**Corollary 3.1.** *The problem (3.18) has a unique solution.*

*Proof.* The functional  $\mathcal{E}_\mu = \frac{1}{2}a(\mathbf{v}, \mathbf{v}) - f(\mathbf{v}) + \mu P(\mathbf{v})$  is strictly convex, and as  $P \geq 0$  then  $\mathcal{E}_\mu$  is coercive. The functional  $\mathcal{E}_\mu$  is continuous from the theorem 3.2 and is convex then it's weakly sequentially lower semicontinuous, or we can use the theorem 3.3 to say that it is Gâteaux differentiable, and because it is convex then it's weakly sequentially lower semicontinuous.  $\square$

**Theorem 3.4.** *Using the same assumptions as above, let the penalty factor  $\mu$  tends to  $+\infty$ , and  $\mathbf{u}_\mu$  the solution of the problem (3.18), then there exist a subsequence of  $\mathbf{u}_\mu$  that converges weakly to the solution  $\mathbf{u}$  of the problem (3.3).*

*Proof.* let  $F(\mathbf{v}) = \frac{1}{2}a(\mathbf{v}, \mathbf{v}) - f(\mathbf{v})$ , because  $\mathbf{u}_\mu$  minimizes  $\mathcal{E}_\mu(\mathbf{v})$  then

$$F(\mathbf{u}_\mu) + \mu P(\mathbf{u}_\mu) \leq F(\mathbf{v}) + \mu P(\mathbf{v}) \quad \forall \mathbf{v} \in \mathbf{V} \quad (3.48)$$

Let  $\mathbf{v} \in \mathbf{K}$ , then  $P(\mathbf{v}) = 0$  and

$$F(\mathbf{u}_\mu) + \mu P(\mathbf{u}_\mu) \leq F(\mathbf{v}) \quad \forall \mathbf{v} \in \mathbf{K} \quad (3.49)$$

Because  $P(\mathbf{u}_\mu) \geq 0$  then

$$F(\mathbf{u}_\mu) \leq F(\mathbf{v}) \quad \forall \mathbf{v} \in \mathbf{K} \quad (3.50)$$

Fixing a  $\mathbf{v} \in \mathbf{V}$  and using the expression (3.50) and the fact that  $F$  is coercive, then  $\exists C > 0$  such that

$$\|\mathbf{u}_\mu\|_1 \leq C \quad (3.51)$$

Since  $\mathbf{V}$  is reflexive then  $\exists$  a subsequence of  $\mathbf{u}_\mu$  (also denoted  $\mathbf{u}_\mu$ ) and  $\mathbf{u} \in \mathbf{V}$  such that  $\mathbf{u}_\mu$  converges weakly to  $\mathbf{u}$ :  $\mathbf{u}_\mu \rightharpoonup \mathbf{u}$ . The functional  $F$  is weakly sequentially lower semicontinuous (see above) then

$$F(\mathbf{u}) \leq \liminf_{\mu \rightarrow +\infty} F(\mathbf{u}_\mu) \quad (3.52)$$

Because  $P \geq 0$  then

$$F(\mathbf{u}) \leq \liminf_{\mu \rightarrow +\infty} F(\mathbf{u}_\mu) \leq \liminf_{\mu \rightarrow +\infty} \mathcal{E}_\mu(\mathbf{u}_\mu) \quad (3.53)$$

Using the expression (3.49) we obtain

$$F(\mathbf{u}) \leq \liminf_{\mu \rightarrow +\infty} \mathcal{E}_\mu(\mathbf{u}_\mu) \leq F(\mathbf{v}) \quad \forall \mathbf{v} \in \mathbf{K} \quad (3.54)$$

Thus it remains to prove that  $\mathbf{u} \in \mathbf{K}$ . Let a  $\mathbf{v}^* \in \mathbf{K}$  be fixed then

$$F(\mathbf{u}_\mu) + \mu P(\mathbf{u}_\mu) \leq F(\mathbf{v}^*) \quad (3.55)$$

$$\Rightarrow P(\mathbf{u}_\mu) \leq \frac{1}{\mu} (F(\mathbf{v}^*) - F(\mathbf{u}_\mu)) \quad (3.56)$$

$$\Rightarrow 0 \leq P(\mathbf{u}_\mu) \leq \frac{1}{\mu} (|F(\mathbf{v}^*)| + |F(\mathbf{u}_\mu)|) \quad (3.57)$$

Otherwise we have  $\|\mathbf{u}_\mu\|_1 \leq C$  and  $F(\mathbf{u}) = \frac{1}{2}a(\mathbf{u}, \mathbf{u}) - f(\mathbf{u})$

$$|F(\mathbf{u}_\mu)| \leq M_1 \|\mathbf{u}_\mu\|_1^2 + m_1 \|\mathbf{u}_\mu\|_1 \leq D \quad (3.58)$$

The expression (3.58) follows from the bilinearity and the linearity of  $a(\cdot, \cdot)$  and  $f(\cdot)$  respectively. We conclude that  $\exists C \geq 0$

$$0 \leq P(\mathbf{u}_\mu) \leq C \frac{1}{\mu} \quad (3.59)$$

Then

$$\liminf_{\mu \rightarrow +\infty} P(\mathbf{u}_\mu) = 0 \quad (3.60)$$

The functional  $P$  is weakly sequentially lower semicontinuous then

$$P(\mathbf{u}) \leq \liminf_{\mu \rightarrow +\infty} P(\mathbf{u}_\mu) = 0 \quad (3.61)$$

Thus  $P(\mathbf{u}) = 0$  and  $\eta(\bar{g}_N - \mathbf{u}, \mathbf{n}) = 0$  a.e. From the second property of the function  $\eta$  we conclude that  $\bar{g}_N - \mathbf{u}, \mathbf{n} \leq 0$  a.e and thus  $\mathbf{u} \in \mathbf{K}$

Finally

$$\mathbf{u} \in \mathbf{K} \text{ and } F(\mathbf{u}) \leq F(\mathbf{v}) \quad \forall \mathbf{v} \in \mathbf{K} \quad (3.62)$$

□

We can prove that the sequence  $\mathbf{u}_\mu$  converges strongly to  $\mathbf{u}$  by the following theorem.

**Theorem 3.5.** *Using the same notations as in the theorem 3.4, the sequence  $\mathbf{u}_\mu$  converges*

strongly to  $\mathbf{u}$ :

$$\mathbf{u}_\mu \xrightarrow{\mu \rightarrow +\infty} \mathbf{u} \quad (3.63)$$

*Proof.* Taking  $\mathbf{v} = \mathbf{u}$  in the expression (3.49)

$$\frac{1}{2}a(\mathbf{u}_\mu, \mathbf{u}_\mu) - f(\mathbf{u}_\mu) + \mu P(\mathbf{u}_\mu) \leq \frac{1}{2}a(\mathbf{u}, \mathbf{u}) - f(\mathbf{u}) \quad (3.64)$$

$$\frac{1}{2}a(\mathbf{u}_\mu, \mathbf{u}_\mu) + \mu P(\mathbf{u}_\mu) \leq \frac{1}{2}a(\mathbf{u}, \mathbf{u}) - f(\mathbf{u}) + f(\mathbf{u}_\mu) \quad (3.65)$$

Because  $P(\mathbf{u}_\mu) \geq 0$

$$a(\mathbf{u}_\mu, \mathbf{u}_\mu) \leq a(\mathbf{u}, \mathbf{u}) + 2(f(\mathbf{u}_\mu) - f(\mathbf{u})) \quad (3.66)$$

As  $\mathbf{u}_\mu \rightharpoonup \mathbf{u}$  weakly and  $f \in \mathbf{V}'$  then  $f(\mathbf{u}_\mu) \xrightarrow{\mu \rightarrow +\infty} f(\mathbf{u})$ . Therefore

$$\liminf_{\mu \rightarrow +\infty} a(\mathbf{u}_\mu, \mathbf{u}_\mu) \leq a(\mathbf{u}, \mathbf{u}) \quad (3.67)$$

and

$$\limsup_{\mu \rightarrow +\infty} a(\mathbf{u}_\mu, \mathbf{u}_\mu) \leq a(\mathbf{u}, \mathbf{u}) \quad (3.68)$$

The application  $a(\cdot, \cdot)$  is weakly sequentially lower semicontinuous then

$$a(\mathbf{u}, \mathbf{u}) \leq \liminf_{\mu \rightarrow +\infty} a(\mathbf{u}_\mu, \mathbf{u}_\mu) \quad (3.69)$$

we conclude from (3.67), (3.68) and (3.69) that

$$\begin{cases} \liminf_{\mu \rightarrow +\infty} a(\mathbf{u}_\mu, \mathbf{u}_\mu) = a(\mathbf{u}, \mathbf{u}) \\ \limsup_{\mu \rightarrow +\infty} a(\mathbf{u}_\mu, \mathbf{u}_\mu) = a(\mathbf{u}, \mathbf{u}) \end{cases} \quad (3.70)$$

We deduce from (3.70) that

$$\lim_{\mu \rightarrow +\infty} a(\mathbf{u}_\mu, \mathbf{u}_\mu) = a(\mathbf{u}, \mathbf{u}) \quad (3.71)$$

Besides

$$a(\mathbf{u} - \mathbf{u}_\mu, \mathbf{u} - \mathbf{u}_\mu) = a(\mathbf{u}, \mathbf{u}) - 2a(\mathbf{u}, \mathbf{u}_\mu) + a(\mathbf{u}_\mu, \mathbf{u}_\mu) \quad (3.72)$$

$\mathbf{u}_\mu \rightharpoonup \mathbf{u}$  weakly, then  $a(\mathbf{u}, \mathbf{u}_\mu) \xrightarrow{\mu \rightarrow +\infty} a(\mathbf{u}, \mathbf{u})$ . From (3.71) and (3.72) we obtain

$$a(\mathbf{u} - \mathbf{u}_\mu, \mathbf{u} - \mathbf{u}_\mu) \xrightarrow{\mu \rightarrow +\infty} 0$$

Finally because the application  $a$  is elliptic

$$\|\mathbf{u} - \mathbf{u}_\mu\|_1^2 \leq \frac{1}{M} a(\mathbf{u} - \mathbf{u}_\mu, \mathbf{u} - \mathbf{u}_\mu) \xrightarrow{\mu \rightarrow +\infty} 0 \quad (3.73)$$

Thus  $\mathbf{u}_\mu$  converges strongly to  $\mathbf{u}$ .  $\square$

### Error analysis

The penalty problem is often employed with the following penalty functional

$$P^+(\mathbf{v}) = \frac{1}{2} \int_{\Gamma_C} ((\bar{g}_N - \mathbf{v} \cdot \mathbf{n})^+)^2 ds \quad (3.74)$$

where  $x^+ = \max(x, 0)$ . Otherwise speaking in our formulation the function  $\eta(x)$  is replaced by the function  $\frac{1}{2} \max(x, 0)^2$ , which is only of class  $C^1$ .

As the errors estimates were studied using the penalty functional (equation (3.74)) as in [22, 26, 70], then we will choose a penalty function  $\eta \in \mathcal{P}$  such that, it approximates the function  $\frac{1}{2} \max(x, 0)^2$ , and therefore we will obtain an error between the solutions of the two penalty methods.

Let  $\eta_\mu \in \mathcal{P}$  be the function already defined in equation (3.22)

$$\eta_\nu(x) = \begin{cases} 0 & \text{if } x < 0 \\ \frac{1}{6\nu} x^3 & \text{if } 0 \leq x < \nu \\ \frac{1}{2} x^2 - \frac{\nu}{2} x + \frac{\nu^2}{6} & \text{if } \nu \leq x \end{cases} \quad (3.75)$$

Its derivative is given by

$$\eta'_\nu(x) = \begin{cases} 0 & \text{if } x < 0 \\ \frac{1}{2\nu} x^2 & \text{if } 0 \leq x < \nu \\ x - \frac{\nu}{2} & \text{if } \nu \leq x \end{cases} \quad (3.76)$$

The function  $(\cdot)^+$  can be written as

$$x^+ = \begin{cases} 0 & \text{if } x < 0 \\ x & \text{if } 0 \leq x < \nu \\ x & \text{if } \nu \leq x \end{cases} \quad (3.77)$$

Then

$$x^+ - \eta'_\nu(x) = 0 \cdot \mathbb{1}_{\mathbb{R}^-} + (x - \frac{1}{2\nu} x^2) \mathbb{1}_{\{0 \leq x < \nu\}} + \frac{\nu}{2} \mathbb{1}_{\{x \geq \nu\}} \quad (3.78)$$

$$= (x - \frac{1}{2\nu} x^2) \mathbb{1}_{\{0 \leq x < \nu\}} + \frac{\nu}{2} \mathbb{1}_{\{x \geq \nu\}} \quad (3.79)$$

Therefore

$$\begin{aligned} |x^+ - \eta'_\nu(x)| &\leq (\nu + \frac{1}{2\nu} \nu^2) + \frac{\nu}{2} \\ &= 2\nu \end{aligned} \quad (3.80)$$

let  $\mathbf{u}_\mu, \mathbf{u}_\mu^*$  be the solutions of the problem (3.18), with the penalty functions  $\eta(x) = \eta_\nu(x)$ ,  $\eta(x) = \frac{1}{2}(x^+)^2$  respectively. By applying the Gâteaux derivative,  $\mathbf{u}_\mu, \mathbf{u}_\mu^*$  verify the two following

differential equations

$$a(\mathbf{u}_\mu, \mathbf{v}) - \mu \int_{\Gamma_C} \eta'_\nu(w_{\mu,N}) \cdot v_N ds = f(\mathbf{v}) \quad \forall \mathbf{v} \in \mathbf{V} \quad (3.81)$$

$$a(\mathbf{u}_\mu^*, \mathbf{v}) - \mu \int_{\Gamma_C} (w_{\mu,N}^*)^+ \cdot v_N ds = f(\mathbf{v}) \quad \forall \mathbf{v} \in \mathbf{V} \quad (3.82)$$

where  $w_{\mu,N} = \bar{g}_N - \mathbf{u}_\mu \cdot \mathbf{n}$ ,  $w_{\mu,N}^* = \bar{g}_N - \mathbf{u}_\mu^* \cdot \mathbf{n}$  and  $v_N = \mathbf{v} \cdot \mathbf{n}$ . Therefore

$$a(\mathbf{u}_\mu - \mathbf{u}_\mu^*, \mathbf{v}) - \mu \int_{\Gamma_C} (\eta'_\nu(w_{\mu,N}) - (w_{\mu,N}^*)^+) \cdot v_N ds = 0 \quad \forall \mathbf{v} \in \mathbf{V} \quad (3.83)$$

By taking  $\mathbf{v} = \mathbf{u}_\mu - \mathbf{u}_\mu^*$ , we obtain

$$a(\mathbf{u}_\mu - \mathbf{u}_\mu^*, \mathbf{u}_\mu - \mathbf{u}_\mu^*) - \mu \int_{\Gamma_C} (\eta'_\nu(w_{\mu,N}) - (w_{\mu,N}^*)^+) \cdot (u_{\mu N} - u_{\mu N}^*) ds = 0 \quad (3.84)$$

Thus

$$\begin{aligned} a(\mathbf{u}_\mu - \mathbf{u}_\mu^*, \mathbf{u}_\mu - \mathbf{u}_\mu^*) &= \mu \int_{\Gamma_C} (\eta'_\nu(w_{\mu,N}) - (w_{\mu,N}^*)^+) \cdot (u_{\mu N} - u_{\mu N}^*) ds \\ &= \mu \int_{\Gamma_C} (\eta'_\nu(w_{\mu,N}) - (w_{\mu,N}^*)^+) \cdot (u_{\mu N} - \bar{g}_N + \bar{g}_N - u_{\mu N}^*) ds \\ &= -\mu \int_{\Gamma_C} (\eta'_\nu(w_{\mu,N}) - (w_{\mu,N}^*)^+) \cdot (w_{\mu,N} - w_{\mu,N}^*) ds \\ &= -\mu \int_{\Gamma_C} (\eta'_\nu(w_{\mu,N}) - (w_{\mu,N})^+ + (w_{\mu,N})^+ - (w_{\mu,N}^*)^+) \cdot (w_{\mu,N} - w_{\mu,N}^*) ds \\ &= -\mu \int_{\Gamma_C} (\eta'_\nu(w_{\mu,N}) - (w_{\mu,N})^+) \cdot (w_{\mu,N} - w_{\mu,N}^*) ds \\ &\quad - \mu \int_{\Gamma_C} ((w_{\mu,N})^+ - (w_{\mu,N}^*)^+) \cdot (w_{\mu,N} - w_{\mu,N}^*) ds \end{aligned} \quad (3.85)$$

Otherwise if  $a \in \mathbb{R}$  then  $a = a^- + a^+$ , where  $a^- = \min(a, 0)$ , and

$$\begin{aligned} (a^+ - b^+)(a - b) &= (a^+ - b^+)(a^- + a^+ - b^- - b^+) \\ &= (a^+ - b^+)((a^+ - b^+) + (a^- - b^-)) \\ &= (a^+ - b^+)^2 + a^+a^- - a^+b^- - b^+a^- + b^+b^- \\ &= (a^+ - b^+)^2 - a^+b^- - b^+a^- \\ &\geq (a^+ - b^+)^2 \geq 0 \end{aligned} \quad (3.86)$$

We used the fact that  $a^+a^- = b^+b^- = 0$ ,  $-a^+b^- \geq 0$  and  $-b^+a^- \geq 0$ . Therefore from the

equation (3.85) we deduce that

$$\begin{aligned}
a(\mathbf{u}_\mu - \mathbf{u}_\mu^*, \mathbf{u}_\mu - \mathbf{u}_\mu^*) &\leq -\mu \int_{\Gamma_C} (\eta'_\nu(w_{\mu,N}) - (w_{\mu,N})^+) \cdot (w_{\mu,N} - w_{\mu,N}^*) ds \\
&= \mu \int_{\Gamma_C} (\eta'_\nu(w_{\mu,N}) - (w_{\mu,N})^+) \cdot (\mathbf{u}_\mu \cdot \mathbf{n} - \mathbf{u}_\mu^* \cdot \mathbf{n}) ds \\
&\leq \mu \int_{\Gamma_C} |(\eta'_\nu(w_{\mu,N}) - (w_{\mu,N})^+)| \cdot |(\mathbf{u}_\mu \cdot \mathbf{n} - \mathbf{u}_\mu^* \cdot \mathbf{n})| ds \quad (3.87)
\end{aligned}$$

Using the inequality (3.80), the inequality (3.87) becomes

$$\begin{aligned}
a(\mathbf{u}_\mu - \mathbf{u}_\mu^*, \mathbf{u}_\mu - \mathbf{u}_\mu^*) &\leq 2\mu\nu \int_{\Gamma_C} |(\mathbf{u}_\mu - \mathbf{u}_\mu^*) \cdot \mathbf{n}| ds \\
&\leq 2\mu\nu C \|\mathbf{u}_\mu - \mathbf{u}_\mu^*\|_{\mathbf{L}^2(\Gamma)} \\
&\leq 2\mu\nu C \|\mathbf{u}_\mu - \mathbf{u}_\mu^*\|_1 \quad (\text{Trace theorem}) \quad (3.88)
\end{aligned}$$

The application  $a(\cdot, \cdot)$  is elliptic thus

$$\|\mathbf{u}_\mu - \mathbf{u}_\mu^*\|_1^2 \leq \frac{1}{M} a(\mathbf{u}_\mu - \mathbf{u}_\mu^*, \mathbf{u}_\mu - \mathbf{u}_\mu^*) \leq \frac{2}{M} \mu\nu C \|\mathbf{u}_\mu - \mathbf{u}_\mu^*\|_1 \quad (3.89)$$

Therefore

$$\|\mathbf{u}_\mu - \mathbf{u}_\mu^*\|_1 \leq \frac{2}{M} \mu\nu C \quad (3.90)$$

Taking  $\nu = \frac{1}{\mu^k}$  with  $k \geq 2$ , we obtain the following error between the two penalty methods

$$\|\mathbf{u}_\mu - \mathbf{u}_\mu^*\|_1 \leq \frac{C}{\mu^{k-1}} \quad (3.91)$$

## 3.2 Finite deformations

In finite deformation, the existence of a solution for hyperelastic materials can be found in [29], and for the Signorini's problem in [29]. In this section we follow the same proof, in order to show the existence of a solution for our penalty method when the hyperelastic materials are used, and when the contact conditions are linearized. Indeed in our algorithm the nonlinearity of the contact in finite deformation is treated as a successive linear constraints, using a fixed point algorithm. The problem can be summarized as follows

$$\min_{\mathbf{v} \in \mathbf{V}} \int_{\Omega} \hat{W} dx - f(\mathbf{v}) + \mu P(\mathbf{v}) \quad (3.92)$$

where  $\hat{W}$  is the strain energy function,  $f$  the work of the loads, and  $P$  the penalty functional as above and has the same properties. The proof of such problems is due to John Ball [14]. Let  $\mathcal{E}_p(\mathbf{v}) = \int_{\Omega} \hat{W} dx - f(\mathbf{v})$  denotes the potential energy and  $\mathcal{E} = \mathcal{E}_p + \mu P$ . In order to prove the existence of our penalty method, we can proceed for example as in [69] (chapter 12), they used the fact that  $\hat{W}$  is polyconvex so  $\mathcal{E}_p$  is weakly sequentially lower semicontinuous, in addition they wrote an equivalent minimization problem on a product space and they proved the coercivity.

In our problem we add the penalty functional which is positive, therefore the coercivity is not affected, also  $P$  is weakly sequentially lower semicontinuous therefore  $\mathcal{E}_p + P$  is always weakly sequentially lower semicontinuous, hence the existence of a solution minimizing the problem (3.92).

Let  $\phi = \mathbf{X} + \mathbf{u}$  denotes the actual position of a material point in the body. We can follow also the proof that can be found in [29]. The proof is long so we will show the steps of the proof where there is a change, and we will use the same notations. First a infimizing sequence  $\phi_k$  is considered, otherwise speaking,  $\phi_k \in \Phi$  (the admissible set without the non-penetration constraints) and

$$\lim_{k \rightarrow +\infty} \mathcal{E}(\phi_k) = \inf_{\psi \in \Phi} \mathcal{E}(\psi) \quad (3.93)$$

The product space  $\mathbf{W}^{1,p}(\Omega) \times \mathbf{L}^q(\Omega) \times L^r(\Omega)$  is reflexive, therefore by the coercivity and the assumption that  $\inf_{\psi \in \Phi} \mathcal{E}(\psi) < +\infty$ , the sequence  $(\phi_l, \mathbf{Cof}\nabla\phi_l, \det\nabla\phi_l)$  is bounded in the reflexive space, thus there exists a subsequence  $(\phi_l, \mathbf{Cof}\nabla\phi_l, \det\nabla\phi_l)$  that converges weakly in  $\mathbf{W}^{1,p}(\Omega) \times \mathbf{L}^q(\Omega) \times L^r(\Omega)$  then

$$\begin{cases} \phi_l \rightharpoonup \phi \text{ in } \mathbf{W}^{1,p}(\Omega) \\ \mathbf{Cof}\nabla\phi_l \rightharpoonup \mathbf{Cof}\nabla\phi \text{ in } \mathbf{L}^q(\Omega) \\ \det\nabla\phi_l \rightharpoonup \det\nabla\phi \text{ in } L^r(\Omega) \end{cases} \quad (3.94)$$

As in [29] we can show that  $\phi \in \Phi$ . It remains to prove that

$$\int_{\Omega} \hat{W}(\mathbf{X}, \nabla\phi(\mathbf{X})) dx + \mu P(\phi) \leq \liminf_{l \rightarrow +\infty} \int_{\Omega} \hat{W}(\mathbf{X}, \nabla\phi_l(\mathbf{X})) dx + \mu P(\phi_l) \quad (3.95)$$

In the same manner as in [29], the following inequality can be shown

$$\int_{\Omega} \hat{W}(\mathbf{X}, \nabla\phi(\mathbf{X})) dx \leq \liminf_{l \rightarrow +\infty} \int_{\Omega} \hat{W}(\mathbf{X}, \nabla\phi_l(\mathbf{X})) dx \quad (3.96)$$

Otherwise we know that  $\phi_l \rightharpoonup \phi$ , and that  $P$  is weakly sequentially lower semicontinuous, therefore

$$\mu P(\phi) \leq \liminf_{l \rightarrow +\infty} \mu P(\phi_l) \quad (3.97)$$

Using the property of the  $\liminf$  and the equations (3.96) and (3.97), we obtain

$$\begin{aligned} \int_{\Omega} \hat{W}(\mathbf{X}, \nabla\phi(\mathbf{X})) dx + \mu P(\phi) &\leq \liminf_{l \rightarrow +\infty} \int_{\Omega} \hat{W}(\mathbf{X}, \nabla\phi_l(\mathbf{X})) dx + \liminf_{l \rightarrow +\infty} \mu P(\phi_l) \\ &\leq \liminf_{l \rightarrow +\infty} \left( \int_{\Omega} \hat{W}(\mathbf{X}, \nabla\phi_l(\mathbf{X})) dx + \mu P(\phi_l) \right) \end{aligned} \quad (3.98)$$

The functional  $f$  is continuous and linear, and  $\phi_l \rightharpoonup \phi$ , therefore

$$\lim_{l \rightarrow +\infty} f(\phi_l) = f(\phi) \quad (3.99)$$

and from equations (3.98) and (3.99)

$$\mathcal{E}(\phi) \leq \liminf_{l \rightarrow +\infty} \mathcal{E}(\phi_l) \quad (3.100)$$

Since  $\phi_l$  is a infimizing sequence thus

$$\liminf_{l \rightarrow +\infty} \mathcal{E}(\phi_l) = \lim_{l \rightarrow +\infty} \mathcal{E}(\phi_l) = \inf_{\psi \in \Phi} \mathcal{E}(\psi) \quad (3.101)$$

We conclude from the equations (3.100) and (3.101)

$$\begin{cases} \phi \in \Phi \\ \mathcal{E}(\phi) \leq \inf_{\psi \in \Phi} \mathcal{E}(\psi) \end{cases} \quad (3.102)$$

Thus

$$\begin{cases} \phi \in \Phi \\ \mathcal{E}(\phi) = \inf_{\psi \in \Phi} \mathcal{E}(\psi) \end{cases} \quad (3.103)$$

Hence the existence of a solution.

### 3.3 Contact between two bodies in linear elasticity

In the following, we consider two elastic bodies  $\Omega^l \subset \mathbb{R}^2$  or  $\mathbb{R}^3$  with  $l = 1, 2$  initially in contact at the border  $\Gamma_C$  (see Figure 3.2), the contact area after loading is supposed to be included in  $\Gamma_C$ . Let  $\Gamma_0^l$  be the border of the body  $\Omega^l$  where a null displacement is imposed, and  $\Gamma_1^l$  where a surface traction  $\mathbf{t}^l$  is imposed. Let  $\Omega = \Omega^1 \cup \Omega^2$  and  $\mathbf{n} := \mathbf{n}^2 = -\mathbf{n}^1$ , where  $\mathbf{n}^1$  and  $\mathbf{n}^2$  are respectively the outward unit normal vector on  $\partial\Omega_1$  and on  $\partial\Omega_2$ . The body force applied on  $\Omega^l$  is noted by  $\mathbf{f}^l$ .

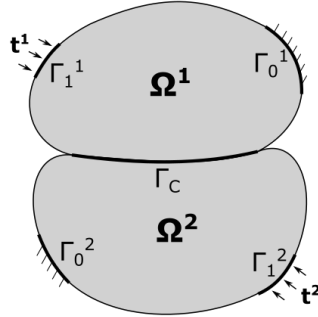


Figure 3.2 – The two bodies in contact

The displacement field  $\mathbf{u}$  is defined by  $\mathbf{u} = (\mathbf{u}^1, \mathbf{u}^2)$  where  $\mathbf{u}^l$  corresponds to the displacement field of the body  $\Omega^l$ , moreover the admissible set is  $\mathbf{V} = \mathbf{V}^1 \times \mathbf{V}^2$  where

$$\mathbf{V}^l = \{\mathbf{v} \in \mathbf{H}^1(\Omega^l) \mid \mathbf{v} = 0 \text{ a.e on } \Gamma_0^l\} \quad (3.104)$$

endowed with the broken norm:

$$\|\mathbf{u}\|_1 = \|(\mathbf{u}^1, \mathbf{u}^2)\|_1 = (\|\mathbf{u}^1\|_1^2 + \|\mathbf{u}^2\|_1^2)^{\frac{1}{2}} \quad (3.105)$$

The non-penetration condition between the two bodies is the following

$$[\mathbf{u}, \mathbf{n}] = (\mathbf{u}^2 - \mathbf{u}^1) \cdot \mathbf{n} \leq 0 \quad \text{on } \Gamma_C \quad (3.106)$$

The contact problem in this case can be written as the following minimization problem

$$\min_{\mathbf{v} \in \mathbf{K}} \frac{1}{2} a(\mathbf{v}, \mathbf{v}) - f(\mathbf{v}) \quad (3.107)$$

where  $\mathbf{K} = \{\mathbf{v} \in \mathbf{V} \mid [\mathbf{v}, \mathbf{n}] \leq 0 \text{ a.e on } \Gamma_C\}$ , and the applications  $a : \mathbf{V} \times \mathbf{V} \rightarrow \mathbb{R}$  and  $f : \mathbf{V} \rightarrow \mathbb{R}$  are defined as follows

$$\begin{cases} a(\mathbf{u}, \mathbf{v}) = a^1(\mathbf{u}, \mathbf{v}) + a^2(\mathbf{u}, \mathbf{v}) \\ f(\mathbf{v}) = f^1(\mathbf{v}) + f^2(\mathbf{v}) \end{cases} \quad (3.108)$$

where for  $l = 1, 2$

$$\begin{cases} a^l(\mathbf{u}, \mathbf{v}) = \int_{\Omega^l} \boldsymbol{\sigma}(\mathbf{u}^l) : \boldsymbol{\epsilon}(\mathbf{v}^l) dv \\ f^l(\mathbf{v}) = \int_{\Omega^l} \mathbf{f}^l \cdot \mathbf{v}^l dv + \int_{\Gamma_1^l} \mathbf{t}^l \cdot \mathbf{v}^l ds \end{cases} \quad (3.109)$$

Taking a penalty factor  $\mu > 0$ , the penalized problem becomes

$$\min_{\mathbf{v} \in \mathbf{V}} \frac{1}{2} a(\mathbf{v}, \mathbf{v}) - f(\mathbf{v}) + \mu P(\mathbf{v}) \quad (3.110)$$

where the penalty functional  $P(\mathbf{v})$ , in this case, is defined by

$$P(\mathbf{v}) = \int_{\Gamma_C} \eta([\mathbf{u}, \mathbf{n}]) ds \quad (3.111)$$

As above, the functional  $P$  is convex and positive, and all theoretical results can be done in the same way as before.

### 3.4 Symmetric contact formulation

Using the finite element approach, for  $l = 1$  or  $2$ , let  $\Omega_h^l$  be the mesh of the body  $\Omega^l$ , which is composed from the triangles family  $\{T_i^l \mid i = 1, \dots, n_T^l\}$ . In addition, consider the following spaces

$$\mathbf{V}_h^l = \left\{ \mathbf{v} = (v_1, v_2) \in C^0(\Omega_h^l) \times C^0(\Omega_h^l) \mid \mathbf{v}|_{T_i^l} \in P_r \times P_r, \forall i = 1, \dots, n_T^l \text{ and } \mathbf{v} = 0 \text{ on } \Gamma_0^l \right\} \quad (3.112)$$

where  $C^0(\Omega_h^l)$  denotes the set of the continuous functions on  $\Omega_h^l$ , and  $P_r$  denotes the linear finite elements for  $r = 1$  and the quadratic ones for  $r = 2$ .

Consider the space  $\mathbf{V}_h$  defined as follows

$$\mathbf{V}_h = \mathbf{V}_h^1 \times \mathbf{V}_h^2 \quad (3.113)$$

Let  $\mathbf{u}_h = (\mathbf{u}_h^1, \mathbf{u}_h^2) \in \mathbf{V}_h$ , the displacement vector field on the mesh  $\Omega_h^l$ , is given by

$$\mathbf{u}_h^l = \sum_i \begin{pmatrix} U_i^{l,x} \\ U_i^{l,y} \end{pmatrix} \hat{w}_i^l \quad (3.114)$$

where  $\hat{w}_i^l$  are the shape functions on the mesh  $\Omega_h^l$ , and  $(U_i^{l,x} \ U_i^{l,y})^T$  are the degrees of freedom of  $\mathbf{u}_h^l$ , otherwise speaking  $U_i^{l,x}$  and  $U_i^{l,y}$  represent respectively the horizontal and vertical displacement of the node  $i$  in the mesh. For the sake of clarity we omit the subscript  $h$  for all vectors.

Let  $\Gamma_{C1}$  and  $\Gamma_{C2}$  be respectively the potential contact area of the slave and master body.

Given  $\mathbf{x} = \mathbf{X} + \mathbf{u}$  the actual position of a material point of  $\Omega_h^1 \cup \Omega_h^2$ , the symmetric non-penetration condition is given as follows

$$\begin{cases} (\mathbf{x} - \bar{\mathbf{x}}_2) \cdot \mathbf{n} \geq 0 & \text{on } \Gamma_{C1} \\ (\mathbf{x} - \bar{\mathbf{x}}_1) \cdot \mathbf{n} \geq 0 & \text{on } \Gamma_{C2} \end{cases} \quad (3.115)$$

or

$$\begin{cases} (\bar{\mathbf{x}}_2 - \mathbf{x}) \cdot \mathbf{n} \leq 0 & \text{on } \Gamma_{C1} \\ (\bar{\mathbf{x}}_1 - \mathbf{x}) \cdot \mathbf{n} \leq 0 & \text{on } \Gamma_{C2} \end{cases} \quad (3.116)$$

where  $\bar{\mathbf{x}}_l$  the projection of  $\mathbf{x}$  on the body  $\phi(\Omega_l)$  for  $l = 1, 2$ , with  $\phi$  the deformation mapping, and  $\mathbf{n}$  the outward unit normal vector at  $\bar{\mathbf{x}}_l$ . Otherwise speaking, this condition means that all points of the first body are forbidden to penetrate the second one and vice versa.

Given a penalty factor  $\mu > 0$ , the symmetric contact formulation using the penalty method becomes

$$\min_{\mathbf{v} \in \mathbf{V}_h} \mathcal{E}_p(\mathbf{v}) + \mu P^1(\mathbf{v}) + \mu P^2(\mathbf{v}) \quad (3.117)$$

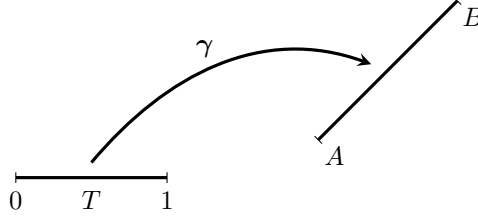
where  $\mathcal{E}_p$  denotes the total potential energy, and the functionals  $P^1$  and  $P^2$  are defined by

$$\begin{cases} P^1(\mathbf{v}) = \int_{\Gamma_{C1}} \eta((\bar{\mathbf{x}}_2 - \mathbf{x}) \cdot \mathbf{n}) \, ds \\ P^2(\mathbf{v}) = \int_{\Gamma_{C2}} \eta((\bar{\mathbf{x}}_1 - \mathbf{x}) \cdot \mathbf{n}) \, ds \end{cases} \quad (3.118)$$

We obtain an unconstrained minimization problem. As the integral is involved in the penalty method, which numerically involves the integration points, therefore this formulation ensures the non-penetration of the integration points of each contact side into the opposite body.

## 3.5 Numerical integration

The two-dimensional case is considered for the sake of simplicity. Consider a parent element  $T = [0, 1]$  and a mapping  $\gamma : T \rightarrow \mathbb{R}^2$ , which transforms  $T$  into a segment  $AB$  in  $\mathbb{R}^2$  (see Figure 3.3).

Figure 3.3 – The mapping  $\gamma$  applied on the parent element

Let  $\hat{N}_1, \hat{N}_2$  be the two linear shape functions on  $T$ , given by

$$\begin{cases} \hat{N}_1(t) = 1 - t \\ \hat{N}_2(t) = t \end{cases} \quad (3.119)$$

We considered the linear case ( $P_1$  finite elements) also for the sake of simplicity.

If  $\mathbf{X} \in AB$ , and  $\mathbf{X}_A = (X_A, Y_A)$ ,  $\mathbf{X}_B = (X_B, Y_B)$  are respectively the point  $A$  and  $B$  of the segment  $AB$ , then

$$\boldsymbol{\gamma}(t) = \mathbf{X}(t) = \hat{N}_1(t)\mathbf{X}_A + \hat{N}_2(t)\mathbf{X}_B \quad (3.120)$$

or

$$\mathbf{X}(t) = (1 - t)\mathbf{X}_A + t\mathbf{X}_B \quad (3.121)$$

In this case, the integral of a function  $f : AB \rightarrow \mathbb{R}$  becomes

$$\int_{AB} f(\mathbf{X}) ds = \int_{AB} f(\boldsymbol{\gamma}) ds = \int_T f(\boldsymbol{\gamma}(t)) \|\boldsymbol{\gamma}'(t)\| ds \quad (3.122)$$

In the linear case,  $\|\boldsymbol{\gamma}'(t)\|$  is equal to the length of  $AB$ , indeed

$$\|\boldsymbol{\gamma}'(t)\| = \|X_B - X_A\| = \|AB\| \quad (3.123)$$

Let  $\{t_{ip} \mid ip = 0, \dots, nip\}$  be the set of integration points on  $T$ , with the corresponding set of weights  $\{w_{ip} \mid ip = 0, \dots, nip\}$ , where  $nip$  is the integration points number. In this case the numerical integration of a function  $F : T \rightarrow \mathbb{R}$  over  $T$  is given, by the following

$$\int_T F(t) dt = \sum_{ip=1}^{nip} F(t_{ip}) \cdot w_{ip} \quad (3.124)$$

The integration of the penalty terms ( equations (3.118)) are done on the reference configurations. In the following, we will discuss two cases, the first one is the linear elasticity where the non-penetration constraints are linear, and the second one is the finite deformation problems where large deformations can occur. We will study the penalty functional  $P^1$ , indeed  $P^2$  is straightforward.

Let  $\{s_i | i = 1, \dots, n_S\}$  be the segments composing  $\Gamma_{C1}$ , therefore

$$P^1(\mathbf{v}) = \int_{\Gamma_{C1}} \eta((\bar{\mathbf{x}}_2 - \mathbf{x}) \cdot \mathbf{n}) ds = \int_{\Gamma_{C1}} \eta((\bar{\mathbf{x}} - \mathbf{x}) \cdot \mathbf{n}) ds = \sum_{i=1}^{n_S} \int_{s_i} \eta((\bar{\mathbf{x}} - \mathbf{x}) \cdot \mathbf{n}) ds \quad (3.125)$$

Let's take a random segment  $s_i$  and suppose that  $A$  and  $B$  are its segment ends. We note  $\mathbf{U}_A$  and  $\mathbf{U}_B$  the degrees of freedom of the displacement field  $\mathbf{u}$  at the nodes  $A$  and  $B$ , in addition  $\mathbf{X}_A$  and  $\mathbf{X}_B$  denote respectively the coordinates in the initial configuration, of the nodes  $A$  and  $B$ . Let  $N_A$  and  $N_B$  denote the shapes functions at  $A$  and  $B$ , then using the parent element  $T$  we can write the following

$$\begin{cases} N_A(\mathbf{X}) = \hat{N}_1(\gamma^{-1}(\mathbf{X})) \\ N_B(\mathbf{X}) = \hat{N}_2(\gamma^{-1}(\mathbf{X})) \\ \mathbf{X} = \mathbf{X}_A \cdot \hat{N}_1(\gamma^{-1}(\mathbf{X})) + \mathbf{X}_B \cdot \hat{N}_2(\gamma^{-1}(\mathbf{X})) \\ \mathbf{u} = \mathbf{U}_A \cdot \hat{N}_1(\gamma^{-1}(\mathbf{X})) + \mathbf{U}_B \cdot \hat{N}_2(\gamma^{-1}(\mathbf{X})) \end{cases} \quad (3.126)$$

Thus the actual position field  $\mathbf{x}$  is given on  $AB$  by

$$\mathbf{x} = (\mathbf{X}_A + \mathbf{U}_A) \cdot \hat{N}_1(\gamma^{-1}(\mathbf{X})) + (\mathbf{X}_B + \mathbf{U}_B) \cdot \hat{N}_2(\gamma^{-1}(\mathbf{X})) \quad (3.127)$$

Note that  $U_A$  and  $U_B$  belongs to the unknowns of our problem. Using the equation (3.122) and the quadrature formula (3.124), the integral over  $s_i$  or  $AB$  in equation (3.125) can be given by

$$\begin{aligned} \int_{s_k^i} \eta((\bar{\mathbf{x}} - \mathbf{x}) \cdot \mathbf{n}) ds &= \int_{AB} \eta((\bar{\mathbf{x}} - \mathbf{x}) \cdot \mathbf{n}) ds \\ &= \sum_{ip=1}^{nip} \eta((\bar{\mathbf{x}}_{ip} - \mathbf{x}_{ip}) \cdot \mathbf{n}_{ip}) \cdot \|\gamma'(t)\| \cdot w_{ip} \\ &= \sum_{ip=1}^{nip} \eta((\bar{\mathbf{x}}_{ip} - \mathbf{x}_{ip}) \cdot \mathbf{n}_{ip}) \cdot \|AB\| \cdot w_{ip} \end{aligned} \quad (3.128)$$

where  $\mathbf{x}_{ip}$  is the actual position of the integration point  $ip$ , given by

$$\mathbf{x}_{ip} = (\mathbf{X}_A + \mathbf{U}_A) \cdot \hat{N}_1(t_{ip}) + (\mathbf{X}_B + \mathbf{U}_B) \cdot \hat{N}_2(t_{ip}) \quad (3.129)$$

It remains to compute the projection point  $\bar{\mathbf{x}}_{ip}$  of  $\mathbf{x}_{ip}$  on the second body, and the normal vector  $\mathbf{n}_{ip}$  at  $\bar{\mathbf{x}}_{ip}$ . In order to compute  $\bar{\mathbf{x}}_{ip}$ , a fixed point algorithm is employed in the case of large displacements, otherwise speaking the previous displacement  $\mathbf{u}^{n-1}$  is used in order to find the closest second body segment to  $\mathbf{x}_{ip}^{n-1}$ . Indeed we do the following actions

1. For  $\mathbf{x}_{ip}^{n-1}$  we look for the closest node of the second body contact area, let's say node  $j$ , we use simply the distance, but we will use in the future a quadtree
2. The set  $\{r_k^j | k = 1, \dots, n_2^*\}$ ,  $n_2^* = 1$  or  $2$ , is the set of segments connected to the node  $j$
3. We look for the point  $P_k$  in each segment  $r_k^j$ , which is the closest to  $\mathbf{x}_{ip}^{n-1}$  (see section 3.7)
4. The closest point  $\bar{P}$  to  $\mathbf{x}_{ip}^{n-1}$  within  $\{P_k | k = 1, \dots, n_2^*\}$ , is chosen

Let  $CD$  be the segment which contains  $\bar{P}$  and  $\bar{\lambda} \in [0, 1]$  such that

$$\bar{P} = (1 - \bar{\lambda})\mathbf{x}_C^{n-1} + \bar{\lambda}\mathbf{x}_D^{n-1} \quad (3.130)$$

with

$$\begin{cases} \mathbf{x}_C^{n-1} = \mathbf{X}_C + \mathbf{U}_C^{n-1} \\ \mathbf{x}_D^{n-1} = \mathbf{X}_D + \mathbf{U}_D^{n-1} \end{cases} \quad (3.131)$$

The principle of the fixed point algorithm is to use at the actual iteration  $n$ , the segment  $CD$  as the closest segment to  $\mathbf{x}_{ip}$ , and  $\bar{\lambda}$  as the position of  $\bar{\mathbf{x}}_{ip}$  in  $CD$ , otherwise speaking the fixed point is on the parameter  $\bar{\lambda}$ . Therefore the actual projection point  $\bar{\mathbf{x}}_{ip}$  will be given by

$$\bar{\mathbf{x}}_{ip} = (1 - \bar{\lambda})\mathbf{x}_C + \bar{\lambda}\mathbf{x}_D \quad (3.132)$$

with

$$\begin{cases} \mathbf{x}_C = \mathbf{X}_C + \mathbf{U}_C \\ \mathbf{x}_D = \mathbf{X}_D + \mathbf{U}_D \end{cases} \quad (3.133)$$

Finally the integral over  $s_i$  or  $AB$  in equation (3.128) can be given by

$$\int_{s_k^i} \eta((\bar{\mathbf{x}} - \mathbf{x}) \cdot \mathbf{n}) ds = \sum_{ip=1}^{nip} \eta((\bar{\mathbf{x}}_{ip} - \mathbf{x}_{ip}) \cdot \mathbf{n}_{ip}) \cdot \|AB\| \cdot w_{ip} \quad (3.134)$$

where  $\mathbf{x}_{ip}$  is the actual position of the integration point  $ip$ , and  $\bar{\mathbf{x}}_{ip}$  its projection. More precisely

$$\begin{cases} \mathbf{x}_{ip} = (\mathbf{X}_A + \mathbf{U}_A) \cdot \hat{N}_1(t_{ip}) + (\mathbf{X}_B + \mathbf{U}_B) \cdot \hat{N}_2(t_{ip}) \\ \bar{\mathbf{x}}_{ip} = (\mathbf{X}_C + \mathbf{U}_C) \cdot \hat{N}_1(\bar{\lambda}) + (\mathbf{X}_D + \mathbf{U}_D) \cdot \hat{N}_2(\bar{\lambda}) \\ \mathbf{n}_{ip} = \mathbf{n}_C \cdot \hat{N}_1(\bar{\lambda}) + \mathbf{n}_D \cdot \hat{N}_2(\bar{\lambda}) \end{cases} \quad (3.135)$$

Note that  $\mathbf{U}_A$  and  $\mathbf{U}_B$  belong to the degrees of freedom of the first body and  $\mathbf{U}_C$  and  $\mathbf{U}_D$  belong to the degrees of freedom of the second body, and these 4 quantities are a part of our unknowns. Moreover  $\mathbf{n}_C$  or  $\mathbf{n}_D$  are computed as follows

$$\mathbf{n}_C = \frac{\sum_{i=1}^{n_C^*} \mathbf{n}_i}{\left\| \sum_{i=1}^{n_C^*} \mathbf{n}_i \right\|} \quad (3.136)$$

where  $n_C^*$  is the number of segments connected to  $C$  and  $\mathbf{n}_i$  is the outward unit normal vector at the segment  $i$  connected to  $C$ , from the previous iteration  $n - 1$ . Another definition of  $\mathbf{n}_C$  can be given as a weighted average, especially when there is a big difference between the length of

the connected segments to  $C$ , indeed

$$\mathbf{n}_C = \frac{\sum_{i=1}^{n_C^*} l_i \mathbf{n}_i}{\left\| \sum_{i=1}^{n_C^*} l_i \mathbf{n}_i \right\|} \quad (3.137)$$

where  $l_i$  is the length, at the previous iteration  $n - 1$ , of the segment  $i$  connected to  $C$ .

**Remark 3.1**

*If two integration points belong to the same segment of the first body, then their projection points can belong to a different segments of the second body, see Figure 3.4.*

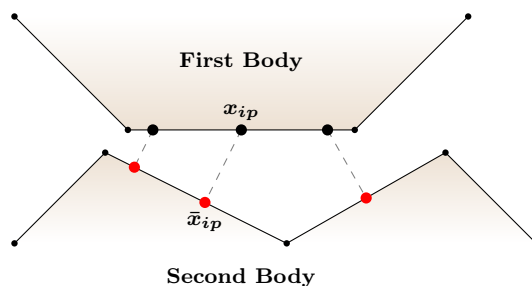


Figure 3.4 – The projection of the first body integration points on the second body

Finally, we can say that this method belongs to the quadrature-point-to-surface (QPTS) discretization scheme.

### 3.6 Symmetric contact algorithm using penalty method

The contact area is not known in advance, thus there is a difficulty to impose contact conditions between the two bodies. More precisely the projection points  $\bar{\mathbf{x}}_1$  or  $\bar{\mathbf{x}}_2$ , which can be seen in the equations (3.116) and (3.118), are the projection of an unknown point  $\mathbf{x} = \mathbf{X} + \mathbf{u}$  on unknown area, therefore there is no way to write explicitly the projection points in term of our degree of freedoms.

As was pointed out in the section 3.5, a fixed point method is used in order to transform the contact problem into a sequence of a minimization ones, with linear constraints, where we apply our penalty method, especially for the finite deformation problems, indeed for the linear elastic problems, the constraints are linear by definition. Such idea can be found in [50, 49, 75], where the geometric non-linearity of the contact is transformed into a sequence of a geometric linear one. More precisely for each iteration of the fixed point algorithm, the previous displacement is

used in order to search for each integration point of the slave contact area, the closest segment (in 2D) or the closest triangle (in 3D) of the master body, and its projection point position on this closest segment or triangle. Therefore, at each iteration the projection points are linear with respect to the degrees of freedom of the problem (see section 3.5, equation (3.135)), especially for the finite deformation problems. The convergence is reached when two geometrical configurations are nearly the same, it will be more detailed in the following.

Let  $\mathbf{U}$  be the degrees of freedom of the problem, otherwise speaking the displacement vector of all nodes. The symmetric algorithm to solve the contact problem is briefly described in the algorithm 3.

---

**Algorithm 3** Symmetric algorithm using penalty method

---

Initialization of the displacement  $\mathbf{U}_0$  and setting the tolerance  $\epsilon_{tol} = 10^{-6}$

**while**  $error \geq \epsilon_{tol}$  **do**

1. Using the displacement vector  $\mathbf{U}_{n-1}$  of the previous iteration  $n - 1$ :

    Compute the projection points' parameters  $\{\bar{\lambda}_i \mid i = 1, \dots, nS\}$  of all slave integration points

    Compute the normal at the projection points  $\{n_i \mid i = 1, \dots, nS\}$  (Using smoothing techniques)

2. For each integration point, its projection point  $\bar{\mathbf{x}}_i$  depends linearly on the actual displacement

3. Reverse the role of the master and the slave body

4. Form the penalty functional

$$E_\mu := \mathcal{E}_p(\mathbf{v}) + \mu P^1(\mathbf{v}) + \mu P^2(\mathbf{v})$$

5. Minimize  $E_\mu$  to obtain the actual displacement  $\mathbf{U}_n$

6.  $error = \frac{\|\mathbf{U}_n - \mathbf{U}_{n-1}\|_\infty}{\|\mathbf{U}_{n-1}\|_\infty}$

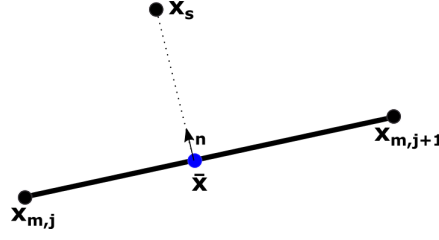
**end while**

---

### 3.7 Projection of the integration points

As was mentioned before, we need to compute the projection of each integration points on the second body, therefore for the sake of simplicity let's use the notion of slave/master body and the linear finite elements in 2D, indeed at the end the algorithm does not use this notion because it's symmetric.

Let  $\mathbf{x}_s = \mathbf{X}_s + \mathbf{U}_s$  be the actual position of an integration point belonging to the contact border of the slave body (see Fig(3.5)), and  $[\mathbf{x}_{m,j}, \mathbf{x}_{m,j+1}]$  the segment of the master contact border, which is the closest to  $\mathbf{x}_s$ .

Figure 3.5 – The projection of a slave integration point  $\mathbf{x}_s$  on the master body

Let  $\bar{\mathbf{x}}$  be the projection of  $\mathbf{x}_s$  on the segment of the master contact border  $[\mathbf{x}_{m,j}, \mathbf{x}_{m,j+1}]$  (see Fig(3.5)), which is supposed to be a parametric curve  $\mathbf{x}_m(\eta)$  and  $\bar{\mathbf{x}} = \mathbf{x}_m(\eta^*)$ . In the case of linear finite elements

$$\bar{\mathbf{x}} = N_1(\eta^*)\mathbf{x}_{m,j} + N_2(\eta^*)\mathbf{x}_{m,j+1} \quad (3.138)$$

where  $N_1(\eta) = 1 - \eta$  and  $N_2(\eta) = \eta$  are the linear shape functions on  $[0, 1]$ . In order to compute the parameter  $\eta^*$ , a constrained minimization problem can be solved, as follows

$$\begin{cases} \min_{\eta} d(\eta) & \text{s.t} \\ 0 \leq \eta \leq 1 \end{cases} \quad (3.139)$$

where  $d(\eta) = \|\mathbf{x}_s - \bar{\mathbf{x}}\|^2 = \|\mathbf{x}_s - N_1(\eta)\mathbf{x}_{m,j} - N_2(\eta)\mathbf{x}_{m,j+1}\|^2$  the distance from the integration point  $\mathbf{x}_s$  to the master segment  $[\mathbf{x}_{m,j}, \mathbf{x}_{m,j+1}]$ .

Consider  $n_S$  integration points in the slave contact area  $\{\mathbf{x}_i^s \mid i = 1, \dots, n_S\}$ , thus in order to compute for each slave point its projection on the master area, we consider for each slave point  $\mathbf{x}_i^s$  the problem (3.139), or as follows

$$\begin{cases} \min_{\eta_i} d_i(\eta_i) & \text{s.t} \\ 0 \leq \eta_i \leq 1 \end{cases} \quad (3.140)$$

where  $d_i$  is the distance from the integration point  $\mathbf{x}_i^s$  to the closest master segment.

Moreover, instead of solving a constrained minimization problem for each slave integration points (problem 3.140), we can solve one constrained minimization problem as follows

$$\begin{cases} \min_{(\eta_1, \dots, \eta_{n_S})} (d_1(\eta_1) + \dots + d_{n_S}(\eta_{n_S})) & \text{s.t} \\ 0 \leq \eta_i \leq 1 \quad \forall i = 1, \dots, n_S \end{cases} \quad (3.141)$$

Besides, we will present a definition and a theorem, which can be found in [86], and which are useful in the following.

**Definition 3.3.** Suppose we have the following problem, a minimization of an objective function  $f$  subjected to an equality constraints  $\{c_i = 0, i \in \mathcal{E}\}$  and to an inequality constraints  $\{c_i \geq$

$0, i \in \mathcal{I}\}$

$$\begin{cases} \min_{x \in \mathbb{R}^n} f(x) & \text{s.t} \\ c_i(x) = 0 & i \in \mathcal{E} \\ c_i(x) \geq 0 & i \in \mathcal{I} \end{cases} \quad (3.142)$$

Then for a feasible point  $x$ , the active set  $\mathcal{A}(x)$  is defined by

$$\mathcal{A}(x) = \mathcal{E} \cup \{i \in \mathcal{I} \text{ s.t } c_i(x) = 0\} \quad (3.143)$$

Given a point  $x$ , we say that the *LICQ* (linear independence constraint qualification) condition is satisfied, if the set of the active constraint gradients  $\{\nabla c_i(x), i \in \mathcal{A}(x)\}$  is linearly independent.

**Theorem 3.6** (First-Order Necessary Conditions [86]). *Suppose that  $x^*$  is a solution of the problem (3.142), the objective function  $f$  and the constraints  $c_i$  are continuously differentiable and the LICQ condition is satisfied at  $x^*$ . Then there exist a Lagrange multiplier vector  $\lambda^*$  of components  $\lambda_i$  where  $i \in \mathcal{E} \cup \mathcal{I}$  such that the following properties are satisfied at  $(x^*, \lambda^*)$*

$$\begin{cases} \nabla_x \mathcal{L}(x^*, \lambda^*) = 0 \end{cases} \quad (3.144)$$

$$\begin{cases} c_i(x^*) = 0 \quad \forall i \in \mathcal{E} \end{cases} \quad (3.145)$$

$$\begin{cases} c_i(x^*) \geq 0 \quad \forall i \in \mathcal{I} \end{cases} \quad (3.146)$$

$$\begin{cases} \lambda_i^* \geq 0 \quad \forall i \in \mathcal{I} \end{cases} \quad (3.147)$$

$$\begin{cases} \lambda_i^* c_i(x^*) = 0 \quad \forall i \in \mathcal{E} \cup \mathcal{I} \end{cases} \quad (3.148)$$

where  $\mathcal{L}(x, \lambda) = f(x) - \sum_{i \in \mathcal{E} \cup \mathcal{I}} \lambda_i c_i(x)$ . Note that these conditions (3.144 – 3.148) are also called *Karush-Kuhn-Tucker (KKT) conditions*.

Back to the problem (3.141), we have only an inequality constraints, which can be reformulated as

$$\begin{cases} \eta_1 \geq 0 \\ 1 - \eta_1 \geq 0 \\ \vdots \\ \eta_{n_S} \geq 0 \\ 1 - \eta_{n_S} \geq 0 \end{cases} \quad (3.149)$$

Given a feasible point  $\eta$  and  $i \in \mathcal{A}(\eta)$ , only one of the conditions  $c(\eta) = \eta_i \geq 0$  and  $c(\eta) = 1 - \eta_i \geq 0$  is active and not both at the same time, in addition  $\nabla c = e_i$  (canonical basis vector) or  $\nabla c = -e_i$ , therefore the *LICQ* condition is satisfied at  $\eta$ . Suppose that  $(\eta^*, \lambda^*)$  satisfies the KKT conditions (3.144 – 3.148), the objective function  $\sum d_i$  in the problem (3.141) is strictly convex in the case of linear finite elements, therefore using the second-order sufficient conditions,  $\eta^*$  is the unique solution of the problem (3.141).

## 3.8 Smoothing techniques

In order to have a smooth normal vector field, several smoothing techniques were developed, here we present a smoothing technique using the Bézier curve, which can be found in [123].

### 3.8.1 Bézier curve

Given a sequence of control points  $\{\mathbf{P}_0, \dots, \mathbf{P}_N\} \subset \mathbb{R}^2$ , the Bézier curve is a parametric curve which passes in the first point  $\mathbf{P}_0$  and in the last point  $\mathbf{P}_N$  but not necessary in the other points. In particular the Bézier curve is contained in the convex hull of the control points. The Bézier curve is defined as follows

$$\begin{pmatrix} x(t) \\ y(t) \end{pmatrix} = \sum_{k=0}^N B_k^N(t) \mathbf{P}_k \quad \forall t \in [0, 1] \quad (3.150)$$

where  $B_k^N$  are the Bernstein polynomials defined by

$$B_k^N(t) = C_N^k t^k (1-t)^{N-k} \quad (3.151)$$

with  $C_N^k$  the binomial coefficient.

#### Example 3.2: Cubic Bézier curve

Given 4 control points  $\{\mathbf{P}_0, \mathbf{P}_1, \mathbf{P}_2, \mathbf{P}_3\}$  the cubic Bézier curve is defined as follows

$$\begin{pmatrix} x(t) \\ y(t) \end{pmatrix} = (1-t)^3 \mathbf{P}_0 + 3t(1-t)^2 \mathbf{P}_1 + 3(1-t)t^2 \mathbf{P}_2 + t^3 \mathbf{P}_3 \quad \forall t \in [0, 1] \quad (3.152)$$

In this part we present the discretization of the master contact surface by the Bézier curve (see [123]), it will be a smooth curve which passes in all the nodes of the master contact surface (curve in 2D). Given a segment  $[\mathbf{x}_1, \mathbf{x}_2]$  of the master contact area, and the following control points  $\{\mathbf{x}_1, \mathbf{x}_1^+, \mathbf{x}_2^-, \mathbf{x}_2\}$ , the segment is approximated by the following Bézier curve

$$\mathbf{x} = B_0^2 \mathbf{x}_1 + B_1^2 \mathbf{x}_1^+ + B_2^2 \mathbf{x}_2^- + B_3^2 \mathbf{x}_2 \quad (3.153)$$

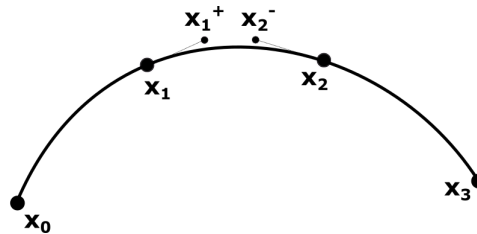


Figure 3.6 – The Bézier curve

We consider also the master node  $\mathbf{x}_0$  before  $\mathbf{x}_1$  and the node  $\mathbf{x}_3$  after  $\mathbf{x}_2$  (see Fig (3.6)). Let  $\mathbf{t}_1 = \frac{\alpha}{2}(\mathbf{x}_2 - \mathbf{x}_0)$  the tangent vector at  $\mathbf{x}_1$  and  $\mathbf{t}_2 = \frac{\alpha}{2}(\mathbf{x}_3 - \mathbf{x}_1)$  the tangent vector at  $\mathbf{x}_2$ , then in order to have a global  $C^1$  curve, the tangent at each node must be continuous. In other words

$$\begin{cases} \frac{d\mathbf{x}}{dt}(0) = \mathbf{t}_1 \\ \frac{d\mathbf{x}}{dt}(1) = \mathbf{t}_2 \end{cases} \Rightarrow \begin{cases} -3\mathbf{x}_1 + 3\mathbf{x}_1^+ = \mathbf{t}_1 = \frac{\alpha}{2}(\mathbf{x}_2 - \mathbf{x}_0) \\ -3\mathbf{x}_2^- + 3\mathbf{x}_2 = \mathbf{t}_2 = \frac{\alpha}{2}(\mathbf{x}_3 - \mathbf{x}_1) \end{cases} \quad (3.154)$$

Therefore we obtain

$$\begin{cases} \mathbf{x}_1^+ = \mathbf{x}_1 + \frac{\alpha}{6}(\mathbf{x}_2 - \mathbf{x}_0) \\ \mathbf{x}_2^- = \mathbf{x}_2 - \frac{\alpha}{6}(\mathbf{x}_3 - \mathbf{x}_1) \end{cases} \quad (3.155)$$

replacing  $\mathbf{x}_1^+$  and  $\mathbf{x}_2^-$  in the equation (3.153) we obtain

$$\mathbf{x} = B'_0\mathbf{x}_0 + B'_1\mathbf{x}_1 + B'_2\mathbf{x}_2 + B'_3\mathbf{x}_3 \quad (3.156)$$

where

$$\begin{cases} B'_0 = -\frac{\alpha}{6}B_1^2 \\ B'_1 = B_0^2 + B_1^2 + \frac{\alpha}{6}B_2^2 \\ B'_2 = B_2^2 + B_3^2 + \frac{\alpha}{6}B_1^2 \\ B'_3 = -\frac{\alpha}{6}B_2^2 \end{cases} \quad (3.157)$$

According to [123] a good choice for  $\alpha$ , is  $\alpha = \frac{1}{3}$ .

Finally the Bézier curves were tested in our contact algorithm. A slight improvement was noted in the accuracy of the result, but the computational time was increased. Thus we preferred to continue with the previous formulation where the normal vector field is continuous on the contact surface.

## 3.9 Numerical validations

### 3.9.1 Compression of two elastic blocks with imposed displacement

A first elastic rectangular block is posed on a second one (see Figure 3.7a). The two blocks have the same properties: a width  $L = 2UL$ , a height  $H = 1UL$ , a Young's modulus  $E = 200 \frac{UF}{UL^2}$ , a Poisson's ratio  $\nu = 0$ . The study is done under the plane strain hypothesis (2D). The frictionless case is always supposed, and a vertical displacement of  $U_0 = -0.1UL$  and a zero horizontal displacement are imposed on the upper face of the first block, the lower face of the second body is clamped. This test was treated in [109].

Theoretically the value of the strain is equal to  $\epsilon = \frac{U_0}{2H} = \frac{-0.1}{2} = -0.05$ , thus the value of the contact pressure is equal to  $p_{theo} = E \cdot \epsilon = -10 \frac{UF}{UL^2}$ .

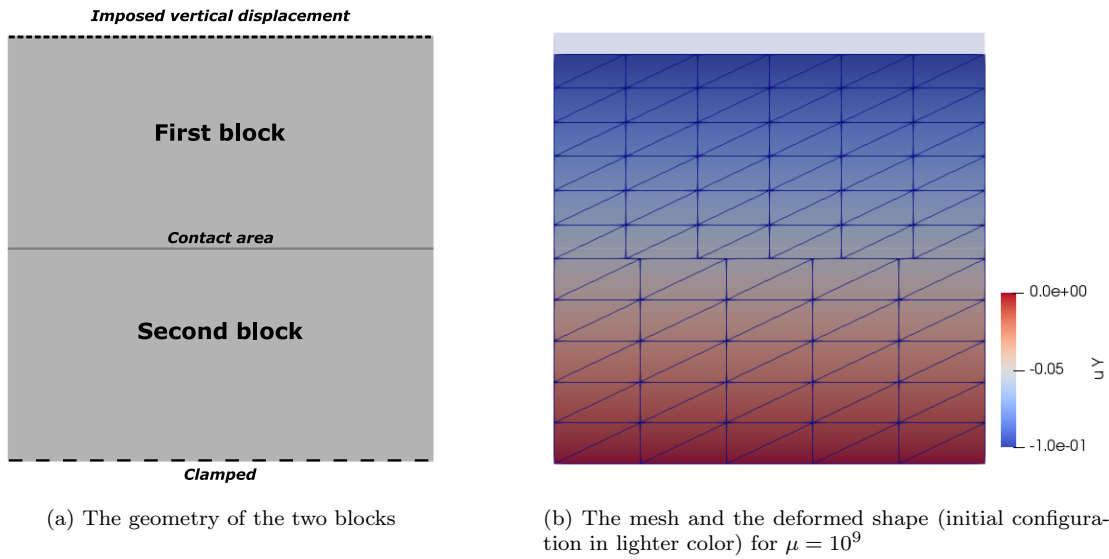


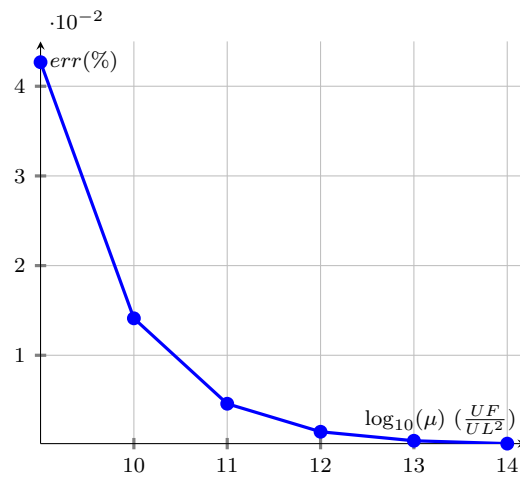
Figure 3.7 – The geometry and the deformed shape of the two blocks

The error between the theoretical contact pressure and the computed one is given as follows

$$err(\%) = \frac{\|p_{theo} - \sigma_y\|_{L^2(\Gamma_C)}}{\|p_{theo}\|_{L^2(\Gamma_C)}} \times 100 \quad (3.158)$$

where  $\Gamma_C$  is the contact area.

Using  $P_1$  finite elements, the variation of the error ( $err$ ) w.r.t the penalty factor  $\mu$  is shown in the Figure 3.8.

Figure 3.8 – The variation of the error ( $err$ ) w.r.t the penalty factor  $\mu$

### 3.9.2 Contact between two cylinders

In order to show that the symmetric algorithm using penalty method can handle the contact between two curved bodies, a contact between two cylinders is considered. This example can be found in [108]. Two concentric cylinders with the same thickness of  $t = 5UL$  are initially in contact, the inner radius of the inner cylinder is equal to  $R_{in} = 10UL$  and the outer radius of the outer cylinder is equal to  $R_{out} = 20UL$ . A radial pressure of  $p = 1 \frac{UF}{UL^2}$  is applied on the outer cylinder. Due to the symmetry of the problem, only one quarter of the problem is considered, as is depicted in the Figure 3.9, the plane strain hypothesis is also considered. The two cylinders are made from a similar elastic material, Young's modulus  $E = 100 \frac{UF}{UL^2}$  and Poisson's ratio  $\nu = 0$ .

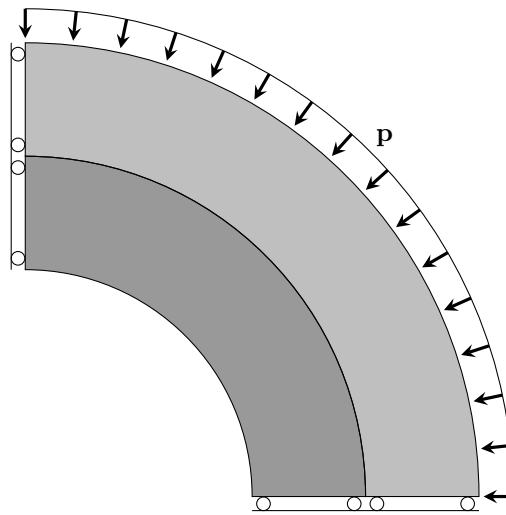


Figure 3.9 – The geometry of the problem

We are interested in the value of the radial stress in the two cylinders, which can be seen in the Figure 3.10 for the linear finite elements ( $P_1$ ) and for a penalty factor of  $\mu = 10^9$ .

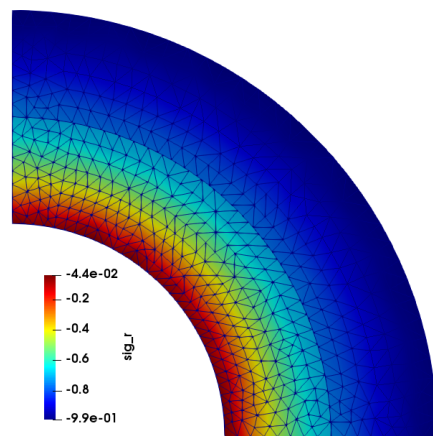


Figure 3.10 – The mesh and the radial stress

We notice the non-conforming meshes in the Figure 3.10, in addition we notice that the radial stress on the inner border is nearly zero, because this border is free, and is nearly equal to 1, the applied pressure, on the outer border. We obtain similar results as in [108].



# Weak contact formulation and a simple symmetric algorithm

## Outline of the current chapter

---

<b>4.1 Weak non-penetration condition for the contact</b>	<b>86</b>
4.1.1 Mesh discretization . . . . .	87
4.1.2 Non-penetration condition . . . . .	88
<b>4.2 Numerical Integration</b>	<b>89</b>
4.2.1 Numerical integration of the weak constraints . . . . .	90
<b>4.3 Contact problems with interior point method</b>	<b>93</b>
4.3.1 Symmetric formulation . . . . .	94
4.3.2 Numerical optimization by the interior point method . . . . .	94
4.3.3 Behavior of the barrier solutions . . . . .	98
4.3.4 Global convergence . . . . .	101
<b>4.4 Alternative formulations</b>	<b>103</b>
4.4.1 First alternative formulation . . . . .	103
4.4.2 Mixed symmetric methods . . . . .	104
<b>4.5 Symmetric contact algorithm</b>	<b>104</b>
<b>4.6 Rigid body motions</b>	<b>105</b>
<b>4.7 Numerical validations</b>	<b>106</b>
4.7.1 Compression of two elastic blocks with imposed displacement . . . . .	106
4.7.2 Hertz contact with two elastic bodies . . . . .	107
4.7.3 Contact between two cylinders . . . . .	109
4.7.4 Disc-in-disc . . . . .	110
4.7.5 Multi-body contact between three beams . . . . .	111

---

In this chapter, an algorithm to solve frictionless contact problems using FreeFEM and IPOPT software is presented. The non-penetration conditions are expressed in a weak form, and the contact problem is written in the form of a sequence of minimization problems with linear constraints especially in the case of large deformations, and each minimization problem is solved using the interior point method. The advantage of this algorithm is its simplicity, in addition the algorithm is symmetric. Moreover we will see how we can take advantage of the interior point method, in order to impose a symmetric non-penetration conditions without having numerical difficulties.

## 4.1 Weak non-penetration condition for the contact

First of all, for any measure  $\lambda$  we consider a measurable set  $\Gamma_C$  and a function  $f$  such that  $f \in L^2(\Gamma_C)$ . We define also the set  $L_+^2(\Gamma_C)$  as:

$$L_+^2(\Gamma_C) = \{\zeta \in L^2(\Gamma_C) \mid \zeta \geq 0 \text{ a.e on } \Gamma_C\} \quad (4.1)$$

We have the following theorem

**Theorem 4.1.** *Using the above notations we have the following property, if*

$$(f, \zeta)_{L^2} = \int_{\Gamma_C} f \cdot \zeta \, d\lambda \geq 0 \quad \forall \zeta \in L_+^2(\Gamma_C) \quad (4.2)$$

Then

$$f \in L_+^2(\Gamma_C) \quad (4.3)$$

*Proof.* Suppose that  $\lambda(\{f < 0\}) > 0$ , we have

$$\int_{\Gamma_C} f \cdot \mathbf{1}_{\{f < 0\}} \, d\lambda \leq 0 \quad (4.4)$$

and by hypothesis, we obtain

$$\int_{\Gamma_C} f \cdot \mathbf{1}_{\{f < 0\}} \, d\lambda = 0 \quad (4.5)$$

Therefore

$$f \cdot \mathbf{1}_{\{f < 0\}} = 0 \text{ a.e on } \Gamma_C \quad (4.6)$$

which is false because  $f \cdot \mathbf{1}_{\{f < 0\}} = f < 0$  on  $\{f < 0\}$  and  $\lambda(\{f < 0\}) > 0$ .

□

As before, The displacement field  $\mathbf{u}$  is defined by  $\mathbf{u} = (\mathbf{u}^1, \mathbf{u}^2)$  where  $\mathbf{u}^l$  corresponds to the displacement field of the body  $\Omega^l$ , with the admissible set  $\mathbf{V} = \mathbf{V}^1 \times \mathbf{V}^2$ , where

$$\mathbf{V}^l = \{\mathbf{v} \in \mathbf{H}^1(\Omega^l) \mid \mathbf{v} = 0 \text{ a.e on } \Gamma_0^l\} \quad (4.7)$$

endowed with the broken norm:

$$\|\mathbf{u}\|_1 = \|(\mathbf{u}^1, \mathbf{u}^2)\|_1 = (\|\mathbf{u}^1\|_1^2 + \|\mathbf{u}^2\|_1^2)^{\frac{1}{2}} \quad (4.8)$$

Let  $\Gamma_{C1}$  be the potential contact area of the slave body, the non-penetration condition as was presented for the contact is the following

$$g(\mathbf{X}) := (\mathbf{x} - \bar{\mathbf{x}}) \cdot \mathbf{n} = (\mathbf{x}^1 - \bar{\mathbf{x}}) \cdot \mathbf{n} \geq 0 \quad \forall \mathbf{X} \in \Gamma_{C1} \quad (4.9)$$

where as before,  $\mathbf{x}^l = \mathbf{X}^l + \mathbf{u}^l$  the actual position and  $\bar{\mathbf{x}}$  its projection on the second body, finally  $\mathbf{n}$  denotes the outward unit normal vector at  $\bar{\mathbf{x}}$ .

The new non-penetration formulation is described by

$$(g, \zeta)_{L^2(\Gamma_{C1})} := \int_{\Gamma_{C1}} g \cdot \zeta \, d\lambda \geq 0 \quad \forall \zeta \in L^2_+(\Gamma_{C1}) \quad (4.10)$$

The formulations (4.9) and (4.10) are equivalent.

### 4.1.1 Mesh discretization

Using the finite element approach, for  $l = 1$  or  $2$ , let  $\Omega_h^l$  be the mesh of the body  $\Omega^l$ , which is composed from the triangles family  $\{T_i^l \mid i = 1, \dots, n_T^l\}$ . In addition, consider the following spaces

$$\mathbf{V}_h^l = \left\{ \mathbf{v} = (v_1, v_2) \in C^0(\Omega_h^l) \times C^0(\Omega_h^l) \mid \mathbf{v}|_{T_i^l} \in P_r \times P_r, \forall i = 1, \dots, n_T^l \text{ and } \mathbf{v} = 0 \text{ on } \Gamma_0^l \right\} \quad (4.11)$$

where  $C^0(\Omega_h^l)$  denotes the set of the continuous functions on  $\Omega_h^l$ , and  $P_r$  denotes the linear finite elements for  $r = 1$  and the quadratic ones for  $r = 2$ .

Consider the space  $\mathbf{V}_h$  defined as follows

$$\mathbf{V}_h = \mathbf{V}_h^1 \times \mathbf{V}_h^2 \quad (4.12)$$

Let  $\mathbf{u}_h = (\mathbf{u}_h^1, \mathbf{u}_h^2) \in \mathbf{V}_h$ , the displacement vector field on the mesh  $\Omega_h^l$ , is given by

$$\mathbf{u}_h^l = \sum_i \begin{pmatrix} U_i^{l,x} \\ U_i^{l,y} \end{pmatrix} \hat{w}_i^l \quad (4.13)$$

where  $\hat{w}_i^l$  are the shape functions on the mesh  $\Omega_h^l$ , and  $(U_i^{l,x} \ U_i^{l,y})^T$  are the degrees of freedom of  $\mathbf{u}_h^l$ , in other words  $U_i^{l,x}$  and  $U_i^{l,y}$  represent respectively the horizontal and vertical displacements of the node  $i$  in the mesh. For the sake of clarity we omit the subscript  $h$  for all vectors.

In addition, we consider the space  $Z_h^+$

$$Z_h^+ = \{ \zeta \in C^0(\Gamma_{C1}) \mid \zeta|_{T_i \cap \Gamma_{C1}} \in P_1, \forall i = 1, \dots, n_T^1 \text{ and } \zeta \geq 0 \} \quad (4.14)$$

which is the trace space on  $\Gamma_{C1}$  of the set of the positive continuous functions which are linear

on each triangle. The minimization problem in this case becomes

Find  $\mathbf{u} \in \mathbf{V}_h$  such that

$$\begin{cases} \mathbf{u} = \arg \min_{\mathbf{V}_h} (\mathcal{E}_p) \\ (g, \zeta)_{L^2} = \int_{\Gamma_{C1}} g \cdot \zeta \, d\lambda \geq 0 \quad \forall \zeta \in Z_h^+ \end{cases} \quad (4.15)$$

where  $\mathcal{E}_p$  is the total potential energy. If  $\zeta$  is a test function  $\zeta \in Z_h^+$  then

$$\zeta = \sum_{i=1}^{n_{C1}} a_i \phi_i \quad (4.16)$$

where  $n_{C1}$  is the nodes number on  $\Gamma_{C1}$ ,  $a_i \in \mathbb{R}$  and  $\phi_i$  are the trace of the shape functions defined at the nodes of  $\Gamma_{C1}$ . The coefficients  $a_i$  are positives, indeed if  $p_i$  is a node of  $\Gamma_{C1}$  then  $\zeta(p_i) = a_i \cdot 1 = a_i \geq 0$ . Thus  $\zeta \in Z_h^+$  iff

$$\zeta = \sum_{i=1}^{n_{C1}} a_i \phi_i \quad \text{where } a_i \geq 0 \quad (4.17)$$

As we have  $P_1$  finite elements for the trace space,  $\phi_i \geq 0$  and  $\phi_i \in Z_h^+$ , therefore we have the following equivalence

$$(g, \zeta)_{L^2} = \int_{\Gamma_{C1}} g \cdot \zeta \, d\lambda \geq 0 \quad \forall \zeta \in Z_h^+ \iff (g, \phi_i)_{L^2} = \int_{\Gamma_{C1}} g \cdot \phi_i \, d\lambda \geq 0 \quad \forall i = 1, \dots, n_{C1} \quad (4.18)$$

### 4.1.2 Non-penetration condition

We recall in the following the non-penetration condition

$$g = (\mathbf{x} - \bar{\mathbf{x}}) \cdot \mathbf{n} \geq 0 \quad (4.19)$$

The weak non-penetration condition becomes

$$\int_{\Gamma_{C1}} g \cdot \phi_i \, d\lambda \geq 0 \quad \forall i = 1, \dots, n_{C1} \quad (4.20)$$

Note that the integration is done on the potential contact border in the initial configuration. In conclusion the minimization problem becomes

$$\begin{cases} \mathbf{u} = \arg \min_{\mathbf{V}_h} (\mathcal{E}_p) \\ \int_{\Gamma_{C1}} g \cdot \phi_i \, d\lambda \geq 0 \quad \forall i = 1, \dots, n_{C1} \end{cases} \quad (4.21)$$

where  $\mathcal{E}_p$  is the total potential energy defined by:

$$\begin{cases} \mathcal{E}_p(\mathbf{v}) = \frac{1}{2}a(\mathbf{v}, \mathbf{v}) - f(\mathbf{v}) \text{ for linear elastic problems} \\ \mathcal{E}_p(\mathbf{v}) = \int_{\Omega_h^1 \cup \Omega_h^2} \hat{W}(\mathbf{v}) dv - f(\mathbf{v}) \text{ for large deformations and hyperelastic problems} \end{cases} \quad (4.22)$$

with  $\hat{W}$  the strain energy function.

In the case of linear elasticity, we can prove the existence and the uniqueness by Stampacchia's theorem. This weak formulation can be seen as the mortar method, treating the contact problems in [15, 59, 97],

In mortar method the shape functions at the element connected to the ends of the contact area  $\Gamma_C$  have a degree less than the others, indeed the goal is to avoid the over constraints when there exist already a constraints at these ends. Assuming that there is no additional constraints at these ends, the shape functions will be here the classical ones  $\phi_i$ .

In the case of quadratic finite elements, the shape functions  $\phi_i$  are taken as the linear ones, at the two ends of the segment, otherwise non physical oscillations are observed at the contact area probably because the quadratic shape functions are not positive.

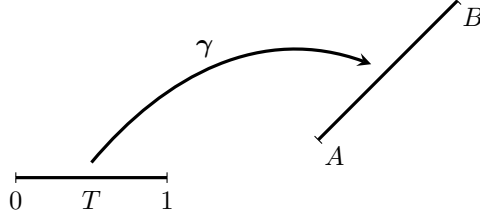
Let  $\mathbf{u} = (\mathbf{u}_1, \mathbf{u}_2)$  be the solution of the contact problem, suppose that  $\mathbf{u}_1 \in H^2(\Omega_1)^2$  and  $\mathbf{u}_2 \in H^2(\Omega_2)^2$ , in addition let  $\mathbf{u}_h$  be the solution of the finite element one, using linear finite elements, where the shape functions  $\phi_i$  in (4.21), connected to the ends of the contact area  $\Gamma_C$  have a degree less than the others, then the error between the two solutions can be found in [59] as follows

$$\|\mathbf{u} - \mathbf{u}_h\|_1 \leq C(\mathbf{u}) \left( h_1^{\frac{1}{4}} + h_2 \right) \quad (4.23)$$

where  $\|\cdot\|_1$  is the broken norm,  $C(\mathbf{u})$  depends only on  $\mathbf{u}_1$  and  $\mathbf{u}_2$ , and finally  $h_1$  and  $h_2$  are respectively the mesh size of the first and the second body.

## 4.2 Numerical Integration

A several notions from the section 3.5 of the chapter 3 are recalled here. In this section the two-dimensional case is considered for the sake of simplicity. First consider a parent element  $T = [0, 1]$  and a mapping  $\gamma : T \rightarrow \mathbb{R}^2$ , which transforms  $T$  into a segment  $AB$  in  $\mathbb{R}^2$  (see Figure 4.1).

Figure 4.1 – The mapping  $\gamma$  applied on the parent element

Let  $\hat{N}_1, \hat{N}_2$  be the two linear shape functions on  $T$ , given by

$$\begin{cases} \hat{N}_1(t) = 1 - t \\ \hat{N}_2(t) = t \end{cases} \quad (4.24)$$

We considered the linear case also for the sake of simplicity.

If  $\mathbf{X} \in AB$ , and  $\mathbf{X}_A = (X_A, Y_A)$ ,  $\mathbf{X}_B = (X_B, Y_B)$  are respectively the points  $A$  and  $B$  of the segment  $AB$ , then

$$\gamma(t) = \mathbf{X}(t) = \hat{N}_1(t)\mathbf{X}_A + \hat{N}_2(t)\mathbf{X}_B \quad (4.25)$$

or

$$\mathbf{X}(t) = (1 - t)\mathbf{X}_A + t\mathbf{X}_B \quad (4.26)$$

In this case, the integral of a function  $f : AB \rightarrow \mathbb{R}$  becomes

$$\int_{AB} f(\mathbf{X}) ds = \int_{AB} f(\gamma) ds = \int_T f(\gamma(t)) \|\gamma'(t)\| ds \quad (4.27)$$

In the linear case,  $\|\gamma'(t)\|$  is equal to the length of  $AB$ , indeed

$$\|\gamma'(t)\| = \|X_B - X_A\| = \|AB\| \quad (4.28)$$

Let  $\{t_{ip} \mid ip = 0, \dots, nip\}$  be the set of integration points on  $T$ , with the corresponding set of weights  $\{w_{ip} \mid ip = 0, \dots, nip\}$ , where  $nip$  is the integration points number. In this case the numerical integration of a function  $F : T \rightarrow \mathbb{R}$  over  $T$  is given, by the following

$$\int_T F(t) dt = \sum_{ip=1}^{nip} F(t_{ip}) \cdot w_{ip} \quad (4.29)$$

### 4.2.1 Numerical integration of the weak constraints

Consider the node  $i$  on  $\Gamma_{C1}$ , as before  $\phi_i$  is the trace of the shape function defined at the node  $i$ . We want to evaluate the following integral

$$\int_{\Gamma_{C1}} g \cdot \phi_i ds = \int_{\Gamma_{C1}} (\mathbf{x} - \bar{\mathbf{x}}) \cdot \mathbf{n} \cdot \phi_i ds \quad (4.30)$$

Let  $n^*$  be the number of segments (triangles in 3D) connected to node  $i$ , and  $\{s_k^i \mid k = 1, \dots, n^*\}$  the connected segments. As  $\phi_i$  is null outside the connected segments, then

$$\int_{\Gamma_{C1}} g \cdot \phi_i ds = \sum_{k=1}^{n^*} \int_{s_k^i} (\mathbf{x} - \bar{\mathbf{x}}) \cdot \mathbf{n} \cdot \phi_i ds \quad (4.31)$$

For example in 2D  $n^* = 1$  or 2.

Let's take a segment  $s_k^i$  connected to the node  $i$ . Suppose that  $A$  and  $B$  are the segment ends of  $s_k^i$ , and  $B$  corresponds to the node  $i$ . We note  $\mathbf{U}_A$  and  $\mathbf{U}_B$  the degrees of freedom of the displacement field  $\mathbf{u}$  at the nodes  $A$  and  $B$ , in addition  $\mathbf{X}_A$  and  $\mathbf{X}_B$  denote respectively the coordinates in the initial configuration, of the nodes  $A$  and  $B$ . Let  $N_A$  and  $N_B$  ( $\phi_i = N_B$ ) denote the shape functions at  $A$  and  $B$ , then using the parent element  $T$  we can write the following

$$\begin{cases} N_A(\mathbf{X}) = \hat{N}_1(\gamma^{-1}(\mathbf{X})) \\ N_B(\mathbf{X}) = \hat{N}_2(\gamma^{-1}(\mathbf{X})) \\ \phi_i(\mathbf{X}) = \hat{N}_2(\gamma^{-1}(\mathbf{X})) \\ \mathbf{X} = \mathbf{X}_A \cdot \hat{N}_1(\gamma^{-1}(\mathbf{X})) + \mathbf{X}_B \cdot \hat{N}_2(\gamma^{-1}(\mathbf{X})) \\ \mathbf{u} = \mathbf{U}_A \cdot \hat{N}_1(\gamma^{-1}(\mathbf{X})) + \mathbf{U}_B \cdot \hat{N}_2(\gamma^{-1}(\mathbf{X})) \end{cases} \quad (4.32)$$

Thus the actual position field  $\mathbf{x}$  is given on  $AB$  by

$$\mathbf{x} = (\mathbf{X}_A + \mathbf{U}_A) \cdot \hat{N}_1(\gamma^{-1}(\mathbf{X})) + (\mathbf{X}_B + \mathbf{U}_B) \cdot \hat{N}_2(\gamma^{-1}(\mathbf{X})) \quad (4.33)$$

Note that  $U_A$  and  $U_B$  belongs to the unknowns of our problem. Using the equation (4.27) and the quadrature formula (4.29), the integral over  $s_k^i$  or  $AB$  in equation (4.31) can be given by

$$\begin{aligned} \int_{s_k^i} (\mathbf{x} - \bar{\mathbf{x}}) \cdot \mathbf{n} \cdot \phi_i ds &= \int_{AB} (\mathbf{x} - \bar{\mathbf{x}}) \cdot \mathbf{n} \cdot \phi_i ds \\ &= \sum_{ip=1}^{nip} (\mathbf{x}_{ip} - \bar{\mathbf{x}}_{ip}) \cdot \mathbf{n}_{ip} \cdot \hat{N}_2(t_{ip}) \cdot \|\gamma'(t)\| \cdot w_{ip} \\ &= \sum_{ip=1}^{nip} (\mathbf{x}_{ip} - \bar{\mathbf{x}}_{ip}) \cdot \mathbf{n}_{ip} \cdot \hat{N}_2(t_{ip}) \cdot \|AB\| \cdot w_{ip} \end{aligned} \quad (4.34)$$

where  $\mathbf{x}_{ip}$  is the actual position of the integration point  $ip$ , given by

$$\mathbf{x}_{ip} = (\mathbf{X}_A + \mathbf{U}_A) \cdot \hat{N}_1(t_{ip}) + (\mathbf{X}_B + \mathbf{U}_B) \cdot \hat{N}_2(t_{ip}) \quad (4.35)$$

It remains to compute the projection point  $\bar{\mathbf{x}}_{ip}$  of  $\mathbf{x}_{ip}$  on the second body, and the normal vector  $\mathbf{n}_{ip}$  at  $\bar{\mathbf{x}}_{ip}$ . In order to compute  $\bar{\mathbf{x}}_{ip}$ , a fixed point algorithm is employed in the case of large displacements, otherwise speaking the previous displacement  $\mathbf{u}^{n-1}$  is used in order to find the closest second body segment to  $\mathbf{x}_{ip}^{n-1}$ . Indeed we do the following actions

1. For  $\mathbf{x}_{ip}^{n-1}$  we look for the closest node of the second body contact area, let's say node  $j$ , we use simply the distance, but we will use in the future a quadtree
2. The set  $\{r_k^j \mid k = 1, \dots, n_2^*\}$ ,  $n_2^* = 1$  or 2, is the set of segments connected to the node  $j$

3. We look for the point  $P_k$  in each segment  $r_k^j$ , which is the closest to  $\mathbf{x}_{ip}^{n-1}$
4. The closest point  $\bar{P}$  to  $\mathbf{x}_{ip}^{n-1}$  within  $\{P_k \mid k = 1, \dots, n_2^*\}$ , is chosen

Let  $CD$  be the segment which contains  $\bar{P}$  and  $\bar{\lambda} \in [0, 1]$  such that

$$\bar{P} = (1 - \bar{\lambda})\mathbf{x}_C^{n-1} + \bar{\lambda}\mathbf{x}_D^{n-1} \quad (4.36)$$

with

$$\begin{cases} \mathbf{x}_C^{n-1} = \mathbf{X}_C + \mathbf{U}_C^{n-1} \\ \mathbf{x}_D^{n-1} = \mathbf{X}_D + \mathbf{U}_D^{n-1} \end{cases} \quad (4.37)$$

The principle of the fixed point algorithm is to use at the actual iteration  $n$ , the segment  $CD$  as the closest segment to  $\mathbf{x}_{ip}$ , and  $\bar{\lambda}$  as the position of  $\bar{\mathbf{x}}_{ip}$  in  $CD$ , otherwise speaking the fixed point is on the parameter  $\bar{\lambda}$ . Therefore the actual projection point  $\bar{\mathbf{x}}_{ip}$  will be given by

$$\bar{\mathbf{x}}_{ip} = (1 - \bar{\lambda})\mathbf{x}_C + \bar{\lambda}\mathbf{x}_D \quad (4.38)$$

with

$$\begin{cases} \mathbf{x}_C = \mathbf{X}_C + \mathbf{U}_C \\ \mathbf{x}_D = \mathbf{X}_D + \mathbf{U}_D \end{cases} \quad (4.39)$$

Finally the integral over  $s_k^i$  or  $AB$  in equation (4.31) can be given by

$$\int_{s_k^i} (\mathbf{x} - \bar{\mathbf{x}}) \cdot \mathbf{n} \cdot \phi_i ds = \sum_{ip=1}^{nip} (\mathbf{x}_{ip} - \bar{\mathbf{x}}_{ip}) \cdot \mathbf{n}_{ip} \cdot \hat{N}_2(t_{ip}) \cdot \|AB\| \cdot w_{ip} \quad (4.40)$$

where  $\mathbf{x}_{ip}$  is the actual position of the integration point  $ip$ , and  $\bar{\mathbf{x}}_{ip}$  its projection. More precisely

$$\begin{cases} \mathbf{x}_{ip} = (\mathbf{X}_A + \mathbf{U}_A) \cdot \hat{N}_1(t_{ip}) + (\mathbf{X}_B + \mathbf{U}_B) \cdot \hat{N}_2(t_{ip}) \\ \bar{\mathbf{x}}_{ip} = (\mathbf{X}_C + \mathbf{U}_C) \cdot \hat{N}_1(\bar{\lambda}) + (\mathbf{X}_D + \mathbf{U}_D) \cdot \hat{N}_2(\bar{\lambda}) \\ \mathbf{n}_{ip} = \mathbf{n}_C \cdot \hat{N}_1(\bar{\lambda}) + \mathbf{n}_D \cdot \hat{N}_2(\bar{\lambda}) \end{cases} \quad (4.41)$$

Note that  $\mathbf{U}_A$  and  $\mathbf{U}_B$  belong to the degrees of freedom of the first body and  $\mathbf{U}_C$  and  $\mathbf{U}_D$  belong to the degrees of freedom of the second body, and these 4 quantities are a part of our unknowns. Moreover  $\mathbf{n}_C$  or  $\mathbf{n}_D$  are computed as follows

$$\mathbf{n}_C = \frac{\sum_{i=1}^{n_C^*} \mathbf{n}_i}{\left\| \sum_{i=1}^{n_C^*} \mathbf{n}_i \right\|} \quad (4.42)$$

where  $n_C^*$  is the number of segments connected to  $C$  and  $\mathbf{n}_i$  is the unit normal vector at the segment  $i$  connected to  $C$ , from the previous iteration  $n - 1$ . Another definition of  $\mathbf{n}_C$  can be given as a weighted average, especially when there is a big difference between the length of the

connected segments to  $C$ , indeed

$$\mathbf{n}_C = \frac{\sum_{i=1}^{n_C^*} l_i \mathbf{n}_i}{\left\| \sum_{i=1}^{n_C^*} l_i \mathbf{n}_i \right\|} \quad (4.43)$$

where  $l_i$  is the length, at the previous iteration  $n - 1$ , of the segment  $i$  connected to  $C$ .

**Remark 4.1**

*If two integration points belong to the same segment of the first body, then their projection points can belong to a different segments of the second body, see Figure 4.2.*

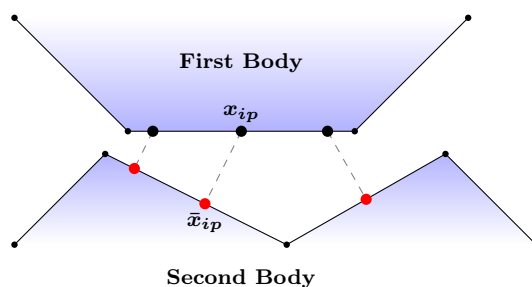


Figure 4.2 – The projection of the first body integration points on the second body

In the case of quadratic finite elements ( $P_2$ ) where the shape functions are quadratic, the same procedure is employed. However the mapping  $\gamma$  is affine, indeed isoparametric elements are not employed, and the boundary of the mesh is polygonal. In addition the shape function  $\phi_i$  in the constraints integrals is considered to be linear.

### 4.3 Contact problems with interior point method

Interior point method is a method to solve constrained minimization problems, one can see [47, 86] for more details about this method. Interior point method was used to solve contact problems, we can cite for example [88] where a primal algorithm was used, with the inverse and the logarithmic barrier functional, in the case of the Signorini's frictionless problem for linear elastic body, in [112] the primal and primal-dual algorithms were considered for the Signorini's frictionless problem, also in the case of linear elastic body. In [116] a primal and dual algorithms were developed to treat the frictionless contact in the case of finite deformation, and it was shown in their formulations that the primal algorithm is more robust than the primal-dual one. In the case of frictional contact problems, a interior point method and a B-differentiable Newton method have been suggested and compared in [28].

In the paper [74], for linear elastic and for Signorini's frictional problems, the problem was written in term of an optimization one, on the Lagrange multipliers (the normal and the tangential contact pressure), otherwise speaking in a dual form. An interior point algorithm was developed, in addition a preconditioner was used in order to solve the generated linear system with iterative methods, the conjugate gradient method.

### 4.3.1 Symmetric formulation

One simple way to create a symmetric formulation, is to take into account an additional non-penetration constraints by considering the second body as slave and the first one as master, thus the additional contact conditions is defined this time on the contact area  $\Gamma_{C2}$  of the second body. In other words the problem becomes

$$\begin{cases} \mathbf{u} = \arg \min_{\mathbf{v} \in \mathbf{V}_h} (\mathcal{E}_p(\mathbf{v})) \\ c_1 := \int_{\Gamma_{C1}} ((\mathbf{x} - \bar{\mathbf{x}}_2) \cdot \mathbf{n}) \cdot \phi_i^{(1)} ds \geq 0 \quad \forall i = 1, \dots, n_{C1} \\ c_2 := \int_{\Gamma_{C2}} ((\mathbf{x} - \bar{\mathbf{x}}_1) \cdot \mathbf{n}) \cdot \phi_i^{(2)} ds \geq 0 \quad \forall i = 1, \dots, n_{C2} \end{cases} \quad (4.44)$$

where  $\bar{\mathbf{x}}_l$  is the projection of  $\mathbf{x}$  on the body  $\phi(\Omega_l)$  for  $l = 1, 2$ , with  $\phi$  the deformation mapping.

For linear elastic problems, the constraints in the problem (4.44) are linear, indeed the deformations are supposed to be small. Otherwise for the finite deformation problems and more specifically for hyperelastic materials, it is not the case, but we can transform the problem (4.44) into a sequence of minimization problems with linear constraints, using a fixed point algorithm. The gradient of the constraints in the problem (4.44) may be linear dependent, and thus generating numerical difficulties. We will see next how to avoid these difficulties.

In the case of using the interior point method, we will see in the next section that the inequality constraints are transformed using the slack variables, and thus generating a constraints Jacobian matrix with full row rank. Also we will show that the matrix  $K$  responsible of the search directions computation is non-singular, therefore numerically the linear dependency between the constraints are not going to be an issue.

### 4.3.2 Numerical optimization by the interior point method

After the finite element discretization, the contact problem is transformed into a constrained optimization one, for this purpose the interior point method is used in order to solve it. Let  $x \in \mathbb{R}^n$  denotes the degrees of freedom vector of the displacement field  $\mathbf{u}$  (using the finite element method), then the problem can be formulated numerically as the following

$$\begin{cases} \min_{x \in \mathbb{R}^n} E(x) = E_1(x) + E_2(x) \quad \text{such that} \\ c_1(x) \geq 0 \\ c_2(x) \geq 0 \end{cases} \quad (4.45)$$

where  $E_1, E_2$  are respectively the total potential energy of the first and second body,  $c_1$  is the constraints vector when taking the first body as slave and  $c_2$  is the constraints vector when taking the second body as slave. In some cases the constraints are linearly dependent especially when the symmetric case is considered. In addition when some methods are used, the Jacobian matrix of the constraints does not have anymore full row rank and therefore numerical difficulties can be generated.

Let  $c : \mathbb{R}^n \rightarrow \mathbb{R}^m$  the linear constraints vector,  $c = (c_1^T, c_2^T)^T$ , with  $m = n_{C1} + n_{C2}$ , where  $n_{C1}$  and  $n_{C2}$  are respectively the components number of  $c_1$  and  $c_2$ . The contact problem becomes

$$\begin{cases} \min_{x \in \mathbb{R}^n} E(x) & \text{such that} \\ c(x) \geq 0 \end{cases} \quad (4.46)$$

Note that the inequality between two vectors is the inequality between each component of these two vectors. Introducing the slack variables  $s$ , the problem (4.46) is equivalent to

$$\begin{cases} \min_{(x,s) \in \mathbb{R}^n \times \mathbb{R}^m} E(x) & \text{such that} \\ c(x) - s = 0 \\ s \geq 0 \end{cases} \quad (4.47)$$

The constraints are linear, therefore the constraints are qualified for the KKT (Karush-Kuhn-Tucker) system, the first-order necessary conditions or the KKT conditions for the problem (4.47) are the following

$$\begin{cases} \nabla_x E(x) + \nabla_x c(x)\lambda = 0 \\ -\lambda - z = 0 \\ c(x) - s = 0 \\ SZe = 0 \\ s, z \geq 0 \end{cases} \quad (4.48)$$

where  $\lambda$  and  $z$  are respectively the Lagrange multipliers of the equality constraints and the bound constraints,  $S$  and  $Z$  are two diagonal matrices where  $S_{ii} = s_i$  and  $Z_{ii} = z_i$ , finally  $e^T = (1, \dots, 1)$ , a unit vector. Applying a homotopy method to the problem (4.48) (see [120]) with the homotopy (also called barrier) parameter  $\mu$ . We obtain the following equations

$$\begin{cases} \nabla_x E(x) + \nabla_x c(x)\lambda = 0 \\ -\lambda - z = 0 \\ c(x) - s = 0 \\ SZe - \mu e = 0 \end{cases} \quad (4.49)$$

with  $s, z \geq 0$  and  $\mu$  converging to zero. Note if  $\mu = 0$  then the problem (4.49) becomes the KKT system (4.48) of the original problem.

Otherwise, the problem (4.49) is equivalent to the following barrier problem

$$\begin{cases} \min_{(x,s) \in \mathbb{R}^n \times \mathbb{R}^m} E_\mu(x) = E(x) - \mu \sum_{i=1}^m \ln(s_i) & \text{such that} \\ c(x) - s = 0 \end{cases} \quad (4.50)$$

For each barrier parameter  $\mu$ , a descent method is applied in order to compute a solution of the primal-dual system (4.49), indeed at the iteration  $k + 1$

$$\begin{cases} x_{k+1} = x_k + \alpha_k d_k^x \\ s_{k+1} = s_k + \alpha_k d_k^s \\ \lambda_{k+1} = \lambda_k + \alpha_k d_k^\lambda \\ z_{k+1} = z_k + \alpha_k d_k^z \end{cases} \quad (4.51)$$

where  $\alpha_k, \alpha_k^z$  are the step sizes allowed to be different [120], and  $d_k^x, d_k^s, d_k^\lambda, d_k^z$  are respectively the descent direction of  $x, s, \lambda, z$ . Besides  $s_{k+1} \geq 0, z_{k+1} \geq 0$  by using the fraction-to-the-boundary rule [120] to choose,  $\alpha_k, \alpha_k^z$ . In the following, a Newton's method is applied in order to compute the descent directions. By considering that our constraints are linear, we obtain the following linear system

$$\begin{bmatrix} \nabla_{xx}E(x_k) & 0 & \nabla_x c(x_k) & 0 \\ 0 & 0 & -I & -I \\ \nabla_x c(x_k)^T & -I & 0 & 0 \\ 0 & Z_k & 0 & S_k \end{bmatrix} \begin{pmatrix} d_k^x \\ d_k^s \\ d_k^\lambda \\ d_k^z \end{pmatrix} = - \begin{pmatrix} \nabla_x E(x_k) + \nabla_x c(x_k) \lambda_k \\ -\lambda_k - z_k \\ c(x_k) - s_k \\ S_k Z_k e - \mu e \end{pmatrix} \quad (4.52)$$

This linear system (4.52) can be reduced into

$$\begin{bmatrix} \nabla_{xx}E(x_k) & 0 & \nabla_x c(x_k) \\ 0 & S_k^{-1} Z_k & -I \\ \nabla_x c(x_k)^T & -I & 0 \end{bmatrix} \begin{pmatrix} d_k^x \\ d_k^s \\ d_k^\lambda \end{pmatrix} = - \begin{pmatrix} \nabla_x E(x_k) + \nabla_x c(x_k) \lambda_k \\ -\mu S_k^{-1} e - \lambda_k \\ c(x_k) - s_k \end{pmatrix} \quad (4.53)$$

with the additional equation  $d_k^z = \mu S_k^{-1} e - z_k - S_k^{-1} Z_k d_k^s$ .

The software IPOPT [120] uses this method in addition to a linear search with a filter method in order to determine the parameters  $\alpha_k$ . Note that in [85], there are different strategies in order to update the barrier parameter  $\mu$ .

In [86] we can find an interesting theorem which gives sufficient conditions in order to make the matrix in (4.53) non-singular. This theorem is recalled below with the same notations.

**Theorem 4.2.** *Let  $A_{m \times n}$  be a full row rank matrix with  $m < n$ ,  $Z_{n \times (n-m)}$  a full rank matrix where its columns are a basis for the null space of  $A$  ( $AZ = 0$ ). If  $G_{n \times n}$  is a matrix such that  $Z^T G Z$  is positive definite then the KKT matrix defined below*

$$K = \begin{bmatrix} G & A^T \\ A & 0 \end{bmatrix} \quad (4.54)$$

*is non-singular.*

*Proof.* In order to prove that the KKT matrix is non-singular we have to show that the zero vector is the only solution of the following equation

$$\begin{bmatrix} G & A^T \\ A & 0 \end{bmatrix} \begin{bmatrix} x \\ y \end{bmatrix} = 0 \quad (4.55)$$

where  $x \in \mathbb{R}^n$  and  $y \in \mathbb{R}^m$ . Otherwise

$$\begin{aligned} \begin{bmatrix} x & y \end{bmatrix}^T \begin{bmatrix} G & A^T \\ A & 0 \end{bmatrix} \begin{bmatrix} x \\ y \end{bmatrix} &= x^T Gx + x^T A^T y + y^T Ax \\ &= x^T Gx + (Ax)^T y + y^T Ax \\ &= x^T Gx \end{aligned} \quad (4.56)$$

because  $Ax = 0$  from the equation (4.55), thus  $x^T Gx = 0$ . since  $Ax = 0$  therefore  $x$  belongs to the null space of  $A$  and can be expressed as  $x = Zv$  with  $v \in \mathbb{R}^{n-m}$ . We obtain then

$$\begin{aligned} x^T Gx &= v^T Z^T GZv \\ &= 0 \end{aligned} \quad (4.57)$$

The matrix  $Z^T GZ$  is positive definite, then from equation (4.57) we deduce that  $v = 0$  and then  $x = 0$ . From equation (4.55) we have  $A^T y = 0$ , as  $A^T$  has full column rank then  $y = 0$ . Therefore the equation (4.55) has only one solution which is zero.  $\square$

In [120] the steps  $\alpha_k$  and  $\alpha_k^z$  are chosen in such a way that the iterates  $s_{k+1}$  and  $z_{k+1}$  are positive (see equation (4.58)).

$$\begin{cases} \alpha_k^z = \max\{\alpha \in ]0, 1] \mid z_k + \alpha d_k^z \geq (1 - \tau_j)z_k\} \\ \alpha_k^{max} = \max\{\alpha \in ]0, 1] \mid s_k + \alpha d_k^s \geq (1 - \tau_j)s_k\} \end{cases} \quad (4.58)$$

where  $0 < \tau_j < 1$ ,  $s_0 \geq 0$  and  $z_0 \geq 0$ .

The matrix multiplied by the descent directions vector in the equation (4.53) has the form of

$$K = \begin{bmatrix} G & A^T \\ A & 0 \end{bmatrix} \quad (4.59)$$

where  $G = \begin{bmatrix} \nabla_{xx} E(x_k) & 0 \\ 0 & S_k^{-1} Z_k \end{bmatrix}$ ,  $A = [\nabla_x c(x_k)^T \quad -I]$ .

**Theorem 4.3.** *Suppose that the matrix  $\nabla_{xx} E(x_k)$  is positive definite (for example a linear elastic material), suppose that  $s_k > 0$  and  $z_k > 0$ , then for a fixed  $\mu$  the matrix  $K$  is non singular.*

*Proof.* First of all, the matrix  $A$  is full row rank (rank =  $m$ ), and the matrix  $S_k^{-1} Z_k$  is a diagonal matrix with strictly positive coefficients.

Let  $X = \begin{bmatrix} U \\ V \end{bmatrix}$ , with  $U \in \mathbb{R}^n$  and  $V \in \mathbb{R}^m$ . We have

$$X^T G X = U^T \nabla_{xx} E(x_k) U + V^T (S_k^{-1} Z_k) V \geq 0 \quad (4.60)$$

Suppose that  $X^T G X = 0$ , thus from the equation (4.60) and from the positive definiteness of  $\nabla_{xx} E(x_k)$  and  $S_k^{-1} Z_k$  we obtain  $U = 0$ , and  $V = 0$ . Then  $G$  is positive definite, and we can use the theorem 4.2 to conclude.  $\square$

Furthermore, we should also point out that if the matrix  $K$  presents some numerical difficulties, like the top-left of the matrix  $K$  is not positive definite on the null space of  $A$ , then the matrix is modified as in [120].

Direct solvers are used to solve the linear system (4.53), one can cite MUMPS (MULTifrontal Massively Parallel sparse direct Solver) [9] or PARDISO [105]. Moreover the software IPOPT offers different choices of direct solvers, that can be used to solve the linear system. In [114] a comparison between different direct solvers within IPOPT is done, it showed also that PARDISO solver performs very well for difficult problems.

By choosing the iterates to minimize the objective function (or the energy), the iterates is encouraged to converge to a minimum point and not just any KKT points.

### 4.3.3 Behavior of the barrier solutions

In this part we will prove that the Lagrange multipliers which are solutions of the KKT system (4.49) are bounded for all barrier parameters  $\mu$ , in addition we will show that the slack variables also solutions of the KKT system (4.49), will not converge dramatically to zero, and are greater than a constant multiplied by  $\mu$ .

Consider two vectors  $\mathbf{x}, \mathbf{y}$  in  $\mathbb{R}^n$ , we say that  $\mathbf{x} \leq \mathbf{y}$  if  $x_i \leq y_i \forall i \leq n$ , and  $\mathbf{x} < \mathbf{y}$  if  $x_i < y_i \forall i \leq n$ . In the proof we will need a theorem of the alternative, due to Gordan [94], which states the following theorem.

**Theorem 4.4.** *Consider a matrix  $A_{n \times m}$ . Exactly one of the following propositions has a solution:*

- 1- There exists  $x \in \mathbb{R}^m$  such that  $Ax > 0$
- 2- There exists  $y \in \mathbb{R}^n$  such that  $y^T A = 0$ ,  $y \geq 0$ ,  $y \neq 0$

In addition, we consider the following assumptions

**Assumption 4.1.**

- The constraints vector  $c : \mathbb{R}^n \rightarrow \mathbb{R}^m$  is linear
- There exists  $\bar{x} \in \mathbb{R}^n$  such that  $c(\bar{x}) > 0$

For each barrier parameter  $\mu$ , let  $x_\mu^*, s_\mu^*, z_\mu^*, \lambda_\mu^*$  be the solution of the following KKT system (Problem (4.49))

$$\begin{cases} \nabla E(x) + \nabla c(x)\lambda = 0 \\ z = -\lambda \\ c(x) - s = 0 \\ SZe = \mu e \\ s \geq 0, z \geq 0 \end{cases} \quad (4.61)$$

Assume that  $\forall \mu \geq 0$ ,  $x_\mu^* \in \mathbb{K}$ , where  $\mathbb{K} \subset \mathbb{R}^n$  a bounded and a closed set. We want to prove next that the corresponding Lagrange multipliers  $\lambda_\mu^*$  and  $z_\mu^*$  are bounded. We will be inspired by a

proof which can be found in [11], first suppose that  $\lambda_\mu^*$  is not bounded, therefore there exists a subsequence also denoted  $\lambda_\mu^*$  such that  $\|\lambda_\mu^*\| \xrightarrow{\mu \rightarrow 0} +\infty$ .

We know from (4.61) that  $\lambda_\mu^* \leq 0$ , let then the vector  $d_\mu$  be defined by  $d_\mu = \frac{\lambda_\mu^*}{e^T \cdot \lambda_\mu^*} \geq 0$  where  $e^T = (1, \dots, 1)$ , besides  $d_\mu \leq 1$  then bounded, therefore there exists a subsequence of  $d_\mu$  also denote  $d_\mu$  such that

$$d_\mu \xrightarrow{\mu \rightarrow 0} d^* \text{ with } d^* \geq 0 \quad (4.62)$$

In addition we have  $e^T \cdot d^* = 1$  and thus  $d^* \neq 0$ .

By assumption  $x_\mu^*$  is bounded, therefore there exists a subsequence also denoted  $x_\mu^*$  such that  $x_\mu^* \xrightarrow{\mu \rightarrow 0} x^*$ . From the first equation of the system (4.61) we obtain

$$\begin{aligned} \nabla c(x_\mu^*) \lambda_\mu^* &= -\nabla E(x_\mu^*) \\ (\times \frac{1}{e^T \cdot \lambda_\mu^*}) \Rightarrow \nabla c(x_\mu^*) d_\mu &= -\frac{1}{e^T \cdot \lambda_\mu^*} \nabla E(x_\mu^*) \end{aligned} \quad (4.63)$$

Since  $\nabla E$  is continuous,  $\nabla E(x_\mu^*)$  is bounded. Thus if  $\mu \rightarrow 0$ , we deduce from the equation (4.63) that

$$\nabla c(x^*) d^* = 0 \quad (4.64)$$

Because the constraints vector  $c$  is continuous we have

$$s_\mu^* = c(x_\mu^*) \xrightarrow{\mu \rightarrow 0} s^* \text{ with } s^* \geq 0 \quad (4.65)$$

From the fourth equation of the system (4.61) we have  $z_\mu^* = -\lambda_\mu^*$  and

$$S_\mu^* Z_\mu^* e = \mu e \quad (4.66)$$

Therefore we have

$$s_{\mu,i}^* \cdot \lambda_{\mu,i}^* = -\mu \quad \forall i = 1, \dots, m \quad (4.67)$$

Multiplying by  $\frac{1}{e^T \cdot \lambda_\mu^*}$ , the equation (4.67) becomes

$$s_{\mu,i}^* \cdot d_{\mu,i} = -\frac{\mu}{e^T \cdot \lambda_\mu^*} \quad \forall i = 1, \dots, m \quad (4.68)$$

Thus by taking  $\mu \rightarrow 0$  we obtain

$$s_i^* \cdot d_i^* = 0 \quad \forall i = 1, \dots, m \quad (4.69)$$

Let  $I = \{i \mid s_i^* = 0\}$ , this set is not empty because if it's not the case, then using the fact that  $d^* \neq 0$  we will have a contradiction with the equation (4.69). If we take a vector  $v \in \mathbb{R}^m$ ,  $v_I$  denotes the vector with the components  $v_i$  where  $i \in I$ . We have  $c_I(x^*) = 0$  and from equation

(4.69) if  $i \notin I$ ,  $d_i^* = 0$ . Thus

$$e_I^T . d_I^* = e^T . d^* = 1 \text{ and } d_I^* \geq 0 \quad (4.70)$$

We conclude that

$$d_I^* \neq 0 \text{ and } d_I^* \geq 0 \quad (4.71)$$

Otherwise from the equation (4.64)

$$\nabla c(x^*) d^* = \nabla c_I(x^*) d_I^* = 0 \quad (4.72)$$

In conclusion we obtain

$$\begin{cases} (d_I^*)^T (\nabla c_I(x^*))^T = 0 \\ d_I^* \geq 0 \\ d_I^* \neq 0 \end{cases} \quad (4.73)$$

By the theorem of the alternative, we deduce that there is no vector  $p$  such that

$$(\nabla c_I(x^*))^T p > 0 \quad (4.74)$$

We will prove next that we have a contradiction.

Otherwise, let  $c_I^{(i)}$  a component of  $c_I$ , we know that  $c_I^{(i)}$  is linear, thus

$$c_I^{(i)}(\bar{x}) - c_I^{(i)}(x^*) = (\nabla c_I^{(i)}(x^*))^T . (\bar{x} - x^*) \quad (4.75)$$

We have  $c_I^{(i)}(x^*) = 0$ , and by the assumption 4.1  $c_I^{(i)}(\bar{x}) > 0$ . Therefore

$$(\nabla c_I^{(i)}(x^*))^T . (\bar{x} - x^*) > 0 \quad (4.76)$$

Besides

$$(\nabla c_I(x^*))^T . (\bar{x} - x^*) = \begin{bmatrix} \vdots \\ (\nabla c_I^{(i)}(x^*))^T \\ \vdots \end{bmatrix} . (\bar{x} - x^*) = \begin{bmatrix} \vdots \\ (\nabla c_I^{(i)}(x^*))^T . (\bar{x} - x^*) \\ \vdots \end{bmatrix} > 0 \quad (4.77)$$

which contradicts the theorem of the alternative, and thus  $\lambda_\mu^*$  is bounded:  $\|\lambda_\mu^*\| \leq M$  where  $M$  does not depend on  $\mu$ .

Moreover, we have from the system (4.61),  $\|z_\mu^*\| \leq M$  and

$$|s_{\mu,i}^*| = \frac{\mu}{|\lambda_{\mu,i}^*|} \geq \frac{\mu}{M} \quad \forall i = 1, \dots, m \quad (4.78)$$

As conclusion there exists a constant  $M^* > 0$  such that

$$\|s_\mu^*\| \geq M^* \mu \quad \forall \mu \geq 0 \quad (4.79)$$

### 4.3.4 Global convergence

In order to solve the minimization problem with linear constraints (4.47), we will solve a sequence of barrier problems (4.49) with a decreasing barrier parameter  $\mu$ , converging to zero. Let  $\epsilon_{tol} > 0$  be a given error tolerance, and  $K > 0$  a given positive constant. For each barrier parameter  $\mu$ , let the error function  $E_\mu$  be defined as

$$E_\mu := \max \{ \|\nabla E + \nabla c \cdot \lambda\|, \|\lambda + z\|, \|c - s\|, \|SZe - \mu e\| \} \quad (4.80)$$

The algorithm to solve the minimization problem with linear constraints (4.47) is described briefly in the following algorithm 4.

---

**Algorithm 4** Interior point algorithm to solve the minimization problem with linear constraints

---

```

while  $E_0 \geq \epsilon_{tol}$  do
  Update the barrier parameter  $\mu$  (in order to converge towards zero)
  while  $E_\mu \geq K \cdot \mu$  do
    Solve the barrier problem (4.49)
  end while
end while

```

---

In the algorithm 4 and for each barrier parameter  $\mu$ , let  $(x_\mu, s_\mu, \lambda_\mu, z_\mu)$  be an approximate solution of each barrier problem, where the error  $E_\mu$  is supposed to satisfy

$$E_\mu(x_\mu, s_\mu, \lambda_\mu, z_\mu) \leq K \cdot \mu \quad (4.81)$$

We want to prove the existence of a limit point of the sequence  $(x_\mu, s_\mu, \lambda_\mu, z_\mu)$  when  $\mu$  converges to zero, and this limit point is the solution of the first-order necessary conditions (4.48) of the original problem which is the minimization problem (4.47), equivalent to the minimization problem (4.46). In order to prove it, we will show that the sequence  $(x_\mu, s_\mu, \lambda_\mu, z_\mu)$  is bounded.

First  $x_\mu$  is assumed to be bounded and thus belongs to a compact set  $\Omega$ . From the inequality (4.81) we have

$$\|c(x_\mu) - s_\mu\| \leq K \cdot \mu \quad (4.82)$$

The application  $c$  is continuous on the compact  $\Omega$ , thus from the inequality (4.82) we deduce that  $s_\mu$  is bounded.

In the algorithm  $s_\mu$  and  $z_\mu$  are chosen to be positive, thanks to the fraction-to-boundary rule. From the inequality (4.81) we obtain

$$\lambda_\mu \leq K\mu - z_\mu \quad (4.83)$$

Next we will also be inspired by the proof which can be found in [11], by proving that the Lagrange multiplier  $\lambda_\mu$  is bounded. Suppose that it is not the case and  $\|\lambda_\mu\| \rightarrow +\infty$ . As was mentioned,  $z_\mu \geq 0$ , we notice from the inequality (4.83) that if a component of  $\lambda_\mu$  is positive then it is of the order of  $K\mu$  and converges to zero. Therefore  $\exists N > 0$  such that  $\forall n \geq N \Rightarrow e^T \cdot \lambda_{\mu_n} \leq 0$ , moreover  $d_n := \frac{\lambda_{\mu_n}}{e^T \cdot \lambda_{\mu_n}}$  is bounded. We deduce that there exists a subsequence

of  $d_n$  also denoted  $d_n$  such that

$$d_n \xrightarrow{n \rightarrow \infty} d^* \text{ with } d^* \geq 0 \quad (4.84)$$

Otherwise  $e^T \cdot d^* = 1$ , thus  $d^* \geq 0$  and  $d^* \neq 0$ .

From the error definition (4.80) and from the inequation (4.81) we have

$$\left\| \frac{\nabla E(x_{\mu_n})}{e^T \cdot \lambda_{\mu_n}} + \nabla c(x_{\mu_n}) \cdot \frac{\lambda_{\mu_n}}{e^T \cdot \lambda_{\mu_n}} \right\| = \frac{1}{|e^T \cdot \lambda_{\mu_n}|} \|\nabla E(x_{\mu_n}) + \nabla c(x_{\mu_n}) \cdot \lambda_{\mu_n}\| \leq \frac{K\mu_n}{|e^T \cdot \lambda_{\mu_n}|} \quad (4.85)$$

Thus if  $n \rightarrow \infty$  then

$$\|\nabla c(x^*) \cdot d^*\| = 0 \Rightarrow \nabla c(x^*) \cdot d^* = 0 \quad (4.86)$$

Doing the same thing

$$\left\| \frac{z_{\mu_n}}{e^T \cdot \lambda_{\mu_n}} + \frac{\lambda_{\mu_n}}{e^T \cdot \lambda_{\mu_n}} \right\| = \frac{1}{|e^T \cdot \lambda_{\mu_n}|} \|z_{\mu_n} + \lambda_{\mu_n}\| \leq \frac{K\mu_n}{|e^T \cdot \lambda_{\mu_n}|} \quad (4.87)$$

As  $d_n = \frac{\lambda_{\mu_n}}{e^T \cdot \lambda_{\mu_n}} \rightarrow d^*$  then  $\frac{z_{\mu_n}}{e^T \cdot \lambda_{\mu_n}} \rightarrow -d^*$ .

We have also from the error definition, that for each component  $i$

$$|s_{\mu_n}^{(i)} \cdot z_{\mu_n}^{(i)} - \mu| \leq K \cdot \mu \quad (4.88)$$

If we multiply the equation (4.88) by  $\frac{1}{|e^T \cdot \lambda_{\mu_n}|}$  and taking  $n \rightarrow \infty$  we obtain

$$s_i^* \cdot d_i^* = 0 \quad \forall i = 1, \dots, m \quad (4.89)$$

Let  $I = \{i | s_i^* = 0\}$ , this set is not empty because if it is not the case, then using the fact that  $d^* \neq 0$  we will have a contradiction with the equation (4.89). If we take a vector  $v \in \mathbb{R}^m$ ,  $v_I$  denotes the vector with the components  $v_i$  where  $i \in I$ . We have  $c_I(x^*) = s_I^* = 0$  and from equation (4.89) if  $i \notin I$ ,  $d_i^* = 0$ . Thus

$$e_I^T \cdot d_I^* = e^T \cdot d^* = 1 \text{ and } d_I^* \geq 0 \quad (4.90)$$

We conclude that

$$d_I^* \neq 0 \text{ and } d_I^* \geq 0 \quad (4.91)$$

Otherwise from the equation (4.86)

$$\nabla c(x^*) \cdot d^* = \nabla c_I(x^*) \cdot d_I^* = 0 \quad (4.92)$$

In conclusion we obtain

$$\begin{cases} (d_I^*)^T (\nabla c_I(x^*))^T = 0 \\ d_I^* \geq 0 \\ d_I^* \neq 0 \end{cases} \quad (4.93)$$

By the theorem of the alternative, we deduce that there is no vector  $p$  such that

$$(\nabla c_I(x^*))^T p > 0 \quad (4.94)$$

We will prove next that we have a contradiction.

Otherwise, let  $c_I^{(i)}$  a component of  $c_I$ , we know that  $c_I^{(i)}$  is linear, thus

$$c_I^{(i)}(\bar{x}) - c_I^{(i)}(x^*) = (\nabla c_I^{(i)}(x^*))^T \cdot (\bar{x} - x^*) \quad (4.95)$$

We have  $c_I^{(i)}(x^*) = 0$ , and by the assumption 4.1  $c_I^{(i)}(\bar{x}) > 0$ . Therefore

$$(\nabla c_I^{(i)}(x^*))^T \cdot (\bar{x} - x^*) > 0 \quad (4.96)$$

besides

$$(\nabla c_I(x^*))^T \cdot (\bar{x} - x^*) = \begin{bmatrix} \vdots \\ (\nabla c_I^{(i)}(x^*))^T \\ \vdots \end{bmatrix} \cdot (\bar{x} - x^*) = \begin{bmatrix} \vdots \\ (\nabla c_I^{(i)}(x^*))^T \cdot (\bar{x} - x^*) \\ \vdots \end{bmatrix} > 0 \quad (4.97)$$

which contradicts the theorem of the alternative, and thus  $\lambda_\mu$  is bounded. This fact implies that the Lagrange multiplier  $z_\mu$  is also bounded.

In conclusion  $y_\mu := (x_\mu, s_\mu, \lambda_\mu, z_\mu)$  is bounded, and thus belongs to a compact set. Then there exists a subsequence of  $y_\mu$  converging to  $y^* = (x^*, s^*, \lambda^*, z^*)$ . Finally using the error definition and the inequality (4.81),  $(x^*, s^*, \lambda^*, z^*)$  satisfies the original KKT system (4.48)

$$\begin{cases} \nabla E(x^*) + \nabla c(x^*)\lambda^* = 0 \\ z^* = -\lambda^* \\ c(x^*) - s^* = 0 \\ S^* Z^* e = 0 \\ s^* \geq 0, z^* \geq 0 \end{cases} \quad (4.98)$$

## 4.4 Alternative formulations

Another symmetric formulations were developed in order to solve the contact problems, more precisely the minimization of the energy with linear constraints.

### 4.4.1 First alternative formulation

Instead of using the minimization problem (4.47), we will penalize the slack variables to be negative, and we obtain the following problem

$$\begin{cases} \min_{(u,s) \in \mathbb{R}^n \times \mathbb{R}^m} E(u) + \sum_{i=1}^m \mu_i \zeta(s_i) \quad \text{such that} \\ c(u) - s = 0 \\ s \geq -\epsilon \end{cases} \quad (4.99)$$

where  $\mu$  the penalty factor ( $\mu \rightarrow \infty$  in this case),  $\epsilon > 0$  and,  $\zeta : \mathbb{R} \rightarrow \mathbb{R}_+$  a  $C^2$  and a convex function with the following property:  $\zeta(x) > 0 \forall x < 0$  and  $\zeta(x) = 0 \forall x \geq 0$ . An example of a penalty function  $\zeta$

$$\zeta(x) = \begin{cases} 0 & \text{if } x \geq 0 \\ -x^3 & \text{if } -1 \leq x < 0 \\ 3x^2 + 3x + 1 & \text{if } x \leq -1 \end{cases} \quad (4.100)$$

In this formulation we ensure that the inequality in the problem (4.99) will not be activated.

#### 4.4.2 Mixed symmetric methods

We can use a penalty function in order to take into account the symmetric constraints, which describes the non-penetration of the master body into the slave one. The problem can be reformulated as follows

$$\begin{cases} \min_{\mathbf{U}} \left( E(\mathbf{U}) + \mu \int_{\Gamma_{C2}} \eta((\mathbf{x} - \bar{\mathbf{x}}_1) \cdot \mathbf{n}) ds \right) \\ \int_{\Gamma_{C1}} g_i \phi_i d\lambda \geq 0 \quad \forall i = 1, \dots, n_{C1} \end{cases} \quad (4.101)$$

where  $\mu$  is the penalty factor and  $\eta$  is the penalty function, note that the same notations as the chapter 3 are used. Since the penalty method is used to ensure the symmetrical constraints, the contact method here is not purely symmetric, however it improves the results.

### 4.5 Symmetric contact algorithm

A fixed point method is used in order to transform the contact problem into a sequence of a minimization ones, with linear constraints, especially for the finite deformation problems, indeed for the linear elastic problems, the constraints are linear by definition. Such idea can be found in [50, 49, 75], where the geometric non-linearity of the contact is transformed into a sequence of a geometric linear one. More precisely for each iteration of the fixed point algorithm, the previous displacement is used in order to search for each integration point of the slave contact area, the closest segment (in 2D) or the closest triangle (in 3D) of the master body, and its projection point position on this closest segment or triangle. The integration points have been employed, because the constraints are written in term of integrals. See section 4.2 for more details.

Let  $\mathbf{U}$  be the degrees of freedom vector of the problem, otherwise speaking the displacement vector of all nodes. Finally the algorithm to solve the contact problems is briefly described in the algorithm 5.

**Algorithm 5** Symmetric algorithm using the fixed point method

---

Initialization of the displacement  $\mathbf{U}_0$  and setting the tolerance  $\epsilon_{tol} = 10^{-6}$

**while**  $error \geq \epsilon_{tol}$  **do**

1. Using the displacement vector  $\mathbf{U}_{n-1}$  of the previous iteration  $n - 1$ :
  - Compute the projection points' parameters  $\{\bar{\lambda}_i \mid i = 1, \dots, nS\}$  of all slave integration points
  - Compute the normal vectors at the projection points  $\{n_i \mid i = 1, \dots, nS\}$
2. For each integration point, its projection point  $\bar{\mathbf{x}}_i$  depends linearly on the actual displacement
3. Reverse the role of the master and the slave body
4. Form the Energy  $E$  and the symmetric linear constraints
5. Use the interior point method in order to solve the minimization problem with linear constraints, and to obtain the actual displacement  $\mathbf{U}_n$
6.  $error = \frac{\|\mathbf{U}_n - \mathbf{U}_{n-1}\|_\infty}{\|\mathbf{U}_{n-1}\|_\infty}$

**end while**

---

Note that the resolution of the linear system generated by the interior point method is solved using direct methods, for example the solver MUMPS (MUltifrontal Massively Parallel sparse direct Solver).

## 4.6 Rigid body motions

In some cases, where the boundary conditions are not sufficient, rigid body motions can appear (translations or rotations) for the bodies in contact. In order to remove the rigid body motions we will slightly modify our contact problem formulation (see problem 4.44).

Suppose we are in  $3D$  case, and we want to remove the rigid body motions, the translations in the directions of the canonical vectors  $\mathbf{e}_1$  and  $\mathbf{e}_2$ , therefore our contact problem formulation becomes as follows

$$\begin{cases} \mathbf{u} = \arg \min_{\mathbf{v} \in \mathbf{V}_h} \left( \mathcal{E}_p(\mathbf{v}) + \frac{1}{2} \int_{\Omega_h^1 \cup \Omega_h^2} (kv_1^2 + kv_2^2) dx \right) \\ c_1 := \int_{\Gamma_{C1}} ((\mathbf{x} - \bar{\mathbf{x}}_2) \cdot \mathbf{n}) \cdot \phi_i^{(1)} ds \geq 0 \quad \forall i = 1, \dots, n_{C1} \\ c_2 := \int_{\Gamma_{C2}} ((\mathbf{x} - \bar{\mathbf{x}}_1) \cdot \mathbf{n}) \cdot \phi_i^{(2)} ds \geq 0 \quad \forall i = 1, \dots, n_{C2} \end{cases} \quad (4.102)$$

where  $v_1, v_2$  are respectively the first and the second component of the vector  $\mathbf{v}$ , and  $k$  is a coefficient small enough. The modified problem (4.102) is equivalent to apply springs with small stiffness on the structure.

## 4.7 Numerical validations

### 4.7.1 Compression of two elastic blocks with imposed displacement

This test is similar to the one in chapter 3. A first elastic rectangular block is posed on a second one (see Figure 4.3a). The two blocks have the same properties: a width  $L = 2UL$ , a height  $H = 1UL$ , a Young's modulus  $E = 200 \frac{UF}{UL^2}$ , a Poisson's ratio  $\nu = 0$ . The study is done under the plan strain hypothesis (2D). The frictionless case is always supposed, and a vertical displacement of  $U_0 = -0.1UL$  and a zero horizontal displacement are imposed on the upper face of the first block, the lower face of the second body is clamped. This test was treated in [109].

Theoretically the value of the strain is equal to  $\epsilon = \frac{U_0}{2H} = \frac{-0.1}{2} = -0.05$ , thus the value of the stress on the contact area is equal to  $p_{theo} = E.\epsilon = -10 \frac{UF}{UL^2}$ .

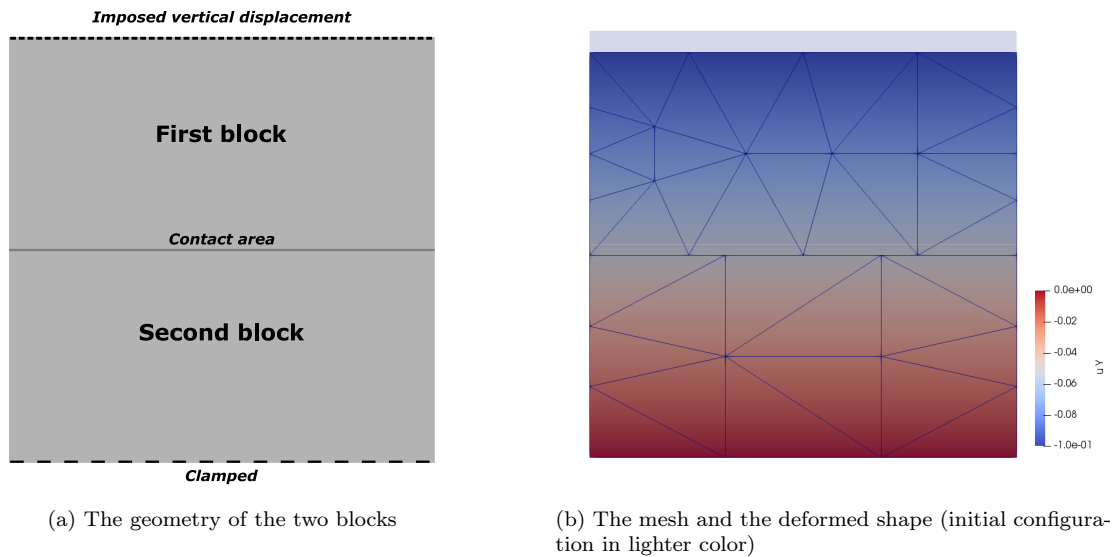


Figure 4.3 – The geometry and the deformed shape of the two blocks

The distribution of the pressure on the contact area is shown in the Figure 4.4.

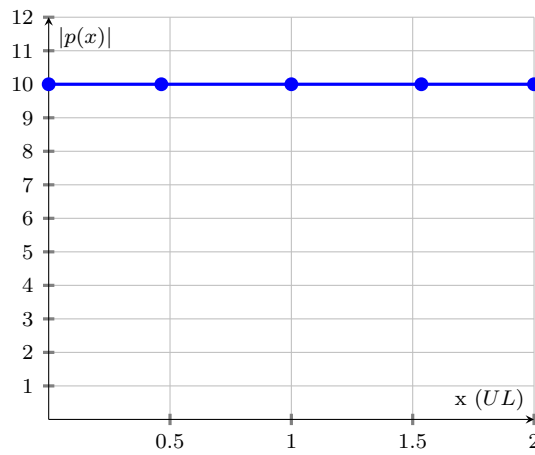


Figure 4.4 – Pressure at the contact area

### 4.7.2 Hertz contact with two elastic bodies

This example studies the contact between an elastic cylinder ( $E_1 = 210 \frac{UF}{UL^2}$ ,  $\nu_1 = 0.3$ ) and an elastic block ( $E_2 = 70 \frac{UF}{UL^2}$ ,  $\nu_2 = 0.3$ ), the cylinder is posed on the block and a force of  $P = 35UF$  is applied on the top of the cylinder, the block is clamped at its base ( $U_x = U_y = 0$ ) (see Figure 4.5a). This test was treated for example in [1, 98, 110]. The study is done under the plane strain hypothesis, therefore the cylinder is modeled by a disc of radius  $R_1 = 100UL$  and the block by a square of dimension  $L = 200UL$ . Due to the symmetry of the problem only the half of the problem is modeled.

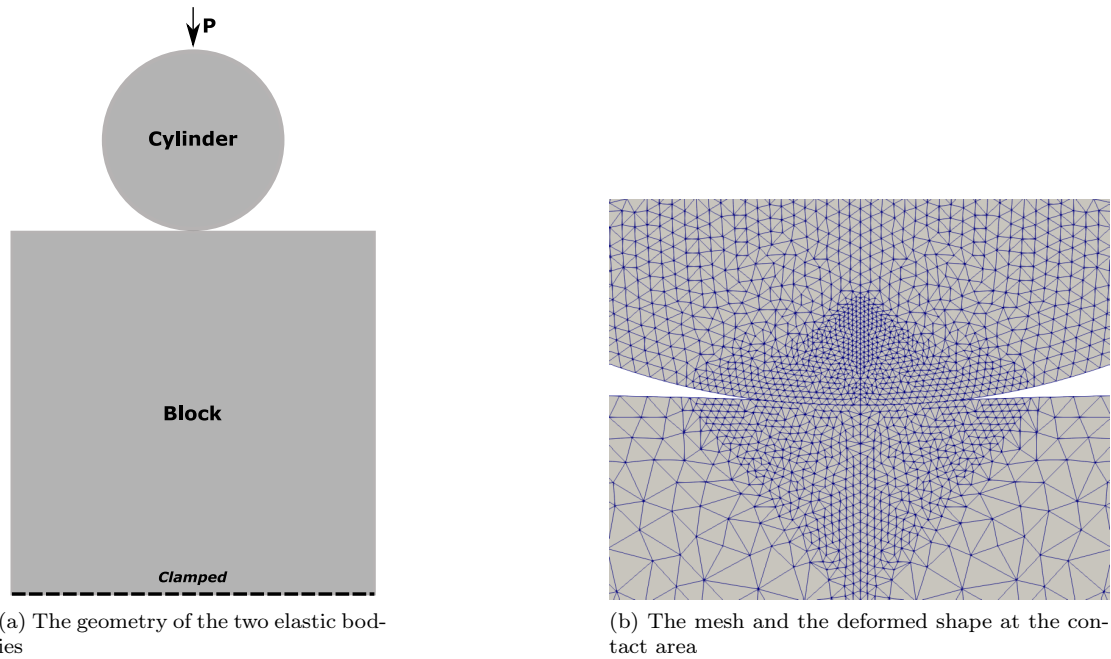


Figure 4.5 – The geometry and the deformed shape of the contact between the elastic cylinder and the elastic block

Using the quadratic finite elements ( $P_2$ ), the deformed shape at the contact area can be seen in the Figure 4.5b. Finally the ratio of the pressure at the contact area  $p(x)$ , computed with our contact method, to the maximum contact pressure  $p_0$ , in addition to the theoretical ratio, are plotted in the Figure 4.6.

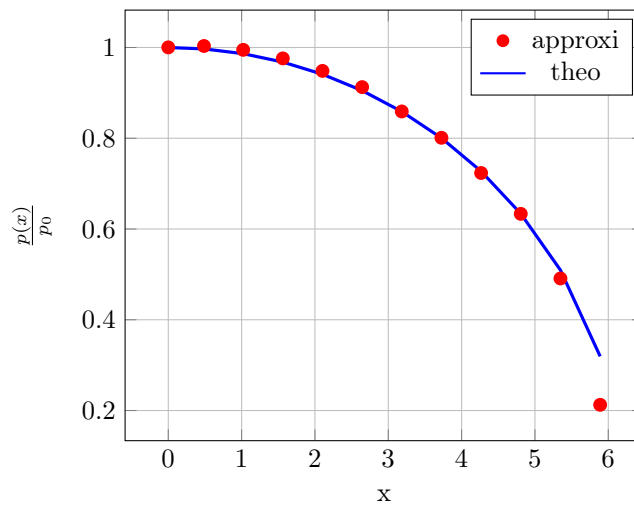


Figure 4.6 – Pressure at the contact area

### 4.7.3 Contact between two cylinders

In order to show that the algorithm or the formulation can handle the contact between two curved bodies, a contact between two cylinders is considered. This example can be found in [108]. Two concentric cylinders with the same thickness of  $t = 5UL$  are initially in contact, the inner radius of the inner cylinder is equal to  $R_{in} = 10UL$  and the outer radius of the outer cylinder is equal to  $R_{out} = 20UL$ . A radial pressure of  $p = 1 \frac{UF}{UL^2}$  is applied on the outer cylinder. Due to the symmetry of the problem, only one quarter of the problem is considered, as is depicted in the Figure 4.7, the plane strain hypothesis is also considered. The two cylinders are made from a similar elastic material, Young's modulus  $E = 100 \frac{UF}{UL^2}$  and Poisson's ratio  $\nu = 0$ .

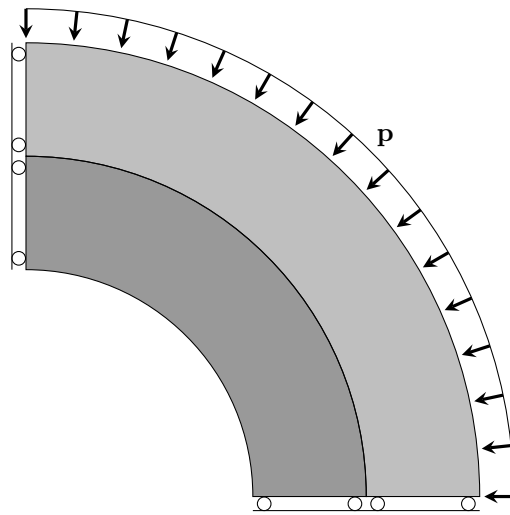


Figure 4.7 – The geometry of the problem

We are interested in the value of the radial stress in the two cylinders, which can be seen in the Figure 4.8 for the linear finite elements ( $P_1$ ) and for the quadratic finite elements ( $P_2$ ).

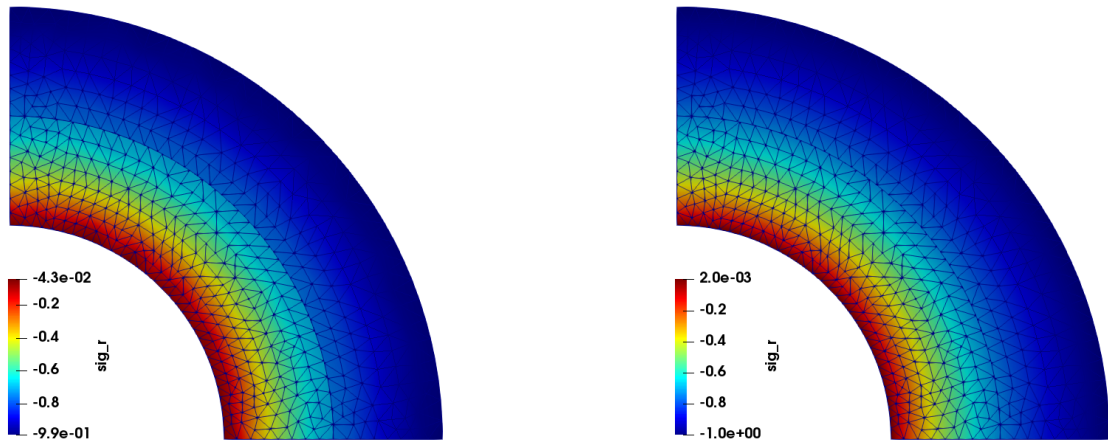


Figure 4.8 – The mesh and the radial stress for  $P_1$  elements (on the left), and for  $P_2$  elements (on the right)

We notice the non-conforming meshes in the Figure 4.8, in addition we notice that the radial stress at the inner border is nearly zero, because this border is free, and is nearly equal to 1, the applied pressure, on the outer border. We obtain similar results as in [108] and as in chapter 3.

#### 4.7.4 Disc-in-disc

The following example, which can be found in [123], is considered in order to show that our algorithm can handle large deformations. In this example the contact is between a hollow disc and an inner disc, as shown in the Figure 4.9, it is a quasi-static study where the inertia is not taken into account. The symmetric formulation was used to consider the contact, and linear finite elements were used. The outer and the inner radius of the hollow disc are respectively  $r_{ho} = 2. UL$ ,  $r_{hi} = 0.7 UL$ , the radius of the inner disc is  $r_{in} = 0.6 UL$ . Neo-Hookean material is considered for the two discs, with the following properties  $E_h = 1000 \frac{UF}{UL^2}$ ,  $\nu_h = 0$  for the hollow disc, and  $E_i = 2000 \frac{UF}{UL^2}$ ,  $\nu_i = 0.3$  for the inner disc, note that  $UF$ ,  $UL$  denote respectively the force and the length unit. We impose a vertical downward displacement at all nodes of the inner disc, the outside of the hollow disc is fixed. The maximal displacement imposed is  $1.125 UL$  and is done by 100 load increments. The deformation states of the two discs at the steps 0, 50, 100 are depicted in the following figure (Figure 4.9).

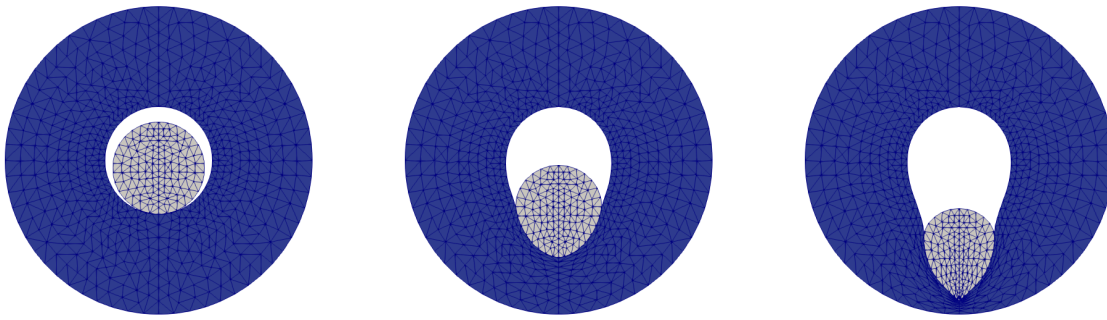


Figure 4.9 – The deformation states at the steps 0, 50, 100

### 4.7.5 Multi-body contact between three beams

In this example we consider the bending of three cantilever beams as shown in the Figure 4.10, the goal of this example is to show that the contact algorithm can work in three-dimensional space and can handle multi-body contact problems. The symmetric formulation was used to consider the contact, and linear finite elements were used. The dimension of the three beams are the same, indeed the length of each beam is  $200.UL$  and each cross section is a square of dimension  $25.UL$ . The three beams have the same elastic material properties  $E = 2.10^5 \frac{UF}{UL^2}$ ,  $\nu = 0$ . We apply a downward vertical surface load of  $f = 100 \frac{UF}{UL^2}$  at the upper surface of the top beam. We can see in the Figure 4.10 the deformations and the sliding between the beams.

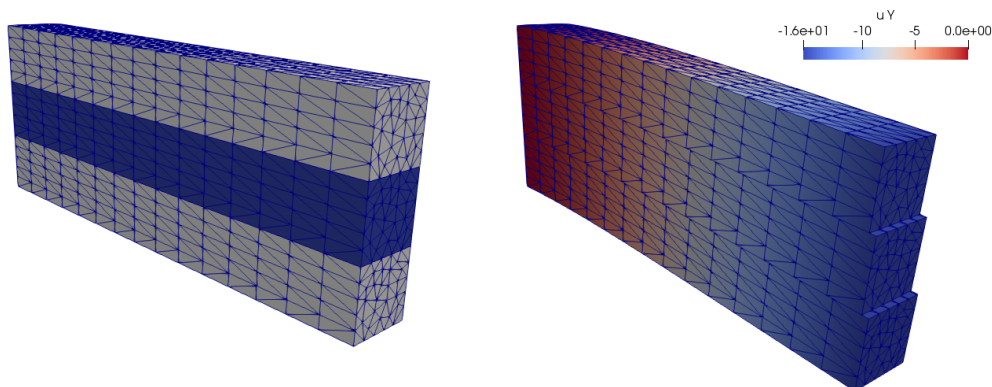


Figure 4.10 – The sliding between beams. The initial configuration (on the left), the deformations and the sliding (on the right)



# Chapter 5

## The dynamic contact

### Outline of the current chapter

<b>5.1 Formulation of the dynamic contact problem as a minimization one</b>	<b>114</b>
5.1.1 The minimization problem using Euler implicit scheme . . . . .	114
5.1.2 The problem using a special case of the Newmark scheme . . . . .	117
<b>5.2 Numerical examples</b>	<b>117</b>
5.2.1 Impact between a ball and a block . . . . .	118
5.2.2 Impact between two balls and a foundation . . . . .	119

In this chapter we will show how to make some modifications on the previous contact formulation (chapter 3 or chapter 4), in order to solve the dynamic contact problem. In the balance equation an inertia term is added, and the constraints remain the same, however the persistency condition can be sometimes considered as an additional contact condition for dynamic contact problems, indeed it ensures the conservation of the energy when the friction is not taken into account [77]. The persistency condition is stated as follows

$$\sigma_n \dot{g}_n = 0 \quad \text{on the contact area} \tag{5.1}$$

where  $\sigma_n$  and  $g_n$  are respectively the normal contact pressure and the material time derivative of the normal gap. This condition means that the contact pressure  $\sigma_n$  is equal to zero when a separation or a coming into contact begins.

In [68] two formulations are presented for the dynamic contact problems in the case of elastic materials, which are energy conserving, the first formulation uses contact conditions based on the velocity (the persistency condition), the second one consists in rewriting the mass matrix of the problem in order to have no inertia for the contact nodes.

## 5.1 Formulation of the dynamic contact problem as a minimization one

In the dynamic problems, the inertia term must be added, which depends on the mass and on the acceleration of the involved bodies. As the inertia term depends on the acceleration and thus on the second derivative of the displacement, we will use some time integration schemes, for instance Euler implicit (5.2) and Newmark (5.3) scheme. Note that other schemes can be easily used, and the principle goal of this chapter is to show how to create an optimization problem given a time integration scheme.

Using the same notations as before, let  $\rho_1, \rho_2$  be respectively the initial density of the first body  $\Omega_1$  and of the second body  $\Omega_2$ . Given a time step  $\Delta t$ , the Euler implicit scheme can be stated as follows

$$\begin{cases} \mathbf{v}_{t+1} = \frac{\mathbf{u}_{t+1} - \mathbf{u}_t}{\Delta t} \\ \mathbf{a}_{t+1} = \frac{\mathbf{v}_{t+1} - \mathbf{v}_t}{\Delta t} \end{cases} \quad (5.2)$$

where  $\mathbf{u}$ ,  $\mathbf{v}$  and  $\mathbf{a}$  are respectively the displacement, the velocity and the acceleration of a material point in  $\Omega_1 \cup \Omega_2$ , moreover the subscripts  $t$  and  $t+1$  denote respectively the previous and actual time.

A special case of the Newmark scheme can be stated as follows

$$\begin{cases} \mathbf{v}_{t+1} = \frac{2}{\Delta t}(\mathbf{u}_{t+1} - \mathbf{u}_t) - \mathbf{v}_t \\ \mathbf{a}_{t+1} = \frac{2}{\Delta t^2}(\mathbf{u}_{t+1} - \mathbf{u}_t) - \frac{2}{\Delta t}\mathbf{v}_t \end{cases} \quad (5.3)$$

In order to be more general, we suppose in the following that the two bodies  $\Omega_1$  and  $\Omega_2$  are two hyperelastic materials with strain energy functions  $\hat{W}_1$  and  $\hat{W}_2$ , in addition we suppose that traction forces  $\mathbf{t}_1$  and  $\mathbf{t}_2$  are applied on their parts of boundaries  $\Gamma_1^1$  and  $\Gamma_1^2$ , and two body forces  $\mathbf{f}_1$  and  $\mathbf{f}_2$  are applied respectively on  $\Omega_1$  and on  $\Omega_2$ . We will use the same notations as the previous chapters, for example  $\mathbf{K}_{t+1}$  describes the non-penetration between the two bodies at the time  $t+1$  and  $\Omega = \Omega_1 \cup \Omega_2$ .

### 5.1.1 The minimization problem using Euler implicit scheme

Using the Euler implicit scheme (5.2) the dynamic contact problem can be formulated as follows

Find  $\mathbf{u}_{t+1} \in \mathbf{K}_{t+1}$  such that

$$\mathbf{u}_{t+1} = \arg \min_{\mathbf{w} \in \mathbf{K}_{t+1}} (E(\mathbf{w})) \quad (5.4)$$

where the energy  $E : \mathbf{V} \rightarrow \mathbb{R}$  is defined by

$$\begin{cases} E(\mathbf{w}) = \frac{1}{2} \int_{\Omega} \rho_0 (\mathbf{v} - \mathbf{v}_t)^2 dx + E_p(\mathbf{w}) \quad \text{s.t} \\ \mathbf{v} = \frac{1}{\Delta t} (\mathbf{w} - \mathbf{u}_t) \end{cases} \quad (5.5)$$

where  $\mathbf{v}_t$  is the previous velocity,  $\rho_0 = \rho_1 \mathbb{1}_{\Omega_1} + \rho_2 \mathbb{1}_{\Omega_2}$  and  $E_p$  the total potential energy given by

$$E_p(\mathbf{w}) = \int_{\Omega_1} \hat{W}_1 dx + \int_{\Omega_2} \hat{W}_2 dx - \int_{\Omega_1} \mathbf{f}_1 \cdot \mathbf{w} dx - \int_{\Omega_2} \mathbf{f}_2 \cdot \mathbf{w} dx - \int_{\Gamma_1^1} \mathbf{t}_1 \cdot \mathbf{w} ds - \int_{\Gamma_1^2} \mathbf{t}_2 \cdot \mathbf{w} ds \quad (5.6)$$

In the following theorem we will justify the use of this optimization problem.

**Theorem 5.1.** *Let  $\mathbf{u}_{t+1}$  be a solution (sufficiently regular) of the problem (5.4), then  $\mathbf{u}_{t+1}$  satisfies the balance equation*

$$\operatorname{div} \mathbf{P} + \mathbf{f} = \rho_0 \mathbf{a}_{t+1} \quad (5.7)$$

where  $\mathbf{P}$  is the first Piola-Kirchhoff stress tensor, with  $\mathbf{P} = \mathbf{P}_1$  for the first body and  $\mathbf{P} = \mathbf{P}_2$  for the second body. Moreover  $\mathbf{f} = \mathbf{f}_1$  the body force on the first body and  $\mathbf{f} = \mathbf{f}_2$  the body force on the second body.

*Proof.* Let  $E_m$  be defined by

$$E_m(\mathbf{w}) = \frac{1}{2} \int_{\Omega} \rho_0 (\mathbf{v} - \mathbf{v}_t)^2 dx \quad (5.8)$$

where  $\mathbf{v} = \frac{1}{\Delta t} (\mathbf{w} - \mathbf{u}_t)$

Let  $\mathbf{X} \in \Omega_1$ , and  $B_1(\mathbf{X}, r) \subset \Omega_1$  the ball of center  $\mathbf{X}$  and of radius  $r > 0$ .

Let  $\mathbf{u}_{t+1} \in \mathbf{K}_{t+1}$  be a solution of the problem (5.4), consider  $\boldsymbol{\theta}$  a sufficiently smooth function with support in  $B_1(\mathbf{X}, r)$ . There exists  $\epsilon_0 = \epsilon(\boldsymbol{\theta}) > 0$  such that  $\mathbf{u}_{t+1}^\epsilon = \mathbf{u}_{t+1} + \epsilon \boldsymbol{\theta} \in \mathbf{K}_{t+1} \quad \forall |\epsilon| \leq \epsilon_0$ .

We have

$$E(\mathbf{u}_{t+1}^\epsilon) - E(\mathbf{u}_{t+1}) \geq 0 \quad (5.9)$$

In addition

$$\begin{aligned} E(\mathbf{u}_{t+1}^\epsilon) - E(\mathbf{u}_{t+1}) &= E(\mathbf{u}_{t+1} + \epsilon \boldsymbol{\theta}) - E(\mathbf{u}_{t+1}) \\ &= E_m(\mathbf{u}_{t+1} + \epsilon \boldsymbol{\theta}) - E_m(\mathbf{u}_{t+1}) + E_p(\mathbf{u}_{t+1} + \epsilon \boldsymbol{\theta}) - E_p(\mathbf{u}_{t+1}) \\ &= E_m(\mathbf{u}_{t+1} + \epsilon \boldsymbol{\theta}) - E_m(\mathbf{u}_{t+1}) + \int_{\Omega_1} \left( \hat{W}_1(\mathbf{u}_{t+1} + \epsilon \boldsymbol{\theta}) - \hat{W}_1(\mathbf{u}_{t+1}) \right) dx \\ &\quad - \epsilon \int_{\Omega_1} \mathbf{f}_1 \cdot \boldsymbol{\theta} dx \end{aligned} \quad (5.10)$$

Otherwise we have

$$\begin{aligned} \hat{W}_1(\mathbf{u}_{t+1} + \epsilon \boldsymbol{\theta}) - \hat{W}_1(\mathbf{u}_{t+1}) &= \epsilon \frac{\partial \hat{W}_1}{\partial \mathbf{F}} : \nabla \boldsymbol{\theta} + o(\epsilon) \\ &= \epsilon \mathbf{P}_1 : \nabla \boldsymbol{\theta} + o(\epsilon) \end{aligned} \quad (5.11)$$

Using the Green formula and the fact that  $\boldsymbol{\theta}$  vanishes in the neighborhood of  $\partial\Omega_1$ , we obtain :

$$\begin{aligned} \int_{\Omega_1} \left( \hat{W}_1(\mathbf{u}_{t+1} + \epsilon\boldsymbol{\theta}) - \hat{W}_1(\mathbf{u}_{t+1}) \right) dx &= \epsilon \int_{\Omega_1} \mathbf{P}_1 : \nabla \boldsymbol{\theta} dx + o(\epsilon) \\ &= -\epsilon \int_{\Omega_1} \operatorname{div}(\mathbf{P}_1) \cdot \boldsymbol{\theta} dx + o(\epsilon) \end{aligned} \quad (5.12)$$

Thus

$$\begin{aligned} E(\mathbf{u}_{t+1}^\epsilon) - E(\mathbf{u}_{t+1}) &= \epsilon \left\{ \frac{E_m(\mathbf{u}_{t+1} + \epsilon\boldsymbol{\theta}) - E_m(\mathbf{u}_{t+1})}{\epsilon} \right\} \\ &\quad + \epsilon \left\{ \int_{\Omega_1} (-\operatorname{div}(\mathbf{P}_1) - \mathbf{f}_1) \cdot \boldsymbol{\theta} dx + \frac{o(\epsilon)}{\epsilon} \right\} \geq 0 \end{aligned} \quad (5.13)$$

Moreover, using the Euler implicit scheme (5.2)

$$\begin{aligned} \lim_{\epsilon \rightarrow 0^-} \frac{E_m(\mathbf{u}_{t+1} + \epsilon\boldsymbol{\theta}) - E_m(\mathbf{u}_{t+1})}{\epsilon} &= \lim_{\epsilon \rightarrow 0^+} \frac{E_m(\mathbf{u}_{t+1} + \epsilon\boldsymbol{\theta}) - E_m(\mathbf{u}_{t+1})}{\epsilon} \\ &= \int_{\Omega} \rho_0 \frac{1}{\Delta t} (\mathbf{v}_{t+1} - \mathbf{v}_t) \cdot \boldsymbol{\theta} dx \\ &= \int_{\Omega} \rho_0 \mathbf{a}_{t+1} \cdot \boldsymbol{\theta} dx \end{aligned} \quad (5.14)$$

Thus taking  $\epsilon > 0$  and taking the limit  $\epsilon \rightarrow 0^+$  in equation (5.13), we obtain

$$\int_{\Omega_1} (\rho_0 \mathbf{a}_{t+1} - \operatorname{div}(\mathbf{P}_1) - \mathbf{f}_1) \cdot \boldsymbol{\theta} dx \geq 0 \quad (5.15)$$

Taking  $\epsilon < 0$  and taking the limit  $\epsilon \rightarrow 0^-$  in equation (5.13), we obtain

$$\int_{\Omega_1} (\rho_0 \mathbf{a}_{t+1} - \operatorname{div}(\mathbf{P}_1) - \mathbf{f}_1) \cdot \boldsymbol{\theta} dx \leq 0 \quad (5.16)$$

Therefore:

$$\int_{\Omega_1} (\rho_0 \mathbf{a}_{t+1} - \operatorname{div}(\mathbf{P}_1) - \mathbf{f}_1) \cdot \boldsymbol{\theta} dx = 0 \quad (5.17)$$

The support of  $\boldsymbol{\theta}$  is in  $B_1(\mathbf{X}, r) \subset \Omega_1$ , thus we obtain:

$$\int_{B_1(\mathbf{X}, r)} (\rho_0 \mathbf{a}_{t+1} - \operatorname{div}(\mathbf{P}_1) - \mathbf{f}_1) \cdot \boldsymbol{\theta} dx = 0 \quad (5.18)$$

We deduce that  $\rho_0 \mathbf{a}_{t+1} = \operatorname{div}(\mathbf{P}_1) + \mathbf{f}_1$  in  $B_1(\mathbf{X}, r)$ , and then it's true in  $\Omega_1$ . The same procedure can be used for  $\Omega_2$ .

Note that we were interested in retrieving the balance equation, where the inertia term occurs, indeed the other contact conditions (for example the negativity of the contact pressure) can be obtained like it is done in the Appendix A.  $\square$

### 5.1.2 The problem using a special case of the Newmark scheme

Using the Newmark scheme (5.3) the dynamic contact problem can be formulated as follows

Find  $\mathbf{u}_{t+1} \in \mathbf{K}_{t+1}$  such that

$$\mathbf{u}_{t+1} = \arg \min_{\mathbf{w} \in \mathbf{K}_{t+1}} (E(\mathbf{w})) \quad (5.19)$$

where the energy  $E : \mathbf{V} \rightarrow \mathbb{R}$  is defined by

$$\begin{cases} E(\mathbf{w}) = \frac{1}{\Delta t^2} \int_{\Omega} \rho_0 (\mathbf{w} - \hat{\mathbf{u}}_t)^2 dx + E_p(\mathbf{w}) & \text{s.t} \\ \hat{\mathbf{u}}_t = \mathbf{u}_t + \Delta t \mathbf{v}_t \end{cases} \quad (5.20)$$

with  $E_p$  already defined in (5.6).

As before, the following theorem will justify the use of this optimization problem.

**Theorem 5.2.** *Let  $\mathbf{u}_{t+1}$  be a solution (sufficiently regular) of the problem (5.19), then  $\mathbf{u}_{t+1}$  satisfies the balance equation*

$$\operatorname{div} \mathbf{P} + \mathbf{f} = \rho_0 \mathbf{a}_{t+1} \quad (5.21)$$

*Proof.* The same proof of the theorem 5.1 can be used again, the only difference is in the definition of  $E_m$ , in this case

$$E_m(\mathbf{w}) = \frac{1}{\Delta t^2} \int_{\Omega} \rho_0 (\mathbf{w} - \hat{\mathbf{u}}_t)^2 dx \quad (5.22)$$

with

$$\hat{\mathbf{u}}_t = \mathbf{u}_t + \Delta t \mathbf{v}_t \quad (5.23)$$

Finally, using the Newmark scheme (5.3)

$$\begin{aligned} \lim_{\epsilon \rightarrow 0^-} \frac{E_m(\mathbf{u}_{t+1} + \epsilon \boldsymbol{\theta}) - E_m(\mathbf{u}_{t+1})}{\epsilon} &= \lim_{\epsilon \rightarrow 0^+} \frac{E_m(\mathbf{u}_{t+1} + \epsilon \boldsymbol{\theta}) - E_m(\mathbf{u}_{t+1})}{\epsilon} \\ &= \int_{\Omega} \rho_0 \frac{2}{\Delta t^2} (\mathbf{u}_{t+1} - \hat{\mathbf{u}}_t) \cdot \boldsymbol{\theta} dx \\ &= \int_{\Omega} \rho_0 \left( \frac{2}{\Delta t^2} (\mathbf{u}_{t+1} - \mathbf{u}_t) - \frac{2}{\Delta t} \mathbf{v}_t \right) \cdot \boldsymbol{\theta} dx \\ &= \int_{\Omega} \rho_0 \mathbf{a}_{t+1} \cdot \boldsymbol{\theta} dx \end{aligned} \quad (5.24)$$

□

## 5.2 Numerical examples

In this section we will present two simple examples using the Euler implicit scheme, in order to show that the total energy, which is the sum of the kinematic and internal energies don't blow up. Assuming no forces are applied on the different bodies  $\Omega_1$  and  $\Omega_2$ , the total energy can be

given by

$$E_{tot} = E_{kin} + E_p \quad (5.25)$$

where  $E_p$  the internal energy defined before, and  $E_{kin}$  the kinematic energy of the two bodies given as follows

$$E_{kin}(\mathbf{w}) = \int_{\Omega} \rho_0 \mathbf{v}^2 dx \quad (5.26)$$

with  $\mathbf{v}$  the material velocity.

### 5.2.1 Impact between a ball and a block

A ball of density  $\rho = 100 \frac{UM}{UL^3}$  and of radius  $R = 30UL$ , is launched with an initial velocity  $\mathbf{v}_0 = -0.1 \frac{UL}{UT}$  in order to hit a rectangular foundation, initially  $0.1UL$  away. Neo-Hookean material is considered for the ball, with the following properties  $E = 2100 \frac{UF}{UL^2}$ ,  $\nu = 0.3$ . The total time of the study is about  $T = 60UT$ , and a time step  $\Delta T = 0.05UT$  (time unit) is considered. The goal of this example is to study the behavior of the total energy  $E_{tot}$ , and to see if any oscillations occur in the total reaction force on the ball.

The deformation shape of the ball at the time  $t = 22UT$  is shown in the Figure 5.1.

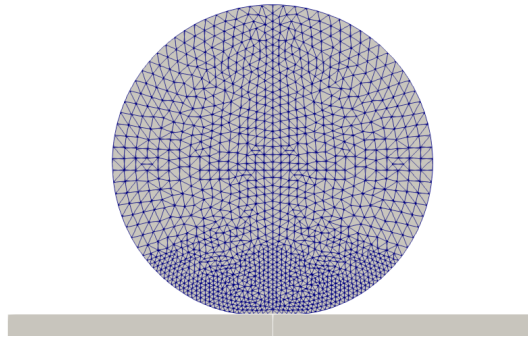


Figure 5.1 – The deformation shape at the time  $t = 22UT$

The variation of the total, potential and kinematic energy are depicted in the Figure 5.2.

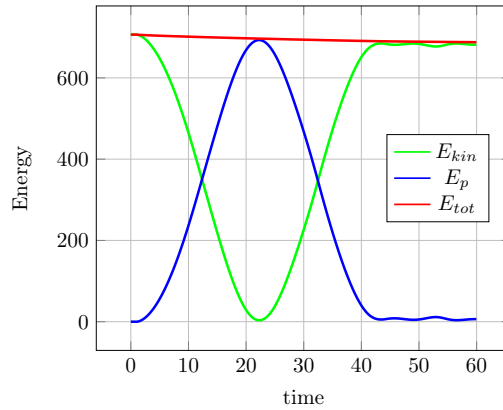


Figure 5.2 – The total, potential and kinematic energy

Moreover the total vertical reaction force on the ball is depicted in the Figure 5.3.

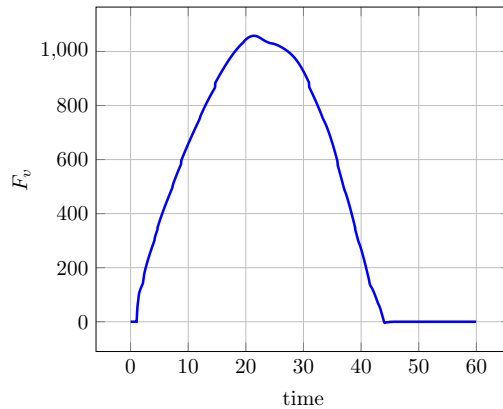


Figure 5.3 – The total vertical reaction force on the ball

We note that there is a little energy dissipation (which begins to vanish when the time step becomes smaller), and no oscillations for the vertical force is noticed.

### 5.2.2 Impact between two balls and a foundation

Two balls with the same radius  $R_1 = R_2 = 30UL$  and with different densities, are launched with the same velocity  $\mathbf{v}_0 = -1.4 \frac{UL}{UT}$  on a rigid foundation, see Figure 5.4. This example imitates the experience of taking a tennis ball on a basket ball and dropping the whole on the floor, which makes the tennis ball fly so high. The two balls are made from the same elastic material  $E = 2.1 \times 10^5 \frac{UF}{UL^2}$ ,  $\nu = 0.29$ . The ball on the top has a density of  $\rho_2 = 5 \frac{UM}{UL^3}$  and the other one has a density of  $\rho_1 = 20 \frac{UM}{UL^3}$ . The total time of the study is about  $T = 8UT$ , and a time step  $\Delta T = 0.001UT$  is considered. The goal of this example is to study the behavior of the total

energy  $E_{tot}$ , and to compare the balls velocities with the theoretical ones, generated from the classical mechanics theory.

The deformation shapes of the whole at the times  $t = 0UT$ ,  $t = 2.64UT$ ,  $t = 4.16UT$  and  $t = 8UT$  are shown in the Figure 5.4.

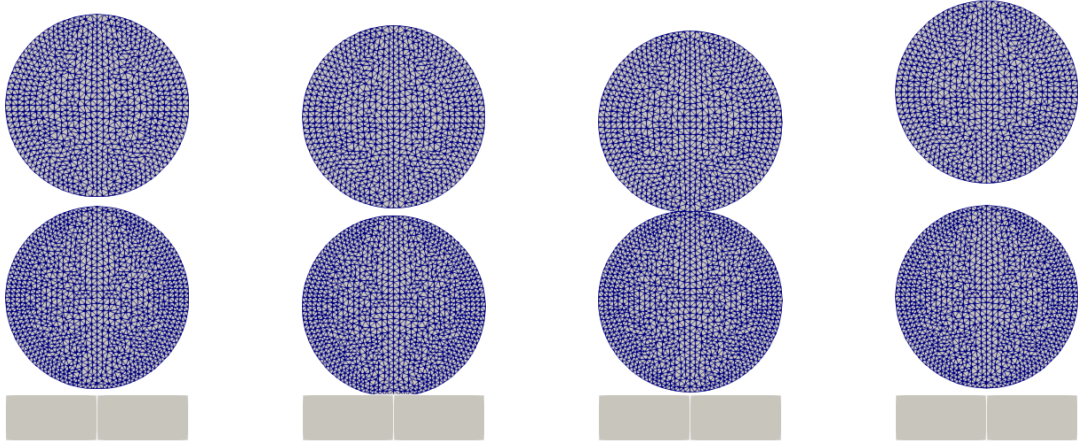


Figure 5.4 – The deformation shapes at the times  $t = 0, 2.64, 4.16, 8UT$  (from left to right)

The variation of the total, potential and kinematic energy are depicted in the Figure 5.5.

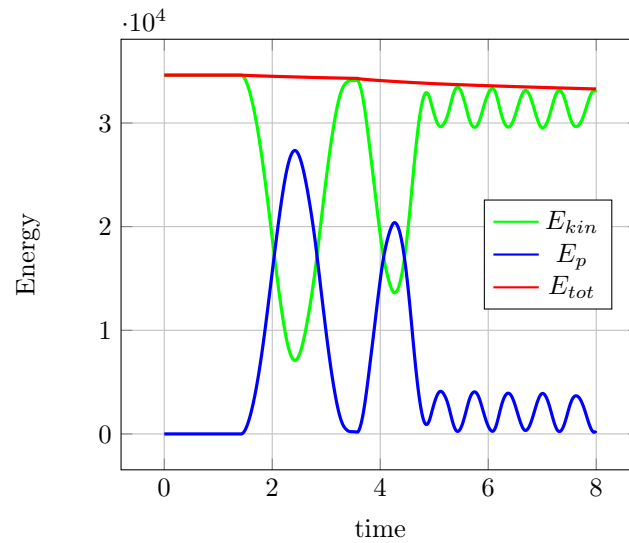


Figure 5.5 – The total, potential and kinematic energy

We note that there is a little energy dissipation (which begins to vanish when the time step becomes smaller).

Otherwise according to the classical mechanics, and supposing an elastic collision, the massive ball will hit the foundation and rebounds with a velocity  $v_{1i} = 1.4 \frac{UL}{UT}$ . At the same time, the less massive ball falls with a velocity  $v_{2i} = -1.4 \frac{UL}{UT}$  and hits the massive ball, thus the velocities of the two balls after the collision  $v_{1f}$  and  $v_{2f}$  are given by

$$\begin{cases} m_1 v_{1i} + m_2 v_{2i} = m_1 v_{1f} + m_2 v_{2f} & \text{(conservation of momentum)} \\ \frac{1}{2} m_1 v_{1i}^2 + \frac{1}{2} m_2 v_{2i}^2 = \frac{1}{2} m_1 v_{1f}^2 + \frac{1}{2} m_2 v_{2f}^2 & \text{(conservation of the kinetic energy)} \end{cases} \quad (5.27)$$

where  $m_1$  and  $m_2$  are the respective masses. Therefore

$$\begin{cases} v_{1f} = \frac{m_1 - m_2}{m_1 + m_2} v_{1i} + \frac{2m_2}{m_1 + m_2} v_{2i} \\ v_{2f} = \frac{m_2 - m_1}{m_1 + m_2} v_{2i} + \frac{2m_1}{m_1 + m_2} v_{1i} \end{cases} \quad (5.28)$$

In our case, we obtain  $v_{1f} = 0.28 \frac{UL}{UT}$  and  $v_{2f} = 3.08 \frac{UL}{UT}$ . Otherwise, the velocities values from our simulation are computed as the average of all nodes vertical velocities. In the Figure 5.6 we can see the variations of the velocities with respect to time.

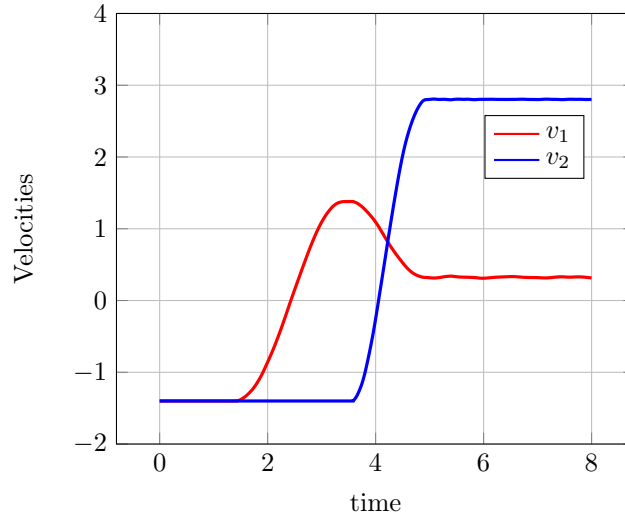


Figure 5.6 – The vertical velocities,  $v_1$  for the massive ball and  $v_2$  for the less massive one

Thus in our simulation, we obtained  $v_{1f} = 0.31 \frac{UL}{UT}$  and  $v_{2f} = 2.8 \frac{UL}{UT}$ , which are reasonable with the theoretical ones, generated from the classical mechanics.



# Frictional contact problems with the interior point method

## Outline of the current chapter

---

<b>6.1 Linear elasticity</b>	<b>124</b>
6.1.1 Tresca criterion . . . . .	125
6.1.2 Variational formulation for Tresca criterion . . . . .	125
6.1.3 Minimization formulation for the Tresca criterion . . . . .	126
6.1.4 Coulomb's criterion as a fixed point problem . . . . .	127
6.1.5 The quasi-static problem for Coulomb's criterion . . . . .	127
<b>6.2 Regularization of the Tresca frictional problem</b>	<b>128</b>
6.2.1 Frictional criterion generated from the regularized problem . . . . .	130
6.2.2 Minimization formulation for the regularized problem . . . . .	134
6.2.3 Error between Tresca's solution and regularized Tresca's solution . .	134
6.2.4 Coulomb's criterion as a fixed point problem for the regularized problem . . . . .	135
6.2.5 Quasi-static problem for the regularized one . . . . .	136
<b>6.3 Finite deformation</b>	<b>137</b>
<b>6.4 Fixed point algorithm convergence for the frictional regularized discretized problem</b>	<b>143</b>
6.4.1 Case of two bodies in contact . . . . .	149
6.4.2 Error between Tresca's discretized solution and regularized Tresca's discretized solution . . . . .	150
<b>6.5 The Algorithm</b>	<b>151</b>
<b>6.6 Numerical validations</b>	<b>154</b>
6.6.1 Validation of the regularized friction law . . . . .	154
6.6.2 Elastic bloc pressed against a rigid foundation . . . . .	155

6.6.3 Contact of a square plate against an obstacle . . . . .	157
6.6.4 Sliding on an inclined interface . . . . .	158
6.6.5 Frictional Hertz contact . . . . .	161
6.6.6 Shallow ironing . . . . .	164

The aim of this chapter is to present an algorithm to solve frictional contact problems by considering the Coulomb's criterion. As it is known, the frictional contact problem using Coulomb's criterion has no minimization principle behind. However in order to take advantage of the algorithms already developed in the previous chapters and which are based on a minimization methods, the frictional contact problem in this chapter is written as an optimization one, more specifically as a sequence of Tresca contact problems until convergence.

Each Tresca contact problem is equivalent to a minimization one, unfortunately the energy to minimize becomes not smooth enough, therefore we introduce a family of regularization functions in order to regularize the non-smooth part. In addition, in some cases, regularization can be justified because tangential slip always occurs, even for a small tangential stress [33, 87]. We can also cite [67], where a micro-displacement is produced between a hard steel ball and the flat end of a hard steel roller in contact, when the tangential force applied on the ball is less than the value necessary to produce slip.

## 6.1 Linear elasticity

We consider here two elastic bodies  $\Omega^l \subset \mathbb{R}^2$  or  $\mathbb{R}^3$  with  $l = 1, 2$  initially in contact at the border  $\Gamma_C$  (see Figure 6.1), the contact area after loading is supposed to be included in  $\Gamma_C$ . Let  $\Gamma_0^l$  be the border of the body  $\Omega^l$  where a null displacement is imposed, and  $\Gamma_1^l$  where a surface traction  $\mathbf{t}^l$  is imposed, in addition  $\Omega = \Omega^1 \cup \Omega^2$ . We call  $\mathbf{n} := \mathbf{n}^1, \mathbf{n}^2$  respectively the outward unit vector on  $\partial\Omega_1$  and on  $\partial\Omega_2$ . Finally, the body force  $\mathbf{f}^l$  is applied on  $\Omega^l$ .

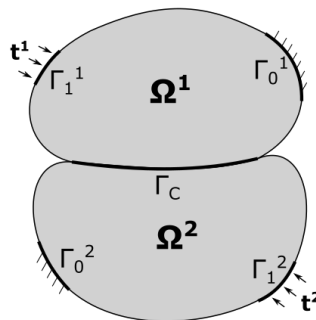


Figure 6.1 – The two bodies in contact

The frictional contact problem using Coulomb's criterion is given as follows

$$\begin{cases} \nabla \cdot \boldsymbol{\sigma}^l + \mathbf{f}^l = 0 & \text{in } \Omega^l \\ \boldsymbol{\sigma}^l = C^l \boldsymbol{\epsilon}^l & \text{in } \Omega^l \quad (\text{Hook's law}) \\ \mathbf{u}^l = \mathbf{0} & \text{on } \Gamma_0^l \\ \boldsymbol{\sigma}^l \mathbf{n}^l = \mathbf{t}^l & \text{on } \Gamma_1^l \end{cases} \quad (6.1)$$

with the following contact conditions

$$\begin{cases} [\mathbf{u} \cdot \mathbf{n}] = \mathbf{u}^1 \cdot \mathbf{n}^1 + \mathbf{u}^2 \cdot \mathbf{n}^2 = (\mathbf{u}^1 - \mathbf{u}^2) \cdot \mathbf{n} \leq 0 & \text{on } \Gamma_C \\ \sigma_n = (\boldsymbol{\sigma}^1 \mathbf{n}^1) \cdot \mathbf{n}^1 = (\boldsymbol{\sigma}^2 \mathbf{n}^2) \cdot \mathbf{n}^2 \leq 0 & \text{on } \Gamma_C \\ \sigma_n \cdot [\mathbf{u} \cdot \mathbf{n}] = 0 & \text{on } \Gamma_C \end{cases} \quad (6.2)$$

Here the normal vector  $\mathbf{n}$  is considered to be equal to  $\mathbf{n}^1$ , in addition at the contact area we have  $\mathbf{n}^1 = -\mathbf{n}^2$ . Given a friction coefficient  $\mu$ , the static Coulomb criterion on  $\Gamma_C$  states

$$\begin{cases} \boldsymbol{\sigma}_T^1 = -\boldsymbol{\sigma}_T^2 \\ |\boldsymbol{\sigma}_T^1| \leq \mu |\sigma_n| \\ \text{if } |\boldsymbol{\sigma}_T^1| < \mu |\sigma_n| \Rightarrow \mathbf{u}_T^1 - \mathbf{u}_T^2 = \mathbf{0} \\ \text{if } |\boldsymbol{\sigma}_T^1| = \mu |\sigma_n| \Rightarrow \exists \lambda \geq 0 \text{ s.t. } \mathbf{u}_T^1 - \mathbf{u}_T^2 = -\lambda \boldsymbol{\sigma}_T^1 \end{cases} \quad (6.3)$$

where the subscript  $T$  means the tangential part, otherwise speaking, for a vector  $\mathbf{v}^l$ ,  $\mathbf{v}_T^l = \mathbf{v}^l - (\mathbf{v}^l \cdot \mathbf{n}^l) \mathbf{n}^l$ , and the tangential stress  $\boldsymbol{\sigma}_T^l$  is given by  $\boldsymbol{\sigma}_T^l = \boldsymbol{\sigma}^l \mathbf{n}^l - ((\boldsymbol{\sigma}^l \mathbf{n}^l) \cdot \mathbf{n}^l) \mathbf{n}^l$ . Moreover the symbol  $|\cdot|$  for a vector means its module.

### 6.1.1 Tresca criterion

Let  $\tau \in L^2(\Gamma_C) \geq 0$ , be the sliding limit of the Tresca criterion, the governing equations are the same, except the system (6.3), which becomes

$$\begin{cases} \boldsymbol{\sigma}_T^1 = -\boldsymbol{\sigma}_T^2 \\ |\boldsymbol{\sigma}_T^1| \leq \tau \\ \text{if } |\boldsymbol{\sigma}_T^1| < \tau \Rightarrow \mathbf{u}_T^1 - \mathbf{u}_T^2 = \mathbf{0} \\ \text{if } |\boldsymbol{\sigma}_T^1| = \tau \Rightarrow \exists \lambda \geq 0 \text{ s.t. } \mathbf{u}_T^1 - \mathbf{u}_T^2 = -\lambda \boldsymbol{\sigma}_T^1 \end{cases} \quad (6.4)$$

where  $\mu |\sigma_n|$  was replaced by the sliding limit  $\tau$ .

### 6.1.2 Variational formulation for Tresca criterion

The displacement field  $\mathbf{u}$  is defined by  $\mathbf{u} = (\mathbf{u}^1, \mathbf{u}^2)$ . We define the admissible set as  $\mathbf{V} = \mathbf{V}^1 \times \mathbf{V}^2$  where

$$\mathbf{V}^l = \{\mathbf{v} \in \mathbf{H}^1(\Omega^l) \mid \mathbf{v} = \mathbf{0} \text{ a.e on } \Gamma_0^l\} \quad (6.5)$$

endowed with the broken norm:

$$\|\mathbf{u}\|_1 = \|(\mathbf{u}^1, \mathbf{u}^2)\|_1 = (\|\mathbf{u}^1\|_1^2 + \|\mathbf{u}^2\|_1^2)^{\frac{1}{2}} \quad (6.6)$$

Let the applications  $a : \mathbf{V} \times \mathbf{V} \rightarrow \mathbb{R}$  and  $f : \mathbf{V} \rightarrow \mathbb{R}$  be defined by

$$\begin{cases} a(\mathbf{u}, \mathbf{v}) = a^1(\mathbf{u}, \mathbf{v}) + a^2(\mathbf{u}, \mathbf{v}) \\ f(\mathbf{v}) = f^1(\mathbf{v}) + f^2(\mathbf{v}) \end{cases} \quad (6.7)$$

where for  $l = 1, 2$

$$\begin{cases} a^l(\mathbf{u}, \mathbf{v}) = \int_{\Omega^l} \boldsymbol{\sigma}(\mathbf{u}^l) : \boldsymbol{\epsilon}(\mathbf{v}^l) dv \\ f^l(\mathbf{v}) = \int_{\Omega^l} \mathbf{f}^l \cdot \mathbf{v}^l dv + \int_{\Gamma_1^l} \mathbf{t}^l \cdot \mathbf{v}^l ds \end{cases} \quad (6.8)$$

We also consider the application  $j_\tau : \mathbf{V} \rightarrow \mathbb{R}_+$  defined by

$$j_\tau(\mathbf{v}) = \int_{\Gamma_C} \tau |\mathbf{v}_T^1 - \mathbf{v}_T^2| ds \quad (6.9)$$

The convex and closed set  $\mathbf{K}$  describes the non-penetration between the two bodies, and is defined by

$$\mathbf{K} = \{\mathbf{v} \in \mathbf{V} \mid [\mathbf{v} \cdot \mathbf{n}] \leq 0 \text{ a.e on } \Gamma_C\} \quad (6.10)$$

where  $[\mathbf{v} \cdot \mathbf{n}] = (\mathbf{u}^1 - \mathbf{u}^2) \cdot \mathbf{n} = (\mathbf{u}^1 - \mathbf{u}^2) \cdot \mathbf{n}^1$ . The variational formulation of the frictional contact problem using Tresca's criterion can be proven to be equal to

Find  $\mathbf{u} \in \mathbf{K}$  such that

$$a(\mathbf{u}, \mathbf{v} - \mathbf{u}) + j_\tau(\mathbf{v}) - j_\tau(\mathbf{u}) \geq f(\mathbf{v} - \mathbf{u}) \quad \forall \mathbf{v} \in \mathbf{K} \quad (6.11)$$

### 6.1.3 Minimization formulation for the Tresca criterion

Before giving the minimization formulation, let's recall a theorem which can be found in [69].

**Theorem 6.1.** *Let  $\mathbf{K}$  be a nonempty, closed and convex, subset of the normed linear space  $\mathbf{V}$ , and consider a function  $F : \mathbf{K} \subset \mathbf{V} \rightarrow \mathbb{R}$  of the form  $F = F_1 + \Phi$  where  $F_1$  and  $\Phi$  are convex and lower semicontinuous and  $F_1$  is Gâteaux differentiable on  $\mathbf{K}$ . Then  $\mathbf{u}$  is a minimizer of  $F$  on  $\mathbf{K}$  if and only if,*

$$\langle DF_1(\mathbf{u}), \mathbf{v} - \mathbf{u} \rangle + \Phi(\mathbf{v}) - \Phi(\mathbf{u}) \geq 0 \quad \forall \mathbf{v} \in \mathbf{K} \quad (6.12)$$

Let  $\mathcal{E}_p$  denotes the total potential energy of the two bodies,  $\mathcal{E}_p$  can be given by

$$\mathcal{E}_p(\mathbf{v}) := \frac{1}{2} a(\mathbf{v}, \mathbf{v}) - f(\mathbf{v}) \quad (6.13)$$

Consider the energy functional  $J_\tau$  given by

$$J_\tau(\mathbf{v}) := \mathcal{E}_p(\mathbf{v}) + j_\tau(\mathbf{v}) \quad (6.14)$$

Then by applying the theorem 6.1 above, by taking  $F = J_\tau$ ,  $F_1 = \mathcal{E}_p$  and  $\Phi = j_\tau$ , the frictional problem (6.11) is equivalent to the following minimization problem

$$\text{Find } \mathbf{u} \in \mathbf{K} \text{ such that} \quad J_\tau(\mathbf{u}) \leq J_\tau(\mathbf{v}) \quad \forall \mathbf{v} \in \mathbf{K} \quad (6.15)$$

#### 6.1.4 Coulomb's criterion as a fixed point problem

The idea to study the Tresca criterion, is that the Coulomb criterion can be equivalent to the fixed point of the following application (see [79, 101])

$$T(\tau) = -\mu\sigma_N(\mathbf{u}_\tau) \quad (6.16)$$

where  $\sigma_N$  the normal stress and  $\mathbf{u}_\tau$  the solution of the Tresca problem with the sliding limit  $\tau \geq 0$ , otherwise speaking, solution of the following problem

$$\text{Find } \mathbf{u}_\tau \in \mathbf{K} \text{ such that} \quad a(\mathbf{u}_\tau, \mathbf{v} - \mathbf{u}_\tau) + j_\tau(\mathbf{v}) - j_\tau(\mathbf{u}_\tau) \geq f(\mathbf{v} - \mathbf{u}_\tau) \quad \forall \mathbf{v} \in \mathbf{K} \quad (6.17)$$

or equivalently

$$\text{Find } \mathbf{u}_\tau \in \mathbf{K} \text{ such that} \quad J_\tau(\mathbf{u}_\tau) \leq J_\tau(\mathbf{v}) \quad \forall \mathbf{v} \in \mathbf{K} \quad (6.18)$$

Otherwise speaking, if  $\tau^*$  is the fixed point of the application  $T$ ,  $\tau^* = -\mu\sigma_N(\mathbf{u}_{\tau^*})$ , then  $\mathbf{u}_{\tau^*}$  is the solution of the frictional problem using Coulomb's criterion.

#### 6.1.5 The quasi-static problem for Coulomb's criterion

In reality the friction depends on the history of the loading, indeed the Coulomb criterion depends on the velocity rather than the displacement, and therefore the friction depends on the state of the previous time step. However the static criterion is very useful to treat the quasi-static case, because as we will see the quasi-static criterion can be written as a sequence of a static criterion when the velocity is discretized.

The quasi-static criterion is given by the following

$$\begin{cases} |\sigma_T^1| \leq \mu|\sigma_n| \\ \text{if } |\sigma_T^1| < \mu|\sigma_n| \Rightarrow \dot{\mathbf{u}}_T^1 - \dot{\mathbf{u}}_T^2 = \mathbf{0} \\ \text{if } |\sigma_T^1| = \mu|\sigma_n| \Rightarrow \exists \lambda \geq 0 \text{ s.t. } \dot{\mathbf{u}}_T^1 - \dot{\mathbf{u}}_T^2 = -\lambda\sigma_T^1 \end{cases} \quad (6.19)$$

where  $\dot{\mathbf{u}}$  denotes the velocity.

For a time step  $\Delta t$  the velocities  $\dot{\mathbf{u}}_T^1$  and  $\dot{\mathbf{u}}_T^2$  are discretized as follows

$$\begin{cases} \dot{\mathbf{u}}_T^1 = \frac{\mathbf{u}_{T,i+1}^1 - \mathbf{u}_{T,i}^1}{\Delta t} \\ \dot{\mathbf{u}}_T^2 = \frac{\mathbf{u}_{T,i+1}^2 - \mathbf{u}_{T,i}^2}{\Delta t} \end{cases} \quad (6.20)$$

where  $i+1$  and  $i$  denotes respectively the actual and the previous state. Therefore the quasi-static criterion becomes

$$\begin{cases} |\sigma_T^1| \leq \mu|\sigma_n| \\ \text{if } |\sigma_T^1| < \mu|\sigma_n| \Rightarrow (\mathbf{u}_{T,i+1}^1 - \mathbf{u}_{T,i}^1) - (\mathbf{u}_{T,i+1}^2 - \mathbf{u}_{T,i}^2) = \mathbf{0} \\ \text{if } |\sigma_T^1| = \mu|\sigma_n| \Rightarrow \exists \lambda \geq 0 \text{ s.t. } (\mathbf{u}_{T,i+1}^1 - \mathbf{u}_{T,i}^1) - (\mathbf{u}_{T,i+1}^2 - \mathbf{u}_{T,i}^2) = -\lambda \sigma_T^1 \end{cases} \quad (6.21)$$

## 6.2 Regularization of the Tresca frictional problem

Recall that the frictional problem using Tresca's criterion is given by

Find  $\mathbf{u} \in \mathbf{K}$  such that

$$a(\mathbf{u}, \mathbf{v} - \mathbf{u}) + j_\tau(\mathbf{v}) - j_\tau(\mathbf{u}) \geq f(\mathbf{v} - \mathbf{u}) \quad \forall \mathbf{v} \in \mathbf{K} \quad (6.22)$$

The application  $j_\tau$  is not differentiable because of its module term. For this reason and for an algorithmic point of view, in order to obtain a smooth problem, the module vector  $|\cdot|$  is approximated by an application  $\eta_\alpha$ .

We suppose that the regularization function  $\eta_\alpha$  approximating the module of a vector, belongs to the set  $\Xi_\alpha$ , defined below.

**Definition 6.1.** Define  $\Xi_\alpha$ , for  $\alpha > 0$ , the set of functions such that

$$\eta_\alpha \in \Xi_\alpha \iff \begin{cases} \eta_\alpha \in C^2(\mathbb{R}^d) \\ \eta_\alpha \text{ is convex} \\ \eta_\alpha(\mathbf{v}) = \eta_\alpha(-\mathbf{v}) \quad \forall \mathbf{v} \in \mathbb{R}^d \\ \eta_\alpha(\mathbf{v}) \geq 0 \quad \forall \mathbf{v} \in \mathbb{R}^d \\ |\eta_\alpha(\mathbf{v}) - |\mathbf{v}|| \leq \alpha \quad \forall \mathbf{v} \in \mathbb{R}^d \\ |\eta_\alpha(\mathbf{v}_1) - \eta_\alpha(\mathbf{v}_2)| \leq ||\mathbf{v}_1| - |\mathbf{v}_2|| \quad \forall \mathbf{v}_1, \mathbf{v}_2 \in \mathbb{R}^d \end{cases} \quad (6.23)$$

Let's give an example of a regularization function belonging to  $\Xi_\alpha$ .

**Lemma 6.1.** For  $\alpha > 0$ , the function  $\bar{\eta}_\alpha : \mathbb{R}^d \rightarrow [0, \infty[$  defined by

$$\bar{\eta}_\alpha(\mathbf{v}) = \sqrt{|\mathbf{v}|^2 + \alpha^2} \quad \forall \mathbf{v} \in \mathbb{R}^d \quad (6.24)$$

belongs to  $\Xi_\alpha$ .

*Proof.* First  $\bar{\eta}_\alpha$  is convex, it remains to prove that

$$\begin{cases} |\bar{\eta}_\alpha(\mathbf{v}) - |\mathbf{v}|| \leq \alpha & \forall \mathbf{v} \in \mathbb{R}^d \\ |\bar{\eta}_\alpha(\mathbf{v}_1) - \bar{\eta}_\alpha(\mathbf{v}_2)| \leq ||\mathbf{v}_1| - |\mathbf{v}_2|| & \forall \mathbf{v}_1, \mathbf{v}_2 \in \mathbb{R}^d \end{cases} \quad (6.25)$$

In order to prove the first equation of (6.25), we consider the function  $f : \mathbb{R} \rightarrow \mathbb{R}$  defined by  $f(x) = \sqrt{x^2 + \alpha^2} - \sqrt{x^2}$ , we have  $f(x) \geq 0$  and we just need to prove that  $f(x) \leq \alpha$ . Indeed  $f$  is symmetric and then if  $x \geq 0$ , its derivative  $f'$  is negative and then  $f(x) \leq f(0) = \alpha$ , and the first equation of (6.25) is proved.

Second, consider the function  $F : [0, +\infty[ \times [0, +\infty[ \rightarrow \mathbb{R}$  such that

$$F(x, y) = (\sqrt{x + \alpha^2} - \sqrt{y + \alpha^2})^2 - (\sqrt{x} - \sqrt{y})^2 \quad (6.26)$$

We want to show that  $F(x, y) \leq 0$ , indeed it's enough to study it on the domain  $D = \{(x, y) \in \mathbb{R}^2 \mid x \geq 0, x \leq y\}$ . After some calculations

$$F(x, y) = 2\alpha^2 + 2(\sqrt{x}\sqrt{y} - \sqrt{x + \alpha^2}\sqrt{y + \alpha^2}) \quad (6.27)$$

If  $y = 0$  then  $F(0, 0) = 0$ , thus we can set  $y > 0$  and consider the function  $f_y(x) = 2\alpha^2 + 2(\sqrt{x}\sqrt{y} - \sqrt{x + \alpha^2}\sqrt{y + \alpha^2})$  for  $y$  fixed, defined on the closed interval  $[0, y]$ . The derivative of  $f_y$  is given by

$$f'_y(x) = \frac{\sqrt{y}}{\sqrt{x}} - \frac{\sqrt{y + \alpha^2}}{\sqrt{x + \alpha^2}} \quad (6.28)$$

We have  $f_y(0) = 2\alpha^2 - 2\sqrt{\alpha^2}\sqrt{y + \alpha^2} < 0$  and  $f_y(y) = 0$ . Suppose that  $\exists z \in ]0, y[$  such that  $f_y(z) > 0$ . As  $f_y$  is continuous on the compact set  $[0, y]$ , therefore there exists  $z^*$  such that  $f_y(z^*)$  is the maximum of  $f_y$  on  $[0, y]$ , we have  $z^* \in ]0, y[$  because  $f_y(z^*) \geq f_y(z) > 0$ . Thus  $f'_y(z^*) = 0$  and from the equation (6.28) we conclude that

$$\frac{y}{z^*} = \frac{y + \alpha^2}{z^* + \alpha^2} \quad (6.29)$$

which implies that  $z^* = y$  and we obtain a contradiction. Therefore  $f_y \leq 0$ , and finally  $F(x, y) \leq 0$  on  $[0, +\infty[ \times [0, +\infty[$ .

We can deduce that  $F(|\mathbf{v}_1|^2, |\mathbf{v}_2|^2) \leq 0$ , thus

$$\left(\sqrt{|\mathbf{v}_1|^2 + \alpha^2} - \sqrt{|\mathbf{v}_2|^2 + \alpha^2}\right)^2 \leq \left(\sqrt{|\mathbf{v}_1|^2} - \sqrt{|\mathbf{v}_2|^2}\right)^2 \quad (6.30)$$

and therefore we obtain the second equation of (6.25).  $\square$

In the following we take a regularization function  $\eta_\alpha$  such that  $\eta_\alpha \in \Xi_\alpha$ . Our regularized frictional problem becomes

Find  $\mathbf{u} \in \mathbf{K}$  such that

$$a(\mathbf{u}, \mathbf{v} - \mathbf{u}) + j_{\alpha, \tau}(\mathbf{v}) - j_{\alpha, \tau}(\mathbf{u}) \geq f(\mathbf{v} - \mathbf{u}) \quad \forall \mathbf{v} \in \mathbf{K} \quad (6.31)$$

where the application  $j_{\alpha,\tau}$  is given by

$$j_{\alpha,\tau}(\mathbf{v}) = \int_{\Gamma_C} \tau \eta_\alpha(\mathbf{v}_T^1 - \mathbf{v}_T^2) ds \quad (6.32)$$

Note that the regularization of frictional problems was considered in many papers like [21, 78, 87].

### 6.2.1 Frictional criterion generated from the regularized problem

In most papers and for Signorini's contact problem, one can cite [40, 69], the variational inequality (6.11) is proved to be equivalent to the contact problem equations (6.1), (6.2), with Tresca's frictional criterion (6.4). Otherwise, regularizing the frictional criterion can be found in [101], and in [87] where a nonlocal friction is used (the normal stress is replaced by a weighed average of the normal stress in the friction criterion) and where we can find a physical interpretation for the regularization, as the elastic and elastoplastic deformation of the junctions (a region in the contact area where an adhesion take place). Here we prove formally, in the case of contact between two bodies, that if the variational inequality (6.31) is satisfied then the equations of the contact problem (6.1), (6.2) are satisfied with a special regularized frictional criterion.

In order to obtain the frictional criterion generated by the regularized problem, we present the following theorem

**Theorem 6.2.** *Let  $\mathbf{u} \in \mathbf{K}$  be sufficiently regular ( $\mathbf{H}^2$ ), and satisfying the following variational inequality*

$$a(\mathbf{u}, \mathbf{v} - \mathbf{u}) + j_{\alpha,\tau}(\mathbf{v}) - j_{\alpha,\tau}(\mathbf{u}) \geq f(\mathbf{v} - \mathbf{u}) \quad \forall \mathbf{v} \in \mathbf{K} \quad (6.33)$$

*Then  $\mathbf{u}$  satisfies the following equations for  $l = 1, 2$*

$$\begin{cases} \nabla \cdot \boldsymbol{\sigma}^l + \mathbf{f}^l = 0 & \text{in } \Omega^l \\ \boldsymbol{\sigma}^l = C^l \boldsymbol{\epsilon}^l & \text{in } \Omega^l \quad (\text{Hook's law}) \\ \mathbf{u}^l = \mathbf{0} & \text{on } \Gamma_0^l \\ \boldsymbol{\sigma}^l \mathbf{n}^l = \mathbf{t}^l & \text{on } \Gamma_1^l \end{cases} \quad (6.34)$$

*with the following contact conditions:*

$$\begin{cases} [\mathbf{u} \cdot \mathbf{n}] = \mathbf{u}^1 \cdot \mathbf{n}^1 + \mathbf{u}^2 \cdot \mathbf{n}^2 = (\mathbf{u}^1 - \mathbf{u}^2) \cdot \mathbf{n} \leq 0 & \text{on } \Gamma_C \\ \sigma_n := (\boldsymbol{\sigma}^1 \mathbf{n}^1) \cdot \mathbf{n}^1 = (\boldsymbol{\sigma}^2 \mathbf{n}^2) \cdot \mathbf{n}^2 \leq 0 & \text{on } \Gamma_C \\ \sigma_n [\mathbf{u} \cdot \mathbf{n}] = 0 & \text{on } \Gamma_C \end{cases} \quad (6.35)$$

*with the following regularized frictional criterion on  $\Gamma_C$*

$$\begin{cases} \boldsymbol{\sigma}_T^1 &= -\boldsymbol{\sigma}_T^2 \\ \boldsymbol{\sigma}_T^1 &= -\tau \cdot \nabla \eta_\alpha(\mathbf{u}_T^1 - \mathbf{u}_T^2) \\ &= -\tau \frac{(\mathbf{u}_T^1 - \mathbf{u}_T^2)}{\sqrt{|\mathbf{u}_T^1 - \mathbf{u}_T^2|^2 + \alpha^2}} \text{ if } \eta_\alpha(\mathbf{v}) = \sqrt{|\mathbf{v}|^2 + \alpha^2} \end{cases} \quad (6.36)$$

*where  $\nabla \eta_\alpha(\cdot) : \mathbb{R}^d \rightarrow \mathbb{R}^d$  the gradient of  $\eta_\alpha$  and  $\nabla \eta_\alpha(\mathbf{u}_T^1 - \mathbf{u}_T^2)$  is supposed to be in the same*

tangent space of  $\sigma_T^1$  (true if  $\eta_\alpha(\mathbf{v}) = \sqrt{|\mathbf{v}|^2 + \alpha^2}$ ).

*Proof.* We recall the Green formula which will be useful in the sequel. For  $l = 1$  or  $2$

$$\int_{\Omega^l} \sigma^l(\mathbf{u}^l) : \epsilon(\mathbf{v}^l) dv = - \int_{\Omega^l} \nabla \cdot \sigma^l(\mathbf{u}^l) \cdot \mathbf{v}^l dv + \int_{\partial\Omega^l} \sigma^l(\mathbf{u}^l) \mathbf{n}^l \cdot \mathbf{v}^l ds \quad (6.37)$$

Therefore

$$a(\mathbf{u}, \mathbf{v} - \mathbf{u}) = \sum_{l=1,2} \left( - \int_{\Omega^l} \nabla \cdot \sigma^l(\mathbf{u}^l) \cdot (\mathbf{v}^l - \mathbf{u}^l) dv + \int_{\partial\Omega^l} \sigma^l(\mathbf{u}^l) \mathbf{n}^l \cdot (\mathbf{v}^l - \mathbf{u}^l) ds \right) \quad (6.38)$$

First consider an application  $\phi \in \mathcal{D}^2(\Omega^1)$  ( $\mathbf{C}^2(\Omega^1)$  with a compact support in  $\Omega^1$ ), we will take the test function  $\mathbf{v} = (\mathbf{v}^1, \mathbf{v}^2)$  such that  $\mathbf{v}^1 = \mathbf{u}^1 \pm \phi$  and  $\mathbf{v}^2 = \mathbf{u}^2$ . Then using the variational inequality (6.33), the Green formula (6.38) and the fact that  $\phi$  is equal to zero on the borders, one obtains

$$- \int_{\Omega^1} \nabla \cdot \sigma^1(\mathbf{u}^1) \cdot \phi dv - \int_{\Omega^1} \mathbf{f}^1 \cdot \phi dv \geq 0 \quad (6.39)$$

and

$$\int_{\Omega^1} \nabla \cdot \sigma^1(\mathbf{u}^1) \cdot \phi dv + \int_{\Omega^1} \mathbf{f}^1 \cdot \phi dv \geq 0 \quad (6.40)$$

Thus

$$\int_{\Omega^1} (\nabla \cdot \sigma^1(\mathbf{u}^1) + \mathbf{f}^1) \cdot \phi dv = 0 \quad (6.41)$$

Otherwise speaking

$$\nabla \cdot \sigma^1(\mathbf{u}^1) + \mathbf{f}^1 = 0 \text{ a.e on } \Omega^1 \quad (6.42)$$

In the same manner if we take  $\mathbf{v}$  such that  $\mathbf{v}^1 = \mathbf{u}^1$  and  $\mathbf{v}^2 = \mathbf{u}^2 \pm \phi$ , we obtain

$$\nabla \cdot \sigma^2(\mathbf{u}^2) + \mathbf{f}^2 = 0 \text{ a.e on } \Omega^2 \quad (6.43)$$

Consider the test function  $\mathbf{v} = (\mathbf{v}^1, \mathbf{v}^2)$  such that  $\mathbf{v}^1 = \mathbf{u}^1 \pm \phi$  and  $\mathbf{v}^2 = \mathbf{u}^2$ , then using the two equilibrium equations (6.42) and (6.43) the variational inequality becomes

$$\int_{\partial\Omega^1} \sigma^1(\mathbf{u}^1) \mathbf{n}^1 \cdot (\pm\phi) ds - \int_{\Gamma_1^1} \mathbf{t}^1 \cdot (\pm\phi) ds + \int_{\Gamma_C} \tau \cdot (\eta_\alpha(\mathbf{v}_T^1 - \mathbf{u}_T^1) - \eta_\alpha(\mathbf{u}_T^1 - \mathbf{u}_T^1)) ds \geq 0 \quad (6.44)$$

In the inequality (6.44) we can take  $\phi \in \mathbf{H}^{1/2}(\partial\Omega^1)$  with  $\text{supp}(\phi) \subset \Gamma_1^1$ , and we will obtain then

$$- \int_{\Gamma_1^1} (\sigma^1(\mathbf{u}^1) \mathbf{n}^1 - \mathbf{t}^1) \cdot \phi ds \geq 0 \quad (6.45)$$

and

$$\int_{\Gamma_1^1} (\sigma^1(\mathbf{u}^1) \mathbf{n}^1 - \mathbf{t}^1) \cdot \phi ds \geq 0 \quad (6.46)$$

Otherwise speaking

$$\int_{\Gamma_1^1} (\sigma^1(\mathbf{u}^1) \mathbf{n}^1 - \mathbf{t}^1) \cdot \phi ds = 0 \quad (6.47)$$

Therefore

$$\boldsymbol{\sigma}^1(\mathbf{u}^1)\mathbf{n}^1 = \mathbf{t}^1 \text{ a.e on } \Gamma_1^1 \quad (6.48)$$

In the same manner if we take  $\mathbf{v} = (\mathbf{v}^1, \mathbf{v}^2)$  such that  $\mathbf{v}^1 = \mathbf{u}^1$  and  $\mathbf{v}^2 = \mathbf{u}^2 \pm \phi$  we obtain

$$\boldsymbol{\sigma}^2(\mathbf{u}^2)\mathbf{n}^2 = \mathbf{t}^2 \text{ a.e on } \Gamma_1^2 \quad (6.49)$$

Because  $\mathbf{u} \in \mathbf{K}$ , then by definition  $[\mathbf{u}, \mathbf{n}] \leq 0$  on  $\Gamma_C$  and  $\mathbf{u}^l = \mathbf{0}$  on  $\Gamma_0^l$ . So it remains to verify the last two equations of (6.35) and the two equations of (6.36).

Using the equations (6.42), (6.43), (6.48), (6.49) and the Green formula, the variational inequality (6.33) becomes

$$\sum_{l=1,2} \int_{\Gamma_C} \boldsymbol{\sigma}^l(\mathbf{u}^l)\mathbf{n}^l \cdot (\mathbf{v}^l - \mathbf{u}^l) ds + \int_{\Gamma_C} \tau \cdot (\eta_\alpha(\mathbf{v}_T^1 - \mathbf{v}_T^2) - \eta_\alpha(\mathbf{u}_T^1 - \mathbf{u}_T^2)) ds \geq 0 \quad \forall \mathbf{v} \in \mathbf{K} \quad (6.50)$$

Taking  $\mathbf{v} = (\mathbf{v}^1, \mathbf{v}^2)$  such that  $\mathbf{v}^1 = \phi \cdot \mathbf{n}^1 + \mathbf{u}^1$  and  $\mathbf{v}^2 = -\phi \cdot \mathbf{n}^2 + \mathbf{u}^2$ , we have the fact that  $\mathbf{v} \in \mathbf{K}$  because  $[\mathbf{v}, \mathbf{n}] = \mathbf{v}^1 \cdot \mathbf{n}^1 + \mathbf{v}^2 \cdot \mathbf{n}^2 = \mathbf{u}^1 \cdot \mathbf{n}^1 + \mathbf{u}^2 \cdot \mathbf{n}^2 = [\mathbf{u}, \mathbf{n}] \leq 0$ . Thus if we inject  $\mathbf{v}$  in the inequality (6.50) one obtains

$$\int_{\Gamma_C} (\boldsymbol{\sigma}^1(\mathbf{u}^1)\mathbf{n}^1) \cdot \mathbf{n}^1 \phi ds - \int_{\Gamma_C} (\boldsymbol{\sigma}^2(\mathbf{u}^2)\mathbf{n}^2) \cdot \mathbf{n}^2 \phi ds \geq 0 \quad (6.51)$$

or

$$\int_{\Gamma_C} ((\boldsymbol{\sigma}^1(\mathbf{u}^1)\mathbf{n}^1) \cdot \mathbf{n}^1 - (\boldsymbol{\sigma}^2(\mathbf{u}^2)\mathbf{n}^2) \cdot \mathbf{n}^2) \phi ds \geq 0 \quad (6.52)$$

In addition if we consider  $-\phi$  instead of  $\phi$ , we can obtain thus

$$\int_{\Gamma_C} ((\boldsymbol{\sigma}^1(\mathbf{u}^1)\mathbf{n}^1) \cdot \mathbf{n}^1 - (\boldsymbol{\sigma}^2(\mathbf{u}^2)\mathbf{n}^2) \cdot \mathbf{n}^2) \phi ds \leq 0 \quad (6.53)$$

Therefore

$$\int_{\Gamma_C} ((\boldsymbol{\sigma}^1(\mathbf{u}^1)\mathbf{n}^1) \cdot \mathbf{n}^1 - (\boldsymbol{\sigma}^2(\mathbf{u}^2)\mathbf{n}^2) \cdot \mathbf{n}^2) \phi ds = 0 \quad (6.54)$$

We can deduce that  $\sigma_n := (\boldsymbol{\sigma}^1\mathbf{n}^1) \cdot \mathbf{n}^1 = (\boldsymbol{\sigma}^2\mathbf{n}^2) \cdot \mathbf{n}^2$  a.e on  $\Gamma_C$  which is the second equation of (6.35).

Now we take  $\mathbf{v} = (\mathbf{v}^1, \mathbf{v}^2)$  such that  $\mathbf{v}^1 = \lambda \cdot \phi \cdot \mathbf{n}^1 + \mathbf{u}_T^1$  and  $\mathbf{v}^2 = \mathbf{u}_T^2$ , where  $\lambda \geq 0$  and  $\phi \in H^{1/2}(\partial\Omega^1) \leq 0$  with  $\text{supp}(\phi) \subset \Gamma_C$ . Clearly  $\mathbf{v} \in \mathbf{K}$  because  $[\mathbf{v}, \mathbf{n}] = \mathbf{v}^1 \cdot \mathbf{n}^1 + \mathbf{v}^2 \cdot \mathbf{n}^2 = \lambda \cdot \phi \leq 0$ . Injecting  $\mathbf{v}$  in the inequality (6.50) and using the fact that  $\mathbf{u}^1 = (\mathbf{u}^1 \cdot \mathbf{n}^1)\mathbf{n}^1 + \mathbf{u}_T^1$  and  $\mathbf{u}^2 = (\mathbf{u}^2 \cdot \mathbf{n}^2)\mathbf{n}^2 + \mathbf{u}_T^2$ , one obtains

$$\int_{\Gamma_C} (\boldsymbol{\sigma}^1(\mathbf{u}^1)\mathbf{n}^1) \cdot \lambda \cdot \phi \mathbf{n}^1 ds - \int_{\Gamma_C} (\boldsymbol{\sigma}^1(\mathbf{u}^1)\mathbf{n}^1) \cdot (\mathbf{u}^1 \cdot \mathbf{n}^1)\mathbf{n}^1 ds - \int_{\Gamma_C} (\boldsymbol{\sigma}^2(\mathbf{u}^2)\mathbf{n}^2) \cdot (\mathbf{u}^2 \cdot \mathbf{n}^2)\mathbf{n}^2 ds \geq 0 \quad (6.55)$$

Then

$$\int_{\Gamma_C} \sigma_n \cdot \lambda \cdot \phi ds - \int_{\Gamma_C} \sigma_n \cdot (\mathbf{u}^1 \cdot \mathbf{n}^1) ds - \int_{\Gamma_C} \sigma_n \cdot (\mathbf{u}^2 \cdot \mathbf{n}^2) ds \geq 0 \quad (6.56)$$

which is equivalent to

$$\lambda \int_{\Gamma_C} \sigma_n \cdot \phi \, ds - \int_{\Gamma_C} \sigma_n \cdot [\mathbf{u}, \mathbf{n}] \, ds \geq 0 \quad (6.57)$$

If  $\lambda \rightarrow 0$  then

$$\int_{\Gamma_C} \sigma_n \cdot [\mathbf{u}, \mathbf{n}] \, ds \leq 0 \quad (6.58)$$

If we divide the inequality (6.57) by  $\lambda$  and taking  $\lambda \rightarrow +\infty$  then

$$\int_{\Gamma_C} \sigma_n \cdot \phi \, ds \geq 0 \quad (6.59)$$

From the inequality (6.59) and from the fact that  $\phi \leq 0$  we deduce that  $\sigma_n \leq 0$ . By definition  $[\mathbf{u}, \mathbf{n}] \leq 0$ , thus  $\sigma_n \cdot [\mathbf{u}, \mathbf{n}] \geq 0$ , therefore from the inequality (6.58) we deduce that  $\sigma_n \cdot [\mathbf{u}, \mathbf{n}] = 0$ . Therefore the equations of (6.35) are verified and it remains to prove the two equations of (6.36).

Let  $\phi = \phi_n \mathbf{n}^1 + \phi_T \in \mathbf{H}^{1/2}(\partial\Omega^1)$  with  $\text{supp}(\phi) \subset \Gamma_C$ . Take  $\mathbf{v} = (\mathbf{v}^1, \mathbf{v}^2)$  such that  $\mathbf{v}^1 = \mathbf{u}^1 \pm \epsilon \phi_T$  and  $\mathbf{v}^2 = \mathbf{u}^2$ , where  $\epsilon \in [0, 1]$ . Clearly  $\mathbf{v} \in \mathbf{K}$ , thus injecting  $\mathbf{v}$  in (6.50) one obtains

$$\int_{\Gamma_C} \boldsymbol{\sigma}^1(\mathbf{u}^1) \mathbf{n}^1 \cdot (\pm \epsilon \phi_T) \, ds + \int_{\Gamma_C} \tau \cdot (\eta_\alpha(\mathbf{u}_T^1 - \mathbf{u}_T^2 \pm \epsilon \phi_T) - \eta_\alpha(\mathbf{u}_T^1 - \mathbf{u}_T^2)) \, ds \geq 0 \quad (6.60)$$

thus and after dividing by  $\epsilon$

$$\int_{\Gamma_C} \boldsymbol{\sigma}_T^1 \cdot (\pm \phi_T) \, ds + \int_{\Gamma_C} \tau \cdot \frac{\eta_\alpha(\mathbf{u}_T^1 - \mathbf{u}_T^2 \pm \epsilon \phi_T) - \eta_\alpha(\mathbf{u}_T^1 - \mathbf{u}_T^2)}{\epsilon} \, ds \geq 0 \quad (6.61)$$

Thanks to the differentiability of  $\eta_\alpha$ , we obtain the following inequality when  $\epsilon \rightarrow 0$

$$\int_{\Gamma_C} \boldsymbol{\sigma}_T^1 \cdot (\pm \phi_T) \, ds + \int_{\Gamma_C} \tau \cdot \nabla \eta_\alpha(\mathbf{u}_T^1 - \mathbf{u}_T^2) \cdot (\pm \phi_T) \, ds \geq 0 \quad (6.62)$$

We deduce that

$$\int_{\Gamma_C} \boldsymbol{\sigma}_T^1 \cdot \phi_T \, ds + \int_{\Gamma_C} \tau \cdot \nabla \eta_\alpha(\mathbf{u}_T^1 - \mathbf{u}_T^2) \cdot \phi_T \, ds = 0 \quad (6.63)$$

Otherwise  $\boldsymbol{\sigma}_T^1 \cdot \phi_T = \boldsymbol{\sigma}_T^1 \cdot \phi$  and  $\nabla \eta_\alpha(\mathbf{u}_T^1 - \mathbf{u}_T^2) \cdot \phi_T = \nabla \eta_\alpha(\mathbf{u}_T^1 - \mathbf{u}_T^2) \cdot \phi$ , (indeed  $\nabla \eta_\alpha(\mathbf{u}_T^1 - \mathbf{u}_T^2)$  is supposed to be in the same tangent space, it's true if  $\eta_\alpha(\mathbf{v}) = \sqrt{|\mathbf{v}|^2 + \alpha^2}$ ), thus

$$\int_{\Gamma_C} (\boldsymbol{\sigma}_T^1 + \tau \cdot \nabla \eta_\alpha(\mathbf{u}_T^1 - \mathbf{u}_T^2)) \cdot \phi \, ds = 0 \quad (6.64)$$

We conclude that

$$\boldsymbol{\sigma}_T^1 = -\tau \cdot \nabla \eta_\alpha(\mathbf{u}_T^1 - \mathbf{u}_T^2) = -\tau \frac{\mathbf{u}_T^1 - \mathbf{u}_T^2}{\sqrt{\|\mathbf{u}_T^1 - \mathbf{u}_T^2\|^2 + \alpha^2}} \text{ a.e on } \Gamma_C \quad (6.65)$$

In the same manner, we take  $\mathbf{v} = (\mathbf{v}^1, \mathbf{v}^2)$  such that  $\mathbf{v}^1 = \mathbf{u}^1$  and  $\mathbf{v}^2 = \mathbf{u}^2 \pm \epsilon \phi_T$ , where  $\epsilon \in [0, 1]$ , and we inject  $\mathbf{v}$  in (6.50). We obtain

$$\int_{\Gamma_C} \boldsymbol{\sigma}^2(\mathbf{u}^2) \mathbf{n}^2 \cdot (\pm \epsilon \phi_T) \, ds + \int_{\Gamma_C} \tau \cdot (\eta_\alpha(\mathbf{u}_T^1 - \mathbf{u}_T^2 \mp \epsilon \phi_T) - \eta_\alpha(\mathbf{u}_T^1 - \mathbf{u}_T^2)) \, ds \geq 0 \quad (6.66)$$

As before we conclude that

$$\boldsymbol{\sigma}_T^2 = \tau \cdot \nabla \eta_\alpha(\mathbf{u}_T^1 - \mathbf{u}_T^2) = -\boldsymbol{\sigma}_T^1 \text{ a.e on } \Gamma_C \quad (6.67)$$

□

## 6.2.2 Minimization formulation for the regularized problem

The variational inequality of the problem is recalled below.

Find  $\mathbf{u} \in \mathbf{K}$  such that

$$a(\mathbf{u}, \mathbf{v} - \mathbf{u}) + j_{\alpha, \tau}(\mathbf{v}) - j_{\alpha, \tau}(\mathbf{u}) \geq f(\mathbf{v} - \mathbf{u}) \quad \forall \mathbf{v} \in \mathbf{K} \quad (6.68)$$

As before, let  $\mathcal{E}_p$  denotes the total potential energy of the two bodies

$$\mathcal{E}_p(\mathbf{v}) := \frac{1}{2}a(\mathbf{v}, \mathbf{v}) - f(\mathbf{v}) \quad (6.69)$$

Consider the energy functional  $J_{\alpha, \tau}$  given by

$$J_{\alpha, \tau}(\mathbf{v}) := \mathcal{E}_p(\mathbf{v}) + j_{\alpha, \tau}(\mathbf{v}) \quad (6.70)$$

where as before, the functional is given by

$$j_{\alpha, \tau}(\mathbf{v}) = \int_{\Gamma_C} \tau \cdot \eta_\alpha(\mathbf{v}_T^1 - \mathbf{v}_T^2) ds \quad (6.71)$$

The functional  $j_{\alpha, \tau}$  is lower semicontinuous, and because  $\eta_\alpha$  is convex then  $j_{\alpha, \tau}$  is convex. Therefore by applying the theorem 6.1 above, by taking  $F = J_{\alpha, \tau}$ ,  $F_1 = \mathcal{E}_p$  and  $\Phi = j_{\alpha, \tau}$ , the frictional problem (6.68) is equivalent to the following minimization problem

Find  $\mathbf{u} \in \mathbf{K}$  such that

$$J_{\alpha, \tau}(\mathbf{u}) \leq J_{\alpha, \tau}(\mathbf{v}) \quad \forall \mathbf{v} \in \mathbf{K} \quad (6.72)$$

Otherwise the energy functional  $J_{\alpha, \tau}$  is convex, Gâteaux differentiable (or continuous) because  $\eta_\alpha$  is differentiable (or continuous), and coercive because  $\mathcal{E}_p$  is coercive and the functional  $j_{\alpha, \tau}$  is positive. We conclude that there exists a solution of the minimization problem (6.72), in addition this minimizer is unique because  $J_{\alpha, \tau}$  is strictly convex.

## 6.2.3 Error between Tresca's solution and regularized Tresca's solution

**Theorem 6.3.** *Let  $\mathbf{u} \in \mathbf{K}$  be the Tresca solution, in other words solution of*

$$a(\mathbf{u}, \mathbf{v} - \mathbf{u}) + j_\tau(\mathbf{v}) - j_\tau(\mathbf{u}) \geq f(\mathbf{v} - \mathbf{u}) \quad \forall \mathbf{v} \in \mathbf{K} \quad (6.73)$$

and let  $\mathbf{u}_\alpha \in \mathbf{K}$  be the regularized Tresca solution, otherwise speaking solution of

$$a(\mathbf{u}_\alpha, \mathbf{v} - \mathbf{u}_\alpha) + j_{\alpha, \tau}(\mathbf{v}) - j_{\alpha, \tau}(\mathbf{u}_\alpha) \geq f(\mathbf{v} - \mathbf{u}_\alpha) \quad \forall \mathbf{v} \in \mathbf{K} \quad (6.74)$$

then there exists a constant  $C \geq 0$  such that

$$\|\mathbf{u}_\alpha - \mathbf{u}\|_1 \leq C\sqrt{\alpha} \quad (6.75)$$

*Proof.* Replacing  $\mathbf{v}$  by  $\mathbf{u}_\alpha$  in the equation (6.73), and  $\mathbf{v}$  by  $\mathbf{u}$  in the equation (6.74), one obtains

$$\begin{cases} a(\mathbf{u}, \mathbf{u}_\alpha - \mathbf{u}) + j_\tau(\mathbf{u}_\alpha) - j_\tau(\mathbf{u}) \geq f(\mathbf{u}_\alpha - \mathbf{u}) \\ a(\mathbf{u}_\alpha, \mathbf{u} - \mathbf{u}_\alpha) + j_{\alpha, \tau}(\mathbf{u}) - j_{\alpha, \tau}(\mathbf{u}_\alpha) \geq f(\mathbf{u} - \mathbf{u}_\alpha) \end{cases} \quad (6.76)$$

or

$$\begin{cases} a(\mathbf{u}, \mathbf{u}_\alpha - \mathbf{u}) + j_\tau(\mathbf{u}_\alpha) - j_\tau(\mathbf{u}) \geq f(\mathbf{u}_\alpha - \mathbf{u}) \\ a(-\mathbf{u}_\alpha, \mathbf{u}_\alpha - \mathbf{u}) + j_{\alpha, \tau}(\mathbf{u}) - j_{\alpha, \tau}(\mathbf{u}_\alpha) \geq f(\mathbf{u} - \mathbf{u}_\alpha) \end{cases} \quad (6.77)$$

Adding these two equations, we obtain

$$a(\mathbf{u} - \mathbf{u}_\alpha, \mathbf{u}_\alpha - \mathbf{u}) + j_\tau(\mathbf{u}_\alpha) - j_{\alpha, \tau}(\mathbf{u}_\alpha) + j_{\alpha, \tau}(\mathbf{u}) - j_\tau(\mathbf{u}) \geq 0 \quad (6.78)$$

Thus

$$\begin{aligned} a(\mathbf{u}_\alpha - \mathbf{u}, \mathbf{u}_\alpha - \mathbf{u}) &\leq j_\tau(\mathbf{u}_\alpha) - j_{\alpha, \tau}(\mathbf{u}_\alpha) + j_{\alpha, \tau}(\mathbf{u}) - j_\tau(\mathbf{u}) \\ &\leq \int_{\Gamma_C} \tau \cdot |\eta_\alpha(\mathbf{u}_{\alpha, T}^1 - \mathbf{u}_{\alpha, T}^2) - |\mathbf{u}_{\alpha, T}^1 - \mathbf{u}_{\alpha, T}^2|| \, ds \\ &\quad + \int_{\Gamma_C} \tau \cdot |\eta_\alpha(\mathbf{u}_T^1 - \mathbf{u}_T^2) - |\mathbf{u}_T^1 - \mathbf{u}_T^2|| \, ds \\ &\leq 2\|\tau\|_{L^2(\Gamma_C)} \cdot \sqrt{\text{meas}(\Gamma_C)} \cdot \alpha \quad (\eta_\alpha \in \Xi_\alpha) \end{aligned} \quad (6.79)$$

Because  $a$  is elliptic then

$$\|\mathbf{u}_\alpha - \mathbf{u}\|_1 \leq C\sqrt{\alpha} \quad (6.80)$$

Note that the differentiability of  $\eta_\alpha$  is not needed.  $\square$

**Corollary 6.1.** *If  $\eta_\alpha(\mathbf{v}) = \sqrt{|\mathbf{v}|^2 + \alpha^2}$  then*

$$\|\mathbf{u}_\alpha - \mathbf{u}\|_1 \leq C\alpha^{1/2} \quad (6.81)$$

#### 6.2.4 Coulomb's criterion as a fixed point problem for the regularized problem

Given a regularized parameter  $\alpha > 0$ , consider the following application

$$T(\tau) = -\mu\sigma_N^1(\mathbf{u}_\tau) \quad (6.82)$$

where  $\sigma_N^1$  is the normal stress and  $\mathbf{u}_\tau$  the solution of the Tresca problem with the sliding limit  $\tau \geq 0 \in L^2(\Gamma_C)$ , otherwise speaking, solution of the following problem

Find  $\mathbf{u}_\tau \in \mathbf{K}$  such that

$$a(\mathbf{u}_\tau, \mathbf{v} - \mathbf{u}_\tau) + j_{\alpha,\tau}(\mathbf{v}) - j_{\alpha,\tau}(\mathbf{u}_\tau) \geq f(\mathbf{v} - \mathbf{u}_\tau) \quad \forall \mathbf{v} \in \mathbf{K} \quad (6.83)$$

or equivalently

Find  $\mathbf{u}_\tau \in \mathbf{K}$  such that

$$J_{\alpha,\tau}(\mathbf{u}_\tau) \leq J_{\alpha,\tau}(\mathbf{v}) \quad \forall \mathbf{v} \in \mathbf{K} \quad (6.84)$$

Let  $\tau^* = T(\tau^*) = -\mu\sigma_N^1(\mathbf{u}_{\tau^*})$  be the fixed point of the application  $T$  and let  $\mathbf{u} = \mathbf{u}_{\tau^*}$ , the corresponding displacement which is supposed to be sufficiently regular, therefore according to the theorem 6.2, the equations (6.34) and (6.35) are verified and the regularized Coulomb's criterion becomes

$$\begin{cases} \sigma_T^1 &= -\sigma_T^2 \\ \sigma_T^1 &= \mu\sigma_N^1(\mathbf{u}) \cdot \nabla \eta_\alpha(\mathbf{u}_T^1 - \mathbf{u}_T^2) \\ &= \mu\sigma_N^1(\mathbf{u}) \frac{(\mathbf{u}_T^1 - \mathbf{u}_T^2)}{\sqrt{|\mathbf{u}_T^1 - \mathbf{u}_T^2|^2 + \alpha^2}} \text{ if } \eta_\alpha(\mathbf{v}) = \sqrt{|\mathbf{v}|^2 + \alpha^2} \end{cases} \quad (6.85)$$

In the section 6.4 we prove for the discretized case, the existence and the uniqueness of a fixed point for the application  $T$  (where  $\sigma_N^1 \in H^{-1/2}(\Gamma_C)$ , the dual of  $H^{1/2}(\Gamma_C)$ ), in addition to the convergence of the fixed point algorithm to solve the frictional contact problem.

#### Remark 6.1

*As the non-smooth character of Coulomb's law is lost, when using regularization, then a phenomena like squeal is hard to be modeled [100].*

### 6.2.5 Quasi-static problem for the regularized one

Given the displacement solution  $\mathbf{u}_i = (\mathbf{u}_i^1, \mathbf{u}_i^2)$  of the previous step, then for each sliding limit  $\tau \geq 0 \in L^2(\Gamma_C)$  of the fixed point algorithm, the following problem is considered

Find  $\mathbf{u}_{\tau,i+1} \in \mathbf{K}$  such that

$$a(\mathbf{u}_{\tau,i+1}, \mathbf{v} - \mathbf{u}_{\tau,i+1}) + j_{\alpha,\tau}(\mathbf{v} - \mathbf{u}_i) - j_{\alpha,\tau}(\mathbf{u}_{\tau,i+1} - \mathbf{u}_i) \geq f(\mathbf{v} - \mathbf{u}_{\tau,i+1}) \quad \forall \mathbf{v} \in \mathbf{K} \quad (6.86)$$

or equivalently

Find  $\mathbf{u}_{\tau,i+1} \in \mathbf{K}$  such that

$$J_{\alpha,\tau}(\mathbf{u}_{\tau,i+1}) \leq J_{\alpha,\tau}(\mathbf{v}) \quad \forall \mathbf{v} \in \mathbf{K} \quad (6.87)$$

where  $j_{\alpha,\tau}(\mathbf{v})$  is replaced by  $j_{\alpha,\tau}(\mathbf{v} - \mathbf{u}_i)$  which is given by

$$j_{\alpha,\tau}(\mathbf{v} - \mathbf{u}_i) = \int_{\Gamma_C} \tau \cdot \eta_\alpha((\mathbf{v}_T^1 - \mathbf{u}_T^1) - (\mathbf{v}_T^2 - \mathbf{u}_T^2)) ds \quad (6.88)$$

As  $\mathbf{u}_T^1$  and  $\mathbf{u}_T^2$  are given, then using the same proof of the theorem 6.2, the two problems

(6.86) and (6.87) will generate the same equations (6.34) and (6.35) of the theorem 6.2, except the friction criterion (6.36) which will be slightly changed to

$$\begin{cases} \sigma_T^1 &= -\sigma_T^2 \\ \sigma_T^1 &= -\tau \cdot \nabla \eta_\alpha((\mathbf{u}_{T,\tau,i+1}^1 - \mathbf{u}_{T,i}^1) - (\mathbf{u}_{T,\tau,i+1}^2 - \mathbf{u}_{T,i}^2)) \\ &= -\tau \frac{(\mathbf{u}_{T,\tau,i+1}^1 - \mathbf{u}_{T,i}^1) - (\mathbf{u}_{T,\tau,i+1}^2 - \mathbf{u}_{T,i}^2)}{\sqrt{|(\mathbf{u}_{T,\tau,i+1}^1 - \mathbf{u}_{T,i}^1) - (\mathbf{u}_{T,\tau,i+1}^2 - \mathbf{u}_{T,i}^2)|^2 + \alpha^2}} \text{ if } \eta_\alpha(\mathbf{v}) = \sqrt{|\mathbf{v}|^2 + \alpha^2} \end{cases} \quad (6.89)$$

Let  $\mathbf{u}_{i+1}$  be the displacement corresponding to the fixed point of the application  $T$  already defined, the regularized Coulomb's criterion for the quasi-static problem becomes

$$\begin{cases} \sigma_T^1 &= -\sigma_T^2 \\ \sigma_T^1 &= \mu \sigma_N^1(\mathbf{u}_{i+1}) \cdot \nabla \eta_\alpha((\mathbf{u}_{T,i+1}^1 - \mathbf{u}_{T,i}^1) - (\mathbf{u}_{T,i+1}^2 - \mathbf{u}_{T,i}^2)) \\ &= \mu \sigma_N^1(\mathbf{u}_{i+1}) \frac{(\mathbf{u}_{T,i+1}^1 - \mathbf{u}_{T,i}^1) - (\mathbf{u}_{T,i+1}^2 - \mathbf{u}_{T,i}^2)}{\sqrt{|(\mathbf{u}_{T,i+1}^1 - \mathbf{u}_{T,i}^1) - (\mathbf{u}_{T,i+1}^2 - \mathbf{u}_{T,i}^2)|^2 + \alpha^2}} \text{ if } \eta_\alpha(\mathbf{v}) = \sqrt{|\mathbf{v}|^2 + \alpha^2} \end{cases} \quad (6.90)$$

### 6.3 Finite deformation

We consider here the Signorini's problem for simplicity, indeed the contact between more than one body can be treated in the same manner. As before a fixed point algorithm is used in order to write the frictional contact problem as a sequence of Tresca contact problems until convergence, here the regularization of the Tresca frictional problem is considered. In the following, and for the sake of convenience, our unknown will be the actual position  $\phi$  instead of the displacement  $\mathbf{u}$ , which is not very different because  $\phi = \mathbf{X} + \mathbf{u}$ .

In the following theorem,  $\Omega$  is the body domain in  $\mathbb{R}^3$  (also works for  $\mathbb{R}^2$ ). In addition, let the borders  $\Gamma_0, \Gamma_1, \Gamma_C$  be disjoint relatively to  $\partial\Omega$ , and  $\Gamma = \partial\Omega = \Gamma_0 \cup \Gamma_1 \cup \Gamma_C$ . The area of the border  $\Gamma_C$  is supposed to be strictly positive.

$\Gamma_0$  is the border where a displacement is imposed,  $\Gamma_1$  is the border where a surface traction is applied, finally  $\Gamma_C$  is the potential contact area, otherwise speaking if  $\phi(\Gamma_C)$  is  $\Gamma_C$  in the actual configuration, then the actual contact area is included in  $\phi(\Gamma_C)$ .

The body force  $\mathbf{f}$  is applied over the body  $\Omega$ , the surface traction  $\mathbf{g}$  is applied over  $\Gamma_1$ , and finally  $\phi_0$  is the imposed position on  $\Gamma_0$ .

The obstacle is described by the open set  $\mathcal{C} \subset \mathbb{R}^3$ , the strain energy function is denoted by  $\hat{W}$ , and the first Piola-Kirchhoff stress by  $\mathbf{P}$ . We have that  $\mathbf{P} = \frac{\partial \hat{W}}{\partial \mathbf{F}}$ , where  $\mathbf{F}$  is the deformation gradient tensor.

The admissible solutions set  $\Phi$  is defined by:

$$\Phi = \{\psi : \bar{\Omega} \rightarrow \mathbb{R}^3; \det(\nabla \psi) > 0 \text{ in } \bar{\Omega}; \psi = \phi_0 \text{ on } \Gamma_0 \text{ with } \psi(\Gamma_C) \subseteq \mathcal{C}^c\} \quad (6.91)$$

The condition  $\psi(\Gamma_C) \subseteq \mathcal{C}^c$  (the complement of  $\mathcal{C}$ ) describes the non-penetration of the first body into the obstacle.

The potential energy of the body is given by

$$\mathcal{E}_p(\psi) = \int_{\Omega} \hat{W}(\nabla\psi) dx - \int_{\Omega} \mathbf{f} \cdot \psi dx - \int_{\Gamma_1} \mathbf{g} \cdot \psi dS \quad (6.92)$$

We define the mapping  $T : \Phi \rightarrow \Phi$ , which for a given  $\zeta \in \Phi$ ,  $T(\zeta)$  is the solution of the following constrained minimization problem

$$\min_{\psi \in \Phi} \left( \mathcal{E}_p(\psi) + \int_{\zeta(\Gamma_C) \cap \partial\mathcal{C}} \tau \eta_{\alpha}(\mathbf{v}_T) ds \right) \quad (6.93)$$

where  $\mathbf{v}(\mathbf{x}) = \psi(\zeta^{-1}(\mathbf{x})) - \zeta^{-1}(\mathbf{x})$ ,  $\forall \mathbf{x} \in \zeta(\Gamma_C) \cap \partial\mathcal{C}$ . Moreover  $\tau(\mathbf{x}) = \tau_0(\zeta^{-1}(\mathbf{x}))$  where  $\tau_0 \in L^2(\Gamma_C) \geq 0$  is the sliding limit of the Tresca criterion and  $\eta_{\alpha} : \mathbb{R}^3 \rightarrow \mathbb{R}_+$  a regularization function belonging to  $\Xi_{\alpha}$ , defined before ( for example  $\eta_{\alpha}(x, y, z) = \sqrt{x^2 + y^2 + z^2 + \alpha^2}$  with  $\alpha > 0$ ). Finally  $\mathbf{v}_T$  is the tangential part of  $\mathbf{v}$ , and can be given by  $\mathbf{v}_T = \mathbf{v} - v_n \mathbf{n}$  with  $v_n$  its normal component and  $\mathbf{n}$  the normal vector at  $\zeta(\Gamma_C) \cap \partial\mathcal{C}$ .

In the following theorem, some elements of the proof, where the friction is not taken into account, are taken from [29].

**Theorem 6.4.** *Let  $\phi \in \Phi$  be the fixed point of the application  $T$  defined above, otherwise speaking  $\phi = T(\phi)$ , which means also that  $\phi$  is solution of*

$$\min_{\psi \in \Phi} \mathcal{E}(\psi) \quad (6.94)$$

where

$$\mathcal{E}(\psi) = \mathcal{E}_p(\psi) + \int_{\phi(\Gamma_C) \cap \partial\mathcal{C}} \tau \cdot \eta_{\alpha}(\mathbf{v}_T) ds \quad (6.95)$$

If  $\phi$  is smooth enough, then  $\phi$  satisfies formally the following properties, corresponding to the frictional contact between a body and an obstacle, with a regularized Tresca criterion.

$$\left\{ \begin{array}{l} -\operatorname{div} \mathbf{P} = \mathbf{f} \text{ in } \Omega \\ \phi = \phi_0 \text{ on } \Gamma_0 \\ \mathbf{P}\mathbf{N} = \mathbf{g} \text{ on } \Gamma_1 \\ \phi(\Gamma_C) \subseteq \mathcal{C}^c \\ \mathbf{P}\mathbf{N} = \mathbf{0} \text{ if } \mathbf{X} \in \Gamma_C \text{ and } \phi(\mathbf{X}) \in \bar{\mathcal{C}}^c \quad (\notin \mathcal{C} \cup \partial\mathcal{C}) \\ (\mathbf{P}\mathbf{N}) \cdot \mathbf{n} = \lambda_n \text{ if } \mathbf{X} \in \Gamma_C \text{ and } \mathbf{x} = \phi(\mathbf{X}) \in \partial\mathcal{C} \text{ where } \lambda_n \leq 0 \\ \boldsymbol{\sigma}_T = -\tau \nabla \eta_{\alpha}(\mathbf{u}_T) = -\tau \frac{\mathbf{u}_T}{\sqrt{|\mathbf{u}_T|^2 + \alpha^2}} \text{ on } \gamma_C = \phi(\Gamma_C) \cap \partial\mathcal{C} \text{ (if } \eta_{\alpha}(\mathbf{v}) = \sqrt{|\mathbf{v}|^2 + \alpha^2}) \end{array} \right. \quad (6.96)$$

where  $\boldsymbol{\sigma}_T, \mathbf{u}_T$  are respectively the tangential stress and displacement,  $\mathbf{N}$  and  $\mathbf{n}$  are respectively the unit outer normal vector on the initial and on the deformed surface of the body.  $\boldsymbol{\sigma}$  is the Cauchy stress tensor and  $\boldsymbol{\sigma}\mathbf{n}$  has the same direction of  $\mathbf{P}\mathbf{N}$ . Finally  $\nabla \eta_{\alpha}(\mathbf{u}_T)$  is supposed to

belong to the tangent plane (it is true if  $\eta_\alpha(\mathbf{v}) = \sqrt{|\mathbf{v}|^2 + \alpha^2}$ ).

*Proof.* The function  $\phi$  is a solution of the minimization problem (6.94), therefore

$$\mathcal{E}(\phi) \leq \mathcal{E}(\psi) \quad \forall \psi \in \Phi \quad (6.97)$$

In the following we need the Green formula, which for a smooth enough tensor  $\mathbf{T}$  states

$$\int_{\Omega} \mathbf{T} : \nabla \boldsymbol{\theta} \, dx = - \int_{\Omega} \operatorname{div}(\mathbf{T}) \cdot \boldsymbol{\theta} \, dx + \int_{\Gamma} \mathbf{T} \mathbf{N} \cdot \boldsymbol{\theta} \, dS \quad \forall \boldsymbol{\theta} \quad (6.98)$$

Consider  $\boldsymbol{\theta}$  a sufficient smooth function that vanishes in a neighborhood of  $\Gamma_0 \cup \Gamma_C$ . There exists  $\epsilon_0 = \epsilon(\boldsymbol{\theta}) > 0$  such that  $\phi_\epsilon = \phi + \epsilon \boldsymbol{\theta} \in \Phi \quad \forall |\epsilon| \leq \epsilon_0$ .

$$\mathcal{E}(\phi_\epsilon) - \mathcal{E}(\phi) \geq 0 \quad (6.99)$$

$$\begin{aligned} \mathcal{E}(\phi_\epsilon) - \mathcal{E}(\phi) &= \mathcal{E}(\phi + \epsilon \boldsymbol{\theta}) - \mathcal{E}(\phi) \\ &= \int_{\Omega} \left( \hat{W}(\nabla \phi + \epsilon \nabla \boldsymbol{\theta}) - \hat{W}(\nabla \phi) \right) dx - \epsilon \left( \int_{\Omega} \mathbf{f} \cdot \boldsymbol{\theta} \, dx + \int_{\Gamma_1} \mathbf{g} \cdot \boldsymbol{\theta} \, dS \right) \end{aligned} \quad (6.100)$$

Otherwise we have:

$$\begin{aligned} \hat{W}(\nabla \phi + \epsilon \nabla \boldsymbol{\theta}) - \hat{W}(\nabla \phi) &= \epsilon \frac{\partial \hat{W}}{\partial \mathbf{F}} : \nabla \boldsymbol{\theta} + o(\epsilon) \\ &= \epsilon \mathbf{P} : \nabla \boldsymbol{\theta} + o(\epsilon) \end{aligned} \quad (6.101)$$

Using the Green formula in equation (6.98) and the fact that  $\boldsymbol{\theta}$  vanishes in a neighborhood of  $\Gamma_0 \cup \Gamma_C$ , we obtain :

$$\begin{aligned} \int_{\Omega} \left( \hat{W}(\nabla \phi + \epsilon \nabla \boldsymbol{\theta}) - \hat{W}(\nabla \phi) \right) dx &= \epsilon \int_{\Omega} \mathbf{P} : \nabla \boldsymbol{\theta} \, dx + o(\epsilon) \\ &= -\epsilon \int_{\Omega} \operatorname{div}(\mathbf{P}) \cdot \boldsymbol{\theta} \, dx + \epsilon \int_{\Gamma_1} \mathbf{P} \mathbf{N} \cdot \boldsymbol{\theta} \, dS + o(\epsilon) \end{aligned} \quad (6.102)$$

Thus

$$\begin{aligned} \mathcal{E}(\phi_\epsilon) - \mathcal{E}(\phi) &= -\epsilon \int_{\Omega} \operatorname{div}(\mathbf{P}) \cdot \boldsymbol{\theta} \, dx + \epsilon \int_{\Gamma_1} \mathbf{P} \mathbf{N} \cdot \boldsymbol{\theta} \, dS \\ &\quad - \epsilon \left( \int_{\Omega} \mathbf{f} \cdot \boldsymbol{\theta} \, dx + \int_{\Gamma_1} \mathbf{g} \cdot \boldsymbol{\theta} \, dS \right) + o(\epsilon) \\ &= \epsilon \left\{ \int_{\Omega} (-\operatorname{div}(\mathbf{P}) - \mathbf{f}) \cdot \boldsymbol{\theta} \, dx + \int_{\Gamma_1} (\mathbf{P} \mathbf{N} - \mathbf{g}) \cdot \boldsymbol{\theta} \, dS + \frac{o(\epsilon)}{\epsilon} \right\} \geq 0 \end{aligned} \quad (6.103)$$

Taking  $\epsilon > 0$  and taking the limit  $\epsilon \rightarrow 0^+$  we have:

$$\int_{\Omega} (-\operatorname{div}(\mathbf{P}) - \mathbf{f}) \cdot \boldsymbol{\theta} \, dx + \int_{\Gamma_1} (\mathbf{P} \mathbf{N} - \mathbf{g}) \cdot \boldsymbol{\theta} \, dS \geq 0 \quad (6.104)$$

Let  $\mathbf{X} \in \Omega$  and  $B(\mathbf{X}, r) \subset \Omega$  the open ball of center  $\mathbf{X}$  with a small radius  $r > 0$  (see Figure 6.2). Consider  $\theta$  a sufficient smooth function with support in  $B(\mathbf{X}, r)$ , thus we deduce that  $-\operatorname{div}(\mathbf{P}) = \mathbf{f}$  in  $B(\mathbf{X}, r)$ , and then it's true in  $\Omega$ .

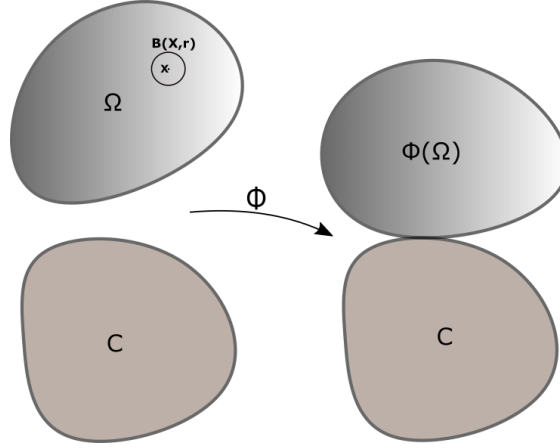


Figure 6.2 – The initial and actual configurations

The equation (6.104) can always be used, thus using the fact that  $-\operatorname{div}(\mathbf{P}) = \mathbf{f}$  in  $\Omega$ , we obtain:

$$\int_{\Gamma_1} (\mathbf{PN} - \mathbf{g}) \cdot \theta \, dS \geq 0 \tag{6.105}$$

We deduce that  $\mathbf{PN} = \mathbf{g}$  on  $\Gamma_1$ .

Let  $\mathbf{X} \in \Gamma_C$  such that  $\phi(\mathbf{X}) \in \bar{\mathcal{C}}^c$  (see Figure 6.3), consider any smooth function  $\theta : \bar{\Omega} \rightarrow \mathbb{R}^3$  with a support in  $B(\mathbf{X}, r) \cap \bar{\Omega}$  where  $r > 0$  and small, there exists a  $\epsilon_2(\theta) > 0$  such that  $\phi_\epsilon = \phi + \epsilon\theta \in \Phi \quad \forall |\epsilon| \leq \epsilon_2$ . As before,  $\mathcal{E}(\phi_\epsilon) - \mathcal{E}(\phi) \geq 0$ , thus using Green's formula and the equations of equilibrium we obtain:

$$\epsilon \left\{ \int_{\Gamma_C} \mathbf{PN} \cdot \theta \, dS + \frac{o(\epsilon)}{\epsilon} \right\} \geq 0 \tag{6.106}$$

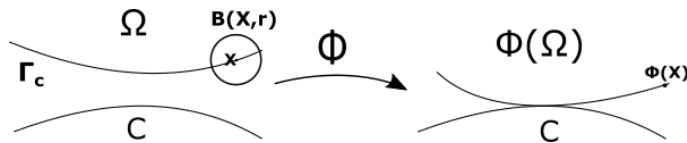


Figure 6.3 – The case where the stress is zero for the point  $\mathbf{X}$

We deduce that  $\mathbf{PN} = \mathbf{0}$  for  $\mathbf{X} \in \Gamma_C$  such that  $\phi(\mathbf{X}) \in \bar{\mathcal{C}}^c$ .

Let  $\gamma_C = \phi(\Gamma_C) \cap \partial\mathcal{C}$ . We will prove next that the coefficient  $\lambda_n$  in the equation (6.96) is negative. We consider  $\mathbf{Y} \in \Gamma_C$  such that  $\mathbf{y} = \phi(\mathbf{Y}) \in \gamma_C$  (see Figure 6.4). Consider any positive

smooth function  $\theta : \bar{\Omega} \rightarrow \mathbb{R}_+$  with support in  $B(\mathbf{Y}, r)$ , then  $\exists \epsilon_4(\theta) > 0$  such that:

$$\phi_\epsilon = \phi - \epsilon \theta \mathbf{n} \in \Phi \quad \forall 0 \leq \epsilon \leq \epsilon_4 \quad (6.107)$$

Thus by the same procedure we obtain:

$$\epsilon \left\{ \int_{\Gamma_C} -\mathbf{PN} \cdot \mathbf{n} \theta dS + \frac{o(\epsilon)}{\epsilon} + \frac{j(\mathbf{u}_\epsilon) - j(\mathbf{u})}{\epsilon} \right\} \geq 0 \quad (6.108)$$

where  $\mathbf{u}_\epsilon, \mathbf{u}$  are respectively the displacement fields of  $\phi_\epsilon$  and  $\phi$ ,  $j$  is defined by

$$j(\mathbf{v}) = \int_{\gamma_C} \tau \cdot \eta_\alpha(\mathbf{v}_T) ds \quad (6.109)$$

As the normal direction is considered then  $j(\mathbf{u}_\epsilon) - j(\mathbf{u}) = 0$ . If  $\epsilon \rightarrow 0^+$  then we have:

$$\int_{\Gamma_C} \mathbf{PN} \cdot \mathbf{n} \theta dS \leq 0 \quad (6.110)$$

Thus  $\lambda_n = \mathbf{PN} \cdot \mathbf{n} \leq 0$  at  $\mathbf{X} \in \Gamma_C$  where  $\phi(\mathbf{X}) \in \gamma_C$ .

We still have the last equations of the problem (6.96) to demonstrate. We also consider  $\mathbf{Y} \in \Gamma_C$  such that  $\mathbf{y} = \phi(\mathbf{Y}) \in \gamma_C$ , supposing that the boundaries of  $\phi(\Omega)$ ,  $\mathcal{C}$  are smooth enough, then we can assume that  $\phi(\Gamma_C)$  and  $\partial\mathcal{C}$  have the same tangent space at the point  $\mathbf{y} = \phi(\mathbf{Y})$ . Let  $V(\mathbf{Y})$  be a neighborhood of  $\mathbf{y}$  and  $\mathbf{t}_1, \mathbf{t}_2, \mathbf{n}$  a 3 smooth fields, such that  $\mathbf{t}_1, \mathbf{t}_2$  span the tangent space at  $V \cap \gamma_C$  and  $\|\mathbf{t}_1\| = \|\mathbf{t}_2\| = 1$ ,  $\mathbf{n}$  is the outer normal vector on the body. Consider the ball  $B(\mathbf{Y}, r)$  such that  $B(\mathbf{Y}, r) \cap \Gamma \subset \Gamma_C$  and  $\phi(B(\mathbf{Y}, r)) \subset V$  (see Figure 6.4), therefore given two smooth functions  $\theta_1, \theta_2 : \bar{\Omega} \rightarrow \mathbb{R}$  with support in  $B(\mathbf{Y}, r)$ , there exist  $\epsilon_3(\theta_1, \theta_2) > 0$  and two functions  $\lambda_1^\epsilon, \lambda_2^\epsilon : \bar{\Omega} \rightarrow \mathbb{R}$  with support in  $B(\mathbf{Y}, r)$  such that:

For  $\beta = 1, 2$

$$\begin{cases} \phi^\epsilon = \phi + \epsilon(\theta_\beta \mathbf{t}_\beta + \lambda_\beta^\epsilon \mathbf{n}) \in \Phi \quad \forall |\epsilon| \leq \epsilon_3 \\ |\lambda_\beta^\epsilon| = o(\epsilon) \end{cases} \quad (6.111)$$

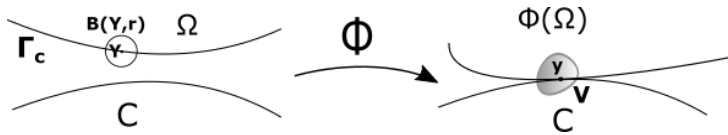


Figure 6.4 – The point  $\mathbf{y} = \phi(\mathbf{Y})$  and its neighborhood

Taking  $\mathcal{E}(\phi^\epsilon) - \mathcal{E}(\phi) \geq 0$  and repeating the same procedure as before, we obtain:

$$\epsilon \left\{ \int_{\Gamma_C} \mathbf{PN} \cdot \theta_\beta \mathbf{t}_\beta dS + \frac{1}{\epsilon} (j(\mathbf{u}_\epsilon) - j(\mathbf{u})) + o(\epsilon) + \frac{o(\epsilon)}{\epsilon} \right\} \geq 0 \quad (6.112)$$

Now the stress tensor  $\mathbf{P}$  is transformed into the Cauchy one  $\boldsymbol{\sigma}$ , which acts on the actual configuration. We can use also the fact that  $\mathbf{PN} dS = \boldsymbol{\sigma} n ds$ , where  $dS$  and  $ds$  are respectively the area

measures in the initial and actual configuration. Therefore

$$\epsilon \left\{ \int_{\gamma_C} \boldsymbol{\sigma} \mathbf{n} \cdot \theta_\beta \mathbf{t}_\beta \, ds + \int_{\gamma_C} \tau \cdot \frac{1}{\epsilon} (\eta_\alpha(\mathbf{u}_T + \epsilon \theta_\beta \mathbf{t}_\beta + \epsilon \mathbf{o}(\epsilon)) - \eta_\alpha(\mathbf{u}_T)) \, ds + o(\epsilon) + \frac{o(\epsilon)}{\epsilon} \right\} \geq 0 \quad (6.113)$$

Using Taylor's theorem we obtain

$$\int_{\gamma_C} \boldsymbol{\sigma} \mathbf{n} \cdot \theta_\beta \mathbf{t}_\beta \, ds + \int_{\gamma_C} \tau \cdot \nabla \eta_\alpha(\mathbf{u}_T) \cdot (\theta_\beta \mathbf{t}_\beta) \, ds + o(\epsilon) + \frac{o(\epsilon)}{\epsilon} \geq 0 \quad (6.114)$$

By taking  $\epsilon \rightarrow 0$  we obtain that

$$\int_{\gamma_C} \boldsymbol{\sigma} \mathbf{n} \cdot \theta_\beta \mathbf{t}_\beta \, ds + \int_{\gamma_C} \tau \cdot \nabla \eta_\alpha(\mathbf{u}_T) \cdot (\theta_\beta \mathbf{t}_\beta) \, ds \geq 0 \quad (6.115)$$

which is equivalent to

$$\int_{\gamma_C} \boldsymbol{\sigma}_T \cdot \theta_\beta \mathbf{t}_\beta \, ds + \int_{\gamma_C} \tau \cdot \nabla \eta_\alpha(\mathbf{u}_T) \cdot (\theta_\beta \mathbf{t}_\beta) \, ds \geq 0 \quad (6.116)$$

and thus we have

$$\int_{\gamma_C} \boldsymbol{\sigma}_T \cdot \theta_\beta \mathbf{t}_\beta \, ds + \int_{\gamma_C} \tau \cdot \nabla \eta_\alpha(\mathbf{u}_T) \cdot (\theta_\beta \mathbf{t}_\beta) \, ds = 0 \quad (6.117)$$

We conclude as before that for  $\beta = 1, 2$  we have

$$\boldsymbol{\sigma}_T \cdot \mathbf{t}_\beta = -\tau \nabla \eta_\alpha(\mathbf{u}_T) \cdot \mathbf{t}_\beta \quad (6.118)$$

$$= -\tau \frac{\mathbf{u}_T}{\sqrt{|\mathbf{u}_T|^2 + \alpha^2}} \cdot \mathbf{t}_\beta \text{ if } \eta_\alpha(\mathbf{v}) = \sqrt{|\mathbf{v}|^2 + \alpha^2} \quad (6.119)$$

$\nabla \eta_\alpha(\mathbf{u}_T)$  is supposed to belong to the tangent plane (it's true if  $\eta_\alpha(\mathbf{v}) = \sqrt{|\mathbf{v}|^2 + \alpha^2}$ ). Therefore for any tangential vector  $\mathbf{t}$  we have

$$(\boldsymbol{\sigma}_T + \tau \nabla \eta_\alpha(\mathbf{u}_T)) \cdot \mathbf{t} = 0 \quad (6.120)$$

We deduce then that  $\boldsymbol{\sigma}_T = -\tau \nabla \eta_\alpha(\mathbf{u}_T) = -\tau \frac{\mathbf{u}_T}{\sqrt{|\mathbf{u}_T|^2 + \alpha^2}}$ .  $\square$

### Remark 6.2

From an algorithmic point of view, we remark that the problem (6.96) can be solved as a fixed point algorithm. Thus at each step  $k$

$$\boldsymbol{\phi}_{k+1} = T(\boldsymbol{\phi}_k) \quad (6.121)$$

**Remark 6.3**

The quasi-static study, as in the linear case, is very similar to the static one, when we discretize the velocity. Indeed we replace  $\mathbf{v}_T$  by  $\mathbf{v}_T - \mathbf{u}_{T,i}$  in the equation (6.95), where  $\mathbf{u}_i$  denotes the solution of the previous state. In addition  $\mathbf{u}_T$  is replaced by  $\mathbf{u}_T - \mathbf{u}_{T,i}$  in the equation (6.96).

## 6.4 Fixed point algorithm convergence for the frictional regularized discretized problem

In the paper [81], the discretized frictional Signorini's problem, using  $P_1$  finite elements was written in term of a fixed point algorithm, and it was proven that there exist a solution for this latter and this algorithm converges for small friction coefficient. In [58], a mixed finite element method was considered, and the friction coefficient threshold for the uniqueness of the solution, depends on the mesh size and on the regularization parameter  $\alpha$ . However we will follow the most part of the proof of [81] with several modifications, in order to treat our regularized problem also for the Signorini's case. Like [81], the friction coefficient threshold for the uniqueness of the solution depends only on the mesh size.

First consider the following finite element spaces for the body  $\Omega_h \subset \mathbb{R}^d$ , where  $d = 2, 3$

$$\begin{cases} X_h &= \{v \in C^0(\bar{\Omega}_h) \mid v|_{T_i} \in P_1, \forall T_i \text{ triangle of } \Omega_h\} \\ \mathbf{V}_h &= \{\mathbf{v} = (v_1, v_2) \in (X_h)^d \mid \mathbf{v} = 0 \text{ on } \Gamma_0\} \\ \mathbf{K}_h &= \{\mathbf{v} \in \mathbf{V}_h \mid v_n = \mathbf{v} \cdot \mathbf{n} \leq 0 \text{ on } \Gamma_C\} \\ \hat{X}_h &= \text{the trace space of } X_h \text{ on } \Gamma_C \\ \hat{\mathbf{V}}_h &= \text{the trace space of } \mathbf{V}_h \text{ on } \Gamma_C \end{cases}$$

where as before  $\Gamma_C$  denotes the contact potential area,  $\mathbf{V}_h$  the admissible set and  $\mathbf{K}_h$  the set describing the non-penetration between the body and the obstacle with  $\mathbf{n}$  the outward unit normal vector on  $\Gamma_C$ .

Let  $\{\hat{w}_i \in \hat{X}_h \mid i = 1, \dots, n_C\}$  be a basis of  $\hat{X}_h$ , otherwise speaking each vector of this basis is the non-zero trace of a vector of the basis of  $X_h$  on  $\Gamma_C$ . The linear application  $R : \hat{\mathbf{V}}_h \rightarrow \mathbf{V}_h$  is defined such that, it associates to  $\hat{\mathbf{v}} \in \hat{\mathbf{V}}_h$ , a unique vector  $\mathbf{v} = R\hat{\mathbf{v}} \in \mathbf{V}_h$  such that this latter is equal to zero at all nodes outside  $\Gamma_C$ .

Let  $\Pi_h$  denotes the restriction to  $\Gamma_C$  of the interpolation operator associated with  $X_h$ ,  $\Pi_h$  has the following property (see [81])

$$|\Pi_h(|\mathbf{v}^h|)|_{L^2(\Gamma_C)} \leq c(h)|\mathbf{v}^h|_{L^2(\Gamma_C)} \quad \forall \mathbf{v}^h \in \hat{\mathbf{V}}_h \quad (6.122)$$

where  $c(h)$  a constant depending on  $h$ . In addition  $\Pi_h$  has the following useful properties

**Lemma 6.2.** *Let  $\phi, \phi^1, \phi^2 \in L^2(\Gamma_C)$ , we have*

$$\begin{cases} \Pi_h(\phi) \geq 0 & \text{if } \phi \geq 0 \\ \Pi_h(\phi^1) \leq \Pi_h(\phi^2) & \text{if } \phi^1 \leq \phi^2 \\ |\Pi_h(\phi)| \leq \Pi_h(|\phi|) \end{cases} \quad (6.123)$$

*Proof.* First of all  $\Pi_h(\phi)$  is given by

$$\Pi_h(\phi) = \sum_i \phi_i \hat{w}_i \quad (6.124)$$

The shape functions  $\hat{w}_i \geq 0$  because we use  $P_1$  finite elements, thus if  $\phi \geq 0$ , then  $\Pi_h(\phi) \geq 0$ . In addition if  $\phi^1 \leq \phi^2$ , then  $\Pi_h(\phi^2 - \phi^1) \geq 0$  and we obtain the second equation of (6.123). Finally

$$|\Pi_h(\phi)| \leq \sum_i |\phi_i| \hat{w}_i = \Pi_h(|\phi|) \quad (6.125)$$

□

According to [81], one can defines two applications

$$\begin{cases} \langle \boldsymbol{\sigma}(\mathbf{v}), \hat{\mathbf{v}} \rangle = a(\mathbf{v}, R\hat{\mathbf{v}}) - f(R\hat{\mathbf{v}}) & \forall \mathbf{v} \in \mathbf{V}_h \text{ and } \forall \hat{\mathbf{v}} \in \hat{\mathbf{V}}_h \\ \langle \sigma_n(\mathbf{v}), \hat{w} \rangle = \langle \boldsymbol{\sigma}(\mathbf{v}), \hat{w}\mathbf{n} \rangle & \forall \mathbf{v} \in \mathbf{V}_h \text{ and } \forall \hat{w} \in \hat{X}_h \end{cases} \quad (6.126)$$

The first one describes the stress vector on  $\Gamma_C$  and the second one describes the normal stress on  $\Gamma_C$  corresponding to a displacement test vector  $\mathbf{v}$ .

#### Remark 6.4

*If  $\mathbf{v}$  is sufficiently regular (let's say  $\mathbf{v} \in H^2$ ), then the Green formula can be used as in theorem 6.2, to obtain*

$$\langle \sigma_n(\mathbf{v}), \hat{w} \rangle = \int_{\Gamma_C} \sigma_n(\mathbf{v}) \hat{w} \, ds \quad (6.127)$$

In the following, the regularization function  $\eta_\alpha$  approximating the module of a vector, belongs to the set  $\Xi_\alpha$ , defined before.

Our regularized frictional problem, approximating Coulomb's criterion is given by

Find  $\mathbf{u}^h \in \mathbf{K}_h$  such that

$$a(\mathbf{u}^h, \mathbf{v} - \mathbf{u}^h) - \langle \mu \sigma_n(\mathbf{u}^h), \Pi_h(\eta_\alpha(\mathbf{v}_T) - \eta_\alpha(\mathbf{u}^h_T)) \rangle \geq f(\mathbf{v} - \mathbf{u}^h) \quad \forall \mathbf{v} \in \mathbf{K}_h \quad (6.128)$$

where  $\mu$  is the friction coefficient.

Let  $H$  denotes the set of all positive linear applications on  $\hat{X}_h$ , otherwise speaking, the set of

applications  $\tau$  such that

$$\langle \tau, \hat{w} \rangle \geq 0 \quad \forall \hat{w} \in \hat{X}_h \geq 0 \quad (6.129)$$

For  $\tau \in H$ , the application  $T$  is defined by

$$\langle T(\tau), \hat{w} \rangle = - \langle \mu \sigma_n(\mathbf{u}_\tau^h), \hat{w} \rangle \quad (6.130)$$

where  $\mathbf{u}_\tau^h$  is the solution of the frictional regularized problem seen before with the sliding limit  $\tau$ , otherwise speaking  $\mathbf{u}_\tau^h$  is the solution of the following problem

Find  $\mathbf{u}_\tau^h \in \mathbf{K}_h$  such that

$$a(\mathbf{u}_\tau^h, \mathbf{v} - \mathbf{u}_\tau^h) + \langle \tau, \Pi_h(\eta_\alpha(\mathbf{v}_T) - \eta_\alpha(\mathbf{u}_\tau^h, T)) \rangle \geq f(\mathbf{v} - \mathbf{u}_\tau^h) \quad \forall \mathbf{v} \in \mathbf{K}_h \quad (6.131)$$

#### Remark 6.5

The problem (6.131) has a unique solution, indeed consider the following energy

$$E(\mathbf{v}) := \frac{1}{2} a(\mathbf{v}, \mathbf{v}) - f(\mathbf{v}) + \langle \tau, \Pi_h(\eta_\alpha(\mathbf{v}_T)) \rangle \quad (6.132)$$

The functional  $\mathbf{v} \rightarrow \langle \tau, \Pi_h(\eta_\alpha(\mathbf{v}_T)) \rangle$  is positive, convex and continuous, therefore the problem (6.131) is equivalent to the minimization of  $E$  over the closed and convex set  $\mathbf{K}_h$ , which assure the existence and the uniqueness of the solution. We can prove the continuity by proving that the mapping:  $\mathbf{v} \rightarrow \Pi_h(\eta_\alpha(\mathbf{v}_T))$  is continuous, and because  $\tau$  is a linear mapping on a finite dimensional vector space then it is continuous. Noting  $|\cdot|_1$  the  $\mathbf{H}^1$  norm, let's take a sequence  $\mathbf{v}^i \rightarrow \mathbf{u}$ , then we have the following inequality (see after in the equation (6.146) for more details)

$$|\Pi_h(\eta_\alpha(\mathbf{v}_T^i)) - \Pi_h(\eta_\alpha(\mathbf{u}_T))|_{H^{1/2}(\Gamma_C)} = |\Pi_h(\eta_\alpha(\mathbf{v}_T^i) - \eta_\alpha(\mathbf{u}_T))|_{H^{1/2}(\Gamma_C)} \leq c \cdot |\mathbf{v}^i - \mathbf{u}|_{L^2(\Gamma_C)} \quad (6.133)$$

By the trace theorem

$$|\Pi_h(\eta_\alpha(\mathbf{v}_T^i)) - \Pi_h(\eta_\alpha(\mathbf{u}_T))|_{H^{1/2}(\Gamma_C)} \leq C \cdot |\mathbf{v}^i - \mathbf{u}|_1 \quad (6.134)$$

and therefore

$$\Pi_h(\eta_\alpha(\mathbf{v}_T^i)) \rightarrow \Pi_h(\eta_\alpha(\mathbf{u}_T)) \quad (6.135)$$

If  $T(\tau) \in H, \forall \tau \in H$ , then we can deduce that the frictional problem (6.128) is equivalent to

Find a fixed point of the application  $T$

$$T(\tau) = \tau \quad (6.136)$$

So we want to prove that  $T(\tau) \in H$ . Let  $\hat{w} \geq 0 \in \hat{X}_h$ , using the definition 6.126 one obtains

$$\langle \sigma_n(\mathbf{u}_\tau^h), \hat{w} \rangle = a(\mathbf{u}_\tau^h, R(\hat{w}\mathbf{n})) - f(R(\hat{w}\mathbf{n})) \quad \forall \hat{w} \in \hat{X}_h \quad (6.137)$$

where  $R$  is a linear application previously defined. As  $\hat{w} \geq 0$  then  $\mathbf{v} = \mathbf{u}_\tau^h - R(\hat{w}\mathbf{n}) \in \mathbf{K}_h$ , so we can inject it in the variational inequality (6.131) to obtain

$$\langle \sigma_n(\mathbf{u}_\tau^h), \hat{w} \rangle = a(\mathbf{u}_\tau^h, R(\hat{w}\mathbf{n})) - f(R(\hat{w}\mathbf{n})) \leq 0 \quad (6.138)$$

Therefore  $\langle T(\tau), \hat{w} \rangle \geq 0$  and  $T(\tau) \in H$ .

In the following we will present some results in order to prove that the application  $T$  has a fixed point, which implies the existence of a solution of the problem (6.128). In addition it will be shown that for a small friction coefficient  $\mu$ , the application  $T$  is a contraction which implies a unique fixed point of  $T$ , and the uniqueness of the solution can be proven. Finally the fixed point algorithm can be easily given in order to solve the problem (6.128) as a sequence of the problem (6.131).

**Lemma 6.3.**

$$|T(\tau_1) - T(\tau_2)|_* \leq \mu C(h) |\tau_1 - \tau_2|_* \quad \forall \tau_1, \tau_2 \in H \quad (6.139)$$

where  $C(h)$  a constant which depends on the mesh size, and the dual norm  $|\cdot|_*$  is defined as follows

$$|\tau|_* = \sup_{\phi \in \hat{X}_h} \frac{|\langle \tau, \phi \rangle|}{|\phi|_{H^{1/2}(\Gamma_C)}} \quad (6.140)$$

*Proof.* Let  $\tau_1, \tau_2 \in H$ , and  $\mathbf{u}_1, \mathbf{u}_2$  respectively the solutions of the equation (6.131) for  $\tau = \tau_1$  and  $\tau = \tau_2$ . Taking  $\mathbf{v} = \mathbf{u}_2$  in the equation (6.131) for  $\tau = \tau_1$  and  $\mathbf{v} = \mathbf{u}_1$  in the equation (6.131) for  $\tau = \tau_2$ , one obtains

$$\begin{cases} a(\mathbf{u}_1, \mathbf{u}_2 - \mathbf{u}_1) + \langle \tau_1, \Pi_h(\eta_\alpha(\mathbf{u}_{2T}) - \eta_\alpha(\mathbf{u}_{1T})) \rangle \geq f(\mathbf{u}_2 - \mathbf{u}_1) \\ a(\mathbf{u}_2, \mathbf{u}_1 - \mathbf{u}_2) + \langle \tau_2, \Pi_h(\eta_\alpha(\mathbf{u}_{1T}) - \eta_\alpha(\mathbf{u}_{2T})) \rangle \geq f(\mathbf{u}_1 - \mathbf{u}_2) \end{cases} \quad (6.141)$$

equivalently

$$\begin{cases} a(\mathbf{u}_1, \mathbf{u}_2 - \mathbf{u}_1) + \langle \tau_1, \Pi_h(\eta_\alpha(\mathbf{u}_{2T}) - \eta_\alpha(\mathbf{u}_{1T})) \rangle \geq f(\mathbf{u}_2 - \mathbf{u}_1) \\ a(-\mathbf{u}_2, \mathbf{u}_2 - \mathbf{u}_1) + \langle \tau_2, \Pi_h(\eta_\alpha(\mathbf{u}_{1T}) - \eta_\alpha(\mathbf{u}_{2T})) \rangle \geq f(\mathbf{u}_1 - \mathbf{u}_2) \end{cases} \quad (6.142)$$

Adding these two equations, one obtains

$$a(\mathbf{u}_1 - \mathbf{u}_2, \mathbf{u}_2 - \mathbf{u}_1) + \langle \tau_1 - \tau_2, \Pi_h(\eta_\alpha(\mathbf{u}_{2T}) - \eta_\alpha(\mathbf{u}_{1T})) \rangle \geq 0 \quad (6.143)$$

Thus

$$a(\mathbf{u}_2 - \mathbf{u}_1, \mathbf{u}_2 - \mathbf{u}_1) \leq \langle \tau_1 - \tau_2, \Pi_h(\eta_\alpha(\mathbf{u}_{2T}) - \eta_\alpha(\mathbf{u}_{1T})) \rangle \quad (6.144)$$

Hence

$$\begin{aligned} a(\mathbf{u}_2 - \mathbf{u}_1, \mathbf{u}_2 - \mathbf{u}_1) &\leq |\tau_1 - \tau_2|_* |\Pi_h(\eta_\alpha(\mathbf{u}_{2T}) - \eta_\alpha(\mathbf{u}_{1T}))|_{H^{1/2}(\Gamma_C)} \\ &\leq C |\tau_1 - \tau_2|_* |\Pi_h(\eta_\alpha(\mathbf{u}_{2T}) - \eta_\alpha(\mathbf{u}_{1T}))|_{L^2(\Gamma_C)} \end{aligned} \quad (6.145)$$

The last inequality is due to the equivalence between the norms  $|\cdot|_{L^2}$  and  $|\cdot|_{H^{1/2}}$  on a finite dimensional space.

Using the fact  $\eta_\alpha \in \Xi_\alpha$  (see the definition 6.1) and the properties of  $\Pi_h$ , one obtains

$$\begin{aligned}
 a(\mathbf{u}_2 - \mathbf{u}_1, \mathbf{u}_2 - \mathbf{u}_1) &\leq C|\tau_1 - \tau_2|_* |\Pi_h(\eta_\alpha(\mathbf{u}_{2T}) - \eta_\alpha(\mathbf{u}_{1T}))|_{L^2(\Gamma_C)} \\
 &\leq C|\tau_1 - \tau_2|_* |\Pi_h(|\eta_\alpha(\mathbf{u}_{2T}) - \eta_\alpha(\mathbf{u}_{1T})|)|_{L^2(\Gamma_C)} \\
 &\leq C|\tau_1 - \tau_2|_* |\Pi_h(|\mathbf{u}_{2T}| - |\mathbf{u}_{1T}|)|_{L^2(\Gamma_C)} \\
 &\leq C|\tau_1 - \tau_2|_* |\Pi_h(|\mathbf{u}_{2T} - \mathbf{u}_{1T}|)|_{L^2(\Gamma_C)} \\
 &\leq C|\tau_1 - \tau_2|_* |\Pi_h(|\mathbf{u}_2 - \mathbf{u}_1|)|_{L^2(\Gamma_C)} \\
 &\leq c|\tau_1 - \tau_2|_* |\mathbf{u}_2 - \mathbf{u}_1|_{L^2(\Gamma_C)}
 \end{aligned} \tag{6.146}$$

Using the fact that  $a$  is elliptic, the above equation becomes

$$|\mathbf{u}_2 - \mathbf{u}_1|_1^2 \leq C_1|\tau_1 - \tau_2|_* |\mathbf{u}_2 - \mathbf{u}_1|_{L^2(\Gamma_C)} \tag{6.147}$$

Considering the trace theorem, we obtain

$$|\mathbf{u}_2 - \mathbf{u}_1|_1^2 \leq C_2|\tau_1 - \tau_2|_* |\mathbf{u}_2 - \mathbf{u}_1|_1 \tag{6.148}$$

Finally

$$|\mathbf{u}_2 - \mathbf{u}_1|_1 \leq C_2|\tau_2 - \tau_1|_* \tag{6.149}$$

Besides, from the definition 6.130, for  $\hat{w} \in \hat{X}_h$

$$\langle T(\tau_2) - T(\tau_1), \hat{w} \rangle = \mu \langle \sigma_n(\mathbf{u}_1) - \sigma_n(\mathbf{u}_2), \hat{w} \rangle \tag{6.150}$$

Otherwise, using the definition 6.126 one obtains

$$\begin{cases} \langle \sigma_n(\mathbf{u}_1), \hat{w} \rangle = a(\mathbf{u}_1, R(\hat{w}\mathbf{n})) - f(R(\hat{w}\mathbf{n})) & \forall \hat{w} \in \hat{X}_h \\ \langle \sigma_n(\mathbf{u}_2), \hat{w} \rangle = a(\mathbf{u}_2, R(\hat{w}\mathbf{n})) - f(R(\hat{w}\mathbf{n})) & \forall \hat{w} \in \hat{X}_h \end{cases} \tag{6.151}$$

where  $R$  is a linear application previously defined. Hence

$$\langle T(\tau_2) - T(\tau_1), \hat{w} \rangle = \mu a(\mathbf{u}_1 - \mathbf{u}_2, R(\hat{w}\mathbf{n})) \tag{6.152}$$

Therefore

$$\begin{aligned}
 |\langle T(\tau_2) - T(\tau_1), \hat{w} \rangle| &\leq \mu |\mathbf{u}_1 - \mathbf{u}_2|_1 |R(\hat{w}\mathbf{n})|_1 \text{ (continuity of } a) \\
 &\leq \mu C_2 |\tau_2 - \tau_1|_* |R(\hat{w}\mathbf{n})|_1 \text{ (equation (6.149))} \\
 &\leq \mu C_3 |\tau_2 - \tau_1|_* |\hat{w}\mathbf{n}|_{L^2} \text{ (continuity of } R) \\
 &= \mu C_3 |\tau_2 - \tau_1|_* |\hat{w}|_{L^2} \\
 &\leq \mu C_4 |\tau_2 - \tau_1|_* |\hat{w}|_{H^{1/2}}
 \end{aligned} \tag{6.153}$$

We conclude that

$$|T(\tau_2) - T(\tau_1)|_* \leq \mu C_4 |\tau_2 - \tau_1|_* \quad \forall \tau_1, \tau_2 \in H \tag{6.154}$$

□

The existence and the uniqueness of the solution of the regularized frictional problem (6.128) depend on the existence and the uniqueness of the fixed point of the application  $T$ . We have the

following theorem

**Theorem 6.5.** *If  $\mu < \frac{1}{C(h)}$ , the application  $T$  has a unique fixed point, and the following fixed point algorithm converges to the fixed point*

$$\tau_{n+1} = T(\tau_n) \quad (6.155)$$

*In addition if  $\mathbf{u}_{n+1}$  is the solution of the problem (6.131) for  $\tau = \tau_{n+1}$  then*

$$\mathbf{u}_{n+1} \xrightarrow[n \rightarrow \infty]{} \mathbf{u}^* \quad (6.156)$$

*where  $\mathbf{u}^*$  is the unique solution of (6.128).*

*Proof.* From the lemma 6.3,  $T$  is a contraction mapping, then using the Banach fixed-point theorem,  $T$  admits a unique fixed point  $\tau^*$  and  $\tau_{n+1}$  converges to  $\tau^*$ .

Moreover from the equation (6.149) we have

$$|\mathbf{u}_{n+1} - \mathbf{u}^*|_1 \leq C_2 |\tau_{n+1} - \tau^*|_* \quad (6.157)$$

Because  $\tau_{n+1} \xrightarrow[n \rightarrow \infty]{} \tau^*$  then  $\mathbf{u}_{n+1} \xrightarrow[n \rightarrow \infty]{} \mathbf{u}^*$ .  $\square$

Next we want to prove only the existence of a solution for the problem (6.128) without any restriction on the friction coefficient. First let's introduce the following lemma

**Lemma 6.4.** *There exists a constant  $C > 0$  such that*

$$|T(\tau)|_* \leq C \quad \forall \tau \in H \quad (6.158)$$

*Proof.* Let  $\mathbf{u}$  be a solution of the problem (6.131) for the sliding limit  $\tau \in H$ , therefore taking  $\mathbf{v} = \mathbf{0} \in \mathbf{K}_h$  in the inequality (6.131) one obtains

$$a(\mathbf{u}, -\mathbf{u}) + \langle \tau, \Pi_h(\eta_\alpha(\mathbf{0}) - \eta_\alpha(\mathbf{u}_T)) \rangle \geq f(-\mathbf{u}) \quad (6.159)$$

Hence

$$a(\mathbf{u}, \mathbf{u}) \leq \langle \tau, \Pi_h(\eta_\alpha(\mathbf{0}) - \eta_\alpha(\mathbf{u}_T)) \rangle + f(\mathbf{u}) \quad (6.160)$$

Because  $\tau \in H$  and  $\eta_\alpha \in \Xi_\alpha$  ( see the definition 6.1), we have  $\langle \tau, \Pi_h(\eta_\alpha(\mathbf{0}) - \eta_\alpha(\mathbf{u}_T)) \rangle \leq 0$ , and thus

$$a(\mathbf{u}, \mathbf{u}) \leq f(\mathbf{u}) \quad (6.161)$$

Using the fact that  $a$  is elliptic and  $f$  is continuous, we deduce the existence of a constant  $C_2 \geq 0$  such that

$$|\mathbf{u}|_1 \leq C_2 \quad (6.162)$$

Besides

$$\begin{aligned}
 |T(\tau)|_* &= \sup_{\phi \in \hat{X}_h} \frac{|\langle T(\tau), \phi \rangle|}{|\phi|_{H^{1/2}(\Gamma_C)}} \\
 &= \mu \sup_{\phi \in \hat{X}_h} \frac{|a(\mathbf{u}, R(\phi \mathbf{n})) - f(R(\phi \mathbf{n}))|}{|\phi|_{H^{1/2}(\Gamma_C)}} \quad (\text{equation (6.151)})
 \end{aligned} \tag{6.163}$$

From the continuity of  $a$  and  $f$  we have

$$\begin{aligned}
 |a(\mathbf{u}, R(\phi \mathbf{n})) - f(R(\phi \mathbf{n}))| &\leq C_3 |\mathbf{u}|_1 |R(\phi \mathbf{n})|_1 + C_4 |R(\phi \mathbf{n})|_1 \\
 &\leq C_5 |\mathbf{u}|_1 |\phi|_{H^{1/2}} + C_6 |\phi|_{H^{1/2}} \quad (\text{like equation (6.153)}) \\
 &= (C_5 |\mathbf{u}|_1 + C_6) |\phi|_{H^{1/2}} \\
 &\leq C_7 |\phi|_{H^{1/2}(\Gamma_C)} \quad (\text{equation (6.162)})
 \end{aligned} \tag{6.164}$$

Therefore

$$|T(\tau)|_* \leq \mu C_7 \tag{6.165}$$

□

Finally we have the following theorem

**Theorem 6.6.** *There exists a fixed point for the application  $T$ .*

*Proof.* We are in a finite dimensional space, thus if we take  $M = H \cap \bar{B}(0, C)$  as the intersection of  $H$  with the closed ball  $\bar{B}(0, C)$ ,  $M$  is compact and convex of the dual of  $\hat{X}_h$ . From the lemma 6.4 we deduce that  $T(M) \subseteq M$  and we know that  $T$  is continuous, therefore by applying Brouwer's fixed-point theorem we conclude that  $T$  admits a fixed point. □

Note that all the above constants do not depend on the regularization parameter  $\alpha$ .

### 6.4.1 Case of two bodies in contact

All previous results can be generalized for the case of contact between two bodies  $\Omega_h^1$  and  $\Omega_h^2$ . Some modifications must be done, for example  $\hat{X}_h$  is the trace space of  $X_h$  which in this case becomes

$$X_h = \{v \in C^0(\Omega_h^1) \mid v|_{T_i} \in P_1, \forall T_i \text{ triangle of } \Omega_h^1\} \tag{6.166}$$

which means that all linear applications (for example  $\sigma_n$ ,  $\tau$ ,  $T(\tau)$ ) applied on  $\hat{X}_h$  depends on the first body  $\Omega_h^1$ . Moreover  $a = a^1 + a^2$  and  $f = f^1 + f^2$ . In equations (6.126, 6.151, 6.152, 6.163, 6.164)  $a = a^1$  and  $f = f^1$ .

In order to extend the above results to the contact between two bodies, the equation (6.146)

is revisited, noting  $\mathbf{u}^l$  the displacement for the body  $\Omega_h^l$  then

$$\begin{aligned} a(\mathbf{u}_2 - \mathbf{u}_1, \mathbf{u}_2 - \mathbf{u}_1) &\leq c|\tau_1 - \tau_2|_* |(\mathbf{u}_2^1 - \mathbf{u}_1^1) - (\mathbf{u}_2^2 - \mathbf{u}_1^2)|_{L^2(\Gamma_C)} \\ &\leq c|\tau_1 - \tau_2|_* (|\mathbf{u}_2^1 - \mathbf{u}_1^1|_{L^2(\Gamma_C)} + |\mathbf{u}_2^2 - \mathbf{u}_1^2|_{L^2(\Gamma_C)}) \end{aligned} \quad (6.167)$$

Let  $|\cdot|_{1,l}$  denotes the  $\mathbf{H}^1$  norm when the vector belongs to  $\Omega_h^l$ , and simply  $|\cdot|_1$  for the  $\mathbf{H}^1$  broken norm on  $\Omega_h = \Omega_h^1 \cup \Omega_h^2$ . Applying the trace theorem on  $\Omega_h^1$  and  $\Omega_h^2$ , the equation (6.167) becomes

$$a(\mathbf{u}_2 - \mathbf{u}_1, \mathbf{u}_2 - \mathbf{u}_1) \leq C|\tau_1 - \tau_2|_* (|\mathbf{u}_2^2 - \mathbf{u}_1^2|_{1,2} + |\mathbf{u}_2^1 - \mathbf{u}_1^1|_{1,1}) \quad (6.168)$$

Using the following identity, for  $x_1, x_2 \in \mathbb{R}$

$$|x_1| + |x_2| \leq \sqrt{2}(x_1^2 + x_2^2)^{1/2} \quad (6.169)$$

equation (6.168) becomes

$$\begin{aligned} a(\mathbf{u}_2 - \mathbf{u}_1, \mathbf{u}_2 - \mathbf{u}_1) &\leq C|\tau_1 - \tau_2|_* (|\mathbf{u}_2^2 - \mathbf{u}_1^2|_{1,2}^2 + |\mathbf{u}_2^1 - \mathbf{u}_1^1|_{1,1}^2)^{1/2} \\ &= C|\tau_1 - \tau_2|_* |\mathbf{u}_2 - \mathbf{u}_1|_1 \end{aligned} \quad (6.170)$$

and the equation (6.148) is recovered. Finally the fact that  $|\cdot|_{1,l} \leq |\cdot|_1$  in equations (6.153, 6.164) finish the proof.

#### 6.4.2 Error between Tresca's discretized solution and regularized Tresca's discretized solution

For the sake of clarity we consider only the Signorini case. We have the following theorem

**Theorem 6.7.** *Let  $\mathbf{u} \in \mathbf{K}_h$  be the Tresca solution, in other words, solution of*

$$a(\mathbf{u}, \mathbf{v} - \mathbf{u}) + \langle \tau, \Pi_h(|\mathbf{v}_T| - |\mathbf{u}_T|) \rangle \geq f(\mathbf{v} - \mathbf{u}) \quad \forall \mathbf{v} \in \mathbf{K}_h \quad (6.171)$$

and let  $\mathbf{u}_\alpha \in \mathbf{K}_h$  be the regularized Tresca solution, otherwise speaking, solution of

$$a(\mathbf{u}_\alpha, \mathbf{v} - \mathbf{u}_\alpha) + \langle \tau, \Pi_h(\eta_\alpha(\mathbf{v}_T) - \eta_\alpha(\mathbf{u}_{\alpha,T})) \rangle \geq f(\mathbf{v} - \mathbf{u}_\alpha) \quad \forall \mathbf{v} \in \mathbf{K}_h \quad (6.172)$$

then there exists a constant  $C \geq 0$  such that

$$|\mathbf{u}_\alpha - \mathbf{u}|_1 \leq C\sqrt{\alpha} \quad (6.173)$$

*Proof.* Replacing  $\mathbf{v}$  by  $\mathbf{u}_\alpha$  in the equation (6.171), and  $\mathbf{v}$  by  $\mathbf{u}$  in the equation (6.172), one obtains

$$\begin{cases} a(\mathbf{u}, \mathbf{u}_\alpha - \mathbf{u}) + \langle \tau, \Pi_h(|\mathbf{u}_{\alpha,T}| - |\mathbf{u}_T|) \rangle \geq f(\mathbf{u}_\alpha - \mathbf{u}) \\ a(\mathbf{u}_\alpha, \mathbf{u} - \mathbf{u}_\alpha) + \langle \tau, \Pi_h(\eta_\alpha(\mathbf{u}_T) - \eta_\alpha(\mathbf{u}_{\alpha,T})) \rangle \geq f(\mathbf{u} - \mathbf{u}_\alpha) \end{cases} \quad (6.174)$$

or

$$\begin{cases} a(\mathbf{u}, \mathbf{u}_\alpha - \mathbf{u}) + \langle \tau, \Pi_h(|\mathbf{u}_{\alpha,T}| - |\mathbf{u}_T|) \rangle \geq f(\mathbf{u}_\alpha - \mathbf{u}) \\ a(-\mathbf{u}_\alpha, \mathbf{u}_\alpha - \mathbf{u}) + \langle \tau, \Pi_h(\eta_\alpha(\mathbf{u}_T) - \eta_\alpha(\mathbf{u}_{\alpha,T})) \rangle \geq f(\mathbf{u} - \mathbf{u}_\alpha) \end{cases} \quad (6.175)$$

Adding these two equations, we obtain

$$a(\mathbf{u} - \mathbf{u}_\alpha, \mathbf{u}_\alpha - \mathbf{u}) + \langle \tau, \Pi_h(|\mathbf{u}_{\alpha,T}| - \eta_\alpha(\mathbf{u}_{\alpha,T}) + \eta_\alpha(\mathbf{u}_T) - |\mathbf{u}_T|) \rangle \geq 0 \quad (6.176)$$

Thus

$$\begin{aligned} a(\mathbf{u}_\alpha - \mathbf{u}, \mathbf{u}_\alpha - \mathbf{u}) &\leq |\tau|_* |\Pi_h(|\mathbf{u}_{\alpha,T}| - \eta_\alpha(\mathbf{u}_{\alpha,T}) + \eta_\alpha(\mathbf{u}_T) - |\mathbf{u}_T|)|_{H^{1/2}(\Gamma_C)} \\ &\leq C|\tau|_* |\Pi_h(|\mathbf{u}_{\alpha,T}| - \eta_\alpha(\mathbf{u}_{\alpha,T}) + \eta_\alpha(\mathbf{u}_T) - |\mathbf{u}_T|)|_{L^2(\Gamma_C)} \\ &\leq C|\tau|_* |\Pi_h(|\mathbf{u}_{\alpha,T}| - \eta_\alpha(\mathbf{u}_{\alpha,T}))| + \Pi_h(|\eta_\alpha(\mathbf{u}_T) - |\mathbf{u}_T||)|_{L^2(\Gamma_C)} \\ &\leq 2C|\tau|_* |\Pi_h(1)|_{L^2(\Gamma_C)} \cdot \alpha \quad (\eta_\alpha \in \Xi_\alpha) \end{aligned} \quad (6.177)$$

Because  $a$  is elliptic then

$$|\mathbf{u}_\alpha - \mathbf{u}|_1 \leq C_1 \sqrt{\alpha} \quad (6.178)$$

□

**Corollary 6.2.** *If  $\eta_\alpha(\mathbf{v}) = \sqrt{|\mathbf{v}|^2 + \alpha^2}$  then*

$$|\mathbf{u}_\alpha - \mathbf{u}|_1 \leq C\alpha^{1/2} \quad (6.179)$$

## 6.5 The Algorithm

Using the finite element approach, for  $l = 1$  or  $2$ , let  $\Omega_h^l$  be the mesh of the body  $\Omega^l$ , which is composed from the triangles family  $\{T_i^l \mid i = 1, \dots, n_T^l\}$ . In addition, consider the following spaces

$$\mathbf{V}_h^l = \left\{ \mathbf{v} = (v_1, v_2) \in C^0(\Omega_h^l) \times C^0(\Omega_h^l) \mid \mathbf{v}|_{T_i^l} \in P_r \times P_r, \forall i = 1, \dots, n_T^l \text{ and } \mathbf{v} = 0 \text{ on } \Gamma_0^l \right\} \quad (6.180)$$

where  $C^0(\Omega_h^l)$  denotes the set of the continuous functions on  $\Omega_h^l$ , and  $P_r$  denotes the linear finite elements for  $r = 1$  and the quadratic ones for  $r = 2$ .

Consider the space  $\mathbf{V}_h$  defined as follows

$$\mathbf{V}_h = \mathbf{V}_h^1 \times \mathbf{V}_h^2 \quad (6.181)$$

Let  $\mathbf{u}_h = (\mathbf{u}_h^1, \mathbf{u}_h^2) \in \mathbf{V}_h$ , the displacement vector field  $\mathbf{u}_h^l$  on the mesh  $\Omega_h^l$  is given by

$$\mathbf{u}_h^l = \sum_i \begin{pmatrix} U_i^x \\ U_i^y \end{pmatrix} \hat{w}_i^l \quad (6.182)$$

where  $\hat{w}_i^l$  are the shape functions on the mesh  $\Omega_h^l$ , and  $(U_i^x \ U_i^y)^T$  are the degrees of freedom of  $\mathbf{u}_h^l$ , otherwise speaking  $U_i^x$  and  $U_i^y$  represent respectively the horizontal and vertical displacement of the node  $i$  in the mesh. In the following  $\mathbf{U} \in \mathbb{R}^n$  denotes the vector of all degrees of freedom of  $\mathbf{u}_h$ , otherwise stated

$$\mathbf{U} = (\dots \ U_i^x \ U_i^y \ \dots)^T \quad (6.183)$$

We will present the algorithm to solve frictional contact problem in general case, otherwise

speaking in the case of large deformations. For the sake of simplicity and in order to be more clear, the algorithm will be split into several algorithms.

The idea behind the algorithm is first to loop on the sliding limits  $\tau$  until convergence, more precisely at each iteration  $k$ , the regularized frictional problem for a given sliding limit  $\tau_k$  is solved, which corresponds to a minimization problem, then we retrieve the normal pressure  $\sigma_{n,k}$  on the contact area, and the next sliding limit  $\tau_{k+1}$  is computed via  $\tau_{k+1} = -\mu\sigma_{n,k}$ . This process continues until the relative error between two successive sliding limits is small enough.

In the sequel,  $\llbracket \tau \rrbracket$  denotes an array containing the value of  $\tau$  at the integration points of the contact area.

The algorithm solving the frictional problem is shown in algorithm 6.

---

**Algorithm 6** Regularized frictional algorithm using the fixed point method

---

Set the error tolerance  $\epsilon_{tol} = 10^{-6}$

Compute  $\sigma_{n,0}$  the normal stress pressure at the contact area for the frictionless problem

Compute  $\tau_0 = -\mu\sigma_{n,0}$ , the first sliding limit

**while**  $error \geq \epsilon_{tol}$  **do**

1. For a given sliding limit  $\tau_k$ , solve Tresca's regularized problem, given in the algorithm 7

2. Retrieve the displacement field  $\mathbf{u}_h$

3. Compute the normal pressure  $\sigma_{n,k}(\mathbf{u}_h)$  on the contact surface

4. Compute the new sliding limit  $\tau_{k+1} = -\mu\sigma_{n,k}$

5.  $error = \frac{\|\llbracket \tau_{k+1} \rrbracket - \llbracket \tau_k \rrbracket\|_\infty}{\|\llbracket \tau_k \rrbracket\|_\infty}$

**end while**

---

The resolution of the contact problem without friction, is to solve the following constrained minimization problem

$$\begin{cases} \mathbf{u}_h = \arg \min_{\mathbf{v} \in \mathbf{V}_h} (\mathcal{E}_p(\mathbf{v})) \text{ s.t} \\ \int_{\Gamma_{C1}} ((\mathbf{x} - \bar{\mathbf{x}}_2) \cdot \mathbf{n}) \cdot \phi_i^{(1)} dS \geq 0 \quad \forall i = 1, \dots, n_{C1} \\ \int_{\Gamma_{C2}} ((\mathbf{x} - \bar{\mathbf{x}}_1) \cdot \mathbf{n}) \cdot \phi_i^{(2)} dS \geq 0 \quad \forall i = 1, \dots, n_{C2} \end{cases} \quad (6.184)$$

where  $\mathbf{x} = \mathbf{X} + \mathbf{v}$  the actual position of a material point, with  $\mathbf{X}$  the initial position of this same point.  $\Gamma_{Cl}$  is the initial potential contact area of the body  $\Omega_h^l$ .  $\bar{\mathbf{x}}_l$  is the projection point of  $\mathbf{x}$  on the body  $\Omega_h^l$ , where  $l = 1, 2$  and  $\mathbf{n}$  is the outward unit normal vector at  $\bar{\mathbf{x}}_l$ . Note that the two constraints in the problem (6.184) describe the non-penetration in a weak sense, and it is a symmetric formulation, in other words the user does not need to specify anymore a slave and a master body, see [63] for details.  $\phi_i^{(l)}$  are the shape functions on the  $n_{Cl}$  nodes of the contact area  $\Gamma_{Cl}$ .

In addition  $\mathcal{E}_p$  is the total potential energy defined by

$$\begin{cases} \mathcal{E}_p(\mathbf{v}) = \frac{1}{2}a(\mathbf{v}, \mathbf{v}) - f(\mathbf{v}) \text{ for linear elastic problems} \\ \mathcal{E}_p(\mathbf{v}) = \int_{\Omega_h^1 \cup \Omega_h^2} \hat{W}(\mathbf{v}) dv - f(\mathbf{v}) \text{ for large deformations and hyperelastic problems} \end{cases} \quad (6.185)$$

where  $\hat{W}$  is the strain energy function.

Moreover, in the case of large deformations, we can remark that the projection points  $\bar{\mathbf{x}}_l$   $l = 1, 2$  in the non-penetration constraints (6.184) depend on the actual solution of the problem. Thus we will use a fixed point algorithm to deal with this issue. Indeed in the fixed point algorithm iteration, we will use the displacement of the previous iteration, and based on this displacement we will compute for each point  $\mathbf{x}$  its closest segment or triangle in the body  $\Omega_h^l$  and its projection parameter, and therefore the projection point  $\bar{\mathbf{x}}_l$  now depends linearly on the actual displacements. Otherwise speaking we obtain a sequence of minimization problems with linear constraints.

The resolution of the Tresca regularized problem, presented in the algorithm 7, will use the theorem 6.4 and therefore as we saw, we can use a fixed point algorithm. We used the same fixed point algorithm treating the constraints. Therefore in the fixed point algorithm iteration, let's say  $n + 1$ , we minimize the following energy  $E_{n+1}$  submitted to the linear constraints.

$$E_{n+1}(\mathbf{v}) = \mathcal{E}_p(\mathbf{v}) + \int_{\gamma_C^n} \tau_k \cdot \eta_\alpha (\mathbf{v}_T^1 - \bar{\mathbf{v}}_T^2) ds \quad (6.186)$$

where  $\tau_k$  is the sliding limit at the iteration  $k$  of the algorithm 6.  $\mathbf{v}^1$  is the admissible displacement field of the first body and  $\bar{\mathbf{v}}^2$  is the admissible displacement field of the second body applied on the projection points of the first body on the second one. Finally  $\gamma_C^n$  is the actual contact area based on the displacements of the previous iteration  $n$ .

---

**Algorithm 7** Symmetric algorithm using the fixed point method for Tresca's regularized problem

---

Initialization of the displacement  $\mathbf{U}_0$  and setting the tolerance  $\epsilon_{tol} = 10^{-6}$

**while**  $error \geq \epsilon_{tol}$  **do**

1. Using the displacement vector  $\mathbf{U}_n$  of the previous iteration  $n$ :
  - Compute the projection points' parameters  $\{\eta_i^* \mid i = 1, \dots, nS\}$  of all slave integration points
  - Compute the normal at the projection points  $\{n_i \mid i = 1, \dots, nS\}$  (Using smoothing techniques)
  - Compute the contact area  $\gamma_C^n$  (by computing the distance between the two bodies)
2. For each integration point, its projection point  $\bar{\mathbf{x}}_i$  depends linearly on the actual displacement
3. Reverse the role of the master and the slave bodies
4. Form the Energy  $E_{n+1}$  (Equation (6.186)) and the symmetric linear constraints
5. Use the interior point method in order to solve the minimization problem with linear constraints, and to obtain the actual displacement  $\mathbf{U}_{n+1}$

$$6. \text{ error} = \frac{\|\mathbf{U}_{n+1} - \mathbf{U}_n\|_\infty}{\|\mathbf{U}_n\|_\infty}$$

**end while**

---

## 6.6 Numerical validations

### 6.6.1 Validation of the regularized friction law

In this first example we will try to validate the regularized friction law given in the equation (6.85). Indeed we will take an elastic rectangular body of dimensions  $(40UL \times 20UL)$  laid on a rigid rectangle body (see Figure 6.5). The elastic body has the following material properties, a Young's modulus  $E = 10^3 \frac{UF}{UL^2}$  and a poisson's ratio  $\nu = 0$ , note that  $UF, UL$  denote respectively the force and the length unit. A vertical force of  $-30 \frac{UF}{UL}$  is uniformly distributed along its top area.

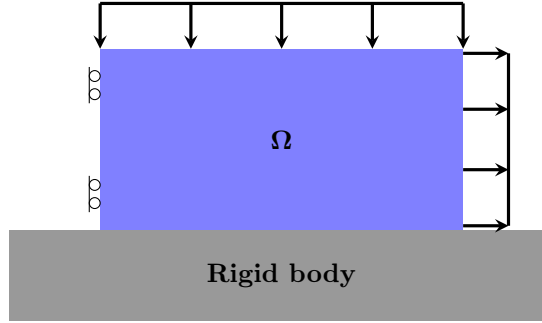


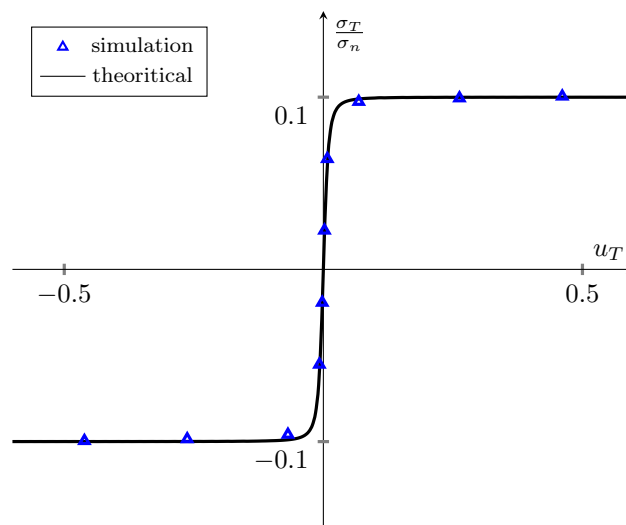
Figure 6.5 – Problem geometry

At the first stage we impose a sliding conditions on its left boundary, and we apply a sequence of an uniformly distributed horizontal force on its right boundary pointing to the right, with the following values 2, 5, 10, 20,  $30 \frac{UF}{UL}$ . In the second stage the sliding conditions are imposed on its right boundary and we apply a sequence of an uniformly distributed horizontal force on its left boundary pointing to the left, with the following values  $-2, -5, -10, -20, -30 \frac{UF}{UL^2}$  (symmetrical loads). Considering the midpoint of the contact area, the goal of this example is to plot the ratio of the tangential and normal stresses  $\frac{\sigma_T}{\sigma_n}$  against the tangential displacement  $u_T$ , and to compare it with the theoretical one seen in the equation (6.85).

In all next examples the regularization function will be  $\eta_\alpha(\mathbf{v}) = \sqrt{|\mathbf{v}|^2 + \alpha^2}$  for  $\mathbf{v} \in \mathbb{R}^2$  or  $\mathbb{R}^3$ . Taking  $\alpha = 10^{-2}$ , then according to the equation (6.85) we have

$$\frac{\sigma_T}{\sigma_n} = \mu \frac{u_T}{\sqrt{u_T^2 + \alpha^2}} \quad (6.187)$$

We consider a friction coefficient  $\mu = 0.1$ , and linear finite elements. The normal stress at the contact area is equal to  $\sigma_n = \sigma_{yy}$  and the tangential stress on the contact area is equal to  $\sigma_T = -\sigma_{xy}$ , moreover the tangential displacement is equal to  $u_T = u_x$ . In the Figure 6.6, the ratio  $\frac{\sigma_T}{\sigma_n}$  against the tangential displacement  $u_T$  is plotted for the different loads mentioned above, and is compared with the theoretical one given by the equation (6.187).

Figure 6.6 –  $\frac{\sigma_T}{\sigma_n}$  vs  $u_T$ 

We can see the consistency between the simulation and the theoretical results, and how regularization can approach Coulomb's law. We saw similar results for quadratic finite elements, three dimensional case and for hyperelastic materials.

### 6.6.2 Elastic bloc pressed against a rigid foundation

In this example an elastic body (Young's modulus  $E = 1000 \frac{UF}{UL^2}$ , Poisson's ratio  $\nu = 0.3$ ) is pressed against a rigid foundation and then pulled by a tangential force. The geometry and the loads are presented in the Figure 6.7 (length units in  $UL$ ). The lower area is composed from a contact area of length  $3.6UL$ , where the friction is active (see Figure 6.7), and from two other parts where a sliding condition is imposed. This example was handled in [89, 124].

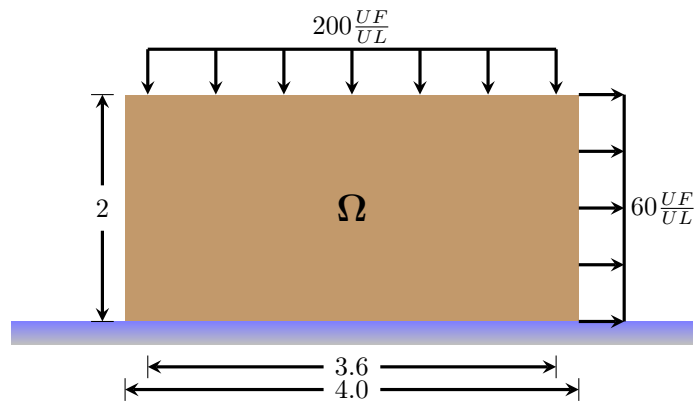


Figure 6.7 – The geometry and the loads

The regularization parameter was taken to be  $\alpha = 10^{-3}$  and quadratic finite elements ( $P_2$ ) were used (in order to test these finite elements). The frictional coefficient is equal to  $\mu = 0.5$ , note that there is no boundary conditions in the horizontal direction in order to avoid the body from sliding to infinity, thus the equilibrium is reached because of the frictional forces. Moreover if  $\mu = 0.1$  then as in [89], the body slide to infinity ( $60 \times 2 > 0.1 \times (200 \times 3.6)$ ).

The mesh and the deformed shape of the elastic body are presented in the following Figure 6.8.

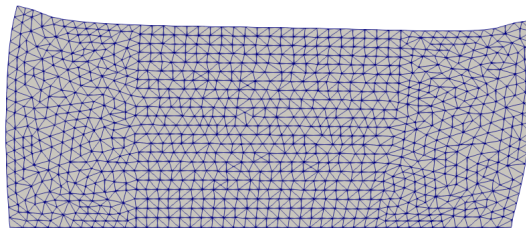


Figure 6.8 – The deformed shape of the elastic body

The normal and tangential contact stresses are depicted in the Figure 6.9, and are close to the ones in [89].

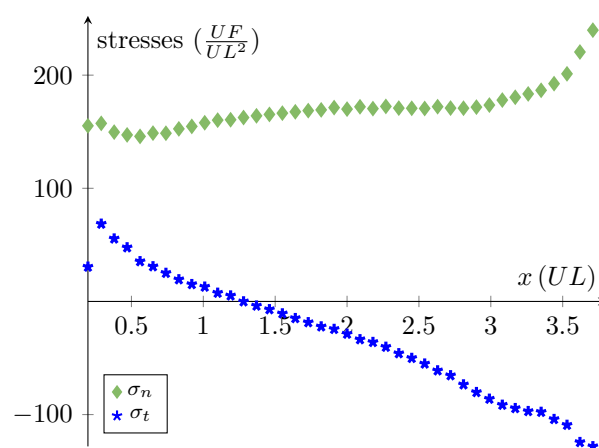


Figure 6.9 – The stresses on the frictional contact area

### 6.6.3 Contact of a square plate against an obstacle

Always in the same spirit, we consider an elastic square plate (Young's modulus  $E = 1.3 \times 10^5 \frac{UF}{UL^2}$ , Poisson's ratio  $\nu = 0.2$ ) in the plane strain configuration (2D). This plate is subjected to a uniformly distributed forces on its top and left area. The geometry and the loads are depicted in the Figure 6.10 (units in  $UL$ ). This example was studied in [111], and the goal is to compute the tangential displacement for a given points on the lower area of the plate.

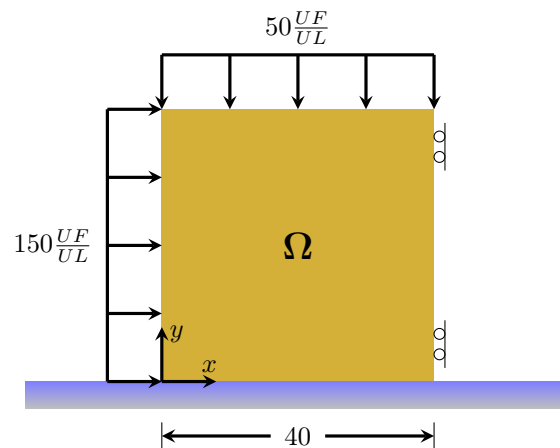


Figure 6.10 – The geometry and the loads

Finally, the body right area is fixed in the horizontal direction, and the friction coefficient is not small and is equal to  $\mu = 1$ . We consider then the following points on the elastic body initial configuration, presented in the following table (6.1).

Points	$x$	$y$
A	0.	0.
B	1.25	0.
C	5.	0.
D	7.5	0.
E	11.25	0.

Table 6.1 – Initial positions ( $UL$ ) of the points

Linear finite elements ( $P_1$ ) were used, and a regularization parameter  $\alpha = 10^{-3}$  was considered. The mesh is shown in the Figure 6.11.

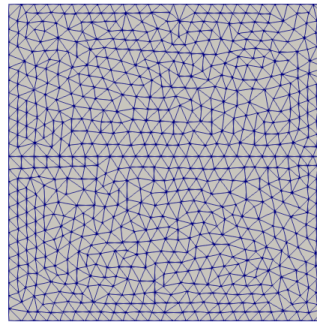


Figure 6.11 – The mesh of the elastic body

The computed tangential displacement for each point and the error with respect to the reference value, computed as an average of different software results, are presented in the following table (6.2).

Points	$u_x$	$u_x$ (reference [111])	error
A	0.0279	0.0286	2.4 %
B	0.0265	0.0272	2.6 %
C	0.0224	0.0228	1.8 %
D	0.0194	0.0198	2.0 %
E	0.0151	0.0150	0.7 %

Table 6.2 – Tangential displacement  $u_x$  ( $UL$ ) of the points

In [111], the errors with respect to the reference values are about 5%.

#### 6.6.4 Sliding on an inclined interface

A two elastic bodies  $\Omega_1$  and  $\Omega_2$  with a common inclined interface in the initial configuration are considered (see Figure 6.12) (units in  $UL$ ). A vertical displacement is imposed on the top area of

the first body  $\Omega_1$ , as shown in the Figure 6.12. In addition, a boundary conditions are imposed in order to avoid the rigid motions when slip occurs at the interface, indeed as we can see in the Figure 6.12, the top right point of the first body  $\Omega_1$  is imposed to slide vertically, the lower right point of the second body  $\Omega_2$  is fixed, and the other parts of the lower area of  $\Omega_2$  can slide horizontally.

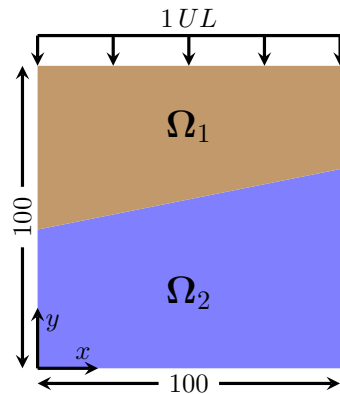


Figure 6.12 – The geometry of the two bodies and the imposed displacement

The equation of the interface is given by the equation  $y = 0.2 * x + 45.86$  with respect to the orthonormal frame shown in Figure 6.12. The two bodies have the same elastic material properties (Young's modulus  $E = 10^4 \frac{UF}{UL^2}$ , Poisson's ration  $\nu = 0.3$ ), finally the plane strain condition is assumed (2D). A vertical displacement of  $1UL$  was imposed in one loading step, on the top area of the first body. This example is a modified version of the one studied in [10].

The goal is to test if there will be no slip between the two bodies when the frictional coefficient  $\mu$  is equal to the slope of the interface, 0.2, as expected.

Linear finite elements ( $P_1$ ) were used, and a regularization parameter  $\alpha = 10^{-3}$  was considered. Taking three frictional coefficients  $\mu = 0, 0.10, 0.2$ , the deformed shape of the three cases are depicted in the Figure 6.13.

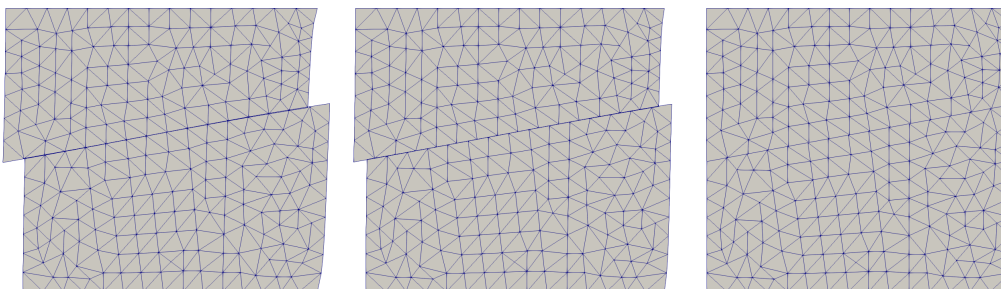


Figure 6.13 – The deformation states (amplification factor =5) for  $\mu = 0, 0.1, 0.2$

The horizontal displacement for the three frictional coefficients can be found in the Figure 6.14.

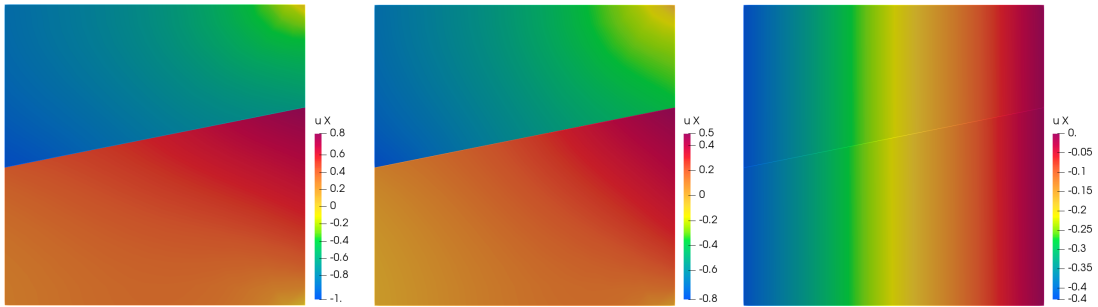


Figure 6.14 – The horizontal displacement field  $u_x$  for  $\mu = 0, 0.1, 0.2$

We can notice that when  $\mu = 0.2$ , the two bodies are stick together, and act like one body. Note that we studied this one body without considering the contact and it gives the same results as if  $\mu = 0.2$ . Moreover a quasi-static study leads to the same results as before.

Now, we consider the three-dimensional case, which is not equivalent to the two-dimensional case, indeed the plain strain condition is not satisfied. The geometry is shown in the Figure 6.15 and the boundary conditions are detailed below, finally all the remaining properties are as the two-dimensional case.

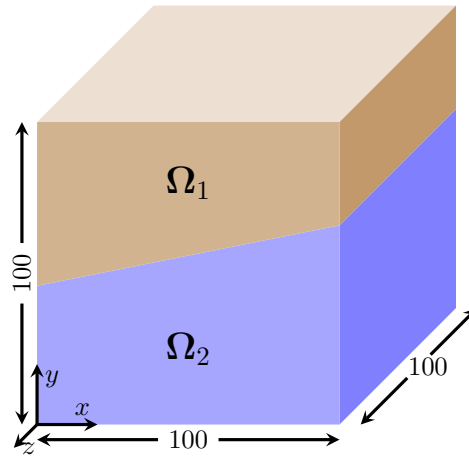


Figure 6.15 – The geometry of the two bodies

The area  $\{z = -100\}$  can slide in the same plane, the area  $\{y = 0\}$  is fixed in the ( $y$ ) direction, the line  $\{x = 100\} \cap \{y = 0\}$  is fixed, and the line  $\{x = 100\} \cap \{y = 100\}$  can slide in the ( $y, z$ ) plane. A downward displacement of  $-1UL$  is imposed on the top area  $\{y = 100\}$ .

The displacement fields  $u_x$  and  $u_z$  are depicted in the Figure 6.16 in addition to the mesh,

we notice that for the frictional coefficient  $\mu = 0.2$ , the two bodies stick together and behave like one body. Moreover, this one body was studied without contact conditions and it provided the same displacement fields.

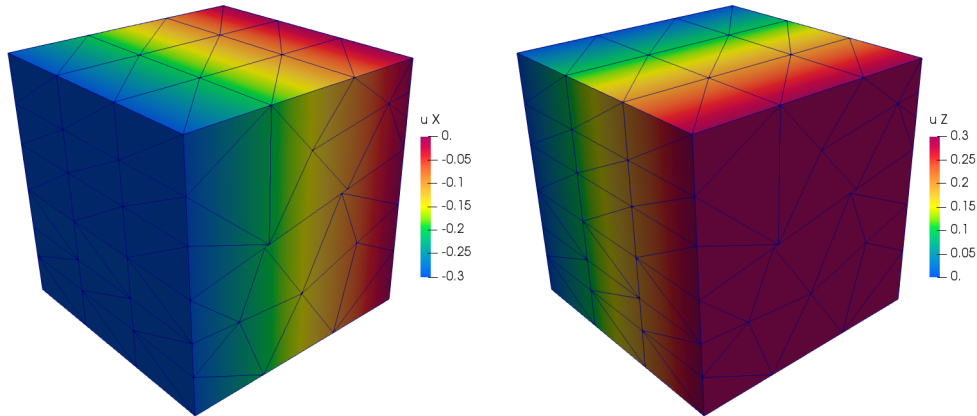


Figure 6.16 – The displacement fields  $u_x$  and  $u_z$  for  $\mu = 0.2$

### 6.6.5 Frictional Hertz contact

We consider a contact between a half elastic cylinder  $\Omega_1$  ( $E_1 = 200 \frac{UF}{UL^2}$ ,  $\nu_1 = 0.3$ ) and an elastic half-space  $\Omega_2$  ( $E_2 = 200 \frac{UF}{UL^2}$ ,  $\nu_2 = 0.3$ ), the geometry and the dimensions are shown in the Figure 6.17 (units in  $UL$ ). The Frictional coefficient is taken relatively big,  $\mu = 0.8$ , and the lower area of  $\Omega_2$  is fixed. First, we impose a downward vertical displacement of  $4.55 UL$  in 3 steps on the top of the half cylinder, then a total horizontal load of  $q = 0.05 \frac{UF}{UL}$  is applied in 7 steps, again on the top of the half cylinder. Obviously it's a quasi-static study.

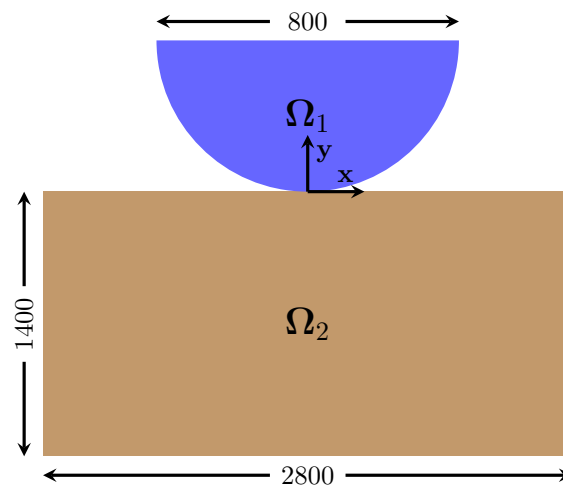


Figure 6.17 – The geometry of the frictional Hertz problem

The imposed vertical displacement gives an equivalent maximal normal pressure of  $p_0 = 2.93 \frac{UF}{UL}$ . Thus the equivalent vertical force is equal to

$$P = \frac{\pi R p_0^2}{E^*} \quad (6.188)$$

where  $R$  is the cylinder radius, and  $E^*$  the effective Young modulus given by

$$E^* = \frac{E_1 E_2}{E_1(1 - \nu_2^2) + E_2(1 - \nu_1^2)} \quad (6.189)$$

According to [66] and with the small deformations hypothesis, there exist two slip zones  $\{c \leq |x| \leq a\}$  and one stick zone  $\{|x| \leq c\}$ , where

$$\begin{cases} a = \sqrt{\frac{4PR}{\pi E^*}} \\ c = a \sqrt{1 - \frac{Q}{\mu P}} \end{cases} \quad (6.190)$$

with  $Q = 2Rq$  and  $a$  the half contact width, moreover the normal and tangential stresses are given by the following.

The normal pressure at the contact zone:

$$p_n = \frac{p_0}{a} \sqrt{a^2 - x^2} \quad (6.191)$$

The tangential pressure at the contact zone:

$$\begin{cases} p_t = \mu \frac{p_0}{a} (\sqrt{a^2 - x^2} - \sqrt{c^2 - x^2}) & \text{if } |x| \leq c \\ p_t = \mu \frac{p_0}{a} \sqrt{a^2 - x^2} & \text{if } c \leq |x| \leq a \end{cases} \quad (6.192)$$

The mesh of the two bodies is shown in the Figure 6.18.

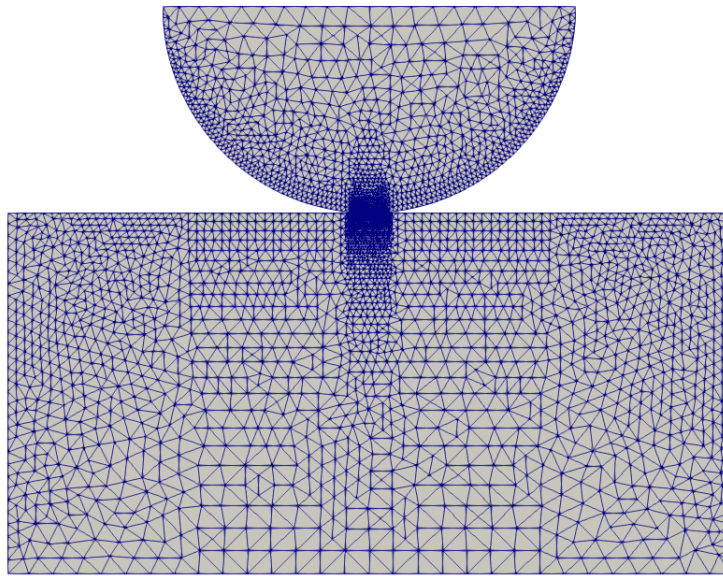


Figure 6.18 – The two bodies mesh

Using the quadratic finite elements ( $P_2$ ), and a regularization parameter  $\alpha = 10^{-3}$ , the computed normal and tangential stresses, in addition to the theoretical ones, are depicted in the Figure 6.19.

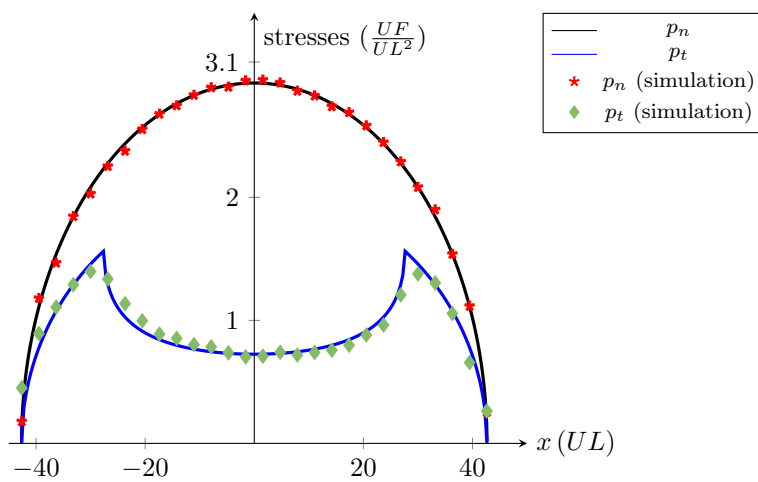


Figure 6.19 – The stresses on the contact area

### 6.6.6 Shallow ironing

This example was studied by many papers, we can cite for example [46, 123, 125]. A small indenter  $\Omega_1$  is pressed into a less stiffer rectangular body  $\Omega_2$  at the first stage, and pulled horizontally to the right at the second stage. The geometries of the two bodies are shown in the Figure 6.20 (units in  $UL$ ), in addition the bottom of the rectangular body is fixed. Neo-Hookean material is assumed for the two bodies (see [123]), with  $(E_1 = 68.96 \times 10^2 \frac{UF}{UL^2}, \nu = 0.32)$  for the small indenter and  $(E_2 = 6.896 \times 10^2 \frac{UF}{UL^2}, \nu = 0.32)$  for the rectangular body, which is 10 times softer than the indenter.

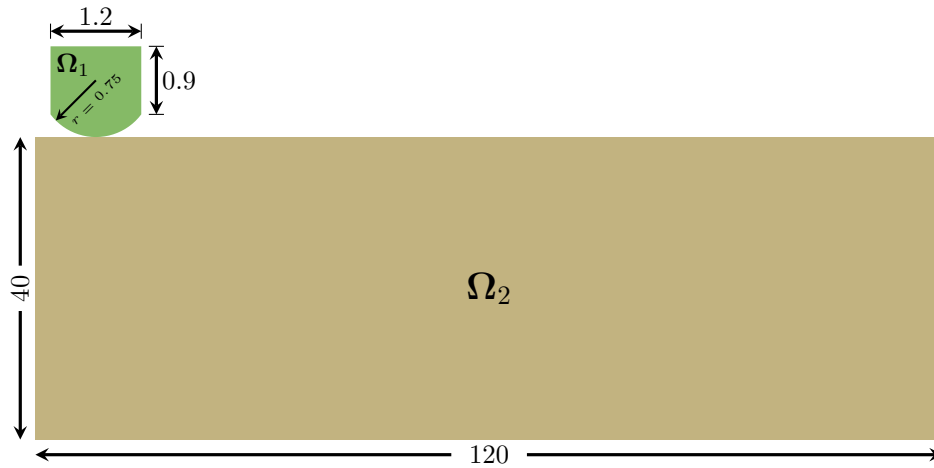


Figure 6.20 – The geometry of the shallow ironing problem

At the first stage a downward vertical displacement of  $8UL$  is applied in 8 time steps on the top of the indenter, in the second stage a horizontal displacement of  $100UL$  is applied on the top of the indenter to the right in 500 time steps. This is a quasi-static study with a friction coefficient  $\mu = 0.3$ .

Using the quadratic finite elements ( $P_2$ ), and a regularization parameter  $\alpha = 10^{-2}$ , the mesh of the two bodies and the deformation shapes at some time steps are shown in the Figure 6.21.

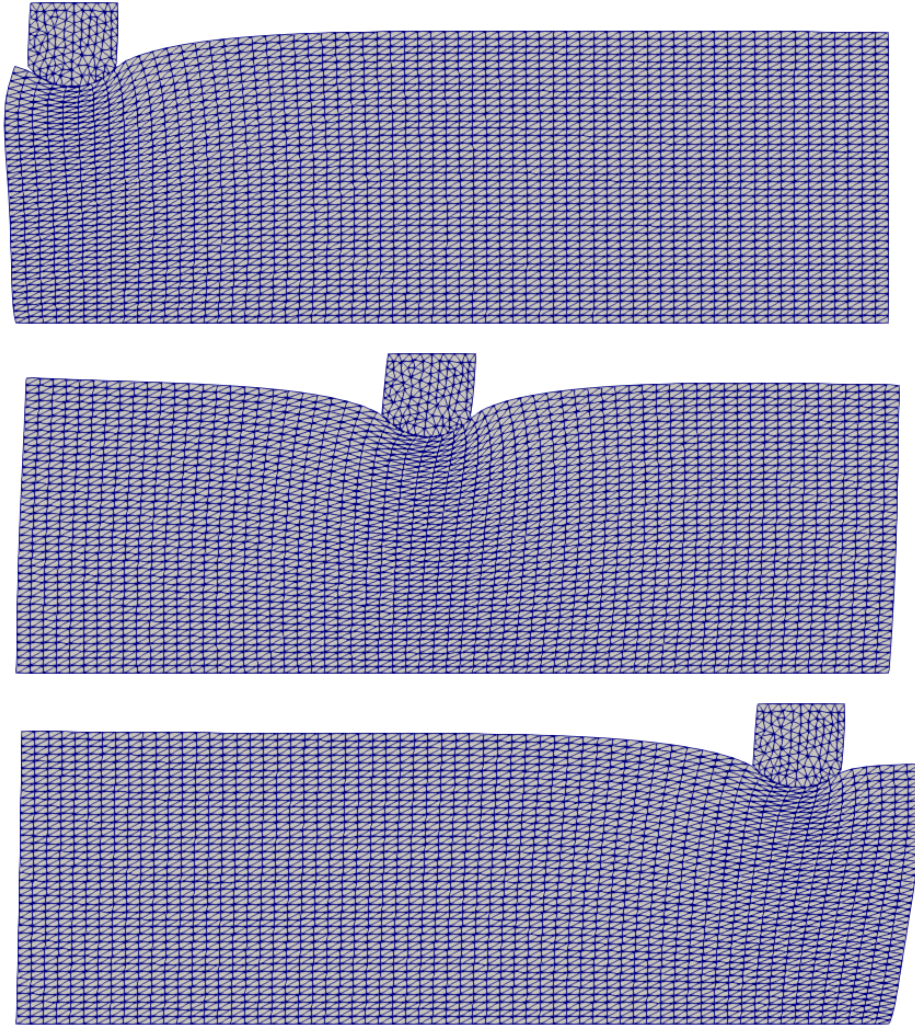


Figure 6.21 – The deformation shapes at  $t = 8, 254, 508$

The vertical and horizontal reactions on the indenter, are depicted in the Figure 6.22.

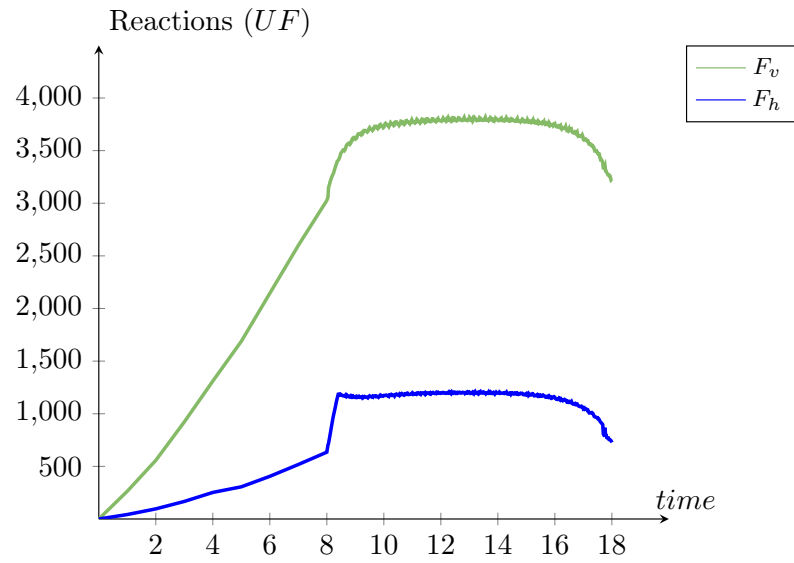


Figure 6.22 – The vertical and horizontal reaction  $F_v$ ,  $F_h$  on the indenter

There was no agreement on the results between the papers which studied this test. However, in order to show that our results are reasonable, we computed the ratio between the horizontal and the vertical reaction, when the indenter slide on the second body. We obtained a ratio approximately equal to 0.32, which is very close to the friction coefficient  $\mu = 0.3$ .

## Conclusion and future works

We developed a simple algorithm to solve Signorini's contact problems, indeed the non-penetration constraints were formulated in a simple form which makes the contact problem formulation well fitted with the interior point method, and there is no need to compute the normal vectors and the projection points on the obstacle, which depend on the solution of the problem, in order to define the non-penetration constraints. Therefore there is no need to use a fixed point algorithm or an active-set strategy, which make the algorithm more simpler and more faster. The drawbacks of this formulation is its restriction for Signorini's problem.

Otherwise all algorithms developed in this manuscript, including the algorithm which solves the frictional contact problem, are based on a minimization methods, which can be a robust way to solve the problem, because we can use optimization techniques such like the line search method in order to converge faster to the solution. In addition, the interior point method was chosen because the matrix structure or sparsity of the generated linear systems remains the same, and the linear dependency of the constraints, when symmetric constraints occur, will not become an issue as in the case of the active-set method.

We developed two symmetric contact algorithms, the first one is based on the penalty method, and the second one is based on the weak formulation of the constraints and on the use of the interior point method to solve the generated minimization problem. In the case of finite deformation, a fixed point method was used in order to transform the contact problem into a sequence of geometric linear ones. Otherwise, the frictional contact problem is transformed as a sequence of Tresca's problems which are based on a minimization principle, in addition a regularization was used to eliminate the non-smooth character of the friction behavior.

Even if the penalty method is employed, we used the interior point method to solve the minimization problem because in the penalty formulation we impose some bounds on the displacement field. Finally we prefer to use the algorithm developed in the chapter 4, where the constraints are in a weak form, indeed we noticed that the penalty method requires more backtracking line search steps especially in the first iterations.

In the future, we would like to make our algorithms work in parallel, in order to run large simulations, and to be coupled with another multiphysics simulations, such like heat transfer or fluid-structure interaction.

# Appendix A

## Contact method using indicator functions defined on triangles

### Outline of the current chapter

<b>A.1 Indicator function of a triangle</b>	<b>175</b>
<b>A.2 Non-penetration condition</b>	<b>177</b>
<b>A.3 Contact problem formulation using indicator functions</b>	<b>178</b>

The frictionless contact problem can be written in the form of a constrained minimization. The solution of the potential energy minimization under the non-penetration constraint is the solution of the contact problem, as it is shown in [29] in the case of the Signorini's contact. We follow the proof given in [29, 31, 30] to prove the same results in the case of contact between two bodies.

In the following theorem,  $\Omega_1$  and  $\Omega_2$  are two domains in  $\mathbb{R}^3$ , which represents respectively the first and the second body. Let  $\Omega = \Omega_1 \cup \Omega_2$ , the border  $\Gamma_0^1, \Gamma_1^1, \Gamma_{C1}$  be disjoint relatively of  $\partial\Omega_1$ , and  $\Gamma_0^2, \Gamma_1^2, \Gamma_{C2}$  be disjoint relatively of  $\partial\Omega_2$ . In addition  $\Gamma_1 = \partial\Omega_1 = \Gamma_0^1 \cup \Gamma_1^1 \cup \Gamma_{C1}$  and  $\Gamma_2 = \partial\Omega_2 = \Gamma_0^2 \cup \Gamma_1^2 \cup \Gamma_{C2}$ . The area of each border  $\Gamma_{C1}$  and  $\Gamma_{C2}$  is supposed to be strictly positive.

$\Gamma_0^1, \Gamma_0^2$  are the borders where a displacement is imposed,  $\Gamma_1^1, \Gamma_1^2$  are the borders where a surface traction is applied, finally  $\Gamma_{C1}, \Gamma_{C2}$  are the potential contact areas in the initial configurations. If a function  $\psi$  is defined on  $\Omega$ , then  $\psi_1 = \psi|_{\Omega_1}$  and  $\psi_2 = \psi|_{\Omega_2}$  represent respectively the restriction of this function on  $\Omega_1$  and  $\Omega_2$ .

The body forces  $f_1$  and  $f_2$  are applied respectively over the bodies  $\Omega_1$  and  $\Omega_2$ , the surface traction  $g_1, g_2$  are applied over  $\Gamma_1^1$  and  $\Gamma_1^2$ , finally  $\phi_0^1$  and  $\phi_0^2$  are the imposed positions on  $\Gamma_0^1$  and  $\Gamma_0^2$ .

The strain energy function is denoted by  $\hat{W}$ , and the first Piola-Kirchhoff stress by  $\mathbf{P}$ . We have that  $\mathbf{P} = \frac{\partial \hat{W}}{\partial \mathbf{F}}$ , where  $\mathbf{F}$  is the deformation gradient tensor.

**Theorem A.1.** *Using the same notations as above, the admissible solutions set  $\Phi$  is defined by:*

$$\Phi = \{\psi : \bar{\Omega} \rightarrow \mathbb{R}^3; \det(\nabla \psi) > 0 \text{ in } \bar{\Omega}; \psi_1 = \phi_0^1 \text{ on } \Gamma_0^1; \psi_2 = \phi_0^2 \text{ on } \Gamma_0^2 \text{ with } \psi_1(\Gamma_{C1}) \subset \psi_2(\Omega_2)^c\} \quad (\text{A.1})$$

The condition  $\psi_1(\Gamma_{C1}) \subset \psi_2(\Omega_2)^c$  describes the non-penetration of the first body with the second body. Let  $\mathcal{E} = \mathcal{E}_1 + \mathcal{E}_2$  denotes the potential energy of the two bodies, and  $\mathcal{E}_1, \mathcal{E}_2$  denote respectively the potential energy of the first body  $\Omega_1$  and of the second body  $\Omega_2$ .

$$\mathcal{E}_1(\psi_1) = \int_{\Omega_1} \hat{W}(\nabla \psi_1) dx - \int_{\Omega_1} \mathbf{f}_1 \cdot \psi_1 dx - \int_{\Gamma_1^1} \mathbf{g}_1 \cdot \psi_1 ds \quad (\text{A.2})$$

$$\mathcal{E}_2(\psi_2) = \int_{\Omega_2} \hat{W}(\nabla \psi_2) dx - \int_{\Omega_2} \mathbf{f}_2 \cdot \psi_2 dx - \int_{\Gamma_1^2} \mathbf{g}_2 \cdot \psi_2 ds \quad (\text{A.3})$$

$$\mathcal{E}(\psi) = \mathcal{E}_1(\psi_1) + \mathcal{E}_2(\psi_2) \quad (\text{A.4})$$

If  $\phi = (\phi_1, \phi_2) \in \Phi$  is smooth enough and solution of the following constrained minimization problem

$$\mathcal{E}(\phi) = \min_{\psi \in \Phi} \mathcal{E}(\psi) \quad (\text{A.5})$$

then  $\phi = (\phi_1, \phi_2)$  satisfies formally the following properties, corresponding to the contact between the two bodies.

$$\left\{ \begin{array}{l} -\operatorname{div} \mathbf{P}_1 = \mathbf{f}_1 \text{ in } \Omega_1 \\ -\operatorname{div} \mathbf{P}_2 = \mathbf{f}_2 \text{ in } \Omega_2 \\ \phi = \phi_0^1 \text{ on } \Gamma_0^1 \\ \phi = \phi_0^2 \text{ on } \Gamma_0^2 \\ \mathbf{P}_1 \mathbf{N}_1 = \mathbf{g}_1 \text{ on } \Gamma_1^1 \\ \mathbf{P}_2 \mathbf{N}_2 = \mathbf{g}_2 \text{ on } \Gamma_1^2 \\ \phi_1(\Gamma_{C1}) \subset \phi_2(\Omega_2)^c \\ \mathbf{P}_1 \mathbf{N}_1 = \mathbf{0} \text{ if } \mathbf{X}_1 \in \Gamma_{C1} \text{ and } \phi_1(\mathbf{X}_1) \notin \phi_1(\partial\Omega_1) \cap \phi_2(\partial\Omega_2) \\ \mathbf{P}_2 \mathbf{N}_2 = \mathbf{0} \text{ if } \mathbf{X}_2 \in \Gamma_{C2} \text{ and } \phi_2(\mathbf{X}_2) \notin \phi_1(\partial\Omega_1) \cap \phi_2(\partial\Omega_2) \\ \mathbf{P}_1 \mathbf{N}_1 = \lambda \mathbf{n}_1 \text{ if } \mathbf{X}_1 \in \Gamma_{C1} \text{ and } \mathbf{x}_1 = \phi_1(\mathbf{X}_1) \in \phi_1(\partial\Omega_1) \cap \phi_2(\partial\Omega_2) \text{ where } \lambda \leq 0 \\ \mathbf{P}_2 \mathbf{N}_2 = \lambda \mathbf{n}_2 \text{ if } \mathbf{X}_2 \in \Gamma_{C2} \text{ and } \mathbf{x}_2 = \phi_2(\mathbf{X}_2) \in \phi_1(\partial\Omega_1) \cap \phi_2(\partial\Omega_2) \text{ where } \lambda \leq 0 \\ \boldsymbol{\sigma}_1 \mathbf{n}_1 \cdot \mathbf{n}_1 = \boldsymbol{\sigma}_2 \mathbf{n}_2 \cdot \mathbf{n}_2 \text{ on } \phi_1(\partial\Omega_1) \cap \phi_2(\partial\Omega_2) \end{array} \right. \quad (\text{A.6})$$

Where  $\mathbf{N}$  and  $\mathbf{n}$  are respectively the outward unit normal vectors on the initial and on the deformed surfaces of the body.  $\boldsymbol{\sigma}$  is the Cauchy stress tensor and  $\boldsymbol{\sigma} \mathbf{n}$  has the same direction of  $\mathbf{P} \mathbf{N}$ .

*Proof.* The function  $\phi$  is a solution of the minimization problem (A.5), therefore

$$\mathcal{E}(\phi) \leq \mathcal{E}(\psi) \quad \forall \psi \in \Phi \quad (\text{A.7})$$

In the following we need the Green formula, which for a smooth enough tensor  $\mathbf{T}$  states

$$\int_{\Omega_1} \mathbf{T} : \nabla \boldsymbol{\theta} \, dx = - \int_{\Omega_1} \operatorname{div}(\mathbf{T}) \cdot \boldsymbol{\theta} \, dx + \int_{\Gamma_1} \mathbf{T} \mathbf{N}_1 \cdot \boldsymbol{\theta} \, ds \quad \forall \boldsymbol{\theta} \quad (\text{A.8})$$

Let  $\mathbf{X} \in \Omega_1$  and  $B_1(\mathbf{X}, r) \subset \Omega_1$  the open ball of center  $\mathbf{X}$  with a small  $r > 0$  (see Figure A.1). Consider  $\boldsymbol{\theta}$  a sufficient smooth function with support in  $B_1(\mathbf{X}, r)$ . There exists  $\epsilon_0 = \epsilon(\boldsymbol{\theta}) > 0$

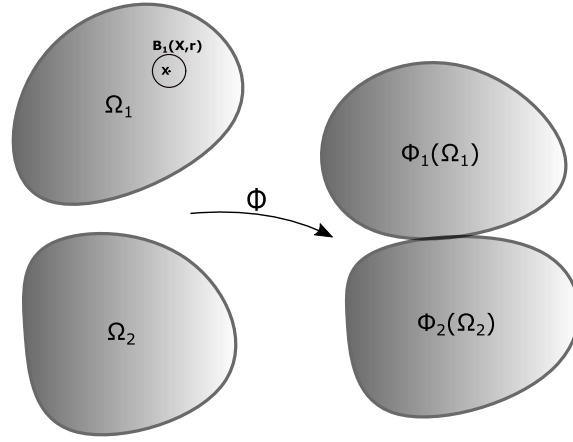


Figure A.1 – The initial and actual configurations

such that  $\phi_\epsilon = \phi + \epsilon \boldsymbol{\theta} \in \Phi \quad \forall |\epsilon| \leq \epsilon_0$ .

$$\mathcal{E}(\phi_\epsilon) - \mathcal{E}(\phi) \geq 0 \quad (\text{A.9})$$

$$\begin{aligned} \mathcal{E}(\phi_\epsilon) - \mathcal{E}(\phi) &= \mathcal{E}(\phi + \epsilon \boldsymbol{\theta}) - \mathcal{E}(\phi) \\ &= \mathcal{E}_1(\phi + \epsilon \boldsymbol{\theta}) + \mathcal{E}_2(\phi) - \mathcal{E}_1(\phi) - \mathcal{E}_2(\phi) \\ &= \mathcal{E}_1(\phi + \epsilon \boldsymbol{\theta}) - \mathcal{E}_1(\phi) \\ &= \int_{\Omega_1} \left( \hat{W}(\nabla \phi_1 + \epsilon \nabla \boldsymbol{\theta}) - \hat{W}(\nabla \phi_1) \right) dx - \epsilon \left( \int_{\Omega_1} \mathbf{f}_1 \cdot \boldsymbol{\theta} \, dx + \int_{\Gamma_1^1} \mathbf{g}_1 \cdot \boldsymbol{\theta} \, ds \right) \end{aligned} \quad (\text{A.10})$$

Otherwise we have

$$\begin{aligned} \hat{W}(\nabla \phi_1 + \epsilon \nabla \boldsymbol{\theta}) - \hat{W}(\nabla \phi_1) &= \epsilon \frac{\partial \hat{W}}{\partial \mathbf{F}} : \nabla \boldsymbol{\theta} + o(\epsilon) \\ &= \epsilon \mathbf{P}_1 : \nabla \boldsymbol{\theta} + o(\epsilon) \end{aligned} \quad (\text{A.11})$$

Using the Green formula in equation (A.8) and the fact that  $\boldsymbol{\theta}$  vanishes in a neighborhood of

$\Gamma_0^1 \cup \Gamma_{C1}$ , we obtain :

$$\begin{aligned} \int_{\Omega_1} \left( \hat{W}(\nabla \phi_1 + \epsilon \nabla \theta) - \hat{W}(\nabla \phi_1) \right) dx &= \epsilon \int_{\Omega_1} \mathbf{P}_1 : \nabla \theta dx + o(\epsilon) \\ &= -\epsilon \int_{\Omega_1} \operatorname{div}(\mathbf{P}_1) \cdot \theta dx + \epsilon \int_{\Gamma_1^1} \mathbf{P}_1 \mathbf{N}_1 \cdot \theta ds + o(\epsilon) \end{aligned} \quad (\text{A.12})$$

Thus

$$\begin{aligned} \mathcal{E}(\phi_\epsilon) - \mathcal{E}(\phi) &= -\epsilon \int_{\Omega_1} \operatorname{div}(\mathbf{P}_1) \cdot \theta dx + \epsilon \int_{\Gamma_1^1} \mathbf{P}_1 \mathbf{N}_1 \cdot \theta ds \\ &\quad - \epsilon \left( \int_{\Omega_1} \mathbf{f}_1 \cdot \theta dx + \int_{\Gamma_1^1} \mathbf{g}_1 \cdot \theta ds \right) + o(\epsilon) \\ &= \epsilon \left\{ \int_{\Omega_1} (-\operatorname{div}(\mathbf{P}_1) - \mathbf{f}_1) \cdot \theta dx + \int_{\Gamma_1^1} (\mathbf{P}_1 \mathbf{N}_1 - \mathbf{g}_1) \cdot \theta ds + \frac{o(\epsilon)}{\epsilon} \right\} \geq 0 \end{aligned} \quad (\text{A.13})$$

Taking  $\epsilon > 0$  and taking the limit  $\epsilon \rightarrow 0^+$  we have:

$$\int_{\Omega_1} (-\operatorname{div}(\mathbf{P}_1) - \mathbf{f}_1) \cdot \theta dx + \int_{\Gamma_1^1} (\mathbf{P}_1 \mathbf{N}_1 - \mathbf{g}_1) \cdot \theta ds \geq 0 \quad (\text{A.14})$$

Taking  $\epsilon < 0$  and taking the limit  $\epsilon \rightarrow 0^-$  we have:

$$\int_{\Omega_1} (-\operatorname{div}(\mathbf{P}_1) - \mathbf{f}_1) \cdot \theta dx + \int_{\Gamma_1^1} (\mathbf{P}_1 \mathbf{N}_1 - \mathbf{g}_1) \cdot \theta ds \leq 0 \quad (\text{A.15})$$

Therefore

$$\int_{\Omega_1} (-\operatorname{div}(\mathbf{P}_1) - \mathbf{f}_1) \cdot \theta dx + \int_{\Gamma_1^1} (\mathbf{P}_1 \mathbf{N}_1 - \mathbf{g}_1) \cdot \theta ds = 0 \quad (\text{A.16})$$

The support of  $\theta$  is in  $B_1(\mathbf{X}, r) \subset \Omega_1$ , thus we obtain:

$$\int_{B_1(\mathbf{X}, r)} (-\operatorname{div}(\mathbf{P}_1) - \mathbf{f}_1) \cdot \theta dx = 0 \quad (\text{A.17})$$

We deduce that  $-\operatorname{div}(\mathbf{P}_1) = \mathbf{f}_1$  in  $B_1(\mathbf{X}, r)$ , and then it's true in  $\Omega_1$

Let's proceed in the same manner for the second body by considering  $\mathbf{X} \in \Omega_2$  and  $B_2(\mathbf{X}, r) \subset \Omega_2$ . For any sufficiently smooth function  $\theta$  with a support in  $B_2(\mathbf{X}, r)$  and  $\theta = 0$  on  $\bar{\Omega}_1$ , there exists  $\epsilon_0 = \epsilon(\theta) > 0$  such that  $\phi_\epsilon = \phi + \epsilon \theta \in \Phi \quad \forall |\epsilon| \leq \epsilon_0$ . We obtain then  $-\operatorname{div}(\mathbf{P}_2) = \mathbf{f}_2$  in  $\Omega_2$ .

Let  $\mathbf{X} \in \Gamma_1^1$  where the surface traction are applied, consider any smooth function  $\theta : \bar{\Omega}_1 \rightarrow \mathbf{R}^3$  with a support in  $B(\mathbf{X}, r) \cap \bar{\Omega}_1$  where  $r > 0$  and small, there exists a  $\epsilon_1(\theta) > 0$  such that  $\phi_\epsilon = \phi + \epsilon \theta \in \Phi \quad \forall |\epsilon| \leq \epsilon_1$ . The equation (A.16) can always be used, thus using the fact that  $-\operatorname{div}(\mathbf{P}_1) = \mathbf{f}_1$  in  $\Omega_1$ , we obtain:

$$\int_{\Gamma_1^1} (\mathbf{P}_1 \mathbf{N}_1 - \mathbf{g}_1) \cdot \theta ds = 0 \quad (\text{A.18})$$

We deduce that  $\mathbf{P}_1\mathbf{N}_1 = \mathbf{g}_1$  on  $\Gamma_1^1$ . Doing the same work for the second body we obtain  $\mathbf{P}_2\mathbf{N}_2 = \mathbf{g}_2$  on  $\Gamma_1^2$ .

Let  $\mathbf{X} \in \Gamma_{C1}$  such that  $\phi_1(\mathbf{X}) \notin \phi_1(\partial\Omega_1) \cap \phi_2(\partial\Omega_2)$  (see Figure A.2), consider any smooth function  $\boldsymbol{\theta} : \tilde{\Omega}_1 \rightarrow \mathbb{R}^3$  with a support in  $B(\mathbf{X}, r) \cap \tilde{\Omega}_1$  where  $r > 0$  and small, there exists a  $\epsilon_2(\boldsymbol{\theta}) > 0$  such that  $\phi_\epsilon = \phi + \epsilon\boldsymbol{\theta} \in \Phi \quad \forall |\epsilon| \leq \epsilon_2$ . As before,  $\mathcal{E}(\phi_\epsilon) - \mathcal{E}(\phi) \geq 0$ , thus using Green's formula and the equations of equilibrium we obtain:

$$\epsilon \left\{ \int_{\Gamma_{C1}} \mathbf{P}_1\mathbf{N}_1 \cdot \boldsymbol{\theta} \, ds + \frac{o(\epsilon)}{\epsilon} \right\} \geq 0 \tag{A.19}$$

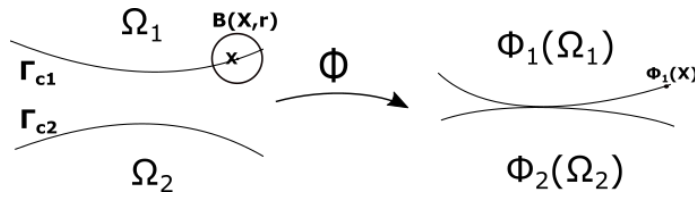


Figure A.2 – The case where the stress is zero for the point  $\mathbf{X}$

We deduce that  $\mathbf{P}_1\mathbf{N}_1 = \mathbf{0}$  for  $\mathbf{X} \in \Gamma_{C1}$  such that  $\phi_1(\mathbf{X}) \notin \phi_1(\partial\Omega_1) \cap \phi_2(\partial\Omega_2)$ . We can do the same work for the second body.

We still have the last equations of the problem (A.6) to demonstrate. We consider  $\mathbf{Y} \in \Gamma_{C1}$  such that  $\mathbf{y} = \phi_1(\mathbf{Y}) \in \phi_2(\partial\Omega_2)$ , supposing that the boundaries of  $\phi_1(\Omega_1)$  and  $\phi_2(\Omega_2)$  are smooth enough, then we can assume that  $\phi_1(\Gamma_{C1})$  and  $\phi_2(\Gamma_{C2})$  have the same tangent space at the point  $\mathbf{y} = \phi_1(\mathbf{Y})$ . Let  $V(\mathbf{Y})$  be a neighborhood of  $\mathbf{y}$  and  $\mathbf{t}_1, \mathbf{t}_2, \mathbf{n}_1$  a 3 smooth fields, such that  $\mathbf{t}_1, \mathbf{t}_2$  are linearly independent and span the tangent space at  $V \cap \phi_1(\Gamma_{C1})$  and  $\|\mathbf{t}_1\| = \|\mathbf{t}_2\| = 1$ ,  $\mathbf{n}_1$  is the outer unit normal vector at  $\phi_1(\Gamma_{C1})$ . Consider the ball  $B(\mathbf{Y}, r)$  such that  $B(\mathbf{Y}, r) \cap \Gamma_1 \subset \Gamma_{C1}$  and  $\phi_1(B(\mathbf{Y}, r)) \subset V$  (see Figure A.3), therefore given two smooth  $\theta_1, \theta_2 : \tilde{\Omega}_1 \rightarrow \mathbb{R}$  with support in  $B(\mathbf{Y}, r)$  and vanish on  $\Omega_2$ , there exist  $\epsilon_3(\theta_1, \theta_2) > 0$  and two functions  $\lambda_1^\epsilon, \lambda_2^\epsilon : \tilde{\Omega}_1 \rightarrow \mathbb{R}$  with support in  $B(\mathbf{Y}, r)$  and vanish on  $\Omega_2$  such that

$$\begin{cases} \phi_\alpha^\epsilon = \phi + \epsilon(\theta_\alpha \mathbf{t}_\alpha + \lambda_\alpha^\epsilon \mathbf{n}_1) \in \Phi \quad \forall |\epsilon| \leq \epsilon_3 \\ |\lambda_\alpha^\epsilon| = o(\epsilon) \end{cases} \tag{A.20}$$

where  $\alpha = 1, 2$ .

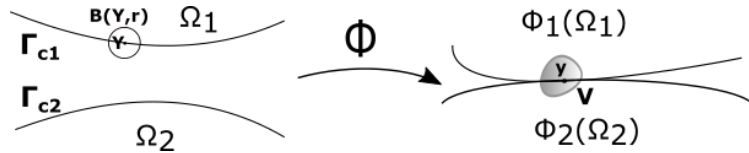


Figure A.3 – The point  $\mathbf{y} = \phi_1(\mathbf{Y})$  and its neighborhood

Taking  $\mathcal{E}(\phi_\alpha^\epsilon) - \mathcal{E}(\phi) = \mathcal{E}_1(\phi_\alpha^\epsilon) - \mathcal{E}_1(\phi) \geq 0$  and repeating the same procedure as before, we

obtain:

$$\epsilon \left\{ \int_{\Gamma_{C1}} \mathbf{P}_1 \mathbf{N}_1 \cdot \theta_\alpha \mathbf{t}_\alpha ds + o(\epsilon) + \frac{o(\epsilon)}{\epsilon} \right\} \geq 0 \quad (\text{A.21})$$

We conclude as before that  $\mathbf{P}_1 \mathbf{N}_1 \cdot \mathbf{t}_\alpha = 0$  for  $\alpha = 1, 2$ , so  $\mathbf{P}_1 \mathbf{N}_1$  is normal to the tangent plane and has the same direction of  $\mathbf{n}_1 \Rightarrow \exists \lambda_1 \in \mathbb{R}$  such that  $\mathbf{P}_1 \mathbf{N}_1 = \lambda_1 \mathbf{n}_1$  at  $\mathbf{X}_1 \in \Gamma_{C1}$  where  $\phi_1(\mathbf{X}_1) \in \phi_2(\partial\Omega_2)$ . The same work can be done for the second body  $\mathbf{P}_2 \mathbf{N}_2 = \lambda_2 \mathbf{n}_2$  but in this case  $\mathbf{n}_2 = -\mathbf{n}_1$ .

We will prove that the coefficients  $\lambda_1, \lambda_2$  are negative. Consider any positive smooth function  $\theta : \bar{\Omega}_1 \rightarrow \mathbb{R}_+$  with support in  $B(\mathbf{Y}, r)$  and vanishes on  $\Omega_2$ , then  $\exists \epsilon_4(\theta) > 0$  such that

$$\phi_\epsilon = \phi - \epsilon \theta \mathbf{n}_1 \in \Phi \quad \forall 0 \leq \epsilon \leq \epsilon_4 \quad (\text{A.22})$$

Thus by the same procedure we obtain

$$\epsilon \left\{ \int_{\Gamma_{C1}} -\mathbf{P}_1 \mathbf{N}_1 \cdot \mathbf{n}_1 \theta ds + \frac{o(\epsilon)}{\epsilon} \right\} \geq 0 \quad (\text{A.23})$$

Then with  $\epsilon \rightarrow 0^+$  we have:

$$\int_{\Gamma_{C1}} \mathbf{P}_1 \mathbf{N}_1 \cdot \mathbf{n}_1 \theta ds \leq 0 \quad (\text{A.24})$$

Thus  $\lambda_1 = \mathbf{P}_1 \mathbf{N}_1 \cdot \mathbf{n}_1 \leq 0$  at  $\mathbf{X}_1 \in \Gamma_{C1}$  where  $\phi_1(\mathbf{X}_1) \in \phi_2(\partial\Omega_2)$ . Same work can be done for the second body  $\Omega_2$  to obtain  $\lambda_2 \leq 0$ .

Finally let  $\gamma = \phi_1(\Gamma_{C1}) \cap \phi_2(\Gamma_{C2})$  where the contact is done and  $\mathbf{x} \in \gamma$ . We consider the ball  $B(\mathbf{x}, r)$  and we call  $\gamma^* = B(\mathbf{x}, r) \cap \gamma$ , and  $\Gamma_1^* = \phi_1^{-1}(\gamma^*) \subset \Gamma_{C1}$ ,  $\Gamma_2^* = \phi_2^{-1}(\gamma^*) \subset \Gamma_{C2}$ .

Given a smooth function  $\theta$  with a support in  $B(\mathbf{x}, r)$ , there exists a small  $\epsilon_5(\theta) > 0$  such that:

$$\phi_\epsilon = \phi + \epsilon \cdot (\theta \circ \phi) \cdot \mathbf{n}_1 \in \Phi \quad \forall |\epsilon| \leq \epsilon_5 \quad (\text{A.25})$$

with  $\mathbf{n}_2 = -\mathbf{n}_1$  on  $\gamma^*$ . We have  $\mathcal{E}(\phi_\epsilon) - \mathcal{E}(\phi) \geq 0$  then  $\mathcal{E}_1(\phi_\epsilon) - \mathcal{E}_1(\phi) + \mathcal{E}_2(\phi_\epsilon) - \mathcal{E}_2(\phi) \geq 0$ . The equilibrium equations and the Green's formula lead to:

$$\epsilon \left\{ \int_{\Gamma_1^*} \mathbf{P}_1 \mathbf{N}_1 \cdot \mathbf{n}_1 \cdot (\theta \circ \phi_1) ds + \int_{\Gamma_2^*} \mathbf{P}_2 \mathbf{N}_2 \cdot \mathbf{n}_1 \cdot (\theta \circ \phi_2) ds + \frac{o(\epsilon)}{\epsilon} \right\} \geq 0 \quad (\text{A.26})$$

Therefore we obtain

$$\int_{\Gamma_1^*} \mathbf{P}_1 \mathbf{N}_1 \cdot \mathbf{n}_1 \cdot (\theta \circ \phi_1) ds - \int_{\Gamma_2^*} \mathbf{P}_2 \mathbf{N}_2 \cdot \mathbf{n}_2 \cdot (\theta \circ \phi_2) ds = 0 \quad (\text{A.27})$$

Otherwise we have a relation between the Cauchy  $\boldsymbol{\sigma}$  and the first Piola-Kirchhoff  $\mathbf{P}$  stress tensor:  $\mathbf{P} = J \boldsymbol{\sigma} \mathbf{F}^{-T}$  and  $\mathbf{n} ds' = J \mathbf{F}^{-T} \mathbf{N} ds$ , where  $\mathbf{F}$  is the deformation gradient tensor and  $J$  its determinant, otherwise speaking  $\boldsymbol{\sigma} \mathbf{n} ds' = \mathbf{P} \mathbf{N} ds$ . Therefore the equation (A.27) becomes

$$\int_{\gamma^*} \boldsymbol{\sigma}_1 \mathbf{n}_1 \cdot \mathbf{n}_1 \theta ds' - \int_{\gamma^*} \boldsymbol{\sigma}_2 \mathbf{n}_2 \cdot \mathbf{n}_2 \theta ds' = 0 \quad (\text{A.28})$$

$$\Rightarrow \int_{\gamma^*} (\boldsymbol{\sigma}_1 \mathbf{n}_1 \cdot \mathbf{n}_1 - \boldsymbol{\sigma}_2 \mathbf{n}_2 \cdot \mathbf{n}_2) \theta \, ds' = 0 \quad (\text{A.29})$$

Therefore  $\boldsymbol{\sigma}_1 \mathbf{n}_1 \cdot \mathbf{n}_1 = \boldsymbol{\sigma}_2 \mathbf{n}_2 \cdot \mathbf{n}_2$ .

□

In contact analysis we have the non-penetration condition to respect, between a body and a foundation or between two bodies. In the following, we create a function which tells if the penetration occurs or not. As the second body in its actual configuration  $\phi_2(\Omega_2)$  is composed of triangles, the non-penetration condition imposes that each material point in  $\phi_1(\Omega_1)$  (more precisely at the contact border of  $\phi_1(\Omega_1)$ ) can not belong to each triangle of  $\phi_2(\Omega_2)$ .

## A.1 Indicator function of a triangle

Let  $\mathcal{T} \subset \mathbb{R}^2$  be a triangle, in this part we create the indicator function of a triangle  $F_{\mathcal{T}} : \mathbb{R}^2 \rightarrow \mathbb{R}_+$  which is a function strictly positive at the interior of the triangle  $\overset{\circ}{\mathcal{T}}$  and equal to zero otherwise. This function will be smooth enough ( $C^2$ ) in order to use it in our optimization process.

The idea begins first by considering a  $C^2$  function which is equal to zero at  $] - \infty, 0]$  and strictly positive at  $]0, +\infty[$ , an example of such functions is shown below

$$f(x) = \begin{cases} 0 & \text{if } x \leq 0 \\ x^3 & \text{if } x > 0 \end{cases} \quad (\text{A.30})$$

Without loss of generality we consider the triangle  $\mathcal{T}_0$  defined by the following points:  $(0, 0)$ ,  $(1, 0)$  and  $(0, 1)$ . Let the functions  $F_1, F_2, F_3 : \mathbb{R}^2 \rightarrow \mathbb{R}_+$  be defined as follows

$$F_1(x, y) = \begin{cases} 0 & \text{if } x \leq 0 \\ x^3 & \text{if } x > 0 \end{cases} \quad (\text{A.31})$$

$$F_2(x, y) = \begin{cases} 0 & \text{if } y \leq 0 \\ y^3 & \text{if } y > 0 \end{cases} \quad (\text{A.32})$$

And

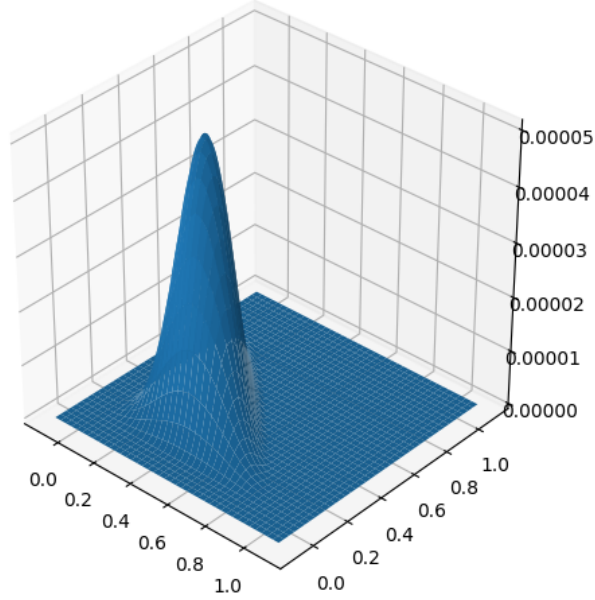
$$F_3(x, y) = \begin{cases} -(y + x - 1)^3 & \text{if } y + x - 1 < 0 \\ 0 & \text{if } y + x - 1 \geq 0 \end{cases} \quad (\text{A.33})$$

The functions  $F_1$ ,  $F_2$  and  $F_3$  are  $C^2(\mathbb{R}^2)$ .

Finally we consider the function  $F_p : \mathbb{R}^2 \rightarrow \mathbb{R}_+$  defined by

$$F_p(x, y) = F_1(x, y) \cdot F_2(x, y) \cdot F_3(x, y) \quad (\text{A.34})$$

Therefore the function  $F_p$  is  $C^2(\mathbb{R}^2)$  and is shown in the Figure A.4.

Figure A.4 – The  $F_p$  function

If  $(X, Y)$  is a point in  $\mathbb{R}^2$  then  $F_p$  satisfies the following properties

$$\begin{cases} F_p(X, Y) > 0 & \text{if } (X, Y) \in \overset{\circ}{\mathcal{T}}_0 \\ F_p(X, Y) = 0 & \text{otherwise} \end{cases} \quad (\text{A.35})$$

We call the function  $F_p$ , the indicator function of the triangle  $\mathcal{T}_0$ .

More generally, consider the triangle  $\mathcal{T}$  defined by the following points  $(x_A, y_A)$ ,  $(x_B, y_B)$ ,  $(x_C, y_C)$ , then the application  $\pi_{\mathcal{T}}$  which transforms  $\mathcal{T}$  into  $\mathcal{T}_0$  is defined below by

$$\pi_{\mathcal{T}}(x, y) = A \cdot \begin{pmatrix} x - x_A \\ y - y_A \end{pmatrix} \quad (\text{A.36})$$

where the matrix  $A$  is defined by

$$A = \frac{1}{\Delta} \begin{bmatrix} y_C - y_A & -(x_C - x_A) \\ -(y_B - y_A) & x_B - x_A \end{bmatrix} \quad (\text{A.37})$$

with  $\Delta = (x_B - x_A)(y_C - y_A) - (x_C - x_A)(y_B - y_A)$ .

Therefore the indicator function of the triangle  $\mathcal{T}$  is the function:

$$F_{\mathcal{T}}(x, y) = F_p(\pi_{\mathcal{T}}(x, y)) \quad \forall (x, y) \in \mathbb{R}^2 \quad (\text{A.38})$$

Same as the function  $F_p$ , if  $(X, Y)$  is a point in  $\mathbb{R}^2$  then  $F_{\mathcal{T}}$  satisfies the following properties

$$\begin{cases} F_{\mathcal{T}}(X, Y) > 0 & \text{if } (X, Y) \in \overset{\circ}{\mathcal{T}} \\ F_{\mathcal{T}}(X, Y) = 0 & \text{otherwise} \end{cases} \quad (\text{A.39})$$

## A.2 Non-penetration condition

The goal here is to try to create a function which is strictly positive at the domain of the second body and equal to zero otherwise, so it can be used in a penalty method for example to avoid the penetration between the bodies. In the finite element configuration the second body in its actual configuration  $\phi_2(\Omega_2)$  or the obstacle is composed of the triangles family  $\{\mathcal{T}_j \mid j = 1, \dots, n_T\}$ , where  $n_T$  is the triangles number. In addition, each triangle is composed from three points  $(x_i, y_i) = (X_i + U_i^x, Y_i + U_i^y)$  with  $i = 1, 2, 3$ , where  $(X_i, Y_i)$  and  $(U_i^x, U_i^y)$  are respectively the initial position and the actual displacement of the node  $i$ .

The indicator function  $F_{\phi_2(\Omega_2)}$  of  $\phi_2(\Omega_2)$  is the sum of the indicator functions of each triangle  $\mathcal{T}_j$ , and is equal to

$$F_{\phi_2(\Omega_2)}(x, y) = \sum_{j=1}^{n_T} F_{\mathcal{T}_j}(x, y) \quad (\text{A.40})$$

The function  $F_{\phi_2(\Omega_2)}$  has the following properties, for  $(X, Y) \in \mathbb{R}^2$

$$\begin{cases} F_{\phi_2(\Omega_2)}(X, Y) > 0 & \text{if } (X, Y) \in \bigcup_{j=1}^{n_T} \overset{\circ}{\mathcal{T}}_j \\ F_{\phi_2(\Omega_2)}(X, Y) = 0 & \text{otherwise} \end{cases} \quad (\text{A.41})$$

The non-penetration condition between the bodies  $\Omega_1$  and  $\Omega_2$  (the edges of  $\Omega_2$  were not taken into account) can be stated as follows

$$F_{\phi_2(\Omega_2)}(\mathbf{x}) = 0 \quad \forall \mathbf{x} \in \phi_1(\Gamma_{C1}) \quad (\text{A.42})$$

where  $\Gamma_{C1}$  is the potential contact area of the first body  $\Omega_1$  and  $\mathbf{x} = \mathbf{X} + \mathbf{u}$  the actual displacement, with  $\mathbf{X}$  the initial position.

Because  $F_{\phi_2(\Omega_2)} \geq 0$  then, a non-penetration condition equivalent to (A.42) can be given by

$$\int_{\Gamma_{C1}} F_{\phi_2(\Omega_2)}(\mathbf{X} + \mathbf{u}) ds = 0 \quad (\text{A.43})$$

### A.3 Contact problem formulation using indicator functions

We consider the following contact problem

$$\begin{cases} \min(\mathcal{E}_p(\mathbf{U})) & \text{subjected to} \\ \int_{\Gamma_{C1}} F_{\phi_2(\Omega_2)}(\mathbf{X} + \mathbf{u}) ds = 0 \end{cases} \quad (\text{A.44})$$

where  $\mathcal{E}_p$  is the total potential energy. One can use the penalty method, and the contact problem becomes

$$\min \left( \mathcal{E}_p(\mathbf{U}) + \mu \int_{\Gamma_{C1}} F_{\phi_2(\Omega_2)}(\mathbf{X} + \mathbf{u}) ds \right) \quad (\text{A.45})$$

where  $\mu$  is the penalty factor. In order to make the problem symmetric, one can define in the same manner an indicator function on  $\phi_1(\Omega_1)$ , in order to obtain

$$\min \left( \mathcal{E}_p(\mathbf{U}) + \mu \int_{\Gamma_{C1}} F_{\phi_2(\Omega_2)}(\mathbf{X} + \mathbf{u}) ds + \mu \int_{\Gamma_{C2}} F_{\phi_1(\Omega_1)}(\mathbf{X} + \mathbf{u}) ds \right) \quad (\text{A.46})$$

The formulation presented above gives an equality constraints for the non-penetration between the bodies, in addition there is no need to an active-set strategy or a fixed point method in order to treat the contact. On the other hand the drawback is that, it is a time consuming and it works only for  $P_1$  finite elements. The formulation can be generalized to the three dimensional case by considering a tetrahedron instead of a triangle, only  $F_p$  changes to become a multiplication of 4 functions instead of 3. Otherwise the indicator function  $F_{\phi_2(\Omega_2)}$  can be defined on a part of  $\phi_2(\Omega_2)$  instead of the whole  $\phi_2(\Omega_2)$ . Finally this method can be interesting to solve contact problems between polygonal bodies.

# Bibliography

- [1] C. M. 5.4. *Structural Mechanics Module - Verification Examples*. 2018.
- [2] M. ABBAS. *Code\_Aster [R5.03.19] Loi de comportement hyperélastique : matériau presque incompressible*. EDF R&D. Aug. 2013.
- [3] M. ABBAS. *Code\_Aster [R5.03.50] - Formulation discrète du contact-frottement*. EDF R&D. Nov. 2017.
- [4] M. ABBAS. *Code\_Aster [V6.04.187] SSNV187 - Validation de la loi ELAS\_HYPER sur un cube*. EDF R&D. May 2018.
- [5] N. El-Abbasi and K.-J. Bathe. “Stability and patch test performance of contact discretizations and a new solution algorithm”. In: *Computers & Structures* 79.16 (2001), pp. 1473–1486.
- [6] R. A. Adams and J. J. Fournier. *Sobolev spaces*. Vol. 140. Elsevier, 2003.
- [7] P. Alart. “Méthode de Newton généralisée en mécanique du contact”. In: *Journal de mathématiques pures et appliquées* 76.1 (1997), pp. 83–108.
- [8] P. Alart and A. Curnier. “A mixed formulation for frictional contact problems prone to Newton like solution methods”. In: *Computer methods in applied mechanics and engineering* 92.3 (1991), pp. 353–375.
- [9] P. R. Amestoy, I. S. Duff, J.-Y. L’Excellent, and J. Koster. “MUMPS: a general purpose distributed memory sparse solver”. In: *International Workshop on Applied Parallel Computing*. Springer. 2000, pp. 121–130.
- [10] C. Annavarapu, M. Hautefeuille, and J. E. Dolbow. “A Nitsche stabilized finite element method for frictional sliding on embedded interfaces. Part I: Single interface”. In: *Computer Methods in Applied Mechanics and Engineering* 268 (2014), pp. 417–436.
- [11] K. M. Anstreicher and J.-P. Vial. “On the convergence of an infeasible primal-dual interior-point method for convex programming”. In: *Optimization methods and software* 3.4 (1994), pp. 273–283.
- [12] M. Astorino, J.-F. Gerbeau, O. Pantz, and K.-F. Traore. “Fluid–structure interaction and multi-body contact: application to aortic valves”. In: *Computer Methods in Applied Mechanics and Engineering* 198.45-46 (2009), pp. 3603–3612.
- [13] S. Auliac. “développement d’outils d’optimisation pour freefem++”. PhD thesis. Université Pierre et Marie Curie-Paris VI, 2014.
- [14] J. M. Ball. “Convexity conditions and existence theorems in nonlinear elasticity”. In: *Archive for rational mechanics and Analysis* 63.4 (1976), pp. 337–403.

- [15] F. B. Belgacem, P. Hild, and P. Laborde. “The mortar finite element method for contact problems”. In: *Mathematical and Computer Modelling* 28.4-8 (1998), pp. 263–271.
- [16] P. Boieri, F. Gastaldi, and D. Kinderlehrer. “Existence, uniqueness, and regularity results for the two-body contact problem”. In: *Applied Mathematics and Optimization* 15.1 (1987), pp. 251–277.
- [17] J. Bonet and R. D. Wood. *Nonlinear continuum mechanics for finite element analysis*. Cambridge university press, 1997.
- [18] d. M. Bonnet and A. Frangi. “Analyse des solides déformables par la méthode des éléments finis”. In: *European Journal of Computational Mechanics/Revue Européenne de Mécanique Numérique* 16.5 (2007), pp. 667–668.
- [19] A. Boukamel. “Modélisation mécaniques et numériques des matériaux et structures en élastomeres”. PhD thesis. Université de la Méditerranée-Aix-Marseille II, 2006.
- [20] H. Brezis. *Functional analysis, Sobolev spaces and partial differential equations*. Springer Science & Business Media, 2010.
- [21] L. Campos, J. Oden, and N. Kikuchi. “A numerical analysis of a class of contact problems with friction in elastostatics”. In: *Computer Methods in Applied Mechanics and Engineering* 34.1-3 (1982), pp. 821–845.
- [22] C. Carstensen, O. Scherf, and P. Wriggers. “Adaptive finite elements for elastic bodies in contact”. In: *SIAM Journal on Scientific Computing* 20.5 (1999), pp. 1605–1626.
- [23] D. Chamoret, P. Saillard, A. Rassineux, and J.-M. Bergheau. “New smoothing procedures in contact mechanics”. In: *Journal of Computational and applied Mathematics* 168.1-2 (2004), pp. 107–116.
- [24] S. Chan and I. Tuba. “A finite element method for contact problems of solid bodies-Part I. Theory and validation”. In: *International Journal of Mechanical Sciences* 13.7 (1971), pp. 615–625.
- [25] F. Chouly and P. Hild. “A Nitsche-based method for unilateral contact problems: numerical analysis”. In: *SIAM Journal on Numerical Analysis* 51.2 (2013), pp. 1295–1307.
- [26] F. Chouly and P. Hild. “On convergence of the penalty method for unilateral contact problems”. In: *Applied Numerical Mathematics* 65 (2013), pp. 27–40.
- [27] F. Chouly, P. Hild, and Y. Renard. “Symmetric and non-symmetric variants of Nitsche’s method for contact problems in elasticity: theory and numerical experiments”. In: *Mathematics of Computation* 84.293 (2015), pp. 1089–1112.
- [28] P. Christensen, A. Klarbring, J.-S. Pang, and N. Strömberg. “Formulation and comparison of algorithms for frictional contact problems”. In: *International Journal for Numerical Methods in Engineering* 42.1 (1998), pp. 145–173.
- [29] P. G. Ciarlet. *Mathematical Elasticity: Volume I: three-dimensional elasticity*. North-Holland, 1988.
- [30] P. G. Ciarlet and J. Nečas. “Injectivity and self-contact in nonlinear elasticity”. In: *Archive for Rational Mechanics and Analysis* 97.3 (1987), pp. 171–188.
- [31] P. G. Ciarlet and J. Nečas. “Unilateral problems in nonlinear, three-dimensional elasticity”. In: *Archive for rational mechanics and analysis* 87.4 (1985), pp. 319–338.
- [32] M. Cocu. “Existence of solutions of Signorini problems with friction”. In: *International journal of engineering science* 22.5 (1984), pp. 567–575.

- [33] J. Courtney-Pratt and E. Eisner. “The effect of a tangential force on the contact of metallic bodies”. In: *Proceedings of the Royal Society of London. Series A. Mathematical and Physical Sciences* 238.1215 (1957), pp. 529–550.
- [34] M. A. Crisfield. *Non-linear finite element analysis of solids and structures, Volume 1: Essentials*. John Wiley & Sons, 2000.
- [35] M. A. Crisfield. *Non-linear finite element analysis of solids and structures, Volume 2: Advanced Topics*. John Wiley & Sons, 2000.
- [36] A. Curnier, Q.-C. He, and J. J. Telega. “Formulation of unilateral contact between two elastic bodies undergoing finite deformations”. In: *Comptes rendus de l’Académie des sciences. Série II, Mécanique, physique, chimie, sciences de l’univers, sciences de la terre* 314 (Jan. 1992).
- [37] L. De Lorenzis, P. Wriggers, and C. Weisenfels. “Computational contact mechanics with the finite element method”. In: *Encyclopedia of computational mechanics second edition* (2017), pp. 1–45.
- [38] G. Drouot and P. Hild. “An accurate local average contact method for nonmatching meshes”. In: *Numerische Mathematik* 136.2 (2017), pp. 467–502.
- [39] G. Dumont. “Algorithme de contraintes actives et contact unilatéral sans frottement”. In: *Revue européenne des éléments finis* 4.1 (1995), pp. 55–73.
- [40] G. Duvaut and J. L. Lions. “Inequalities in mechanics and physics”. In: (1976).
- [41] C. Eck and J. Jarusek. “Existence results for the static contact problem with Coulomb friction”. In: *Mathematical Models and Methods in Applied Sciences* 8.03 (1998), pp. 445–468.
- [42] Z.-Q. Feng, J.-M. Cros, and B. Magnain. “Un algorithme efficace pour les problèmes d’impact avec frottement”. In: *Revue Européenne des Eléments* 14.1 (2005), pp. 65–86.
- [43] Z.-Q. Feng, B. Magnain, and J.-M. Cros. “FER/Impact: logiciel de simulation numérique des problèmes d’impact”. In: *European Journal of Computational Mechanics/Revue Européenne de Mécanique Numérique* 15.1-3 (2006), pp. 175–186.
- [44] G. Fichera. *Problemi elastostatici con vincoli unilaterali: il problema di Signorini con ambigue condizioni al contorno*. Accademia nazionale dei Lincei, 1964.
- [45] K. Fischer and P. Wriggers. “Frictionless 2D contact formulations for finite deformations based on the mortar method”. In: *Computational Mechanics* 36.3 (2005), pp. 226–244.
- [46] K. A. Fischer and P. Wriggers. “Mortar based frictional contact formulation for higher order interpolations using the moving friction cone”. In: *Computer methods in applied mechanics and engineering* 195.37-40 (2006), pp. 5020–5036.
- [47] A. Forsgren, P. E. Gill, and M. H. Wright. “Interior methods for nonlinear optimization”. In: *SIAM review* 44.4 (2002), pp. 525–597.
- [48] A. Francavilla and O. Zienkiewicz. “A note on numerical computation of elastic contact problems”. In: *International Journal for Numerical Methods in Engineering* 9.4 (1975), pp. 913–924.
- [49] E. de France. *Code\_Aster [R5.03.52] - Eléments de contact dérivés d’une formulation hybride continue*. EDF R&D. 2019.
- [50] E. de France. *Finite element code\_aster, Analysis of Structures and Thermomechanics for Studies and Research*. Code\_Aster. Open source on [www.code-aster.org](http://www.code-aster.org). 1989–2017.

- [51] D. Gabriel, J. Plešek, and M. Ulbin. “Symmetry preserving algorithm for large displacement frictionless contact by the pre-discretization penalty method”. In: *International journal for numerical methods in engineering* 61.15 (2004), pp. 2615–2638.
- [52] A. Giannakopoulos. “The return mapping method for the integration of friction constitutive relations”. In: *Computers & structures* 32.1 (1989), pp. 157–167.
- [53] N. I. Gould and P. L. Toint. “Numerical methods for large-scale non-convex quadratic programming”. In: *Trends in Industrial and Applied Mathematics* (2002), pp. 149–179.
- [54] J. Hallquist, G. Goudreau, and D. Benson. “Sliding interfaces with contact-impact in large-scale Lagrangian computations”. In: *Computer methods in applied mechanics and engineering* 51.1-3 (1985), pp. 107–137.
- [55] F. Hecht. “New development in FreeFem++”. In: *J. Numer. Math.* 20.3-4 (2012), pp. 251–265.
- [56] P. Hild. “A sign preserving mixed finite element approximation for contact problems”. In: *International Journal of Applied Mathematics and Computer Science* 21.3 (2011), pp. 487–498.
- [57] P. Hild. “An example of nonuniqueness for the continuous static unilateral contact model with Coulomb friction”. In: *Comptes Rendus Mathématique* 337.10 (2003), pp. 685–688.
- [58] P. Hild. “On finite element uniqueness studies for Coulomb’s frictional contact model”. In: *International Journal of Applied Mathematics and Computer Science* 12 (2002), pp. 41–50.
- [59] P. Hild. “Problèmes de contact unilatéral et maillages éléments finis incompatibles”. PhD thesis. 1998.
- [60] P. Hild and Y. Renard. “A stabilized Lagrange multiplier method for the finite element approximation of contact problems in elastostatics”. In: *Numerische Mathematik* 115.1 (2010), pp. 101–129.
- [61] C. Hogue. “Shape representation and contact detection for discrete element simulations of arbitrary geometries”. In: *Engineering Computations* 15.3 (1998), pp. 374–390.
- [62] C. O. Horgan and G. Saccomandi. “Constitutive models for compressible nonlinearly elastic materials with limiting chain extensibility”. In: *Journal of Elasticity* 77.2 (2004), pp. 123–138.
- [63] H. Houssein, S. Garnotel, and F. Hecht. “Contact Problems in Industrial Applications Using FreeFEM”. In: *14th WCCM-ECCOMAS Congress 2020*. Vol. 2500. 2021.
- [64] S. Hüeber and B. I. Wohlmuth. “A primal–dual active set strategy for non-linear multi-body contact problems”. In: *Computer Methods in Applied Mechanics and Engineering* 194.27-29 (2005), pp. 3147–3166.
- [65] T. J. Hughes, R. L. Taylor, J. L. Sackman, A. Curnier, and W. Kanoknukulchai. “A finite element method for a class of contact-impact problems”. In: *Computer methods in applied mechanics and engineering* 8.3 (1976), pp. 249–276.
- [66] K. L. Johnson. *Contact mechanics*. Cambridge university press, 1985.
- [67] K. L. Johnson. “Surface interaction between elastically loaded bodies under tangential forces”. In: *Proceedings of the royal society of London. Series A. Mathematical and physical sciences* 230.1183 (1955), pp. 531–548.

- [68] H. B. Khenous, P. Laborde, and Y. Renard. “On the discretization of contact problems in elastodynamics”. In: *Analysis and simulation of contact problems*. Springer, 2006, pp. 31–38.
- [69] N. Kikuchi and J. T. Oden. *Contact problems in elasticity: a study of variational inequalities and finite element methods*. Vol. 8. siam, 1988.
- [70] N. Kikuchi and Y. J. Song. “Penalty/finite-element approximations of a class of unilateral problems in linear elasticity”. In: *Quarterly of Applied Mathematics* 39.1 (1981), pp. 1–22.
- [71] G. Kloosterman, R. M. van Damme, A. H. van den Boogaard, and J. Huetink. “A geometrical-based contact algorithm using a barrier method”. In: *International Journal for Numerical Methods in Engineering* 51.7 (2001), pp. 865–882.
- [72] J. Kopačka, D. Gabriel, R. Kolman, and J. Plešek. “A symmetry preserving contact treatment in isogeometric analysis”. In: *Proceedings of the 7th GACM Colloquium on Computational Mechanics for Young Scientists from Academia and Industry* (2017).
- [73] R. H. Krause and B. I. Wohlmuth. “A Dirichlet–Neumann type algorithm for contact problems with friction”. In: *Computing and visualization in science* 5.3 (2002), pp. 139–148.
- [74] R. Kučera, J. Machalová, H. Netuka, and P. Ženčák. “An interior-point algorithm for the minimization arising from 3D contact problems with friction”. In: *Optimization methods and software* 28.6 (2013), pp. 1195–1217.
- [75] A. Kudawoo, M. Abbas, T. De-Soza, F. Lebon, and I. Rosu. “Computational Contact Problems: Investigations on the Robustness of Generalized Newton Method, Fixed-Point method and Partial Newton Method”. In: *International Journal for Computational Methods in Engineering Science and Mechanics* 19.4 (2018), pp. 268–282.
- [76] T. Laursen. *Computational contact and impact mechanics, 2002*. 2002.
- [77] T. Laursen and V. Chawla. “Design of energy conserving algorithms for frictionless dynamic contact problems”. In: *International Journal for Numerical Methods in Engineering* 40.5 (1997), pp. 863–886.
- [78] F. Lebon. “Two-grid method for regularized frictional elastostatics problems”. In: *Engineering computations* (1995).
- [79] F. Lebon and M. Raous. “Multibody contact problem including friction in structure assembly”. In: *Computers & structures* 43.5 (1992), pp. 925–934.
- [80] J.-P. LEFEBVRE. *Code\_Aster [U4.43.01] Operator DEFI\_MATERIAU*. EDF R&D. July 2018.
- [81] C. Licht, E. Pratt, and M. Raous. “Remarks on a numerical method for unilateral contact including friction”. In: *Unilateral Problems in Structural Analysis IV*. Springer, 1991, pp. 129–144.
- [82] D. G. Luenberger and Y. Ye. *Linear and nonlinear programming*. Springer New York, 2008.
- [83] G. Marckmann and E. Verron. “Comparison of hyperelastic models for rubber-like materials”. In: *Rubber chemistry and technology* 79.5 (2006), pp. 835–858.
- [84] A. G. Neto, P. M. Pimenta, and P. Wriggers. “A master-surface to master-surface formulation for beam to beam contact. Part I: frictionless interaction”. In: *Computer Methods in Applied Mechanics and Engineering* 303 (2016), pp. 400–429.

- [85] J. Nocedal, A. Wächter, and R. A. Waltz. “Adaptive barrier update strategies for nonlinear interior methods”. In: *SIAM Journal on Optimization* 19.4 (2009), pp. 1674–1693.
- [86] J. Nocedal and S. Wright. *Numerical optimization*. Springer Science & Business Media, 2006.
- [87] J. T. Oden and E. Pires. “Nonlocal and nonlinear friction laws and variational principles for contact problems in elasticity”. In: (1983).
- [88] J. Oden and S. Kim. “Interior penalty methods for finite element approximations of the Signorini problem in elastostatics”. In: *Computers & Mathematics with Applications* 8.1 (1982), pp. 35–56.
- [89] J. Oden and E. Pires. “Algorithms and numerical results for finite element approximations of contact problems with non-classical friction laws”. In: *Computers & Structures* 19.1-2 (1984), pp. 137–147.
- [90] J. Oden and E. Pires. “Numerical analysis of certain contact problems in elasticity with non-classical friction laws”. In: *Computers & Structures* 16.1-4 (1983), pp. 481–485.
- [91] R. W. Ogden. “Large deformation isotropic elasticity—on the correlation of theory and experiment for incompressible rubberlike solids”. In: *Proc. R. Soc. Lond. A* 326.1567 (1972), pp. 565–584.
- [92] O. Pantz. “A frictionless contact algorithm for deformable bodies”. In: *ESAIM: Mathematical Modelling and Numerical Analysis* 45.2 (2011), pp. 235–254.
- [93] J. PELLET. *Code\_Aster [U3.01.00] Description of the file of grid of Code\_Aster*. EDF R&D. Mar. 2016.
- [94] C.-t. Perng. “On a class of theorems equivalent to farkas’s lemma”. In: *Applied Mathematical Sciences* 11.44 (2017), pp. 2175–2184.
- [95] O. Pironneau. “Handling contacts in an Eulerian frame: a finite element approach for fluid structures with contacts”. In: *International Journal of Computational Fluid Dynamics* 32.2-3 (2018), pp. 121–130.
- [96] A. Popp. “State-of-the-Art Computational Methods for Finite Deformation Contact Modeling of Solids and Structures”. In: *Contact Modeling for Solids and Particles*. Springer, 2018, pp. 1–86.
- [97] A. Popp, M. W. Gee, and W. A. Wall. “A finite deformation mortar contact formulation using a primal–dual active set strategy”. In: *International Journal for Numerical Methods in Engineering* 79.11 (2009), pp. 1354–1391.
- [98] M. N. R3. *MD User’s Guide - Application Examples*. 2008.
- [99] A. Raoult. “Non-polyconvexity of the stored energy function of a Saint Venant-Kirchhoff material”. In: *Aplikace matematiky* 31.6 (1986), pp. 417–419.
- [100] M. Raous. “Art of Modeling in Contact Mechanics”. In: *The Art of Modeling Mechanical Systems*. Springer, 2017, pp. 203–276.
- [101] M. Raous. “Quasistatic Signorini problem with Coulomb friction and coupling to adhesion”. In: *New developments in contact problems*. Springer, 1999, pp. 101–178.
- [102] J. N. Reddy. *An introduction to continuum mechanics*. Cambridge university press, 2013.
- [103] Y. Renard. “A uniqueness criterion for the Signorini problem with Coulomb friction”. In: *SIAM journal on mathematical analysis* 38.2 (2006), pp. 452–467.
- [104] J. Salençon. *Mécanique des milieux continus*. Vol. 1. Editions Ecole Polytechnique, 2013.

- [105] O. Schenk, K. Gärtner, W. Fichtner, and A. Stricker. “PARDISO: a high-performance serial and parallel sparse linear solver in semiconductor device simulation”. In: *Future Generation Computer Systems* 18.1 (2001), pp. 69–78.
- [106] A. Signorini. “Sopra alcune questioni di elastostatica”. In: *Atti della Societa Italiana per il Progresso delle Scienze* 21.II (1933), pp. 143–148.
- [107] J. Simo and T. Laursen. “An augmented Lagrangian treatment of contact problems involving friction”. In: *Computers & Structures* 42.1 (1992), pp. 97–116.
- [108] J. M. Solberg, R. E. Jones, and P. Papadopoulos. “A family of simple two-pass dual formulations for the finite element solution of contact problems”. In: *Computer methods in applied mechanics and engineering* 196.4-6 (2007), pp. 782–802.
- [109] T. D. SOZA. *Code\_Aster [V6.03.121] SSNP121 - Intégration des termes de contact en 2D et 3D*. EDF R&D. July 2015.
- [110] T. D. SOZA. *Code\_Aster [V6.03.154] SSNP154 - Benchmark NAFEMS de validation du contact 1 : cylinder roller contact*. EDF R&D. June 2016.
- [111] T. D. SOZA. *Code\_Aster [V6.04.128] SSNV128 - Plaque avec contact et frottement sur un plan rigide*. EDF R&D. Dec. 2017.
- [112] G. Tanoh, Y. Renard, and D. Noll. “Computational experience with an interior point algorithm for large scale contact problems”. In: *Optimization Online* 10.2 (2004).
- [113] N. Tardieu, F. Youbissi, and E. Chamberland. “Un algorithme de Gradient Conjugué Projeté préconditionné pour la résolution de problèmes unilatéraux”. In: *Comptes rendus Mécanique* 336.11-12 (2008), pp. 840–845.
- [114] B. Tasseff, C. Coffrin, A. Wächter, and C. Laird. “Exploring Benefits of Linear Solver Parallelism on Modern Nonlinear Optimization Applications”. In: *arXiv preprint arXiv:1909.08104* (2019).
- [115] R. L. Taylor and P. Papadopoulos. “On a patch test for contact problems in two dimensions”. In: *Computational methods in nonlinear mechanics* 690 (1991), p. 702.
- [116] I. Temizer, M. Abdalla, and Z. Gürdal. “An interior point method for isogeometric contact”. In: *Computer Methods in Applied Mechanics and Engineering* 276 (2014), pp. 589–611.
- [117] I. Temizer, P. Wriggers, and T. Hughes. “Contact treatment in isogeometric analysis with NURBS”. In: *Computer Methods in Applied Mechanics and Engineering* 200.9-12 (2011), pp. 1100–1112.
- [118] M. Tur, F. Fuenmayor, and P. Wriggers. “A mortar-based frictional contact formulation for large deformations using Lagrange multipliers”. In: *Computer Methods in Applied Mechanics and Engineering* 198.37-40 (2009), pp. 2860–2873.
- [119] A. Wächter. “Short tutorial: getting started with ipopt in 90 minutes”. In: *Dagstuhl Seminar Proceedings*. Schloss Dagstuhl-Leibniz-Zentrum für Informatik. 2009.
- [120] A. Wächter and L. T. Biegler. “On the implementation of an interior-point filter line-search algorithm for large-scale nonlinear programming”. In: *Mathematical programming* 106.1 (2006), pp. 25–57.
- [121] B. I. Wohlmuth. “A mortar finite element method using dual spaces for the Lagrange multiplier”. In: *SIAM journal on numerical analysis* 38.3 (2000), pp. 989–1012.
- [122] P. Wriggers and M. Imhof. “On the treatment of nonlinear unilateral contact problems”. In: *Archive of Applied Mechanics* 63.2 (1993), pp. 116–129.

- 
- [123] P. Wriggers. *Computational Contact Mechanics, Second Edition*. Springer-Verlag, 2006.
  - [124] P. Wriggers, T. V. Van, and E. Stein. “Finite element formulation of large deformation impact-contact problems with friction”. In: *Computers & Structures* 37.3 (1990), pp. 319–331.
  - [125] V. Yastrebov. “Computational contact mechanics: geometry, detection and numerical techniques”. PhD thesis. École Nationale Supérieure des Mines de Paris, 2011.
  - [126] O. C. Zienkiewicz, R. L. Taylor, and R. L. Taylor. *The finite element method: solid mechanics*. Vol. 2. Butterworth-heinemann, 2000.



## FINITE ELEMENT MODELING OF MECHANICAL CONTACT PROBLEMS FOR INDUSTRIAL APPLICATIONS

### Abstract

The Airthium company uses FreeFEM software in order to study its energy storage system, and contact mechanics is a part of these studies. Therefore the principal aim of this thesis is to develop an algorithm, using FreeFEM and its tools, to solve mechanical contact problems between two bodies or more, for linear elastic or finite deformation problems.

The contact problem is considered as a minimization problem of an energy, where we can take advantage of several optimization techniques, in order to converge faster to the solution. For several reasons, the interior point method is the optimization method chosen to solve the generated minimization problems.

An algorithm is proposed in order to solve the frictionless contact between a hyperelastic body and a rigid foundation (obstacle). The non-penetration constraints between the body and the obstacle are described in a simple way, where there is no need to compute the normal vectors or the projection points on the obstacle, which simplifies the resolution of the contact problem.

The second aim of this thesis is to develop a symmetric algorithm where the user no longer needs to specify a slave body and a master one. Thus two algorithms were developed, one based on the penalty method, and the second one uses the interior point method. In the two cases a sequence of minimization problems with linear (or affine) constraints, using a fixed point algorithm, is employed in order to consider the non-penetration for finite deformation problems, where large deformations occur.

The friction is also taken into account, and the problem using Coulomb's criterion is written into a sequence of problems with Tresca's criterion, in order to obtain a sequence of minimization problems. A family of regularization for the Tresca's criterion are proposed, in order to obtain sufficiently smooth problems, which in some situations can have an experimental justifications.

**Keywords:** contact mechanics, signorini problem, friction, regularization , optimization, fixed point, penalization , interior point method, symmetric algorithm

---

## Résumé

La société Airthium utilise le logiciel FreeFEM afin d'étudier son système de stockage d'énergie, et la mécanique du contact fait partie de ces études. L'objectif principal de cette thèse est donc de développer un algorithme, utilisant FreeFEM et ses outils, pour résoudre des problèmes de contact mécanique entre deux corps ou plus, pour des problèmes d'élasticité linéaire ou de grandes déformations.

Le problème de contact est considéré comme un problème de minimisation d'une énergie, où nous pouvons tirer parti de plusieurs techniques d'optimisation, afin de converger plus rapidement vers la solution. Pour plusieurs raisons, la méthode de points intérieurs est la méthode d'optimisation choisie pour résoudre les problèmes de minimisation générés.

Un algorithme est proposé afin de résoudre le contact sans frottement entre un corps hyperélastique et une fondation rigide (obstacle). Les contraintes de non-pénétration entre le corps et l'obstacle sont décrites d'une manière simple, où il n'est pas nécessaire de calculer les vecteurs normaux ou les points de projection sur l'obstacle, ce qui simplifie la résolution du problème de contact.

Le second objectif de cette thèse est de développer un algorithme symétrique où l'utilisateur n'a plus besoin de spécifier un corps esclave et un corps maître. Ainsi deux algorithmes ont été développés, l'un basé sur la méthode de pénalisation, et le second utilise la méthode de points intérieurs. Dans les deux cas, une suite de problèmes de minimisation avec des contraintes linéaires (ou affines), utilisant un algorithme à point fixe, est employée afin de considérer la non-pénétration pour les problèmes où de grandes déformations se produisent.

Le frottement est également pris en compte, et le problème utilisant le critère de Coulomb est écrit en une séquence de problèmes avec le critère de Tresca, afin d'obtenir une séquence de problèmes de minimisation. Une famille de régularisation pour le critère de Tresca est proposée, afin d'obtenir des problèmes suffisamment lisses, qui dans certaines situations peuvent avoir une justification expérimentale.

**Mots clés :** mécanique des contacts, problème de signorini, frottement, régularisation, optimisation, point fixe, pénalisation, méthode des points intérieurs, algorithme symétrique

---

